THE UNIVERSITY *of* LIVERPOOL

Model Predictive Control of the HVAC System in Industrial Cleanrooms for Energy Saving

Thesis submitted in accordance with the
requirements of the University of Liverpool
for the degree of Doctor of Philosophy

in

Electrical Engineering and Electronics

by

Shuji Chen, B.Sc.(Eng.)

December 2016

Model Predictive Control of the HVAC System in Industrial Cleanrooms for Energy Saving

by

Shuji Chen

Acknowledgements

I would like to express my special thanks of gratitude to my supervisor, Dr. L. Jiang. He kindly helped and guided my research. My supervisor also taught me how to research which will take benefits for me throughout my life.

I also would like to thank Prof. Q.H. Wu and Dr. J. Counsell, for their kindly encouragement.

I offer my regards and blessings to all of the members of Smart Grid Control and Renewable Energy Subgroup, the University of Liverpool, especially to Dr. C.K. Zhang and Ms. Q. Zhu. I also thank my friends, Dr. W. Yao, Ms. L.Y. Li, Mr. Y.X. Ren, Mr. S. Rind, Mr. R.T. Wang, Ms. X.J. Zheng, Mr. Y.J. Wang, Ms. Y.F. Du, Mr. K. Shi, Mr. Y. Liu, Mr. C. Duan, Mr. Y.Y. Sang, Mr. W.Z. Deng and Mr. H.T. Xu, for their support and friendship. My thanks also go to the Department of Electrical Engineering and Electronics at the University of Liverpool, for providing the research facilities that made it possible for me to carry out this research.

I gratefully acknowledge the funding received towards my PhD from the Centre for Global Eco-Innovation (CGE) and Energy Efficiency Consultancy Ltd (EECO2). Thanks to Mr. M. Harris from EECO2 for his kindly support and cooperation.

Finally, I would thank my family for their loving and heartening me in these years.

Abstract

20-40% of the total final energy consumption, which includes both residential and commercial users, is spent on buildings, and its amount has been increasing at a rate 0.5-5% per year in developed countries. The heating, ventilation and air conditioning (HVAC) system is widely installed in commercial buildings to provide thermal comfort and acceptable indoor air quality. Cleanrooms are one of the most common applications which have a high requirement of air cleanliness. About 40% of the total energy in a commercial sector is used for heating, cooling and ventilating the buildings' environment. This thesis deals with the reduction of the energy consumption of the HVAC system in industrial cleanrooms via model predictive control (MPC). A cleanroom laboratory has been built with the HVAC system to simulate a pharmaceutical factory where the MPC is implemented.

Literature reviews of MPC approaches and its applications in HVAC systems are carried out. The schematic of the cleanroom laboratory has been investigated, including the detailed specification of the HVAC hardware and software. The laboratory consists of four rooms: the entrance room and three cleanrooms constructed with different levels of air cleanliness: the change room, the small lab and the large lab. The original control of the air ventilation is implemented by proportional-integral (PI) control installed in a building management system (BMS). The data used for further applications are collected through the object linking and embedding for process control (OPC) server connecting the HVAC hardware with the OPC Toolbox in Matlab.

A black-box model of the cleanroom laboratory has been developed based on the measured data. The indoor air quality of cleanrooms is maintained by controlling the air change rate and the air pressure via the HVAC system. Modelling of the

cleanroom laboratory includes single-input single-output (SISO) modelling of each PI control loop and two multi-input multi-output (MIMO) subsystems: the change room related subsystem and the small/large lab related subsystem. Three parameter estimation methods: prediction error identification method (PEM), least squares (LS) method and instrumental variable (IV) method, and three model structures including autoregressive exogenous (ARX), state space (SS) and transfer function (TF) have been investigated, respectively. The model identification is implemented by the System Identification Toolbox in Matlab. For each system model, the model structure with the best performance index has been found by comparing the prediction results with the experimental results using model validation approach.

The MPC controllers are designed based on the identified models to maintain the steady air change rate and air pressure. Both SISO and MIMO MPC are investigated. The original PI controllers are replaced by the SISO MPC controllers. The SISO MPC shows a better transient performance and lowers energy consumption. MIMO MPC controllers are necessary to use in the HVAC system since the HVAC system exhibits a MIMO nature with coupled controlled variables and the interactions are not negligible. The MIMO MPC shows better control performance and lowers energy consumption than SISO MPC and PI control.

The closed-loop control of the particle concentration has been built to maintain the air cleanliness in the laboratory. The particle counters are installed in the cleanroom laboratory to monitor the number of particles within a specified air volume. The particle counter based controllers have been designed and tested including the PI control, the SISO MPC and the MIMO MPC, respectively. The comparison among these control methods shows that the MIMO MPC has the best performance and consumes the least energy.

The PI control and MPC have been developed in programmable logic controller (PLC) devices. A PLC based industrial personal computer (IPC) has been installed to construct a workstation panel. The Matlab based controllers have been transferred into the PLC language. The PLC based controllers have been tested controlling the airflow, air pressure and the particle concentration. The test results demonstrate that the PLC based controllers perform better and spend less energy than those in Matlab.

Declaration

The author hereby declares that this thesis is a record of work carried out in the Department of Electrical Engineering and Electronics at the University of Liverpool during the period from October 2012 to December 2016. The thesis is original in content except where otherwise indicated.

Contents

List of Figures

List of Tables

List of Abbreviations

ACR	Air Change Rate
AE	Absolute Error
AHU	Air Handling Unit
AP	Air Pressure
APE	Absolute Percentage/relative Error
ARMAX	AutoregRessive-Moving Average with eXogenous terms
ARX	AutoregRessive eXogenous
ASHRAE	American Society of Heating, Refrigerating and penalised Engineers
BMS	Building Management System
CC	Correlation Coefficient
COP	Coefficient of performance
CV	Coefficient of Variation
DMC	Dynamic Matrix Control
EHAC	Extended Horizon Adaptive Control
EPSAC	Extended Prediction Self Adaptive Control
EtherCAT	Ethernet for control automation technology
GPC	Generalised Predictive Control
HVAC	Heating, Ventilation and Air Conditioning
IAE	integral of Absolute Error
IAQ	Indoor Air Quality
IPC	Industrial Personal Computer (PC)
ISE	integral of Squared Error
ISO	International organisation for Standardisation
ITAE	integral of Time multiplied Absolute Error
ITSE	integral of Time multiplied Squared Error
IV	Instrumental Variable

LS	Least Squares
LQR	LinearQuadratic Regulator
MAE	Mean Absolute Error
MAPE	Mean Absolute Percentage/relative Error
MBE	Mean Bias Error
MIMO	Multi-Input Multi-Output
MPC	Model Predictive Control
MV	Manipulated Variable
OPC	Object linking and embedding for Process Control
PEM	Prediction Error identification Method
PFC	Predictive Functional Control
PI	Proportional-Integral
PID	Proportional-Integral-Derivative
PLC	Programmable Logic Controller
QP	Quadratic Programming
RMSE	Root Mean Square Error
SISO	Single-Input Single-Output
SP	Set-Point
SS	State Space
TcCOM	TwinCAT Component Object Model
TF	Transfer Function
TwinCAT	The Windows Control and Automation Technology
VAV	Variable Air Volume

Chapter 1

Introduction

1.1 Background

Cleanrooms are widely employed in high-technology fabrication, such as pharmaceutical, semiconductor and optoelectronic manufacturing, to meet the stringent requirements of high air cleanliness levels in the processing environment [1]. The high-technology manufacturing environment is based on a series of cleanrooms whose airborne particle levels are controlled. As defined by the international cleanroom standard (ISO) [2], a cleanroom is: "A room within which the number concentration of airborne particles is controlled and classified, and which is designed, constructed and operated in a manner to control the introduction, generation and retention of particles inside the room." Cleanrooms are typically classified according to their use and confirmed by the air cleanliness [3]. There are two main standards by which pharmaceutical cleanrooms are classified: EU good manufacturing practice (GMP) [4] and ISO 14644 [2]. The standards grade cleanrooms based on the permitted maximum number of particles allowed within a cubic metre of air which is called the particle concentration. The particle concentration is measured and controlled by the heating, ventilation and air conditioning (HVAC) system which circulates air in cleanrooms with a relatively high air change rate (ACR) [5]. ACR is a measure of the air volume added to or removed from a space divided by the volume of the space [5]. To reach the required ACR, the controlled environmental variables

of the HVAC system include the air pressure (AP) and the supply airflow rate into the space [6].

The particle concentration is measured by the particle counter with a standard flow rate: 1 cubic foot per minute. The data of particle concentration can be collected every 35.3 seconds. The distribution of particles inside a cleanroom is not homogeneous. For a given cleanroom, multiple particle counters are installed with different locations. The maximum particle concentration defined among these particle counters is chosen as the output variables of a particulate controller.

A cleanroom is an enclosed working space where delicate work is done that needs protecting from contamination by impurities in the ambient air. The air quality, the temperature and the humidity are regulated to protect the contents of the room from the dust and bacteria contaminated particles that exist naturally in the atmosphere and the ambient air around the cleanroom, and also those that might be generated within the cleanroom itself [7]. Natural, "fresh" air contains about 35 million particles of 0.5 μm in diameter, or larger, per cubic metre. Even if the factory is built in as rural a surrounding area as the planning regulations will allow, the chances are that other nearby emissions will pollute the ambient air to a poorer quality [7].

It should be noticed that a particle 200 times smaller than a human hair, which is approximately 75-100 μm in diameter, can cause major damage to sensitive equipment. Without the availability of cleanrooms, the creation of structures and devices with feature sizes that are equal to or less than that of a dust particle would be impossible. One oversized particle settling at a critical point of a circuit board could cause the whole board to fail [7]. Thus cleanroom manufacturers pay strict attention to air particles, with most cleanroom design and manufacturing companies targeting the elimination of air particles 0.5 μm in size or larger, which has been the function of cleanroom air filters. However, some industries are now imposing even smaller air particle standards [7].

HVAC is designed to satisfy the environmental requirements of a process or comfort, in a specific building and a particular geographic locale [8]. It is defined as the simultaneous control of temperature, humidity, radiant energy, air motion and

air quality within a space [8]. HVAC systems play a significant role in the control of indoor air quality (IAQ) and thermal comfort. A bad indoor environmental quality can be caused by poor ventilation, improper temperature and humidity which results in irritation of the eyes and nose, fatigue, headache and shortness of breath. So that people get sick more often with a bad IAQ since they spend the most time indoors. A control that maintains a fixed set-point of fresh air ventilation based on the designed occupancy of the space is typically employed by HVAC systems to guarantee a good IAQ. This is an inefficient method, since it often provides much more fresh air than necessary, especially in the areas with frequently varying occupancy, such as laboratories and conference rooms [9].

The HVAC system contains three central functions: heating, ventilation and air conditioning. They are interrelated with the need to provide thermal comfort, and acceptable IAQ within reasonable installation, operation, and maintenance cost [10]. HVAC systems can provide ventilation, reduce air infiltration, and maintain pressure relationships between spaces [10]. The process of air delivery and removal from spaces is known as room air distribution [11]. The HVAC system is used to regulate the temperature and humidity using fresh air from outdoors in residential structures such as family homes, apartment buildings and hotels; industrial and office buildings such as factories, skyscrapers and hospitals; and on-board vessels. Ventilation is one of the most important factors for maintaining acceptable IAQ in buildings [12]. It is the process of exchanging or replacing air in any space to remove unwanted smells and excessive moisture, introduce outside air, keep interior building air circulating, and prevent stagnation of the interior air [13].

Commercial HVAC systems provide a comfortable and safe work environment for the people working inside buildings with conditioned air. Many factors can reflect the respond of people to their work environment with respect to their health, attitude and productivity. Air quality and air condition are two critical factors. To make air conditioned and in good quality, air should be clean, and the temperature, humidity, and movement of the air should be within certainly acceptable comfort ranges. The standards established by the American society of heating, refrigerating and penalised engineers (ASHRAE) summarise indoor comfort conditions which

are thermally acceptable to 80% or more of occupants in a commercial building [5]. These comfort conditions are between $68°F$ and $75°F$ for winter and $73°F$ to $78°F$ during the summer [14]. Both these ranges are for room air at approximately 50% relative humidity and moving at a slow speed of 30 feet per minute or less [14].

A wide range of equipment is involved in HVAC systems: air handling units (AHUs), fans, variable air volumes (VAVs), dampers, chillers, boilers, pumps and so on. Figure 1.1 shows a diagram of a basic HVAC system which integrates the equipment presented above. The outside air flows into the AHU, mixed with the return air from the cleanroom. The mixed air is filtered, accelerated, heated or chilled and filtered again in the AHU. So that the AHU provides clean air with required temperature and velocity into the cleanroom. A VAV is installed between the AHU and the cleanroom which is used to control the airflow rate. The clean air flows through the cleanroom and flows out via another VAV. The extracted air is accelerated by another fan before it flows outside or returns to the AHU. A detailed explanation of the equipment will be given in Chapter 3.

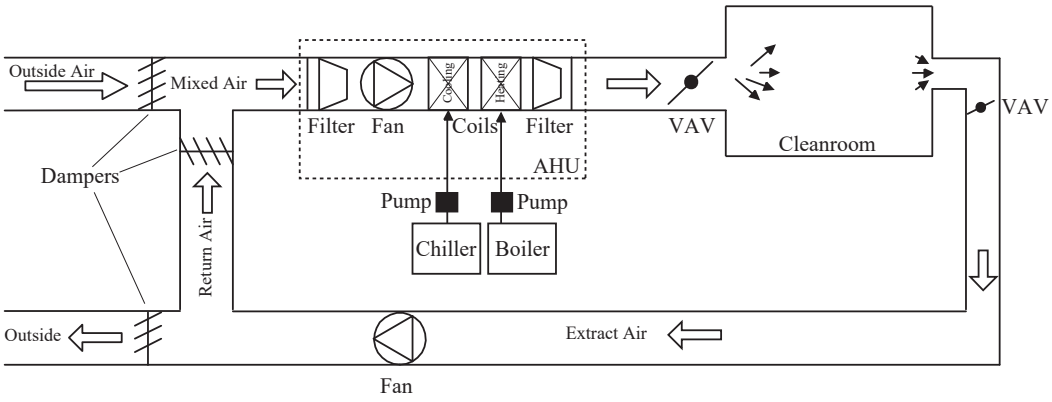

Figure 1.1: Diagram of a basic HVAC system.

HVAC control systems aim to operate the equipment efficiently as well as provide a high-quality environment. In operation, each HVAC system should be suitable for the requirements of the facility. In combination, HVAC system controls provide the link between varying thermal loads and maintaining suitable indoor environmental conditions. The designed HVAC system will not operate as expected

without an adequately designed and properly functioning control system. A control loop includes a controller, a sensor and a control device. The controller compares the data from sensors with the set-point, relaying a command to the controlled device, which passes to the process plant. The command will have an effect on the controlled variable, and then the process will start all over again [15].

1.2 Motivations

The importance of IAQ has increased for both health and comfort, especially for commercial cleanrooms. The growing requirements for higher IAQ of the working environments in laboratories, hospitals, and industrial facilities have rapidly increased the energy demands. The controller designers of the cleanroom HVAC system meet the challenge for both the reduction of energy consumption and the control of the air cleanliness. To address the challenge, a more advanced controller with the optimisation of the energy consumption can be designed compared with the traditional control method, PI control. Also, the feedback control of the particle concentration based on real-time measurements by particle counters can be introduced to improve the dynamic response of air cleanliness control.

HVAC systems aim to maintain IAQ and thermal comfort in cleanrooms. Thermal comfort relates to the air temperature in cleanrooms which has been well studied by researchers. The mathematical models of temperature can be obtained through either physical process models or model identification. For commercial cleanrooms, IAQ also plays a significant role since it carries huge implications for the product quality and people's health. To address this, the mathematical models of IAQ should be achieved including the modelling of the airflow rate, the AP, the concentration of particles and CO_2, etc. This thesis focuses on the modelling of the airflow rate, the AP and the particle concentration while the black-box model approach will be applied to identify their mathematical models.

The MPC uses a system model to predict the future states of the system and generates a control vector that minimises a certain cost function over the prediction horizon in the presence of disturbances and constraints [72]. The identified models

of IAQ can be used by MPC controllers as prediction models. Compared with PI control, MPC shows benefits for optimal energy consumption and improved control performance by optimising the objective function in MPC controllers. The objective function is defined by QP which minimises the difference between measured outputs and set-points and the increment of the control input.

The mathematical models of the particle levels in the cleanroom can be identified based on the measured data from particle counters. The black-box modelling approach is applied to identify them considering the relationship between supply fan speed, supply VAVs and the particle concentrations. The particle counter based MPC is designed to build the feedback control of the particle levels using the real-time measurements of the particle concentration. Thus the control of the air cleanliness can be more intuitive which improves the dynamic response and reduces the energy consumption.

The novelties of this thesis include a new cleanroom laboratory constructed to simulate a pharmaceutical factory, control of ventilation in the HVAC system, closed-loop control of the particle concentration, energy savings compared to traditional PI controllers.

1.3 Objective

The objective of this project is to develop a programmable logic control (PLC) system to control a cleanroom ventilation system, using proprietary tools or developing bespoke electronics.

Cleanrooms are designed to meet strict air cleanliness requirements, the associated equipment necessary for operations which include HVAC systems, create a substantial energy demand as a result. However, the stringent standards under which they operate means that existing technologies developed for industrial or commercial controls are not sufficient to meet customer needs, particularly in existing facilities.

This project aims to develop a predictive sensor-based dynamic control of the cleanroom HVAC system to maintain the required air cleanliness while maximising

energy efficiency. It will be a modular, retrofit control solution, easily expanded as the cleanroom environment changes. It will communicate with third-party products for complete integration with the overall building energy management system. Bespoke control algorithms will be developed based on real-world cleanroom applications in the test facility, potentially to be a Title 21 CFR Part 11 compliant software solution.

The control system is applicable to any cleanroom configuration whether new or existing facility and employs sensors that include real-time particle counters to ensure optimum equipment control according to the number of criteria that include but are not limited to, particulate concentration, the moisture content of air, temperature and pressure (absolute and differential).

1.4 Main Contributions

The publications produced from this research work are listed in this section as follows:

1. S. Chen, L. Jiang, W. Yao and Q.H. Wu, "Application of Switched System Theory in Power System Stability," in *Power Engineering Conference (UPEC), 2014 49th International Universities*, Cluj-Napoca, pp. 1-6, 2014.
2. S. Chen, C.K. Zhang, L. Jiang and M. Harris, "Black-box modelling of a cleanroom pharmaceutical laboratory equipped with the HVAC system," submitted to *Energy and Building*, 2016.
3. S. Chen, C.K. Zhang, L. Jiang and M. Harris, "Model predictive control of air change rate and air pressure of the cleanroom HVAC system," Due to submit to *Applied Energy*, 2016.
4. S. Chen, C.K. Zhang, L. Jiang and M. Harris, "Model predictive control of air cleanliness based on real-time data of particle counters for energy saving," Due to submit to *Building and Environment*, 2016.

Regarding the submitted and drafted publications, the contributions of the second author, C.K. Zhang, include the demonstration of the controller design, review and comments on papers structure and content. The fourth author, M. Harris, is the

manager of this project who provided technical support for the construction of the cleanroom laboratory.

1.5 Thesis outline

- Chapter 1 provides the background of the research, the motivations of the work, the objectives, the main contributions and the thesis outline.
- Chapter 2 gives a detailed literature review on energy demand in buildings and HVAC systems, control methods in cleanrooms, MPC strategy and its applications in the HVAC system.
- Chapter 3 introduces the schematic of the original cleanroom HVAC laboratory controlled by PI control. Then, the specification of the HVAC hardware and software, which are combined to build the original laboratory, is summarised. Finally, the energy consumption of the hardware is analysed that the integral of the fan speed is calculated instead of the integral of fan power. That is because there is no direct measurement of the power.
- Chapter 4 presents the modelling of the cleanroom HVAC laboratory in both SISO and MIMO models. The laboratory is divided into two subsystems, each of which is modelled as a MIMO model. The black-box modelling approach is applied that the models are identified with three parameter estimation methods and three model structures. The subsystem models identified through prediction error estimation method (PEM) and autoregressive exogenous (ARX) model structure result in the best performance.
- Chapter 5 proposes the MPC controllers designed based on the identified models presented in Chapter 4. The ACR and AP of the laboratory are regulated by the MPC. Compared with PI control and SISO MPC, MIMO MPC shows a better performance for both dynamics and energy consumption of the cleanroom HVAC system.
- Chapter 6 investigates the particle counter based MPC in the cleanroom HVAC system. Several particle counters are installed in the laboratory to count the number of particles. The measured outputs of the MPC are the values of the

maximum particle concentrations inside cleanrooms. The results show that the particle counter based MIMO MPC has better performance and consumes less power than SISO MPC and PI control.

- Chapter 7 develops the programmable logic controller (PLC) platform for the implementation of PI control and MPC in the laboratory. A PLC based industrial personal computer (IPC) has been installed to develop the PLC platform. It provides the software which allows the transformation from Matlab program into PLC program. For the regulation of airflow rate and AP, the dynamic performance and the energy consumption of the Matlab based PI control, PLC based PI control and MPC are compared. The particle counter based MPC is tested in PLC which can maintain the particle concentration at a particular level.
- Chapter 8 presents the conclusion and the future work.

Chapter 2

Literature review

2.1 Energy demand in buildings and HVAC systems

In recent years, the world energy consumption has become a major concern that the energy saving has been demonstrated by the governments of many developed countries. For instance, the EU presented targets concerning energy cuts defining goals until 2020 in Reference [16]. The similar goals have been stated by the U.S. government with minor differences on the level of each state [17].

Total world energy consumption continuously rises by 48% from 549 quadrillion Btu in 2012 to 815 quadrillion Btu in 2040 [18]. The non-organisation for economic cooperation and development (non-OECD) nations, which have relatively strong, long-term economic growth, contribute most of the energy growth whose energy consumption increases by 71% compared with an increase of 18% in OECD nations [18]. The end users which the use of energy delivered to contain three sectors: buildings, industrial, and transportation sectors. The industry accounts for the largest share of delivered energy consumption, consuming about 54% of the world's total delivered energy [18].

From the energy outlook given in Reference [19] for 2013, buildings in the U.S. consume 70% of the electricity, about 50% of which is generated from the combustion of fossil fuels. Although the efficiency of individual equipment has increased reasonably with better design, manufacturing and engineering, the energy consump-

tion in buildings has continued to rise because of more use of energy intensive devices and evolved demand on indoor thermal comfort [20]. Buildings are increasingly expected to meet higher requirements such as being sustainable and energy efficient at the same time as a healthy and comfortable indoor environment should be achieved [21]. The use of advanced technology for digital and power electronic devices can increase the energy efficiency. However, the total energy consumption of HVAC systems is difficult to decrease since the fans and boilers spend most of the energy and the higher requirement of the air quality needs higher output from them. The reduction of power consumption is necessary due to the significant requirement of the energy saving and environment sustainability.

The rising costs of drug development, manufacturing and a more voracious competitive landscape cause the increased pressures placed upon the pharmaceutical industry. Stricter controls over energy spending have become a necessity rather than a luxury [22]. According to the Energy Star, run by the US department of energy, pharmaceutical companies in the US spend over $1 billion on energy per annum [23]. The pharmaceutical companies have been looking to seek out energy efficiency opportunities that would increase output hand in hand with energy reduction. Energy efficiency in cleanroom technology is now a high priority to successfully cut costs while protecting operations from any interruptions [22]. There are obvious financial benefits to reduce the burden of energy bills on drug manufacturing sites where HVAC systems are required to control particle counts effectively and in accordance with the ISO 14644 standard [2]. It does reflect well on a company's corporate environmental responsibility and contributes towards overarching carbon emissions reduction targets (CERT).

Energy efficiency is driven by not only the environmental responsibility but also the financial prudence. Given the significant scale on which successful energy reduction programmes ought to be based on maximising their benefits, the rate of return on investment in an energy reduction programme is equally as important [22]. A review of cleanroom costs in Europe indicated that energy consumption accounts for 65-75% of the annual cost of running a cleanroom [25]. Furthermore, of the total level of cleanroom energy usage, 36-67% is derived from the HVAC system

alone [25]. According to GSK, HVAC accounted for around 65% of total energy consumption and is, therefore, a top priority for the company to reduce overall consumption. This amounted to a spend of $44 million back in 2008 [22]. A study by the Carbon Trust in the UK indicated that UK businesses could save up to 1.6 billion pounds per annum on energy and that investing in efficiency programmes resulted in a 48% internal rate of return and payback in three years on average [24]. There is a clear and present need within the pharmaceutical industry for the excesses of unnecessary energy expenditure to be reduced, offering substantial benefits both economically and environmentally. Through the adoption of more intelligent HVAC controls, it is possible to see between 10% and 20% energy cost savings per annum [23].

At present, for pharmaceutical manufacturing, open-loop control [6] and closed-loop proportional-integral-derivative (PID) type control [26] are used for regulating the ACR to maintain the air cleanliness level without in deep consideration of energy saving, and thus results in the extra consumption of energy and more pollutants (such as CO_2 and SO_2) emitted. The PID control of ACR is not dynamic, and the set-point is always kept at a high constant value. Also, PID control is more useful for a simple system, but HVAC systems are complex with a large number of drivers and sensors. Thus, PID controllers are not the best option for regulating ACR when the controlled system is complex, and the regulation is dynamic. The reduction of building energy consumption has become main concerns given the growing focus on energy saving and environment protection in recent years, which desires proper design of the HVAC system with optimum energy efficiency, more accurate model and advanced control methods.

2.2 Control methods in cleanrooms

Four fundamental rules defined in ISO 14644-1 [2] apply to cleanrooms:

1. Contaminants must not be introduced into the controlled environment from outside.
2. The equipment within the controlled environment must not generate or give

rise to contaminants.

3. Contaminants must not be allowed to accumulate in the controlled environment.
4. Existing contaminants must be eliminated to the greatest extent possible, and as rapidly as possible.

These objectives are achieved and maintained by taking an incredible amount of technology such as high-efficient air filter, strict guarding process, protection of the operation equipment, enough supplied clean air, effective air distribution inside the cleanroom and so on. A critical factor in cleanroom design is the ACR which refers to the number of times per hour that filtered air from outside replaces the present volume in a chamber or building. The air changes 0.5 to 2 times per hour in a normal home. However, in a cleanroom, it reaches much higher that the ACR can be 10 to more than 600 times per hour due to classification and usage. Higher ACRs equate to higher airflows and more energy use but do not always achieve the desired air cleanliness. The industrial cleanrooms, such as pharmaceutical factories, require an extremely high level of air cleanliness which recommends high ACR. Fan power is proportional to the cube of ACR. A higher ACR means a higher energy consumption. The optimum ACRs are required to reduce the power consumption.

A building management system (BMS) is a computer-based system that can be used to monitor and control the mechanical, electrical and electromechanical equipment in buildings. Such equipment can include power, lighting, security and HVAC system. HVAC systems are one of the most commonly used applications, in particular for the air cleanliness control in cleanrooms. The BMS in a cleanroom HVAC system provides the monitoring of the sensor readings inducing the particle concentration, pressure, temperature, humidity and occupancy, and the control of the supply fan speed for proper airflow and the return airflow for proper pressure. The closed-loop control, which mostly uses the proportional-integral (PI) control, of the airflow and the AP gives a steady ACR in cleanrooms. Thus the particle levels are controlled by maintaining a particular value of ACR.

The control of the particle concentration in cleanrooms, using the ventilation system is over-designed as the design exists on the rule-of-thumb values published

in standard or code such as Federal Standard FS-209 [27], IEST Recommended Practices RP-12.1 [28], and ISO 14644-4 [29]. The energy intensities of HVAC systems of cleanrooms in California are about 4-100 times greater than the average commercial building, depending on the required cleanliness classification [30]. Fan energy use for ISO Classes 3-5 cleanrooms composes around 80% of the fan energy consumption for cleanrooms of all classes [31].

At present, only trial-and-error methods are used for regulating the ACR to improve the indoor cleanliness level and accomplish energy saving, without deep consideration of indoor heat and particle generations [1]. The BMS is used in cleanrooms to achieve a proper ACR. The values of the ACR are normally over-designed that reduce the energy efficiency. To control the air cleanliness inside a cleanroom, the ACR needs to be controlled to ensure enough clean air flowing into the cleanroom. The present HVAC control systems in pharmaceutical manufactories do not treat air cleanliness as a controlled variable. Instead, they maintain a high and steady ACR to make sure the air would not become dirty. In this project, the particulate control via MPC put the particle concentration into closed-loop which provide dynamic control of ACR and air cleanliness. Efficient management of energy usage has become essential in view of the growing focus on energy conservation and building electricity utility rating systems in recent years. Thus, proper design of HVAC system with optimum energy efficiency is necessary. Various mathematical models [32]- [37] have been proposed to represent the relationship between the ACR and the particle concentration in cleanrooms, but most have been considered to be approximations and oversimplified. Several crucial measures have been disregarded in these models, such as particle gain or removal owing to air leakage [32]- [34], and particle deposition on indoor space surface [32]- [35], airlocks and mini-environment [36].

2.3 Model predictive control

Model predictive control (MPC) originated in the late seventies and had been developed considerably since then. It makes explicit use of a model of the process to

obtain the control signal by minimising an objective function. The ideas, appearing in greater or lesser degree in the predictive control family, are [38]:

- Explicit use of a model to predict the process output at future time instants (horizon);
- Calculation of a control sequence penalised an objective function;
- Receding strategy, at each instant the horizon is displaced towards the future, which involves the application of the first control signal of the sequence calculated at each step.

The various MPC algorithms differ among themselves in the model used to represent the process and the noises and cost function to be minimised. Within MPC, many works have been developed and are widely received by the academic world and industry. MPC presents a series of advantages over other methods [38]:

- It is particularly attractive to staff with only a limited knowledge of control because the concepts are very intuitive, and the tuning is relatively easy.
- It can be used to control a great variety of processes, from those with relatively simple dynamics to more complex ones.
- Its extension to the treatment of constraints is conceptually simple, and these can be systematically included during the design process.
- It is a totally open methodology based on certain basic principles which allow for future extensions.

As is logical, however, it also has its drawbacks:

- Although the resulting control law is easy to implement and requires little computation, its derivation is more complex than that of the traditional PID controllers.
- The greatest drawback is the need for an appropriate model of the process to be available. The design algorithm is based on prior knowledge of the model and is independent of it, but it is evident that the benefits obtained will be affected by the discrepancies existing between the real process and the model used. In practice, MPC has proved to be a reasonable strategy for industrial control, despite the initial lack of theoretical results at some crucial points

such as stability and robustness.

Compared to PID or linearquadratic regulator (LQR), MPC can predict future events and can take control actions accordingly. PID controllers are well designed for the simple system, while the model used in the MPC can represent the complex dynamic system. Large time delays and high-order dynamics are the common dynamic characteristics that PID controllers are difficult to deal with. LQR is used for optimal control where the system dynamics are described by a set of linear differential equations, and the cost is described by a quadratic function. It can be applied in MPC as the optimisation algorithms. However, LQR does not have the ability to predict future events compared to MPC.

Basic strategy

Figure 2.1 [62] shows a block diagram of a single-input single-output (SISO) MPC application. The main objective is to hold a single output, $\overline{y}$, at a reference value (or set-point), r, by adjusting a single manipulated variable (MV), u. The block labelled MPC represents an MPC feedback controller designed to achieve the control objective. v is a measured disturbance and d is an unmeasured disturbance.

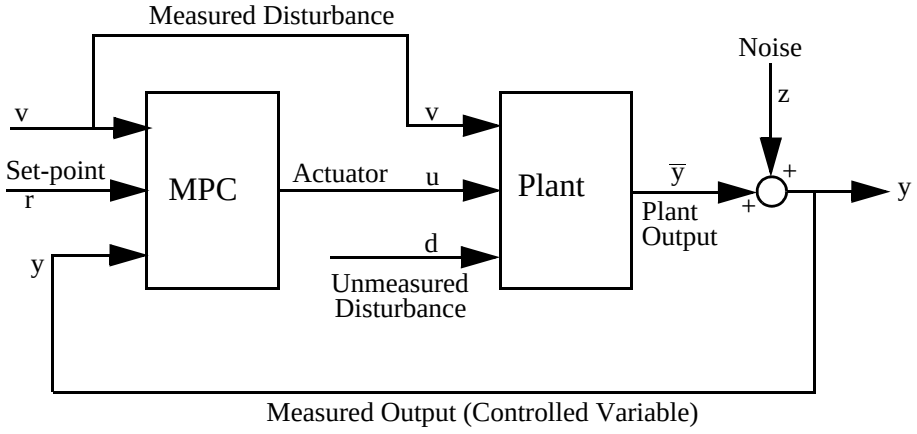

Figure 2.1: Block diagram of a SISO MPC application [62].

The methodology of the MPC is characterised by the following strategy, represented in Figure 2.2 [38].

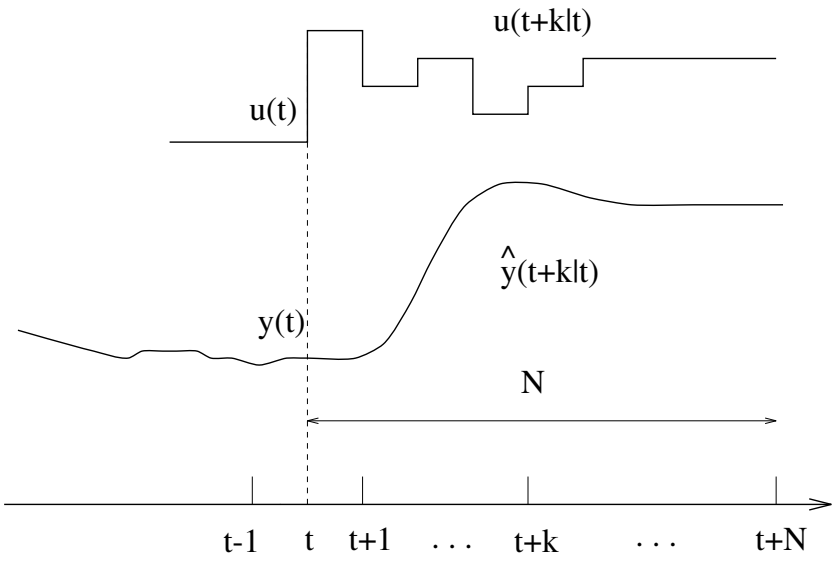

Figure 2.2: MPC strategy [38].

1. With the prediction horizon N, the future outputs are predicted at each instant t using the process model resulting in predicted outputs $y(t+k|t)$ for $k = 1...N$. These predicted outputs depend on the known values up to instant t (past inputs and outputs) and on the future control signals $u(t+k|t),\ k = 0...N-1$, which are those to be sent to the system and calculated.
2. The future control signals are calculated by optimising a determined criterion, which is called objective function, to keep the process as close as possible to the reference trajectory $w(t+k)$. This objective function usually takes the form of a quadratic function representing the errors between the predicted output signal and the predicted reference trajectory. In most cases, the control effort is included in the objective function. An explicit solution can be obtained if the objective function is quadratic, the model is linear, and there are no constraints; otherwise, an iterative optimisation method has to be used.
3. The control signal $u(t|t)$ is sent to the process while the next control signals calculated are rejected, because at the next sampling instant $y(t+1)$ is already known and step 1 is repeated with this new value and all the sequences are brought up to date. Thus $u(t+1|t+1)$ is calculated using the receding horizon concept.

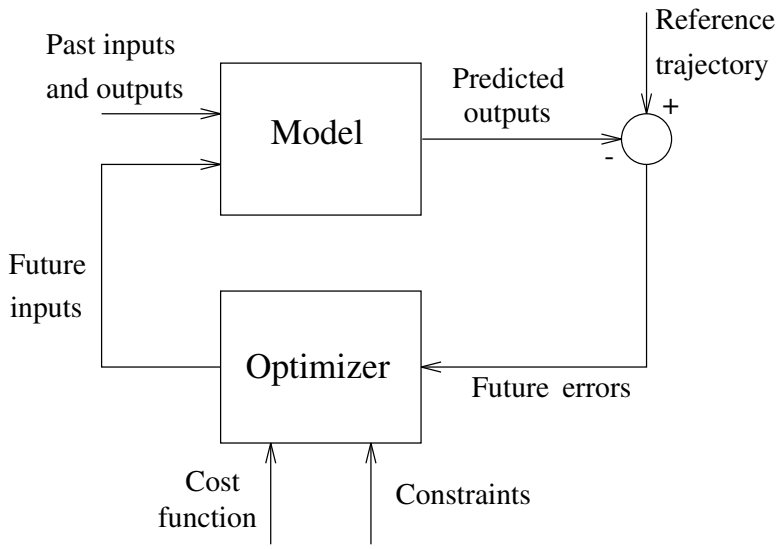

Figure 2.3: Basic structure of MPC [38].

To implement this strategy, the basic structure shown in Figure 2.3 [38] is used. A model is used to predict the future plant outputs, based on the past and current values and the proposed optimal future control actions. These actions are calculated by the optimizer considering the cost function (or called objective function) as well as the constraints.

The process model plays a crucial role in the MPC controller. The chosen model must be able to capture the process dynamics to precisely predict the future outputs and be simple to implement and understand. As the MPC is not a unique technique but rather a set of different methodologies, there are many types of models used in various formulations. The optimizer is another fundamental part of the strategy as it provides the control actions. If the cost function is quadratic, its minimum can be obtained as a specific function (linear) of past inputs and outputs and the future reference trajectory. In the presence of inequality constraints, the solution has to be obtained by more complex numerical algorithms. The size of the optimisation problems depends on the number of variables and the prediction horizons used and usually turns out to be a relatively modest optimisation problem which does not require solving sophisticated computer codes.

Historical background

MPC is a popular advanced control method in industrial processes. MPC has an exceptional history from the early investigation in the academic literature to the explosive growth in the process industries where it is proved to be highly successful [39]. As reviewed in References [40] and [41], the ideas of MPC can be traced back to the 1960s. However, the interest in this field only started to be popular since the introduction of the software identification and command (IDCOM) presented in Reference [42] in 1978 and dynamic matrix control (DMC) was outlined in References [43] and [44] in 1979.

The MPC concept was developed initially from the 1960s related to linear programming (LP). Zadeh and Whalen [45] investigated the connections between minimum time optimal control problem and LP. Propoi [46] proposed the core of all MPC algorithms that the moving horizon approach was presented to solve the LP problem at each sampling period. It became known as "Open Loop Optimal Feedback" named by Reference [47]. To connect this work with MPC, Chang and Seborg [48] developed a feedback control strategy for multi-variable problems solving the LP problems with inequality constraints on the state and at variables. MPC became popular due to its successful industrial applications. A survey of industrial MPC technology was given in Reference [49] including the reported applications until mid-1999. A detailed review of the MPC algorithm was given in Reference [38].

Model predictive heuristic control MPC was firstly recognised in control applications in 1976 by Richalet et al. [50] named as model predictive heuristic control (MPHC) with the solution software, IDCOM. An improved version, named IDCOM-M, was presented with a very similar hierarchy by Grosdidier et al. [51].

IDCOM is very similar to the previous method with a few differences. Firstly, it uses an impulse response model valid only for stable processes, in which the value of $u(t)$ appears instead of $\triangle u(t)$. Furthermore, it makes no use of the control horizon concept so that in the calculations as many control signals as future outputs appear. It introduces a reference trajectory as a first-order system which evolves from the

actual output to the set-point according to a determined time constant. The variance of the error between this trajectory and the output is what one aims at minimising in the objective function.

It also takes into account constraints in the actuators and the internal variables or secondary outputs. Various algorithms can be used for optimising in the presence of constraints, from the ones presented initially by Richalet et al. that can also be used for identifying the impulse response, to others that are shown in Reference [52].

Dynamic matrix control An initial application was developed in 1973 by engineers from Shell Oil with their own independent MPC technology. An unconstrained multivariable control algorithm named as DMC was presented by Cutler and Ramaker at the 1979 National AIChE Meeting [43] and the 1980 Joint Automatic Control Conference [53].

DMC uses the step response to model the process and only takes into account the first N terms, therefore assuming the process to be stable and without integrators. In regards to the disturbances, their value will be considered to be the same as at instant t all along the horizon, that is, to be equal to the measured value of the output (y_m) minus the one estimated by the model ($\hat{y}\,(t|t)$)

Optimisation is carried out at each sampling instant, and the value of $u(t)$ is sent to the process as is typically done in all MPC methods. The inconveniences of this approach are the size of the process model required and the inability to work with unstable processes.

The initial IDCOM and DMC algorithms represent the first generation of MPC technologies which had an enormous impact on industrial process control and served to define the industrial MPC paradigm [49]. The original IDCOM and DMC algorithms provided excellent control of unconstrained multivariable processes.

Generalised predictive control An adaptive MPC method, generalised predictive control (GPC), was developed by Clarke et al [54] [55]. The theoretical basis of the GPC algorithm has been widely studied, and it has been shown in Reference [56] that, for limiting cases of parameter choices, this algorithm is stable, and also that

popular controller such as mean level and deadbeat control are inherent in the GPC structure.

Predictive functional control Predictive functional control (PFC) was developed by Richalet [57] for the case of fast processes. It uses a state space (SS) model of the process and allows for nonlinear and unstable linear internal models. Nonlinear dynamics can be entered in the form of a nonlinear SS model. PFC has two distinctive characteristics: the use of coincidence points and basis functions. The concept of coincidence points is used to simplify the calculation by considering only a subset of points in the prediction horizon. The desired and the predicted future outputs are required to coincide at these points, not in the whole prediction horizon.

The controller parametrizes the control signal using a set of polynomial basis functions which allows a relatively complex input profile to be specified over a long horizon using a small number of parameters. Choosing the family of basis functions establishes many of the features of the computed input profile. These functions can be selected to follow a polynomial set-point with no lag, an important feature for mechanical servo control applications.

Extended prediction self adaptive control Extended prediction self adaptive control (EPSAC) was proposed by Dekeyser [58] in 1988. The implementation of EPSAC is different to the previous methods. For predicting, the process is modelled by the TF. The model can be extended by a term $D(z^{-1})d(t)$, with $d(t)$ being a measurable disturbance in order to include feed-forward effect. Using this method the prediction is obtained as shown in Reference [59].

One characteristic of the method is that the control law structure is very simple, as it is reduced to consider that the control signal is going to stay constant from instant t, that is, $\triangle u(t+k) = 0$ for $k > 0$. In short, the control horizon is reduced to 1 and therefore the calculation is reduced to one single value $u(t)$.

Extended horizon adaptive control Extended horizon adaptive control (EHAC) was developed by Ydstie et al. [60] in 1988. This formulation considers the process modelled by its TF without taking a model of the disturbances into account.

It aims at minimising the discrepancy between the model and the reference at instant $t+N : \hat{y}\,(t+N|t) - w\,(t+N)\,,$ with $\mathrm{N} \geq \mathrm{d}$. The solution to this problem is not unique (unless $\mathrm{N} = \mathrm{d}$) [61].

Thus the control law only depends on the process parameters and can therefore easily be made self-tuning if it has an online identifier. As can be seen, the only parameter of adjustment is the horizon of prediction N, which simplifies its use but provides little freedom for the design. One sees that the reference trajectory cannot be used because the error is only considered at one instant $(t + N)$, neither is it possible to ponder the control efforts at each point so that certain frequencies in the performance cannot be eliminated.

Main elements

All the MPC algorithms possess common elements, and different options can be chosen for each element giving rise to different algorithms. These elements are [38]:

- Prediction model
- Objective function
- Control law
- Parameter tuning

Prediction model The model is the cornerstone of MPC. A complete design should include the necessary mechanisms for obtaining the best possible model, which should be complete enough to fully capture the process dynamics and allow the predictions to be calculated. The use of the process model is determined by the necessity to calculate the predicted output at future instants.

Practically every possible form of modelling a process appears in a given MPC formulation, the following being the most commonly used:

- Impulse response. Also known as weighting sequence or convolution model. The output y is related to the input u by the equation

$$\mathrm{y}\,(\mathrm{t}) = \sum_{i=1}^{\infty} h_i u\,(t-i) \tag{2.3.1}$$

where h_i is the sampled output when the process is excited by a unitary impulse. This sum is truncated and only N values are considered (thus only stable processes without integrators can be represented), having

$$\mathrm{y}\left(\mathrm{t}\right) = \sum_{i=1}^{N} h_i u\left(t-i\right) = H\left(z^{-1}\right) u\left(t\right) \tag{2.3.2}$$

where $H(z^{-1}) = h_1 z^{-1} + h_2 z^{-2} + \cdots + h_N z^{-N}$ and z^{-1} is the backward shift operator. The prediction will be given by:

$$\hat{y}(t+k \mid t) = \sum_{i=1}^{N} h_i u(t+k-i \mid t) = H\left(z^{-1}\right) u(t+k \mid t) \tag{2.3.3}$$

- Step response. Used by DMC and its variants, this is very similar to impulse response except that the input signal is a step. For stable systems, the truncated response is given by:

$$y(t) = y_0 + \sum_{i=1}^{N} g_i \triangle u(t-i) = y_0 + G(z^{-1})(1-z^{-1})u(t) \tag{2.3.4}$$

where g_i are the sampled output values for the step input and $\triangle u(t) = u(t) - u(t-1)$. The value of y_0 can be taken to be 0 without loss of generality, so that the predictor will be:

$$\hat{y}(t+k|t) = \sum_{i=1}^{N} g_i \triangle u(t+k-i|t) \tag{2.3.5}$$

- Transfer function. This uses the concept of the TF, $G = B/A$, so that the output is given by:

$$\mathrm{A}\left(z^{-1}\right) \mathrm{y}\left(\mathrm{t}\right) = \mathrm{B}\left(z^{-1}\right) \mathrm{u}\left(\mathrm{t}\right) \tag{2.3.6}$$

with

$$\mathrm{A}\left(z^{-1}\right) = 1 + a_1 z^{-1} + a_2 z^{-2} + \cdots + a_{na} z^{-na} \tag{2.3.7}$$

$$\mathrm{B}\left(z^{-1}\right) = 1 + b_1 z^{-1} + b_2 z^{-2} + \cdots + b_{nb} z^{-nb} \tag{2.3.8}$$

Thus the prediction is given by

$$\hat{y}(t+k \mid t) = \frac{\mathrm{B}\left(z^{-1}\right)}{\mathrm{A}\left(z^{-1}\right)} u(t+k \mid t) \tag{2.3.9}$$

- State space. It has the following representation:

$$x(t) = Ax(t-1) + Bu(t-1) \tag{2.3.10}$$

$$y(t) = Cx(t) \tag{2.3.11}$$

where x is the state and A, B and C are the matrices of the system, input and output respectively. The prediction for this model is given by

$$\hat{y}(t+k \mid t) = C\hat{x}(t+k \mid t) = C\left[A^k x(t) + \sum_{i=1}^{k} A^{i-1} Bu(t+k-i \mid t)\right] \tag{2.3.12}$$

- Others. Nonlinear models can also be used to represent the process, but they cause the optimisation problem to be more complicated. Neural networks and fuzzy logic are other forms of representation used in some applications.

Objective function The various MPC algorithms propose different objective functions (or called cost functions) for obtaining the control law. The aim is that the future output (y) on the considered horizon should follow a determined reference signal (w) and, at the same time, the control effort ($\triangle u$) necessary for doing so should be penalised [38]. The general expression for an objective function will be:

$$J(N_1, N_2, N_u) = \sum_{j=N_1}^{N_2} \delta(j)[\hat{y}(t+j|t) - w(t+j)]^2 + \sum_{j=1}^{N_u} \lambda(j)[\triangle u(t+j-1)]^2 \tag{2.3.13}$$

In the objective function it is possible to consider:

- Parameters: N_1 and N_2 are the minimum and maximum prediction horizons, and N_u is the control horizon. The meaning of N_1 and N_2 is rather intuitive. They mark the limits of the instants in which it is desirable for the output to follow the reference. Thus, if a high value of N_1 is taken, it is because of no importance if there are errors in the first instant. This will originate a smooth response of the process. Note that in processes with dead time d there is no reason for N_1 to be less than d because the output will not begin to evolve until instant $t+d$. Also if the process is a non-minimum phase, this parameter will allow the first instant of inverse response to be eliminated from the objective

function. The coefficients $\delta(j)$ and $\lambda(j)$ are sequences that consider the future behaviour; usually, constant values or exponential sequences are considered. It is possible to obtain an exponential weight of $\delta(j)$ along the horizon by using:

$$\delta(j) = \alpha^{N_2 - j} \tag{2.3.14}$$

If α is given a value between 0 and 1, the errors farthest from instant t are penalised more than those nearer to it, giving rise to smoother control with less effort. If on the other hand, $\alpha > 1$, the first errors are more penalised, provoking tighter control. All these values can be used as tuning parameters to cover an ample scope of options, from standard control to a made-to-measure design strategy for a particular process.

- Reference trajectory: One of the advantages of predictive control is that if the future evolution of the reference is known a priori, the system can react before the change has effectively been made, thus avoiding the effects of delay in the process response. The future evolution of reference $r(t+k)$ is known beforehand in many applications, such as robotics, servos or batch processes. In other applications a noticeable improvement in performance can be obtained even though the reference is constant by simply knowing the instant when the value changes and getting ahead of this circumstance. In minimisation (5.2.6), the majority of methods usually uses a reference trajectory $w(t+k)$ which does not necessarily have to coincide with the real reference. It is normally a smooth approximation from the current value of the output $y(t)$ towards the known reference by means of the first-order system:

$$w\,(t) = y\,(t) \quad w\,(t+k) = \alpha w\,(t+k-1) + (1-\alpha)\,r\,(t+k) \quad k = 1 \ldots N \tag{2.3.15}$$

where α is a parameter between 0 and 1 (the closer to 1 the smoother the approximation) that constitutes an adjustable value that will influence the dynamic response of the system. In Figure 2.4 [38] the form of the trajectory is shown from when the reference $r(t+k)$ is constant and for two different values of α: small values of this parameter provide fast tracking w_1; if it is increased then the reference trajectory becomes w_2, giving rise to a smoother

response.

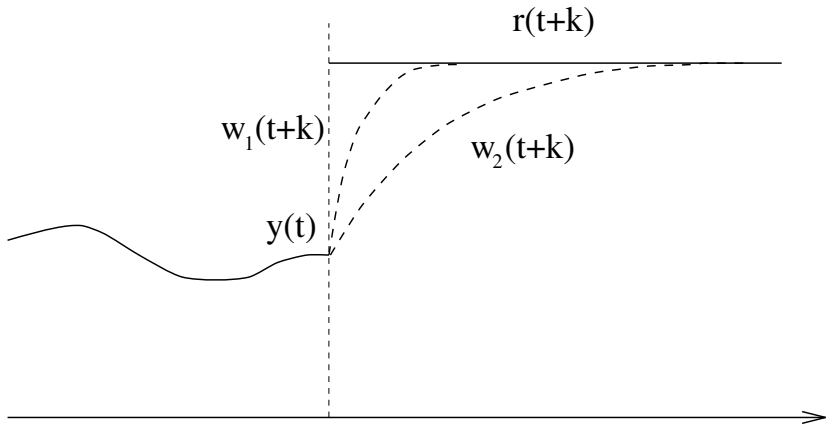

Figure 2.4: Reference trajectory [38].

- Constraints: In practice, all processes are subject to constraints. The actuators have a limited field of action and a determined slew rate, as is the case of the valves, limited by the positions of totally open or closed and by the response rate. Limits in the process variables can be caused by constructive reasons, safety issues, environmental restriction or the scopes of sensors, such as levels in tanks, flows in piping, or maximum temperatures and pressures. Moreover, the operational conditions are commonly defined by the intersection of certain constraints for basically economic reasons, so that the control system will operate close to the boundaries. All of these limitations make the introduction of constraints in the function to be minimised. Many predictive algorithms intrinsically take into account constraints (MPHC, DMC) and have therefore been very successful in the industry, while others can incorporate them a posteriori (GPC). Bounds in the amplitude and the slew rate of the control signal u and limits in the output y will be considered

$$u_{\min} \leq u(t) \leq u_{max} \quad \forall t \tag{2.3.16}$$

$$du_{\min} \leq u(t) - u(t-1) \leq du_{\max} \quad \forall t \tag{2.3.17}$$

$$y_{\min} \leq y(t) \leq y_{\max} \quad \forall t \tag{2.3.18}$$

By adding these constraints to the objective function, the minimisation be-

comes more complex, so that the solution cannot be obtained explicitly as in the unconstrained case.

Control Law In order to get values $u(t+k|t)$ it is necessary to minimise the functional J of Equation 5.2.6. The values of the predicted outputs $\hat{y}(t+k|t)$ are calculated as a function of past inputs and outputs and future control signals using the prediction model chosen and substituted in the objective function. An expression is obtained whose minimisation leads to the desired values. An analytical solution can be obtained for the quadratic criterion if the model is linear and there are no constraints. Otherwise, an iterative method of optimisation should be used. Whatever the method, obtaining the solution is not easy because there will be $N_2 - N_1 + 1$ independent variables, a value which can be high. To reduce this degree of freedom, a certain structure may be imposed by the control law.

Furthermore, it has been proved that this control law produces an improvement in robustness and the general behaviour of the system, basically due to the fact of allowing the free evolution of the MVs which may lead to unwanted high-frequency control signals and at the worst to instability.

This structure is sometimes imposed by the use of the control horizon concept (N_u) applied in DMC, GPC, EPSAC and EHAC that consists of considering that after a certain interval $N_u < N_2$ there is no variation in the proposed control signals, that is:

$$\triangle u(t+j-1) = 0 \quad j > N_u \tag{2.3.19}$$

which is equivalent to giving infinite weights to the changes in the control from a certain instant. The extreme case would be to consider N_u equal to 1 with which all future actions would be equal to $u(t)$. Another way of structuring the control law is by using base functions, a procedure used in PFC which consists of representing the control signal as a linear combination of certain predetermined base functions:

$$u\,(t+k) = \sum_{i=1}^{n} \mu_i\,(t)\,B_i\,(k) \tag{2.3.20}$$

The B_i are chosen according to the nature of the process and the reference. They are usually polynomial type $B_0 = 1 \;\; B_1 = k \;\; B_2 = k^2 \ldots$.

As has been indicated previously, an explicit solution does not exist in the presence of constraints, so that quadratic programming (QP) methods have to be used. Reference [38] presents the detailed algorithm to solve the QP problem. The equality constrained QP problem can be stated as

$$\text{minimise} \qquad \tfrac{1}{2}u^{\mathrm{T}}Hu + b^{\mathrm{T}}u + f_0 \tag{2.3.21}$$

$$\text{subject to :} \qquad Au = \mathrm{a} \tag{2.3.22}$$

where A is an $m \times n$ matrix and a is an m vector. It is assumed that $m < n$ and that $\mathrm{rank(A)} = \mathrm{m}$.

A direct way of solving the problem is to use the constraints to express m of n variables as a function of the remaining $n - m$ variables and then to substitute them in the objective function. The problem is reduced to minimising a quadratic function of $n - m$ variables without constraints.

Usually, a generalised elimination method is used instead of a direct elimination procedure. The idea is to express u as a function of a reduced set of $n-m$ variables: $u = Ya + Zv$, where Y and Z are $n \times m$ and $n \times (n - m)$ matrices such that $AY = I, \; AZ = 0$ and the matrix $[Y \; Z]$ has full rank. Notice that matrix Y can be interpreted as a generalised left inverse of A^T and that Zv is the null column space of A^T.

If this substitution is made, the equality constraints hold and the objective function

$$\begin{aligned} J(v) &= \frac{1}{2}[Ya + Zv]^{\mathrm{T}}H[Ya + Zv] + b^{\mathrm{T}}[Ya + Zv] + f_0 \\ &= \frac{1}{2}v^{\mathrm{T}}Z^{\mathrm{T}}HZv + \left[b^{\mathrm{T}} + a^{\mathrm{T}}Y^{\mathrm{T}}H\right]Zv + \left[\frac{1}{2}a^{\mathrm{T}}Y^{\mathrm{T}}H + b^{\mathrm{T}}\right]Ya + f_0 \end{aligned}$$

that is, an unconstrained QP problem of $n - m$ variables. If the matrix Z^THZ is positive definite, there is only one global optimum point that can be found solving the linear set of equations

$$Z^{\mathrm{T}}HZ = -Z^{\mathrm{T}}(b + HYa) \tag{2.3.23}$$

Notice that if u^k is a point satisfying the constraint $Au^k = a$, any other point u satisfying the constraints can be expressed as $u = u^k + Zv$. Thus the vector Ya can be made equal to any point satisfying the constraints. Vector v can be expressed as the solution of the following linear equation

$$Z^{\mathrm{T}} H Z v \;=\; -Z^{\mathrm{T}}\, \mathrm{g}\left(u^k\right) \tag{2.3.24}$$

where $g(u^k) = Hu^k + b$ is the gradient of $J(u)$ at u^k. A general way of obtaining appropriate Y and Z matrices is to choose a $(n - m) \times n$ matrix W such that the matrix $[A\ W]^T$ is non-singular. The inverse can then be expressed as:

$$\begin{bmatrix} A \\ W \end{bmatrix}^{-1} = [Y\ Z] \tag{2.3.25}$$

It then follows that $AY = I$ and $AZ = 0$.

If matrix W is chosen as $[0\ I]$, the method coincides with the direct elimination method. Another way of choosing W is related to the active set method that will be described later. The idea is to use inactive constraints (a_i) as the rows of W. If an inactive constraint present in W becomes active (the rows of R where $r_i u = c_i$), the corresponding row of W is transferred to A. When an active constraint becomes inactive, the corresponding row of A is transferred to W. By doing this, the inverse of the matrix need not be recomputed to calculate Y and Z.

Consider a feasible point u^0; that is, $Ru^0 \leq c$ and the set of active constraints (all the equality constraints and the rows of R where $r_i u = c_i$). Form matrix A and vector a by adding these rows (r_i) and corresponding limits (c_i) and the equality constraints.

The problem can now be solved with the method described previously. Suppose that u^1 is the solution to the equally constrained QP problem. If u^1 is feasible on the inactive constraints, a test for optimality has to be performed to check if the global optimum has been found. This can be accomplished by verifying that the Lagrange multipliers for all equality constraints $\lambda_i \geq 0$. If this is not the case, the constraint with the most negative Lagrange multiplier is dropped from the active constraint set, and the previous steps are repeated.

If point u^1 is not feasible on the inactive constraints, the nearest intersection from u^0 of the line joining points u^0 and u^1, and the inactive constraints is computed. The corresponding constraint is added to the active set, and the previous steps are repeated.

Parameter tuning A typical MPC law has many tunable parameters. A review of tuning guidelines for MPC from theoretical and practical perspectives was provided in Reference [63]. Off-line tuning methods are suggested in which each parameter are individually tuned as given below.

- Prediction horizon

  The prediction horizon, p, is the number of future control intervals the MPC controller must evaluate by prediction when optimising its MVs at current control interval k. Recommended practice is to choose p early in the controller design and then hold it constant while tuning other controller settings. The value of p should be such that the controller is internally stable and anticipates constraint violations early enough to allow corrective action. If the desired closed-loop response time is T and the control interval is T_s, try p such that $T \approx pT_s$.
- Control horizon

  The control horizon affects how aggressive or conservative the control action is. This leads to a trade-off: increasing the control horizon from 1 creates a more robust, but more aggressive controller with an increased computational load; however, keeping it at 1 increases the conservativeness and decreases the robustness of the controller but at a savings of computation.
- Weights on the outputs

  Weights on the output are used to scale the control variables and direct more control efforts toward more significant controlled outputs to achieve tighter control of these controlled outputs.
- Weights on the rate of change of inputs

  Penalising the rate of change yields a more robust controller, but the cost of the controller is more sluggish. Setting a small penalty or none whatsoever

gives a more aggressive controller that is less robust.

- Weights on the magnitude of the inputs

  This parameter penalises access controller action. It is a way to remove a constraint from the optimisation problem and thus make it more computationally attractive. This appropriate penalty allows one to remove the constraints on the minimum and maximum sizes of the inputs.

- Constraint parameters

  Typically, the objective to tune the constraints involves knowing the window when the constraints are active or inactive to make the optimisation problem feasible.

2.4 Applications of model predictive control in HVAC systems

In the industrial applications, most of the controllers commissioned in HVAC systems are of the PID type [64]. This is because its relatively simple structure makes it easy to be understood and applied in practice. It is more acceptable in the first position of view when designing an HVAC control system unless there is evidence showing it cannot satisfy the conditions or more advanced functions are required. However, the tuning of the PID controller can be a time-consuming, expensive and challenging task, and the re-tuning of the controller is sometimes needed because of the change in operating and environmental conditions [65]. A workable PID controller may take several days for tuning which increases the cost and time of projects [26]. The PID controllers are used in the HVAC system for the dynamic control of cooling coil units [66], supply AP control [67] [68], supply air temperature control [69] and room temperature control [70].

The need for high-quality products, reduced energy consumption, increasing market competition and lower cost, makes the necessity to apply the advanced control method with improved control performance [71]. In recent years, there have been suggestions that MPC may offer benefits when applied to the HVAC system. The MPC uses a system model to predict the future states of the system and gen-

erates a control vector that minimises a certain cost function over the prediction horizon in the presence of disturbances and constraints [72]. The using of MPC is particularly attractive to staff with a limited knowledge of control because the concepts are very intuitive, and the tuning is relatively easy [38]. A significant advantage of MPC is that it can apply to a wide range of processes such as delayed, none minimum phase and unstable systems [73]. By replacing PID controllers with MPC controllers in the HVAC system, there is no need for the adjustment of coefficients since the MPC controllers are tunable online without tuning the coefficients before testing the controllers [74]. A significant amount of literature has been published on applications of MPC to HVAC systems. Reference [74] proposes the idea of using MPC to control the speed of air supply fan. The zone temperature and damper position in a simulated VAV system were controlled using MPC in Reference [75].

There are thousands of applications of MPC in many industries. The majority of applications (see surveys by Qin and Badgwell [76] [77]) are in the area of refining, one of the original application fields of MPC, where it has a solid background. A substantial number of applications can be found in petrochemicals and chemicals. Significant growth areas include pulp and paper, food processing, aerospace, and automotive industries. Other areas such as gas, utility, furnaces, or mining and metallurgy also appear in the report. Some applications in the cement industry or pulp factories can be found in Reference [78]. Although the MPC technology has not yet penetrated deeply into areas where process nonlinearities are strong and frequent changes in operation conditions occur, the number of nonlinear MPC applications is clearly increasing.

A significant number of applications involving mechanical and electronic system are now being reported in Reference [79]. This is made possible by the implementation of MPC at sample rates that are orders-of-magnitude faster than in traditional process applications. The applications include vehicle traction control, direct injection stratified charge engines, ducted fan in a thrust-vectored flight control experiment, automotive powertrains, magnetically actuated mass spring damper system, power converters, multi-core thermal management, and so on.

A large amount of literature has been published on applications of MPC in

HVAC systems [72] [80]. A robust MPC strategy was presented in Reference [75], to improve the supply air temperature control of AHUs. The associated uncertainties and constraints were taken into account directly. The performance of the MPC controller was compared with that of the PI controller, controlling the supply airflow rate. The MPC controller displayed better transient response, which includes the compare of rise time, settling time and percentage overshoot, and was more robust in the presence of air duct pressure disturbances. Two types of set-points were regulated: at a low set-point, the PI controller responded sluggishly which needed additional time to reach the set-point; at a high set-point, the PI controller produced excessive overshoots which made the response too aggressive. By contrast, the MPC controller produced consistent responses and achieved faster settling time and lower overshoot in both cases. Two typical inlet conditions were used for the performance test of the supply air temperature control: hot summer condition with $26°C$ air temperature, and cool winter condition with $17°C$ air temperature. In both conditions, the conventional PI and the MPC controllers tracked the set-point well. In the hot summer condition, the PI controller took less time to reach the set-point but exhibited much more fluctuation than the MPC controller. In the cool winter condition, the PI controller took much more time to reach the set-point which suggests re-tuning the parameters, and the MPC controller spent less response time and had a much better control performance.

Reference [81] presented the simulations of thermal regulation in buildings using a distributed MPC algorithm which took the advantages of decentralised control and centralised control. The MPC strategy was first presented for a single zone building then extended to a multi-zone building. Both centralised and distributed MPC regulated the zone temperature well at the set-point coupling the effects between adjacent zones. For the purpose of comparison, the conventional controllers (On/Off and PI controller) were tested acting as decentralised controllers. Each of them controls the zone temperature individually in a multi-zone building without any knowledge of the others' behaviour. The decentralised MPC scheme improves the performance slightly while the thermal coupling is not included. However, the centralised and distributed MPC controllers accounted for the coupling effects of the adjacent zones

by making predictions for the coupling effects and communicating the control decisions to the neighbouring controllers. Compared with the conventional controllers, decentralised MPC could reduce the energy consumption by about 5.5%, and the centralised and distributed MPC strategies were able to achieve a 36.7% increase in thermal comfort and the meantime reduce the energy consumption with 13.4%.

Reference [82] adopts an MPC-based multi-input multi-output (MIMO) controller to implement temperature and ventilation control of a virtual building composed of six zones and an all-air VAV system. The virtual building simulated an educational building on a campus with daily occupancy and internal heat gain profiles. Four typical weather conditions were applied to compare the performance of conventional PI control and MPC whose weather data was randomly chosen between June and August of 1988-1990 from SAMSON. The multi-zone MPC used a MIMO linear model for predicting the temperature of the zones and solved a constrained convex quadratic optimisation problem to find the control actions guaranteeing enough airflow for every zone. All the simulation showed that the multi-zone MPC met the ventilation requirements set by ASHRAE Standard 62.1 and outperformed the PI control.

To keep the indoor temperature within a defined comfort interval, the forthcoming supply fluid temperature for a water-based floor heating system in residential buildings was computed using both a detailed numerical Simulink model and a simplified 2-node lumped model in Reference [83]. The MPC method was applied to determine the optimal supply water temperature using weather prediction and accounting for the dead time of the building. The accuracy of the results obtained from the simplified model is better in comparison to the Simulink model. The exact solution method based on the numerical Simulink model was unable to maintain the room temperature at the at all times because it did not use weather forecasting. Hence, the explicit solution based on the simplified model can be utilised to evaluate simple control methods for low energy buildings.

In Reference [84], MPC was used for zone temperature control to reduce energy and demand costs for building HVAC systems. A simulated multi-zone commercial building equipped with a VAV cooling system was built in Energyplus with real-time

data exchange between Energyplus and a Matlab controller. The min-max optimisation problem with an economic objective was transferred into a linear program and solved at each time step which minimised the costs on a daily basis. By employing the MPC technique, the pre-cooling effect was automatically triggered, and the peak demand was shifted away from on-peak hours. Compared with the baseline night setup strategy (0%), MPC yielded higher savings (28%) than did the linear-up (17%) and step-up (24%) strategies.

To meet the separate temperature requirements of two cooling zones, MPC was used to control the water flow valve (WFV) in Reference [85]. A novel control architecture was presented with a flexible two-level structure. The MPC method was used at both levels to control the temperatures of two different cooling zones while maximising the energy efficiency. The pressure and cooling values for the evaporators were calculated to minimise a quadratic cost function by controlling the electronic expansion valve (EEV) and compressor speed. Local level PI controllers were also implemented for comparison. The results showed that the MPC outperformed the PI controllers with improved regulation of superheat temperature and evaporator pressure. The coefficient of performance (COP) of the system was improved by 9.5% if adding supervisory MPC to the system resulting in higher energy efficiency.

Reference [86] presented an MPC based on Takagi-Sugeno fuzzy model to control the dry bulb temperature of the off-coil air from the AHU in HVAC systems. To compensate uncertainties of the model, the feedback regulation was developed. In the simulation test, the proposed MPC had better tracking effect and robustness than PID control with less overshoot and shorter setting time. The MPC controller also showed improved performance from the test results in a lab-scale HVAC system.

Both numerical simulation and experimental tests were proposed in Reference [87] to control the supply air temperature of a test room using prescribed error dynamics and MPC techniques with feedback linearisation. A simplified model was derived from thermodynamic equations. The comparison results demonstrated that the MPC controller performed better than the other with better trajectory tracking. The plant dead time and future values of the reference signal can be taken into ac-

count in the MPC controllers.

For zone temperature control in a large university building, the performance of the MPC was compared with that of a finely tuned weather compensated controller that also used weather forecasting in Reference [88] and the heating curve method in Reference [89]. The MPC used 29% less energy while maintaining the same thermal comfort level in both applications.

The zone temperature and humidity of a thermal chamber in a university lab were controlled with an MPC and a neural-fuzzy controller in Reference [90]. Compared with the neural-fuzzy controller, the MPC demonstrated superior performance: it improved the settling time by 25% and the steady-state error for temperature and humidity by 100% and 400%, respectively.

A comparison of on/off control with learning-based MPC (LBMPC) was carried out in Reference [91] using a single heat pump air-conditioning (AC) system installed in a university lab. LBMPC reduced the energy consumption by 30-70% compared with the on/off control. The energy savings were reduced as the occupancy and temperature of outside air increased, resulting in a higher thermal load on the AC.

Summarised from the above applications, most researchers focus on maintaining the thermal comfort in the HVAC system by controlling the temperature and humidity. The test beds the above applications used are mostly residential buildings, normal university buildings or just simulated buildings. This thesis concentrates not only on the simulated plant but also a constructed cleanroom laboratory which simulates a pharmaceutical factory. The novelty of this thesis is that the HVAC control system focus on the ventilation system inside the cleanroom to maintain the ACR, AP and the desired particulate levels. The particulate control with MPC is a new direction to control the air cleanliness.

The challenges of the MPC design include the communication between controllers and facilities, the definition and identification of the accurate model, the large computational load the MPC algorithm needs and so on. The controllers are designed in Matlab at first. The communication between Matlab and the facilities should be implemented through the OPC server. An OPC Toolbox is installed in

Matlab to achieve that. To identify accurate system models, several model structures and several parameter estimation methods are studied. The best system models are found by model validation approach. The MPC algorithm needs a large computation at each time step. A more powerful computer is introduced to run the programs. The HVAC process is slow enough to run complex MPC controllers on this computer. For a cleanroom HVAC system, the heat transfer and the ventilation process inside the cleanroom are time-consuming. The response time ranges from minutes to days. Thus, the sample time of the MPC controller should be designed with a large value to ensure the stability of the system.

Chapter 3

Configuration and setup of the cleanroom laboratory

This chapter will present the configuration and setup of the cleanroom HVAC laboratory built by a company called Energy Efficiency Consultancy Ltd (EECO2) located in Macclesfield, UK. The laboratory aims to simulate the operation of the cleanroom HVAC system used in a pharmaceutical factory. The traditional PI controllers have been implemented in the BMS to monitor and control the IAQ inside the cleanroom laboratory. Then, the working principles of the main hardware and software installed in the HVAC system will be introduced. At last, the energy consumption of the hardware will be analysed to figure out how to compare the consumed energy between different control methods.

3.1 Schematic of the cleanroom laboratory

Figure 3.1 [96] shows the schematic of the cleanroom laboratory whose hardware is controlled by PI controllers implemented in the BMS. The cleanroom laboratory consists of four rooms (in red line) and some HVAC facilities. The zone in red lines represents the clean zone of a pharmaceutical factory where the medicines are produced and packed. It is sealed by glass and rubber which makes the laboratory isolated from the outdoor air. Four rooms are classified and separated depending

on functions and air cleanliness levels: the entrance room, the change room, the small lab and the large lab. Some sensors are installed inside the laboratory to measure and collect the operational variable data required for monitoring, modelling and controlling the cleanroom HVAC system.

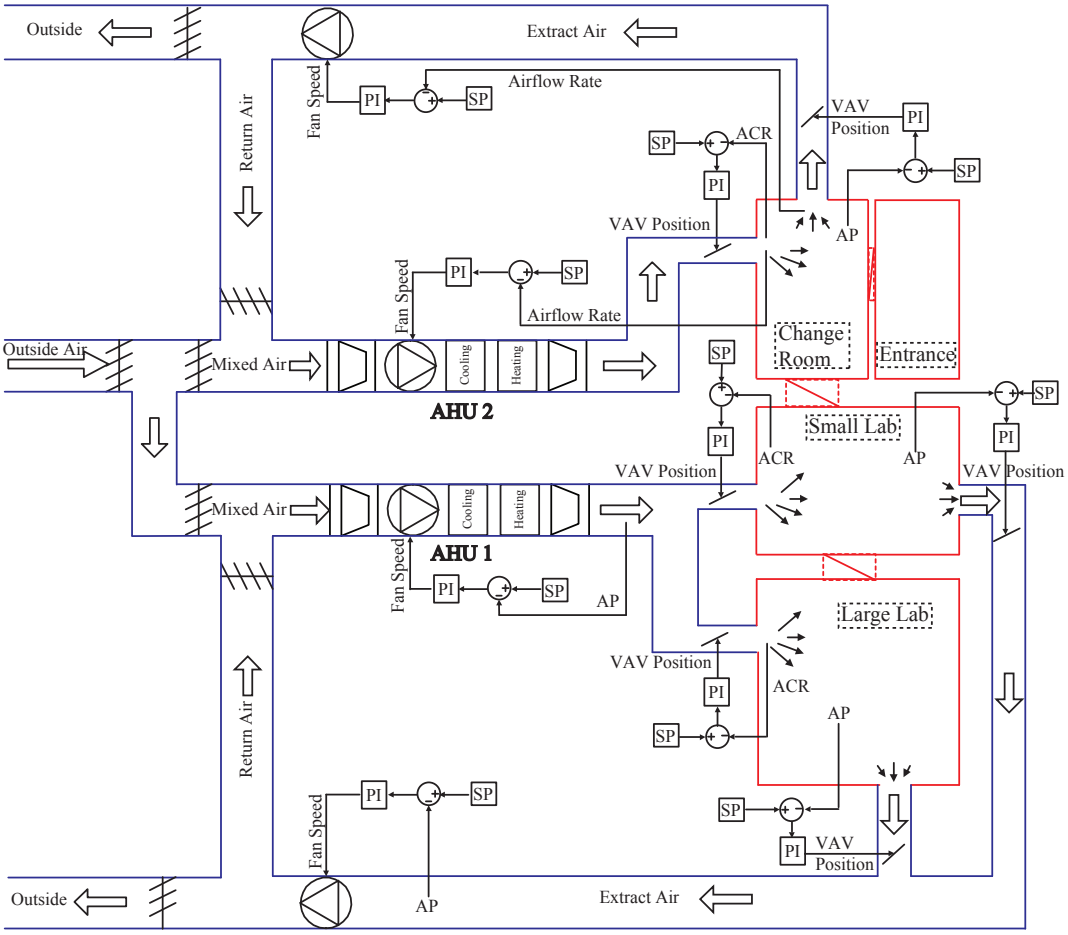

Figure 3.1: Schematic of the cleanroom laboratory with HVAC control system [96].

Figure 1.1 shows a diagram of a basic HVAC system and its basic operation is presented in Section 1.1. In addition to the basic schematic, Figure 3.1 shows the schematic of the cleanroom laboratory whose hardware is controlled by PI controllers implemented in the BMS. Each PI controller is designed to control a fatality within the HVAC system including the supply fans inside the AHUs, the extract fans and the supply and extract VAVs. The original design of the HVAC system requires the PI controllers to maintain the steady state of the supply airflow rate and

air pressure of each cleanrooms.

3.2 HVAC hardware

The laboratory has two separate AHUs which allow a wide variety of performance testing options. The testing experiments are taken in the cleanroom laboratory via the HVAC system. The HVAC system cleans and circulates the air from outdoors to the cleanrooms, the functionality of which is achieved by the operation of the hardware including AHUs, VAVs, Extract fans, sensors, grilles and diffusers.

3.2.1 Air handling unit

An AHU is a central air conditioner station that handles the air supplied into the buildings by the ventilation ductwork with thermal, hygrometric and IAQ treatment. The accuracy of the treatment will depend on the specificity of each project. The AHU treats the air by filtering, cooling or heating, humidifying or dehumidifying. The AHU is typically constructed around a framing system with metal infill panels as required to suit the configuration of the components.

The AHU consists of several components depending on the complexity and requirements of each specific building and application. In this laboratory, two AHUs have been constructed with the same type and the same number of components. The AHU1 supplies air to the small lab and the large lab, and the AHU2 supplies air to the change room.

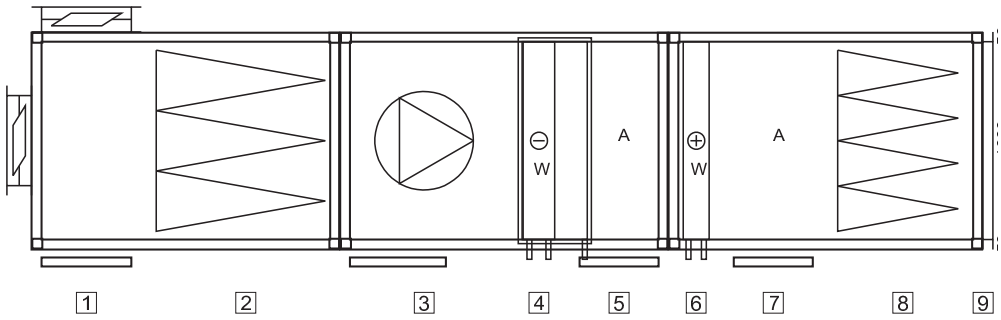

Figure 3.2: Schematic of the AHU [92].

The structure of an AHU is decided based on the requirement of the condition of the air supplied into cleanrooms. In this project, the supply air needs to be cleaned with required air velocity, so that the filter and fan are needed. The heating and cooling coils are added because they are useful to keep the thermal comfort and will be requested for the further design.

The components described from the return duct (input to the AHU), through the unit, to the supply duct (AHU output), are presented in Figure 3.2 [92] with the number from 1 to 9 as introduced below:

- 1 Mixing box

  The AHU allows the introduction of outside air into cleanrooms and the exhausting of air from cleanrooms. To approach the desired supply air temperature, the right amount of cooler outside air is mixed in the mixing box with warmer return air. A mixing box is therefore used which has dampers controlling the ratio of the return, outside, and exhaust air.
- 2 and 8 Bag filter

  Air filtration is applied to provide clean air to the building occupants. A bag filter is an air pollution control device that removes particles out of the air to control the emission of air pollutants into buildings. Most bag filters use long, cylindrical bags, made of woven or felted fabric, as a filter medium. The life of the filter is assessed by monitoring the pressure drop through the filter medium at a designed airflow rate. This is done using a visual display using a pressure gauge.
- 3 Plenum fan

  The AHU employs a plenum fan, which is shown in Figure 3.3(a) [95], driven by an AC induction electric motor to move the air. The fan is driven by a variable frequency drive to allow a wide range of airflow rates. All fans and motors are located on a rigid steel frame to form an assembly. All assemblies are isolated from the main AHU chassis via anti-vibration mountings. On direct drive fan assemblies, the motor must be run at the fan speed shown on the technical specification to achieve the correct duty point. This is obtained by modulating the frequency (Hz) of the inverter as shown in Figure 3.3(b)

[94]. The motor will be selected to run at a frequency other than 50 Hz. Failure to set this correctly will result in the unit operating either over volume and possible damage to components or under volume.

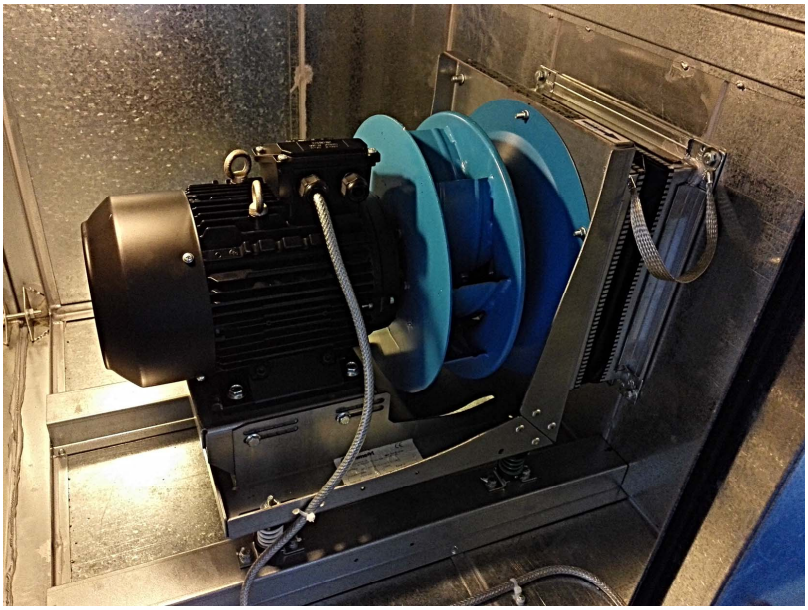

(a) Plenum fan in the AHU

(b) Controlling inverter of the fan

Figure 3.3: The plenum fan [95] in the AHU and the inverter [94].

The ideal power consumption for a fan (without losses) can be expressed as

$$P_i = QH \tag{3.2.1}$$

where P_i is the ideal power consumption, Q is the volumetric flow rate, and H is the static pressure developed by the fan.

By using manufacturers' specifications for actual fans, the fan efficiency is given to represent the performance of the fan. The fan efficiency is the ratio between power delivered to the air and the power supplied to the shaft of the fan. The fan efficiency is independent of the air density and can be expressed as:

$$\eta_f = \frac{QH}{P} \tag{3.2.2}$$

where η_f is the fan efficiency, Q is the volumetric flow rate, H is the static pressure developed by the fan, and P is the power used by the fan.

Then, the shaft power used by the fan can be expressed as:

$$P = \frac{QH}{\eta_f} \tag{3.2.3}$$

Figures 3.4 [95] and 3.5 [95] present the fan curves of the AHU1 supply fan and AHU2 supply fan produced by COMEFRI [95], respectively. The figures show the relationship among static pressure ($\triangle pstat$), volumetric flow rate (V), rotational speed (RPM), fan efficiency (the percentage values), shaft power (values in kW) and sound power level (values in dB). The intersection points of area 1 and area 2 in these figures give the maximum fan efficiency. The fan efficiency decays from this point along area 1 or area 2. On the bottom, a scale on the performance, K_η, is given for a serious of RPM. The fan efficiency read in the figure with percentage values can be corrected using K_η that

$$\eta_t = \eta_f \times K_\eta \tag{3.2.4}$$

where η_t is the corrected total efficiency, η_f is the fan efficiency read from the curve, and K_η is the performance scale.

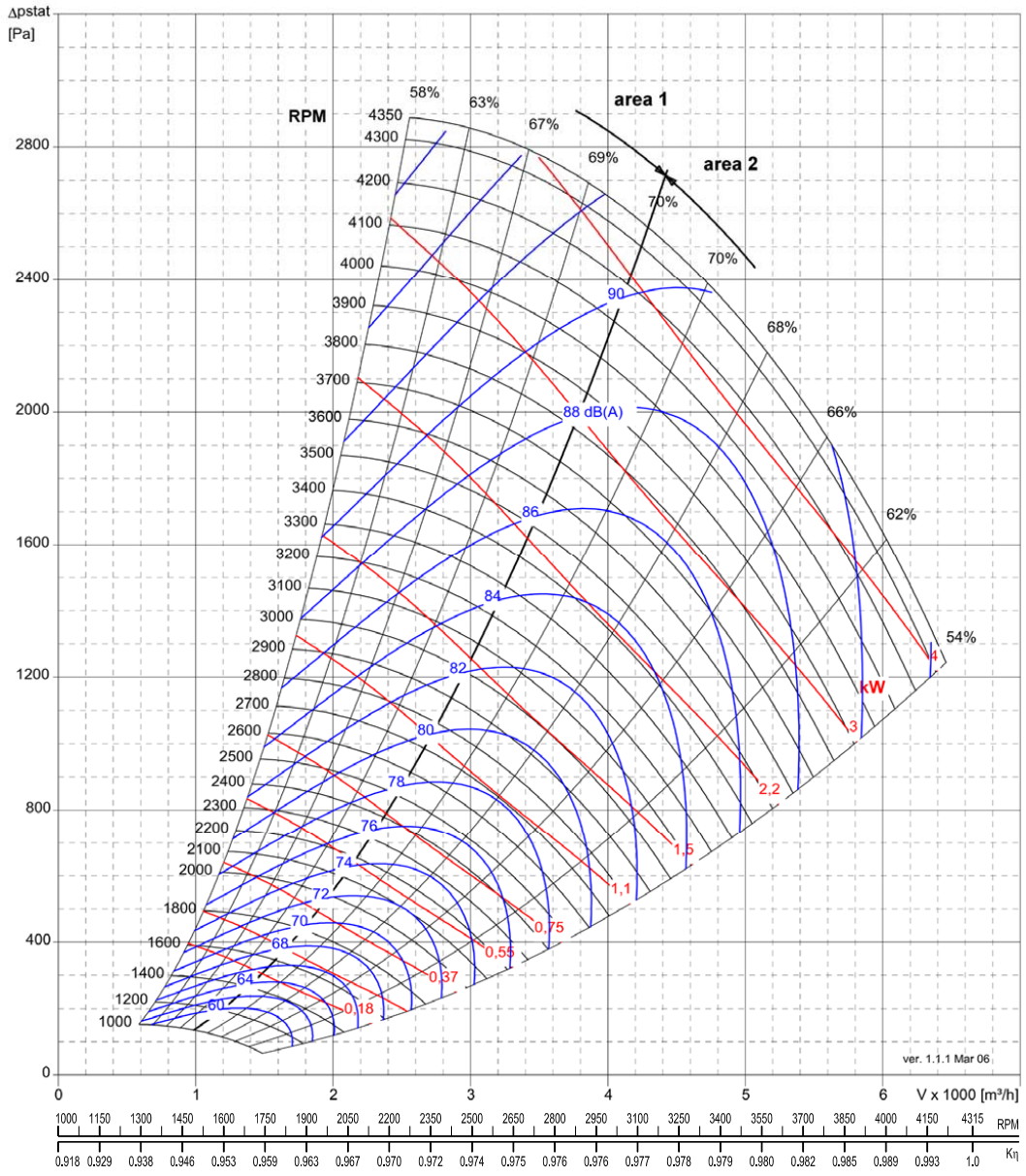

Figure 3.4: The fan curve of the AHU1 supply fan [95].

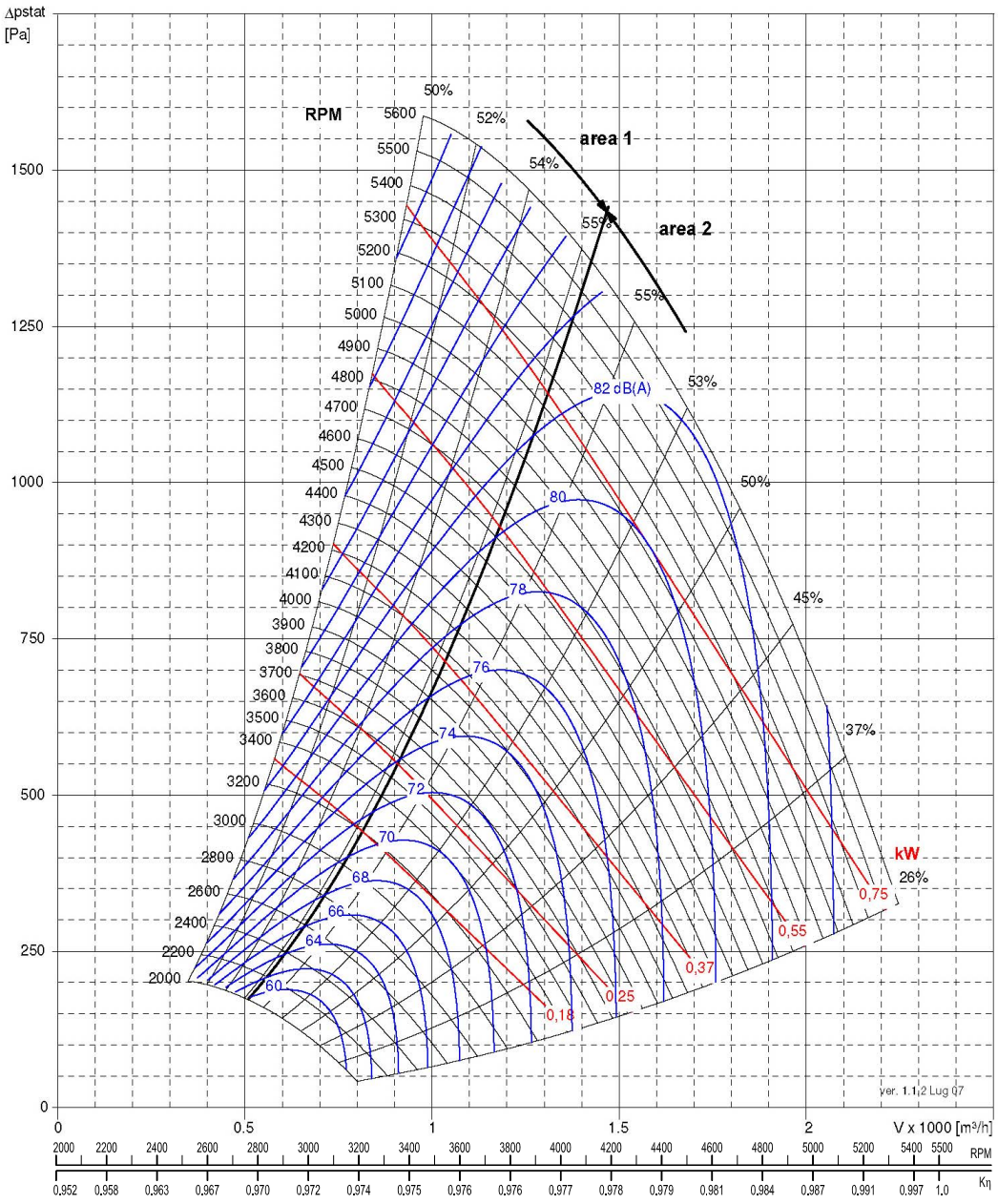

Figure 3.5: The fan curve of the AHU2 supply fan [95].

- 4 and 6 Water cooling and heating coil

  The AHU provides heating, cooling, or both to change the supply air temperature. Such conditioning is provided by heat exchanger coils within the AHU air stream, and such coils may be direct or indirect about the medium provid-

ing the heating or cooling effect [93]. The coils use hot water for heating and chilled water for cooling. Coils are manufactured by copper for the tubes to aid heat transfer. The hot water is provided by a central boiler, and the chilled water is provided by a central chiller. The coils are usually of open header box construction and completely self-supporting. They are designed to slide into the AHU and are retained without any internal fixing.

- 5 and 7 Access
  Access doors are installed for maintenance.
- 9 Outlet
  The outlet is connected with the ductwork to let the clean and conditioned air flow into cleanrooms.

In the AHU, the air will enter the mixing box, be cleaned by the first filter, be accelerated by the supply fan, be cooled or warmed by the coils, be cleaned by the second filter and flow into cleanrooms. The constructed AHUs are shown in Figure 3.6 [96].

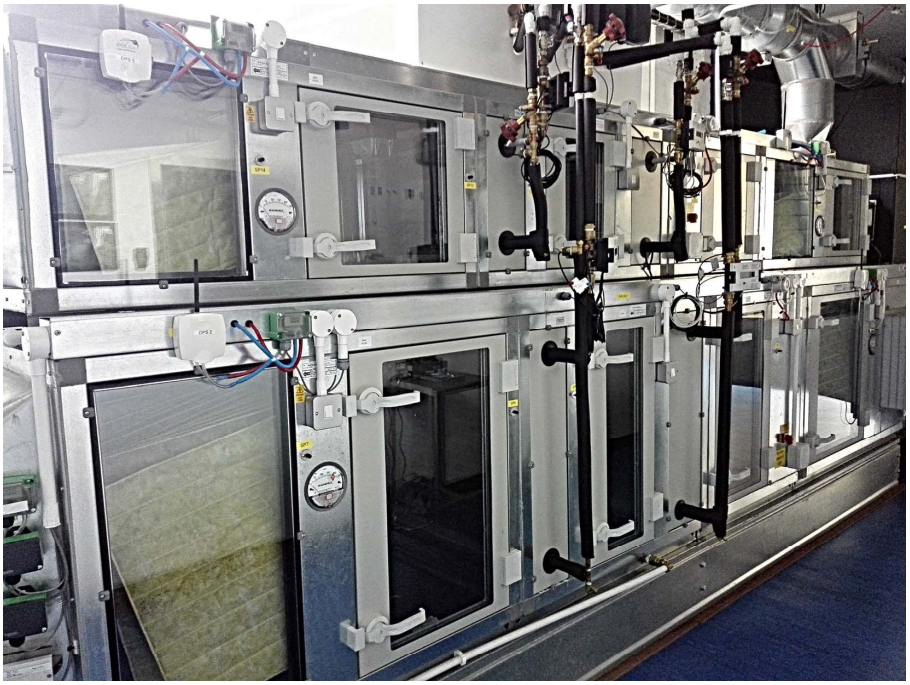

Figure 3.6: The constructed AHUs [96].

3.2.2 Variable air volume

A VAV varies the volume flow rate of the supply air to maintain the room air temperature and pressure at the set-point [97]. A VAV box is a calibrated air damper with an automatic actuator. The air volume flows through the VAV box relate to the position of the damper installed inside it. In this thesis, the VAV system is responsible for maintaining the static airflow rate and AP. Six VAVs have been installed in the HVAC system, three of them control the air supplied into the rooms, and the other three control the air extracted from rooms.

Figure 3.7 [98] shows a VAV box produced by CMR where the actuator is installed on the top. The actuator has a digital motor control which can be commissioned with a PC. The actuator has been built in overload control, and the motor is capable driving against a block without end switches. The rotation angle $(0 \ldots 90°)$ can be adjusted via mechanical end stops for opening and closing. Feedback from the actuator can be adapted to be $0 \ldots 10V$. The rotation direction is adjustable via a dip switch under the motor cover. The VAV is driven by a 24 V 50 Hz AC voltage, and the power consumption is 12 W [98].

Figure 3.7: The VAV box [98].

The VAV installed in the laboratory is embedded with a pressure-based VAV

airflow sensor which infers the airflow velocity pressure and converts it to a VAV airflow rate. The VAV airflow rate is calculated from the measured VAV differential pressure using the following equation [101]:

$$Q_{VAV} = K\sqrt{\triangle P_{VAV}} \tag{3.2.5}$$

where, Q_{VAV} is the VAV volumetric airflow (l/s), $\triangle P_{VAV}$ is the VAV differential pressure (Pa), and K is the conversion factor provided by the VAV manufacturer.

3.2.3 Extract fan

The extract fan accelerates the air extracted from cleanrooms. As shown in Figure 3.1, two extract fans are installed near two AHUs. The extract fan near AHU1 is called AHU1 extract fan, and the one near AHU2 is named AHU2 extract fan. The extract fans produced by SYSTEMAIR, which are shown in Figure 3.8 [99] [100], are installed in the ducts beside the outlet of air into the outside. The extract fans can affect the air circulation in the HVAC system.

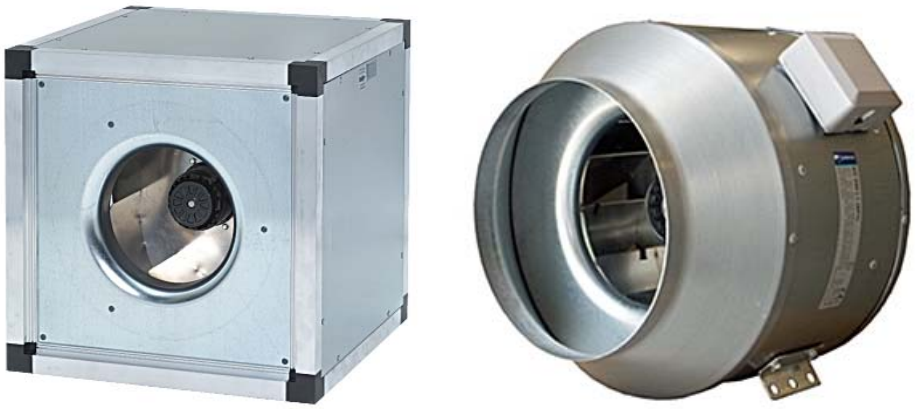

(a) AHU1 extract fan (b) AHU2 extract fan

Figure 3.8: The extract fans installed in the HVAC system [99] [100].

Figures 3.9 and 3.10 present the fan curves of the AHU1 extract fan and AHU2 extract fan respectively produced by SYSTEMAIR [99] [100]. The figures show the relationship among static pressure (Ps), volumetric flow rate (Q) and power (P).

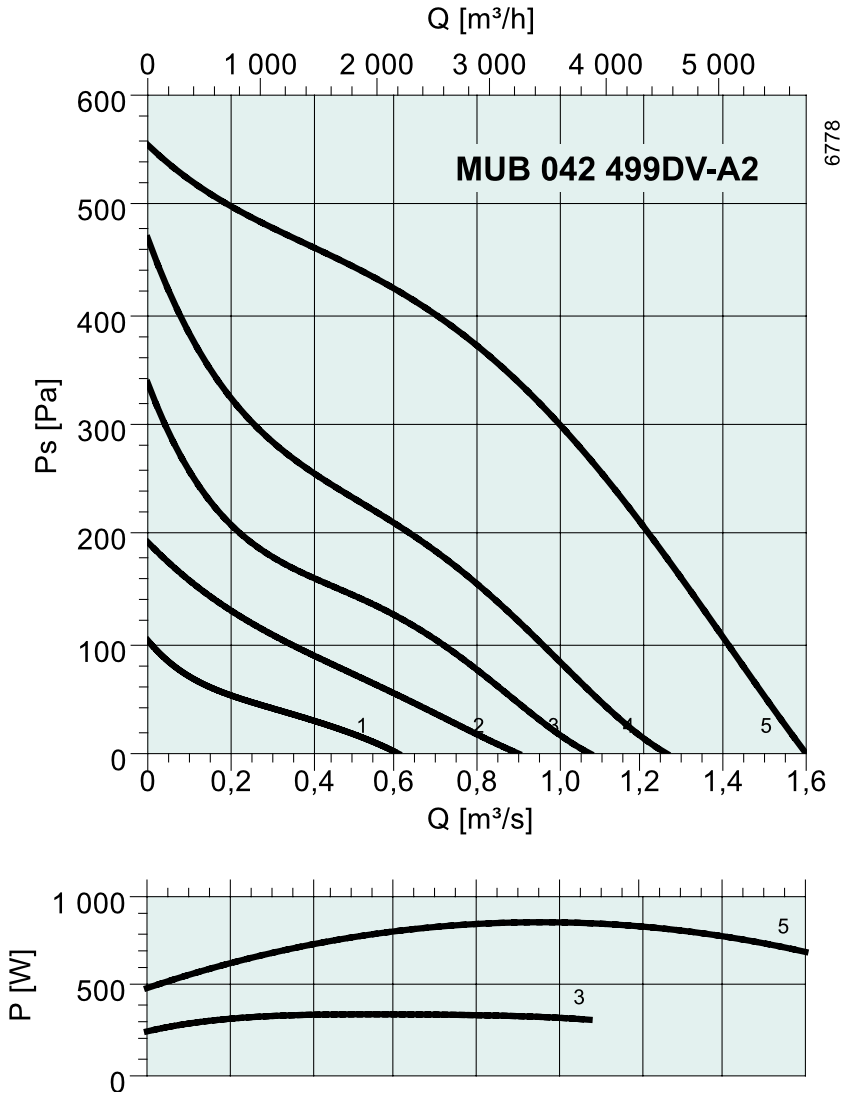

Figure 3.9: The fan curve of the AHU1 extract fan [99].

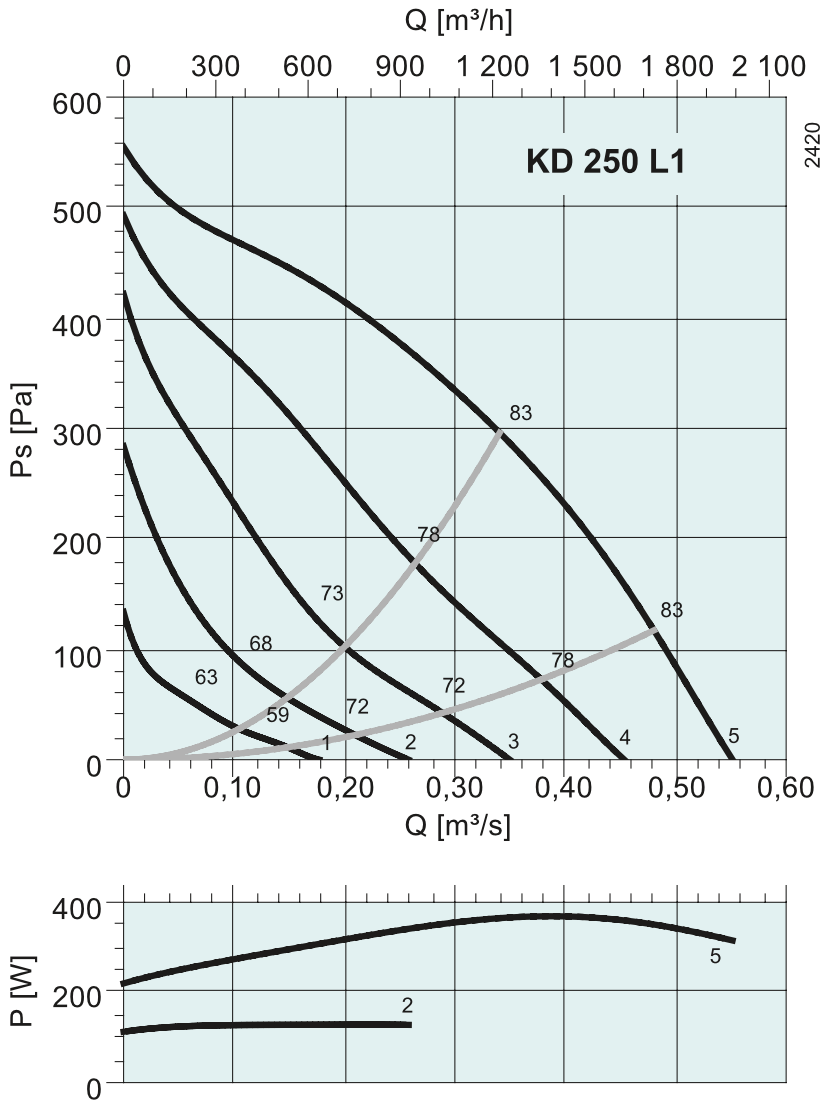

Figure 3.10: The fan curve of the AHU2 extract fan [100].

3.2.4 Others

Since the project focuses on the sensor-based controller designed in the cleanroom HVAC system, several types of sensors have been installed:

- Static pressure, measured at the outlet of AHUs and in cleanrooms.
- Differential pressure, measured at some testing points in the ducts, at VAVs and the outlet of AHUs.

- Temperature and humidity, measured at the cooling and heating coils, the inlet of fresh air, the outlet from extract fans and in cleanrooms.
- Particle counter measured in cleanrooms and ducts.

A grille is a device to supply or extract air vertically without any deflection. A diffuser normally has profiled blades to direct the air at an angle as it leaves the unit into the space. Diffusers are part of room air distribution systems in HVAC systems serving several purposes:

- To deliver both conditioning and ventilating air
- Evenly distribute the flow of air, in the desired directions
- To enhance mixing of room air into the primary air being discharged
- To create low-velocity air movement in the occupied portion of room
- Accomplish the above while producing the minimum amount of noise

3.3 HVAC software

Figure 3.11 presents the data communication between the HVAC hardware and the software in the cleanroom laboratory. The hardware contains sensors and drivers: the sensors are used to measure the system output (y: airflow rate and AP), and the drivers receive the controller output data (u) from PI controllers implemented in the BMS to operate the HVAC facilities (supply fans, extract fans and VAVs). The software is the BMS installed in a computer as the workstation. The BMS is provided by Trend which monitors and controls the HVAC hardware to maintain steady airflow rate and AP of the cleanroom laboratory. The data communication between the sensors and drivers and the BMS is achieved by Modbus, which is a serial communication protocol enabling communication among devices within the same network.

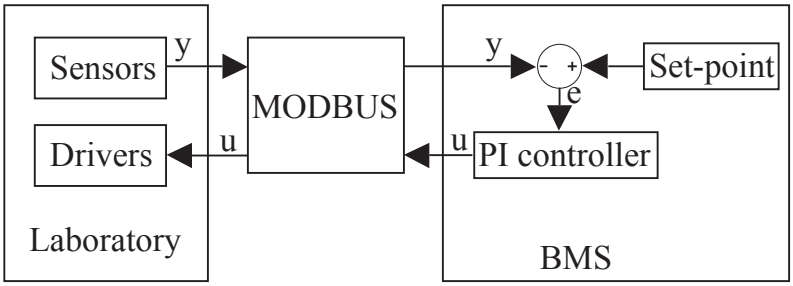

Figure 3.11: Data communication between the hardware and the software in the laboratory.

3.4 Energy consumption analysis

Due to the progress of this project, the data of voltage and current cannot be collected when the MPC controllers were tested. So that the energy consumption of the fans with different controllers has to be compared using the fan law.

The affinity laws for fans are used in HVAC systems to express the relationship among variables involved in fan performance (such as head, volumetric flow rate, shaft speed) and power. The fan affinity laws offer a quick way to evaluate fan performance when wheel speed or diameter is changed. In this thesis, the diameter (D) of the fan's impeller is kept constant after the construction of the whole system. Thus the simplified version of the fan affinity laws with the impeller diameter (D) held constant are as follows [102]:

- Fan law 1: The change in flow rate (Q_2 to Q_1) is directly proportional to changes in speed (N_2 to N_1).

$$Q_1 = \frac{N_1}{N_2} \times Q_2 \tag{3.4.1}$$

- Fan law 2: Static pressure (H_2 to H_1) is proportional to the square of the change in speed (N_2 to N_1).

$$H_1 = (\frac{N_1}{N_2})^2 \times H_2 \tag{3.4.2}$$

- Fan law 3: Fan brake horsepower (P_2 to P_1) changes are proportional to the cube of changes in speed (N_2 to N_1).

$$P_1 = (\frac{N_1}{N_2})^3 \times P_2 \tag{3.4.3}$$

where

- Q_i $(i = 1, 2)$ is the volumetric flow rate (e.g. cubic foot per minute (CFM) or litre per second (l/s)),
- N_i $(i = 1, 2)$ is the shaft rotational speed (e.g. revolutions per minute (rpm) or Hertz),
- H_i $(i = 1, 2)$ is the static pressure developed by the fan (e.g. psi or Pascal),
- P_i $(i = 1, 2)$ is the shaft power (e.g. W).

These laws assume that the fan efficiency (η) and gas density (ρ) at inlet conditions remain constant. The P given above is the instantaneous power of the fan. Thus the energy (E) during a time interval 0-t can be calculated as:

$$E(t) = \int_0^t P(t)dt \tag{3.4.4}$$

Since the ventilation system is the main concentration of this thesis, the heating part is not taken into account, such as boilers and chillers. Then the total energy consumption of this HVAC system contains the hardware:

- Fans

  To compare the energy consumption of each fan operated by different controllers, the energy E should be compared. From (3.4.3), the compare of the cube of the rotational speed can reflect the compare of the power. Thus, the compare of the integral of the rotational speed's cube can reflect the energy consumption of fans.
- VAVs, dampers, sensors, etc.

  They are driven by a $24V$ voltage. They are running in a nominal power which is constant whatever the signal voltage is and whatever the controller is. The energy consumption of these hardware remains the same between different control methods. So, when comparing the energy consumption with different controllers, the energy consumption of this hardware is not taken into account.

3.5 Conclusion

In this chapter, the cleanroom laboratory has been introduced in detail with the configuration of the laboratory, the HVAC hardware and software, and the analysis of the energy consumption. The HVAC hardware provides the foundation to implement the operation of the HVAC system to achieve the thermal comfort and IAQ. The data related to the hardware can be collected through the BMS which is the HVAC software that runs PI controllers to achieve a steady state in the airflow rate and the AP inside the cleanroom laboratory.

Since the combination of the hardware provides a platform which is capable of implementing a variety of control algorithm, the laboratory can be operated by other control methods, such as MPC. The software based BMS communicates with the hardware, collecting the data from sensors and drivers. These data will be useful for further chapters as the black-box models of the laboratory can be identified based on (in Chapter 4). Then the MPC controllers will be designed based the identified models as presented in Chapter 5.

Chapter 4

Black-box model identification of the cleanroom laboratory

The performance of MPC is highly sensitive to model mismatch. To reduce the influence of model mismatch, it is necessary to figure out the system models as accurate as possible. This chapter investigates a black-box approach based modelling of the cleanroom laboratory installed with an HVAC system, based on measurements from sensors installed in the laboratory. The cleanroom HVAC laboratory is modelled with several SISO models based on individual devices such as supply fans in AHUs, extract fans and VAVs. The system models are identified using the black-box modelling approach while the model structure is ARX and the model parameters are estimated using PEM. The system model is also identified as two MIMO models that the ACR and the AP of each cleanroom are modelled as the system outputs. The ARX model has been identified via three different parameter estimation methods: PEM, least squares (LS) method and instrumental variable (IV) method. The one with the best performance, the PEM has been obtained and then applied to the other two model structures, SS model and TF model, for comparison. The performance of the identified system models is verified based on the cleanroom laboratory, and it is found that the ARX model performs the best.

4.1 Introduction

Closed-loop controllers can be implemented for cleanrooms to reduce their power consumption [104]. As the performance of the controllers depends on the accuracy of the cleanroom models, the development of an accurate model is necessary and useful for either tuning controllers' parameter (such as PID control) or developing model-based controllers, such as MPC. Three types of models have been used for the modelling of the cleanroom HVAC system [12]: white-box model (also known as physical based, analytical and forward model) [105] [106], black-box model (also known as data-driven and inverse model) [107] [108] [109] [110] and grey-box model [111] [112]. White-box models are developed depending on the knowledge of underlying process and physical principles [109]. Black-box models are identified based on the measured input and output data. When building a grey-box model, a white-box model is designed first, but the parameters of the model are estimated by the black-box approach.

The HVAC systems are designed for two purposes: thermal comfort for representing the satisfaction with the thermal environment, and acceptable IAQ for presenting a required low levels of contaminants. Modelling of buildings installed with HVAC systems with thermal comfort has been well studied. In Reference [108], a building model, which focus on the temperature inside the building, is identified by autoregressive moving average with exogenous terms (ARMAX) model identification and subspace identification methods respectively, and the performance of the two methods are compared. Reference [109] describes a comparison result among several identification methods which are used to identify the model of several HVAC subsystems installed in a residential building. The temperatures of air and water are defined as the model outputs. In Reference [110], an energy resource station is designed to achieve the thermal comfort by applying the identified models using the neural network approach. However, the research related to the IAQ mainly focuses on the hardware implementation and experimental test, such as a experimental study describing the influences of ACR and free area ratio of raised-floor on cleanroom particle concentrations in Reference [113], test results for air quality control from an in-vitro fertilisation facility constructed according to cleanroom standards for air

particulate matter and volatile organic compounds [114], and a set of measurements in class 1000 cleanroom to demonstrates that humans are the predominant source of particles in a cleanroom [115].

4.2 System models and data acquisition

This section presents the SISO and MIMO system models of the cleanroom laboratory and the data acquisition from the laboratory.

4.2.1 SISO system models

As shown in Figure 3.1, ten PI controllers have been designed to maintain the steady airflow rate and AP inside the original cleanroom laboratory. The SISO models can be defined and identified based on each PI control loop. The controlled facilities consist of two supply fans in AHUs, two extract fans and six VAVs. The structure of a closed-loop system with PI control is shown in Figure 4.1. To find the mathematical model, the black-box modelling method is applied to the process in the block diagram while MV is the input and PV is the output. The description of the system models is shown in Table 4.1.

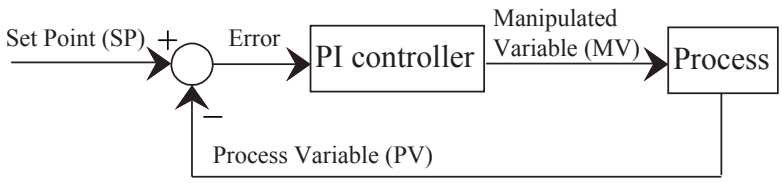

Figure 4.1: Closed-loop with PI control.

Table 4.1: Description of the SISO system models.

Models	Inputs	Outputs
AHU1 supply fun	AHU1 supply fan speed	AHU1 supply air pressure
AHU1 extract fun	AHU1 extract fan speed	AHU1 extract air pressure
AHU2 supply fun	AHU2 supply fan speed	AHU2 supply airflow rate
AHU2 extract fun	AHU2 extract fan speed	AHU2 extract airflow rate
Change room supply VAV	Change room supply VAV position	Change room supply airflow rate
Small lab supply VAV	Small lab supply VAV position	Small lab supply airflow rate
Large lab supply VAV	Large lab supply VAV position	Large lab supply airflow rate
Change room extract VAV	Change room extract VAV position	Change room extract airflow rate
Small lab extract VAV	Small lab extract VAV position	Air pressure in the small lab
Large lab extract VAV	Large lab extract VAV position	Air pressure in the large lab

4.2.2 MIMO system models

The cleanroom laboratory models are classified based on the ventilation system implemented by the HVAC system. The whole system is divided into two subsystems depending upon two ventilation cycles: the AHU1 related and the AHU2 related subsystems. Each subsystem represents the operation of a group of facilities as shown below.

- AHU1 related subsystem

  The HVAC subsystem among the AHU1 and two labs (the small lab and the large lab) is shown in Figure 4.2. The air flows through the AHU1 to the labs is controlled by the AHU1 supply fan, the supply VAVs of the labs, the extract VAVs of the labs and the AHU1 extract fan. The control objective is to regulate the ACR and the AP inside both labs to the proper levels.
- AHU2 related subsystem

  The HVAC subsystem between the AHU2 and the change room is shown in Figure 4.3. The air flows into the change room from the AHU2 is controlled by the AHU2 supply fan, the supply VAV and the extract VAV of the change room, and the AHU2 extract fan to maintain the required ACR and AP of the change room.

The inputs and outputs of these two subsystem models are represented in Figure

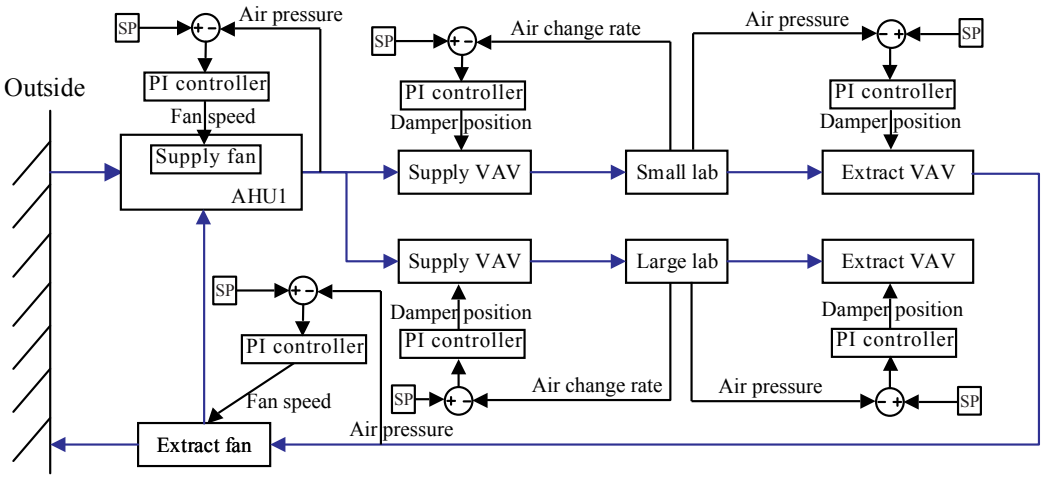

Figure 4.2: AHU1 related subsystem.

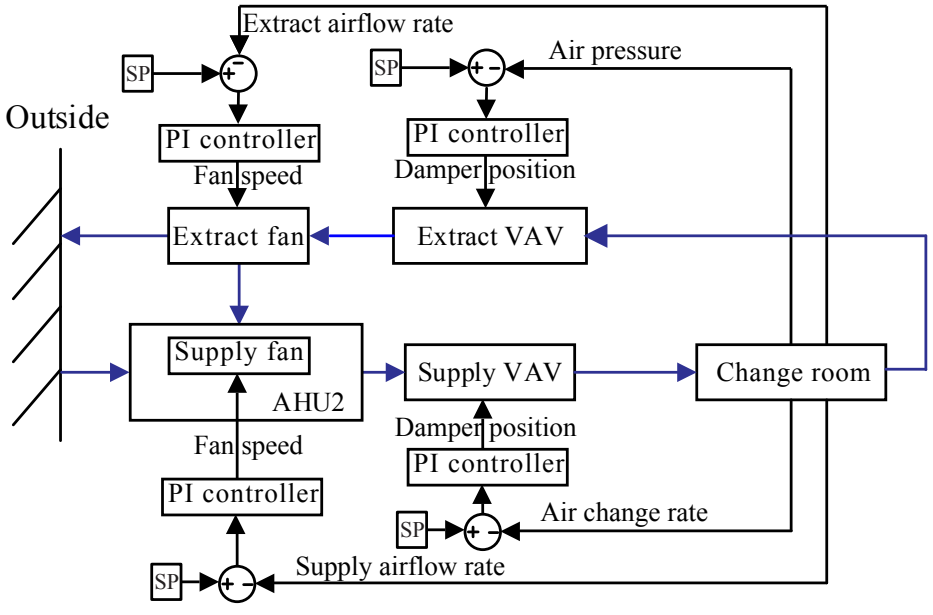

Figure 4.3: AHU2 related subsystem.

4.4. Both of them are MIMO models: the AHU1 related subsystem has six inputs and four outputs, and the AHU2 related subsystem has four inputs and two outputs.

4.2.3 Data acquisition

As shown in Figure 4.5, the controller inputs and system outputs of the subsystems are collected from the object linking and embedding for process control (OPC) server installed in a computer. Sensors and drivers are installed in the laboratory, in which the sensors are used to measure the system output (ACR and AP), and the drivers receive the controller output data from PI controllers implemented in the BMS to operate the HVAC facilities (fans and VAVs). The BMS installed is provided by Trend which controls the HVAC facilities to maintain a steady ACR and AP of the cleanroom. The communication between the sensors and drivers and the BMS is achieved by a Modbus based OPC server. OPC is the interoperability standard for the secure and reliable exchange of data in the industrial automation space and other industries [116]. The data transferred through the OPC server can be collected by the OPC Toolbox in Matlab installed in the same computer. These data can be used by the system identification toolbox to identify the mathematical system models.

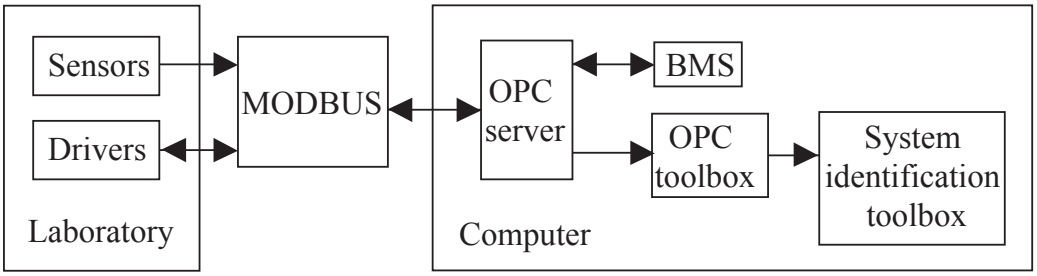

Figure 4.5: Data acquisition from the laboratory

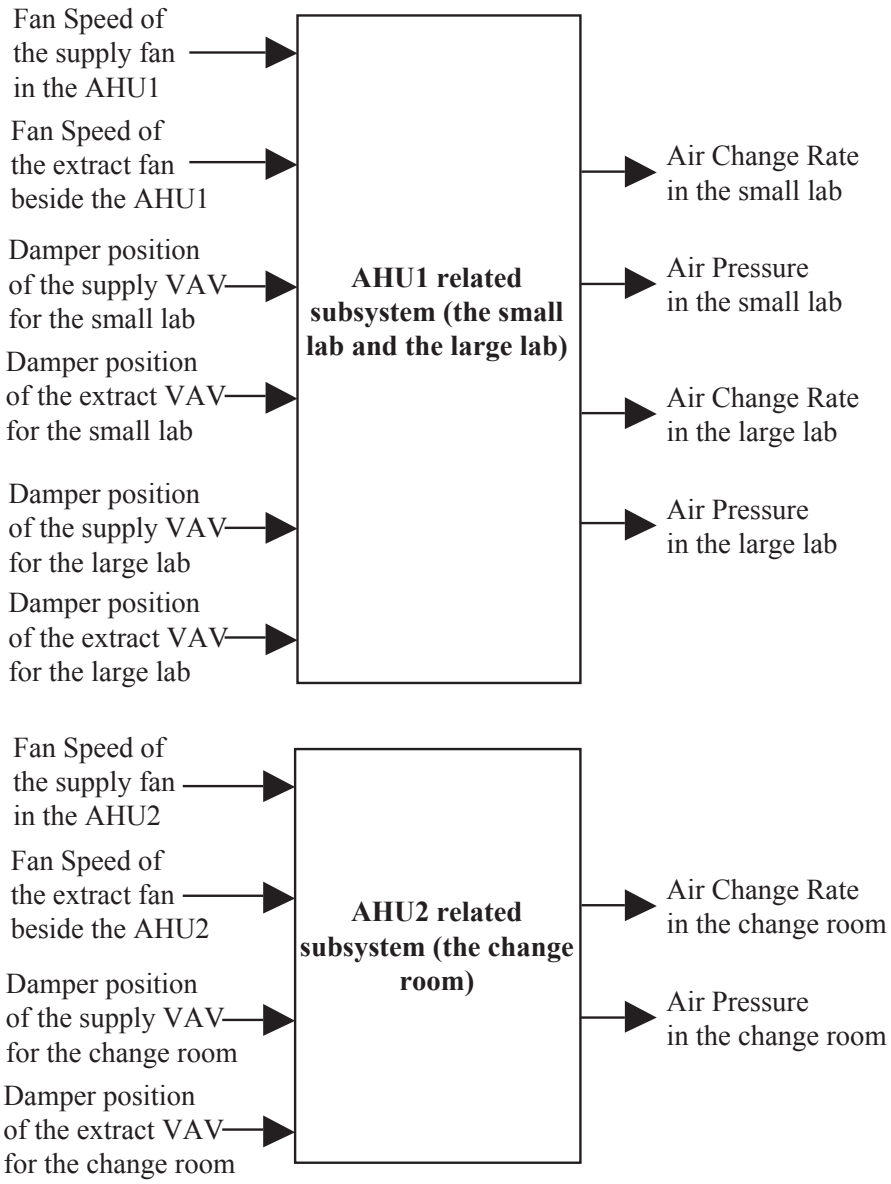

Figure 4.4: Inputs and outputs of two subsystems

4.3 Black-box modelling based on system identification methodology

Three model identification methods: PEM, LS and IV method are compared at first. The best method PEM is applied to three types of system models including ARX model, SS model and TF model, respectively. The model validation approach is used to obtain the model structure with the best performance.

4.3.1 System identification procedure

The mathematical model plays an important role on system controller design, especially for MPC. To figure out the appropriate mathematical model of the cleanroom laboratory, the system identification procedure has been applied which is represented as follows [117].

Step 1. Data preparation and model structures

(1) Operational measurements from the cleanroom laboratory
Setup all the facilities of the HVAC system in the cleanroom laboratory and operate them via the BMS installed, design several experimental tests and run them, then collect data from the OPC server for the inputs and outputs.

In most of the case in identification is done in the open-loop system means without having any feedback system. However, for the cleanroom laboratory presented in this thesis, the open-loop system is not practical because of safety issues and the limitation of the sensor's measurement. In this case, closed-loop system identification becomes important. In closed-loop identification, data are collected from a closed-loop test where an underlying process is fully under feedback control. Since the HVAC system has been operated by BMS with PI control, the closed-loop data are easy to collect.

Disturbances affecting the process will highly influence the modelling,

and therefore priori assumptions on the noise are required to describe the process. The main disturbance of this system is the disturbance affecting the process internally such as the air leakage, the distribution of the hardware, time delay of the sensors, etc. A white noise signal is generated and integrated into the input to overcome such uncertainties.

(2) Model type and structure

A system model consists of a model structure and model parametrisation. By applying the black-box modelling approach, three model structures are investigated: ARX model, SS model and TF model, respectively. Model parametrisation deals with the choice of the adjustable parameters [118].

(3) Criterion function

A criterion function is specified to measure the fitness between the outputs of the identified model and the operational measurements. Also, a proper identification method is chosen to estimate the system parameters.

Step 2. Model identification

The system model is identified based on the data collected in step 1, by using System Identification Toolbox in Matlab.

Step 3. Model validation

The Simulink in Matlab is used to verify the identified models. Outputs from the identified model are compared with the measured outputs through several metrics. It is necessary to repeat the above steps if the model is not accurate enough.

4.3.2 Model structure selection

The problem of model structure selection can be divided into three sub-problems [119]. The first one is to specify the type of model set to use, involving selection between linear and nonlinear models, between white-box, black-box and grey-box models, and so forth. Next, the size of the model set must be decided, including

the choice of possible variables and combination of variables to use in the model description. It also involves fixing orders and degrees of the model types. The last item to consider is how to parametrise the model set so that the estimation algorithms stand as good chances as possible to find reasonable parameter values.

In practice, all systems are nonlinear, and the output is a nonlinear function of the input variables. Some phenomena are inherently nonlinear in nature which normally are identified as nonlinear models, such as dry friction in mechanical systems, actuator power saturation, and sensor nonlinearities in electromechanical systems. However, a linear model is often sufficient to describe the system dynamics accurately. In most cases, the linear models are fit firstly.

The selection of a model structure and its order are required in advance for the estimation of a model using measurement data. This choice is influenced by prior knowledge about the system being modelled, but can also be motivated by an analysis of data itself. There are various possibilities for structure - state-space, transfer functions and polynomial forms. The choice of the reasonable structure may not be obvious if the detailed prior knowledge, such as its noise characteristics and the indication of feedback, is unknown. The order of the model needs to be specified before the corresponding parameters are estimated.

In lack of prior knowledge, it is advisable to try out various available choices and use the one that seems to work the best. Three most common model structures have been investigated in this chapter including ARX, SS and TF models. Once a model structure has been chosen to use, the next task is to determine the order. In general, the order is decided not higher than necessary. This can be determined by analysing the improvement in % fit as a function of model order. When doing this, it is advisable to use a separate, independent dataset for validation. Choosing an independent validation data set would improve the detection of over-fitting. In addition to a progressive analysis of multiple model orders, explicit determination of optimum orders can be performed for some model structures.

4.3.3 Three types of model structures

The models of each subsystem are identified with three types of model structures: ARX model, SS model and TF model, respectively.

Autoregressive exogenous model

In Reference [120], various statistical black-box models have been introduced to achieve different aspects about regression. From the results of comparison, it is found that ARX model can satisfy the requirement of closed-loop system design. With the measured inputs and outputs, the discrete-time ARX models are applied with the basic structure [109]:

$$A(z)y(k) = B(z)u(k - n_k) + e(k) \tag{4.3.1}$$

where z is the delay operator, n_k is the delay, u is the input, y is the output and e is the white-noise disturbance value, $A(z)$ and $B(z)$ are:

$$\begin{aligned} A(z) &= 1 + a_1 z^{-1} + \ldots + a_{n_a} z^{-n_a} \\ B(z) &= b_1 + b_2 z^{-1} + \ldots + b_{n_b} z^{-n_b+1} \end{aligned}$$

where n_a and n_b are the orders of the ARX model.

Given a MIMO system that the number of inputs is n_u and the number of outputs is n_y, the jth output y^j of the MIMO ARX model can be expressed as:

$$A^j(z)y^j = -\sum_{i=1}^{n_y} A_i^j(z)y_i(k) + \sum_{i=1}^{n_u} B_i^j(z)u_i(k) \;\; i \neq j \tag{4.3.2}$$

State space model

The discrete-time SS model is represented as follows:

$$x(k+1) = Ax(k) + Bu(k) + Ke(k) \tag{4.3.3}$$

$$y(k) = Cx(k) + Du(k) + e(k) \tag{4.3.4}$$

where A, B, C, D and K are system matrices, $u(k)$ is the input, $e(k)$ is the disturbance, $x(k)$ is the state and $y(k)$ is the output.

Transfer function model

A TF is the ratio of the output of a system to the input of a system. In the discrete-time case, the output of a TF model is defined as:

$$Y(z^{-1}) = G(z^{-1})U(z^{-1}) + E(z^{-1}) \tag{4.3.5}$$

where $Y(z^{-1})$, $U(z^{-1})$ and $E(z^{-1})$ represent the output, input and noise, respectively. $G(z^{-1}) = \text{num}(z^{-1})/\text{den}(z^{-1})$ is the desired TF relating the input to the output.

4.3.4 Parameter estimation methods

Three common parameter estimation methods: PEM, LS and IV method, are used to estimate the parameters of the models of the two subsystems. The methods presented in this section are concluded based on Reference [118].

Prediction error identification method

Recall the identification procedure, a model set $M(\theta)$ has been selected and is parametrised as three model structures: ARX, SS and TF, using a parameter vector θ. Thus, the determination of the best model within the set becomes a problem of estimating θ. The equation (4.3.5) can be then rewritten as:

$$y(t) = G(q, \theta)u(t) + H(q, \theta)e(t) \tag{4.3.6}$$

One-step-ahead prediction of $y(t)$ is derived as :

$$y(t|t-1) = H^{-1}(q)G(q)u(t) + [1 - H^{-1}(q)]y(t) \tag{4.3.7}$$

Given a certain model $M(\theta_*)$, the prediction error is defined as:

$$\varepsilon(t, \theta_*) = y(t) - \hat{y}(t|\theta_*) \tag{4.3.8}$$

where $\hat{y}$ is the predictor. Since a data set Z^N has been collected from the system:

$$Z^N = [y(1), u(1), y(2), u(2), \ldots, y(N), u(N)] \tag{4.3.9}$$

the errors defined in (4.3.8) can be computed for $t = 1, 2, \ldots, N$.

The best identification model aims to minimise the error. In other words, at time $t = N$, the parameter θ becomes $\hat{\theta}_N$ so that the prediction error $\varepsilon(t, \hat{\theta}_N)$ becomes as small as possible. That is the basic idea of a parameter estimation method.

Given a prediction-error sequence from (4.3.8), let it be filtered through a stable linear filter $L(q)$:

$$\varepsilon_F(t, \theta) = L(q)\varepsilon(t, \theta), \quad 1 \leq t \leq N \tag{4.3.10}$$

Then derive the following norm:

$$V_N(\theta, Z^N) = \frac{1}{N} \sum_{t=1}^{N} l(\varepsilon_F(t, \theta)) \tag{4.3.11}$$

where l is a scalar-valued function.

The estimation of $\hat{\theta}_N$ is then defined by minimisation of the above norm

$$\hat{\theta}_N = \arg\min_{\theta \in D_M} V_N(\theta, Z^N) \tag{4.3.12}$$

This way of estimating θ denotes the general term: PEM.

Least squares method

The LS method is a standard approach to estimate the unknown models from measured data by minimising the sum of squared prediction errors or residuals between the measured output and the observed output. The residual is defined as:

$$\varepsilon(t, \theta) = y(t) - \phi(t)^T \theta \tag{4.3.13}$$

where y is the measured output, ϕ is the regressor with known elements relating the states to the observations, and θ is the unknown static states.

The sum of squared residuals, also known as the LS objective function is defined as:

$$J(\theta) = \sum_{t=1}^{N} \varepsilon^2(t) = \sum_{t=1}^{N} (y(t) - \phi(t)^T \theta)^2 \tag{4.3.14}$$

Since the model contains m parameters and $t = 1, \ldots, N$, Φ is defined as an $N \times m$ matrix with elements $\Phi_{t_j} = \phi_j(t), j = 1, \ldots, m$. Thus (4.3.14) can be written as

$$J(\theta) = \varepsilon^T \varepsilon = (y^T - \theta^T \Phi^T)(y - \Phi\theta) \tag{4.3.15}$$

The minimum of $J(\theta)$ is found by setting the gradient to zero, so that

$$\frac{\partial J(\theta)}{\partial \theta} = -2\Phi^T y + 2\Phi^T \Phi\theta = 0 \tag{4.3.16}$$

The gradient of $J(\theta)$ is zero if and only if

$$\Phi^T \Phi\hat{\theta} = \Phi^T y \Rightarrow \hat{\theta} = (\Phi^T \Phi)^{-1}\Phi^T y \tag{4.3.17}$$

which means $J(\theta)$ has a minimum at $\hat{\theta}$.

A concept called forgetting exists when estimating the parameters that the earlier data is gradually discarded for more recent information. In the least square method, to present forgetting, a forgetting factor is introduced into the objective function which gives less weight to older data and more weight to recent data. The modified objective function is then defined as follows:

$$J(\theta) = \sum_{t=1}^{N} \lambda^{N-t}(y(t) - \phi(t)^T\theta)^2 \tag{4.3.18}$$

where λ is the forgetting factor and $0 < \lambda \leqslant 1$.

Instrumental variable method

The IV method is used in estimation when correlation between the explanatory variables and the error term is suspected. The LS estimate of θ can be expressed as

$$\hat{\theta}_N^{LS} = \text{sol}\{\sum_{t=1}^{N}(y(t) - \phi(t)^T\theta)^2 = 0\} \tag{4.3.19}$$

For the instrumental variables method, a sequence of correlation vectors called instrumental variables are introduced. This gives

$$\hat{\theta}_N^{IV} = \text{sol}\{\sum_{t=1}^{N}\zeta(t)(y(t) - \phi(t)^T\theta)^2 = 0\} \tag{4.3.20}$$

where the elements of ζ are called instruments or instrumental variables.

Good instruments ζ should be uncorrelated with the noise, sufficiently correlated with the state and orthogonal to the inputs. The instruments are usually chosen from the past inputs and outputs.

4.3.5 Model validation

For the visual inspection of the model responses, it is hard to see the difference in performance for the models having similar responses [109]. In order to compare the performance of the models identified with various model structures, the comparison metric, which is called goodness of fit (G), is used [107]. A larger value of G indicates the better fit.

$$\mathrm{G} = (1 - \frac{\sqrt{\sum_{i=1}^{n}(y_i^* - y_i)^2}}{\sqrt{\sum_{i=1}^{n}(y_i - \frac{1}{n}\sum_{i=1}^{n} y_i)^2}}) \times 100 \tag{4.3.21}$$

4.4 Identification of the SISO models

As shown in Table 4.1, ten SISO models have been defined in the cleanroom HVAC laboratory based on ten facilities. The mathematical models of these subsystems have been identified using the black-box modelling approach. The identified models can be used for process models in the simulation tests for PI control and MPC, and prediction models of MPC. Because of the simpleness of the SISO models, there is a minor difference in performance between different model structures and parameter estimation methods. Thus, it is not necessary to show the comparison results. The ARX models of the SISO model are chosen as examples. The polynomials of the SISO ARX models are:

- AHU1 supply fun
  $A(z) = 1 - 0.8524z^{-1} - 0.2248z^{-2} - 0.3095z^{-3} + 0.239z^{-4} + 0.1584z^{-5}$
  $B(z) = 0.01551z^{-1} + 0.2458z^{-2} + 1.392z^{-3} - 1.583z^{-4}$

- AHU1 extract fun
  $A(z) = 1 - 0.6242z^{-1} - 0.3686z^{-2} - 0.5286z^{-3} + 0.1461z^{-4} + 0.3854z^{-5}$
  $B(z) = 0.008118z^{-1} + 0.06171z^{-2} + 0.1452z^{-3} - 0.1312z^{-4}$

- AHU2 supply fun
  $A(z) = 1 - 0.6077z^{-1} - 0.3928z^{-2} - 0.5829z^{-3} + 0.2415z^{-4}$
  $B(z) = 0.1566z^{-7} - 0.1232z^{-8} + 0.1483z^{-9} - 0.1362z^{-10}$

- AHU2 extract fun

  $A(z) = 1 - 0.9679z^{-1} - 0.1713z^{-2} + 0.04889z^{-3} - 0.03278z^{-4} + 0.1479z^{-5}$

  $B(z) = -0.1841z^{-1} + 0.1293z^{-2} + 0.2736z^{-3} - 0.1945z^{-4} - 0.05819z^{-5}$

- Change room supply VAV

  $A(z) = 1 - 0.9133z^{-1} - 0.08681z^{-2}$

  $B(z) = 1.854z^{-3} - 1.114z^{-4} - 0.3413z^{-5} - 0.3992z^{-6}$

- Small lab supply VAV

  $A(z) = 1 - 0.6287z^{-1} - 0.3236z^{-2} - 0.754z^{-3} + 0.2123z^{-4} + 0.2972z^{-5}$

  $B(z) = 0.1055z^{-8} + 0.1443z^{-9} + 0.03696z^{-10} - 0.09832z^{-11} - 0.02543z^{-12}$

- Large lab supply VAV

  $A(z) = 1 - 0.9152z^{-1} - 0.0854z^{-2} - 0.4572z^{-3} + 0.3568z^{-4}$

  $B(z) = -0.3253z^{-1} + 4.284z^{-2} - 3.416z^{-3} - 0.5402z^{-4}$

- Change room extract VAV

  $A(z) = 1 - 0.9178z^{-1} - 0.1009z^{-2} - 0.3969z^{-3} + 0.3365z^{-4} - 0.00919z^{-5}$

  $B(z) = -3.754z^{-7} + 3.786z^{-8} - 1.649z^{-9} + 6.339z^{-10} - 1.231z^{-11}$

- Small lab extract VAV

  $A(z) = 1 - 0.7686z^{-1} - 0.1929z^{-2} - 0.5283z^{-3} + 0.3187z^{-4} + 0.1582z^{-5}$

  $B(z) = 0.02352z^{-1} - 0.0452z^{-2} - 0.3691z^{-3} + 0.2158z^{-4} + 0.0963z^{-5}$

- Large lab extract VAV

  $A(z) = 1 - 1.606z^{-1} + 0.1258z^{-2} - 0.6232z^{-3} + 1.451z^{-4} + 0.3341z^{-5}$

  $B(z) = 0.1214z^{-1} - 0.1515z^{-2} - 0.213z^{-3} + 0.1972z^{-4}$

The SISO models defined above are identified using black-box modelling approach. Ten SISO models have been identified, each of which represents an individual equipment. Two supply fans in AHUs, two extract fans, three supply VAVs

and three extract VAVs have been modelled. The predicted output results of the identified models and the measured output results are compared by plotting both of them in the same figure and by plotting the absolute error and relative error between them.

4.4.1 Supply fans in AHUs

The model of the supply fan represents the process that the air flows through the supply fan inside the AHU and accelerates by a specified fan speed and then flows into cleanrooms. Two supply fans are installed in the AHU1 and AHU2 respectively: the supply fan in the AHU1 serves the small lab and large lab, and the supply fan in the AHU2 serves the change room.

In the AHU1 supply fan model, the AP is measured by the pressure sensor beside the export of AHU1 from the PI control loop. The control objective is to keep the AP after the AHU1 stable by controlling the AHU1 supply fan speed. Thus the input is fan speed of the supply fan, and the output is the measured AP. The measured and the predicted outputs of the identified model, the absolute error and the relative error are shown in Figure 4.6.

In the AHU2 supply fan model, the airflow rate supplied after the AHU2 is measured based on the PI control loop. The control objective is to maintain the supply airflow rate by controlling the AHU2 supply fan speed. The input is the fan speed of the supply fan, and the output is the supply airflow rate. The measured and the predicted outputs of the identified model, the absolute error and the relative error are presented in Figure 4.7.

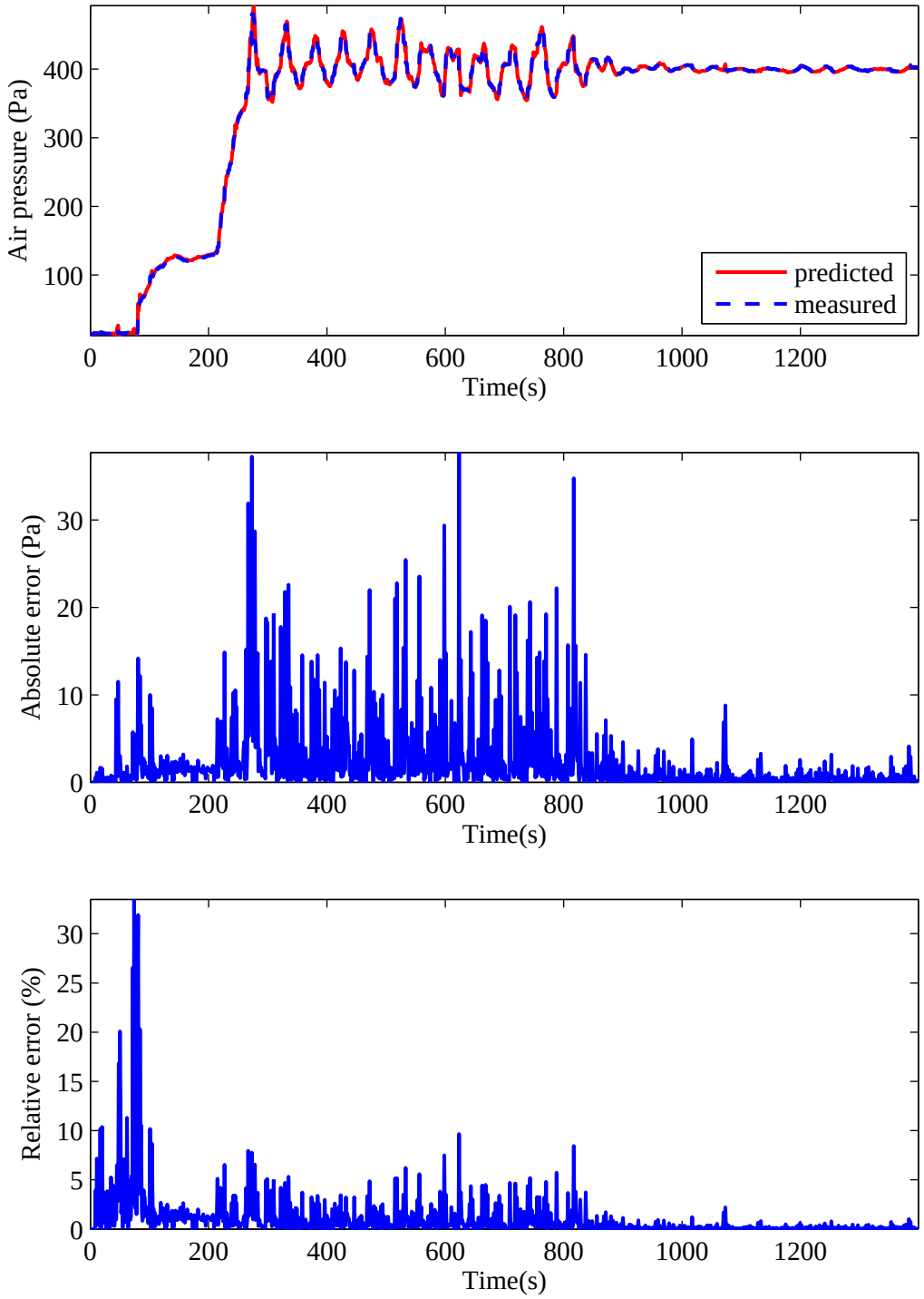

Figure 4.6: Comparison results of the output of the AHU1 supply fan model.

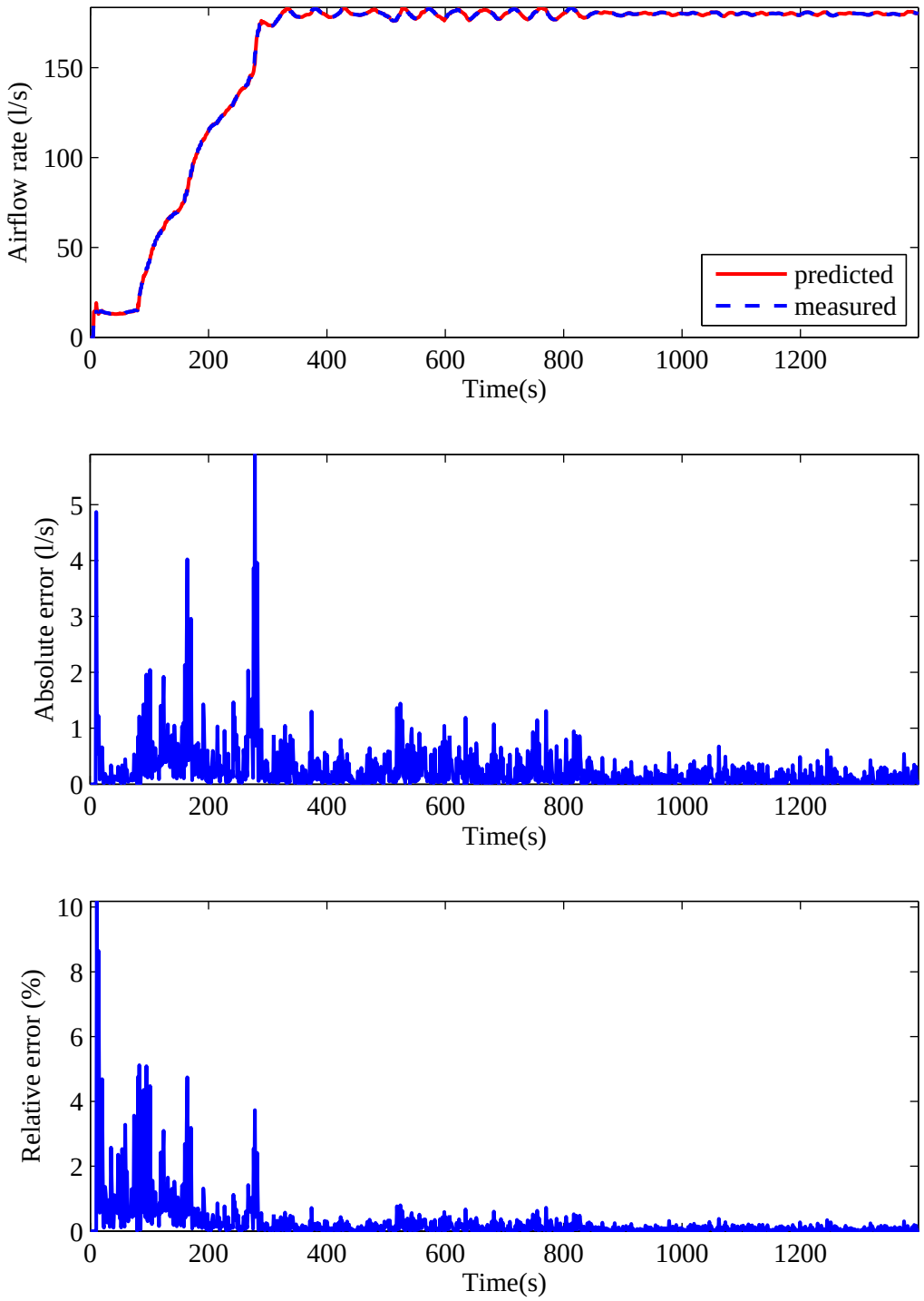

Figure 4.7: Comparison results of the output of the AHU2 supply fan model.

4.4.2 Extract fans

The extract fan model represents the process: the air, which is extracted from cleanrooms, flows through the extract fan beside the export and accelerates by a specified fan speed. The air extracted from the small lab and the large lab is controlled by the AHU1 extract fan, and that from the change room is controlled by the AHU2 extract fan.

For the AHU1 extract fan model, the AP beside this fan is measured from the PI control loop. The control objective is to keep a stable AP of the air extracted into outdoors by controlling the extract fan speed. The input is thus the fan speed of the fan, and the output is the measured AP. Figure 4.8 presents the measured and the predicted outputs of the identified model, the absolute error and the relative error, respectively.

The extract airflow rate is measured based on the PI control loop for the AHU2 extract fan model. The control objective is to keep the extract airflow rate a stable value by controlling the extract fan speed. The input is the fan speed of the extract fan, and the output is the extract airflow rate. Figure 4.9 shows the measured and the predicted outputs of the identified model, the absolute error and the relative error.

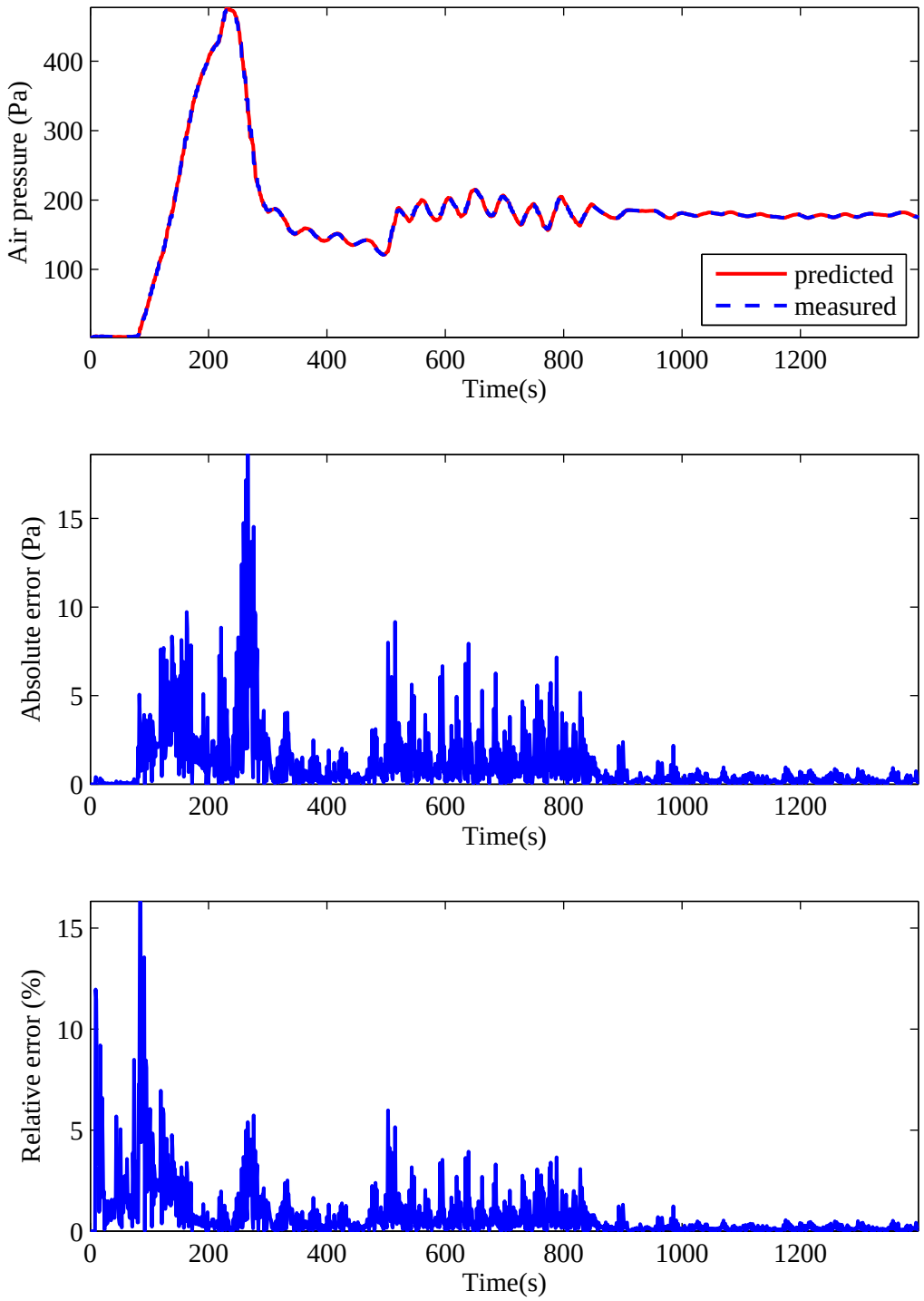

Figure 4.8: Comparison results of the output of the AHU1 extract fan model.

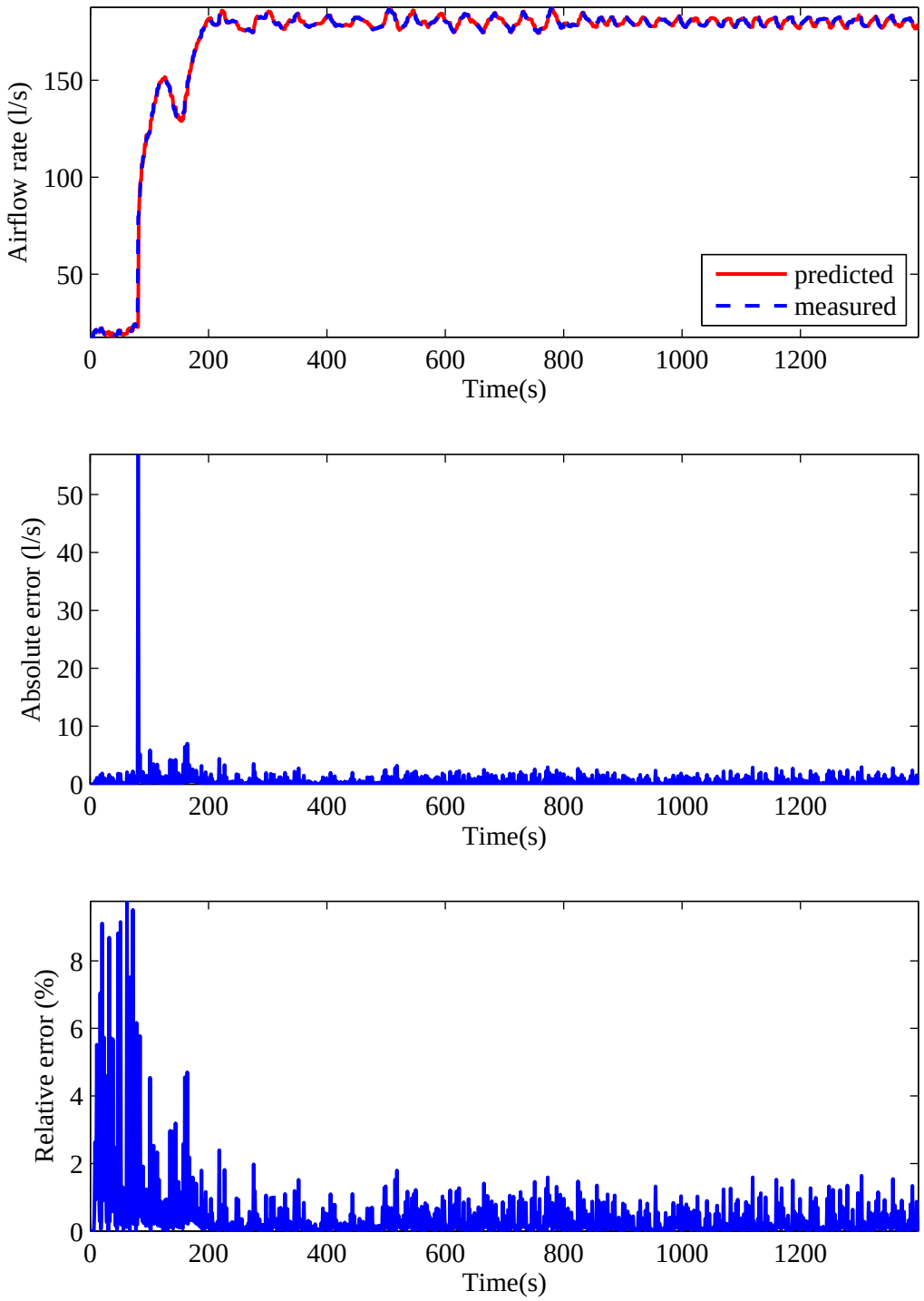

Figure 4.9: Comparison results of the output of the AHU2 extract fan model.

4.4.3 Supply VAVs

The model of the supply VAV represents the process that the air, which is supplied from the AHU, flows through the supply VAV and flows into cleanrooms. Three supply VAVs are installed for three cleanrooms: the change room, the small lab and the large lab, respectively. The airflow rate supplied into each cleanroom is measured. The input is the position of the VAV, and the output is the airflow rate supplied into the cleanroom. The control objective of the PI controller is to maintain the supply airflow rate into the cleanroom by controlling the position of the supply VAV. The measured and the predicted outputs of the identified models, the absolute error and the relative error are shown in Figures 4.10-4.11 for the supply VAV model of the change room, the small lab and the large lab, respectively.

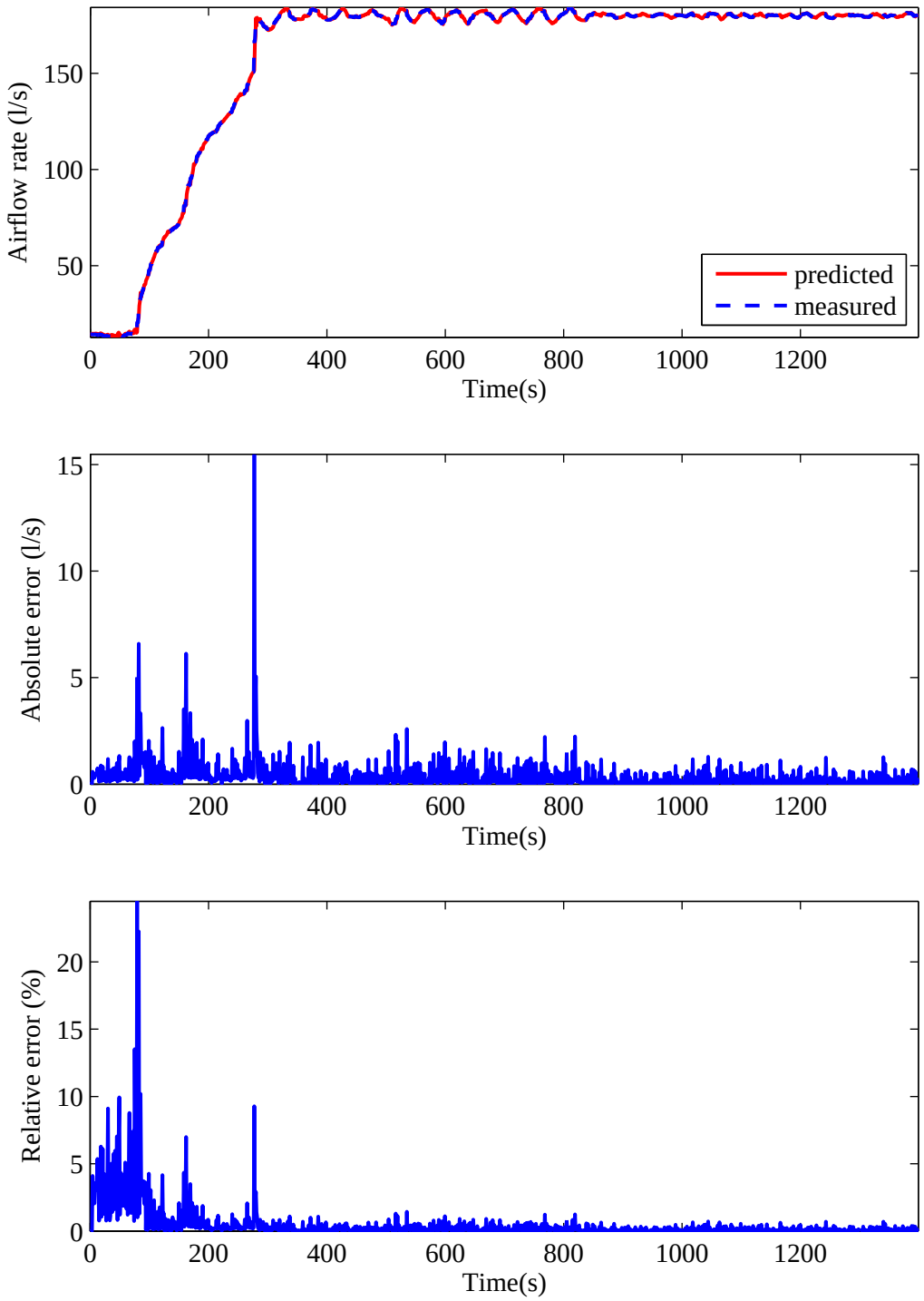

Figure 4.10: Comparison results of the output of the change room supply VAV model.

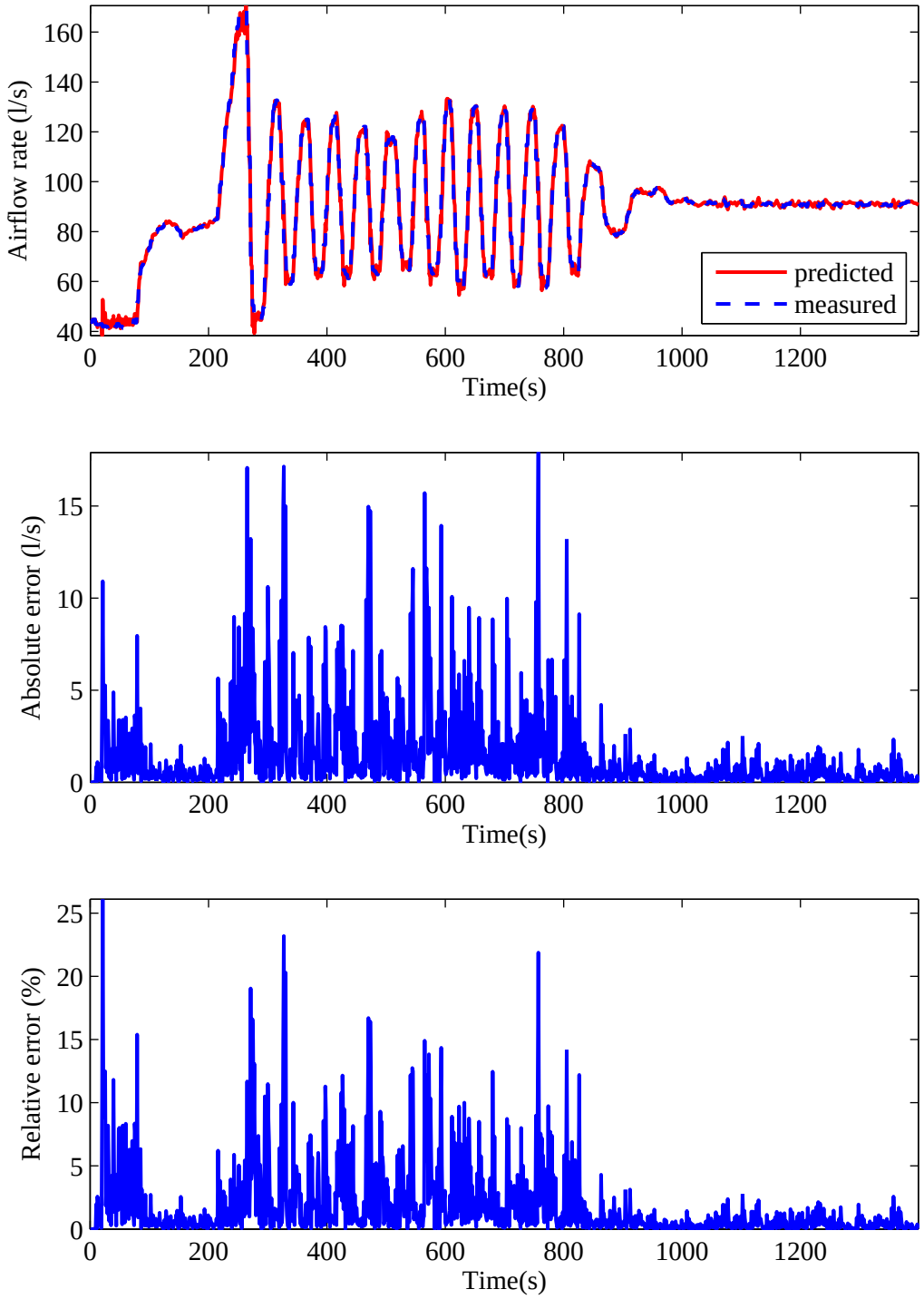

Figure 4.11: Comparison results of the output of the change room supply VAV model.

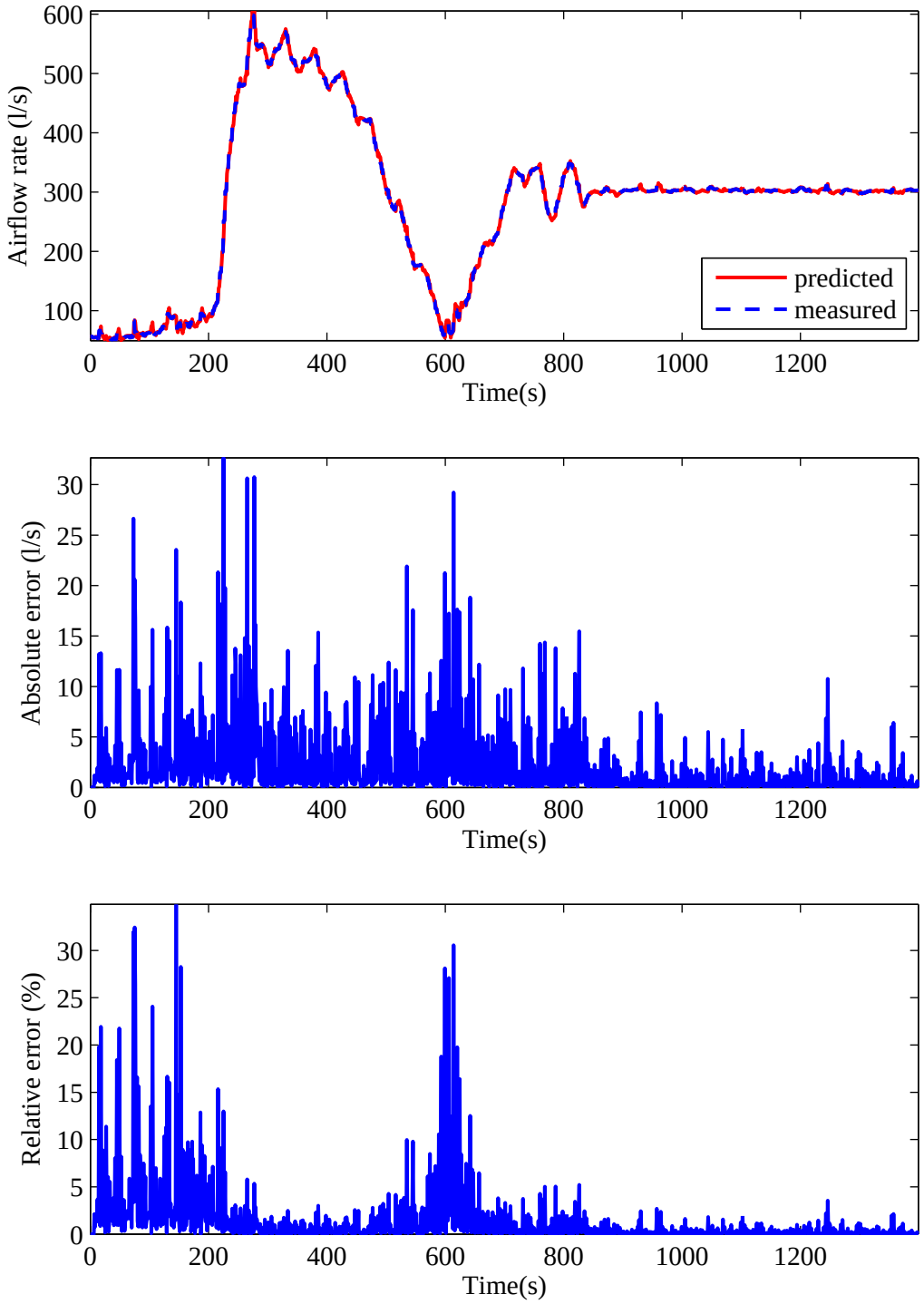

Figure 4.12: Comparison results of the output of the change room supply VAV model.

4.4.4 Extract VAVs

The model of the extract VAV represents the process: the air extracted from the cleanroom flows through the extract VAV. Three extract VAVs for three cleanrooms are installed. For the model of the change room extract VAV, the airflow rate extracted from the change room is measured. The control objective of the corresponding PI controller is to keep the extract airflow rate from the change room a stable value by controlling the position of the extract VAV. The input is the position of the VAV, and the output is the airflow rate extracted from the change room. The measured and the predicted outputs of the identified model, the absolute error and the relative error are shown in Figure 4.13.

The extract VAV models of the small lab and large lab are identified from the PI control process whose control objective is to maintain the AP in the lab by controlling the position of the extract VAV. The input is the position of the extract VAV, and the output is the AP in the lab. The measured and the predicted outputs of the identified models, the absolute error and the relative error are shown in Figures 4.14 and 4.15 for the small lab and large lab, respectively.

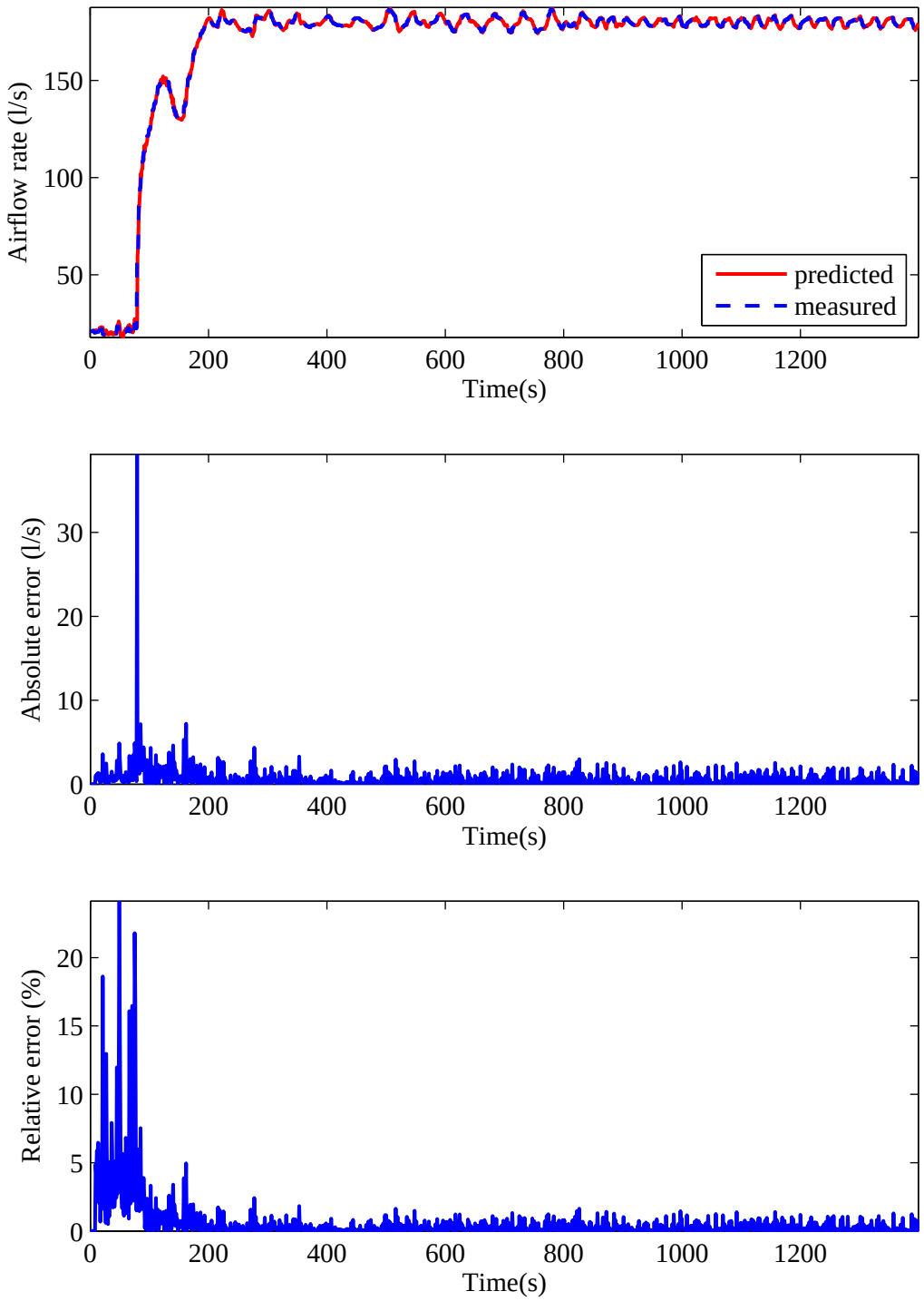

Figure 4.13: Comparison results of the output of the change room extract VAV model.

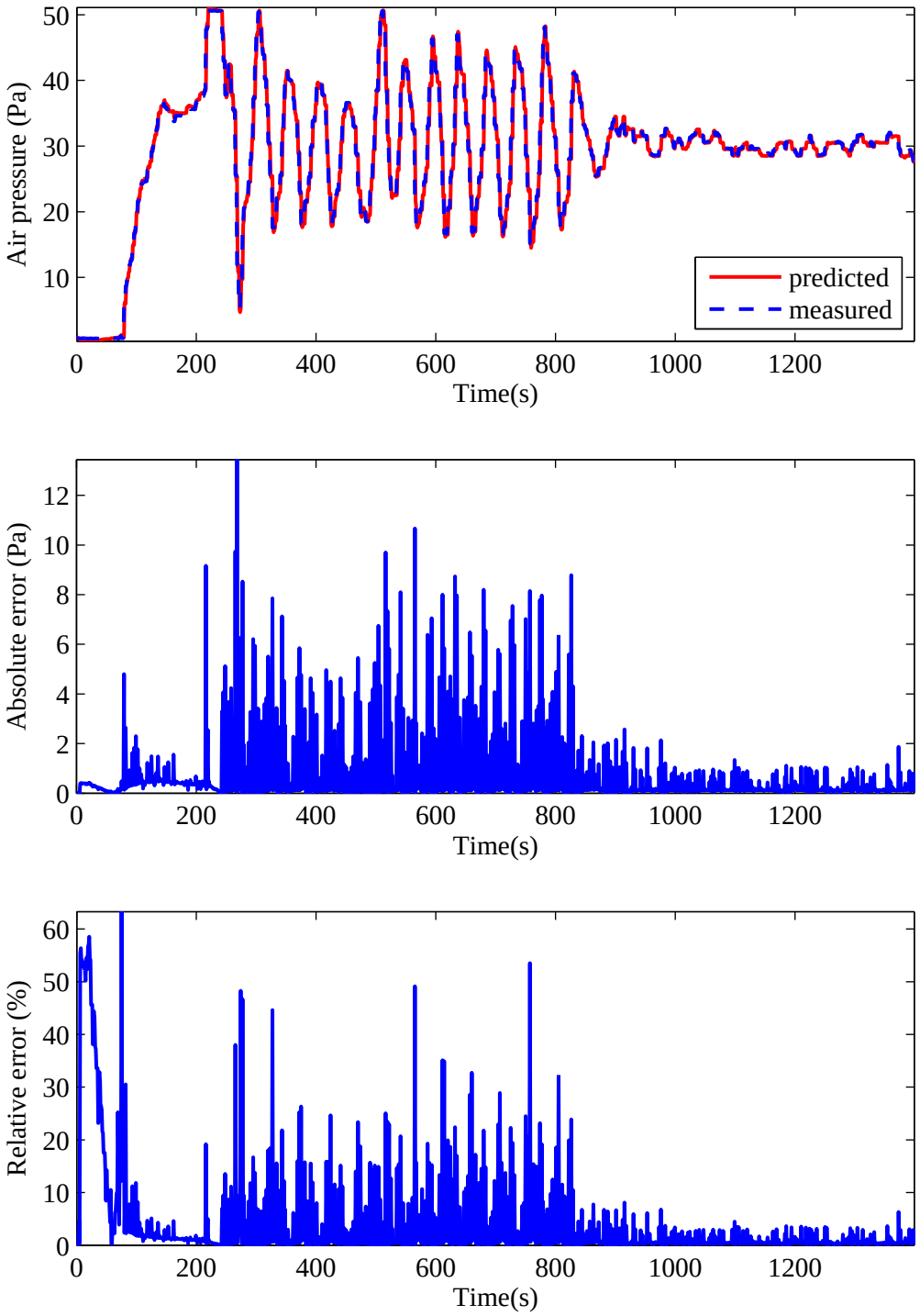

Figure 4.14: Comparison results of the output of the change room extract VAV model.

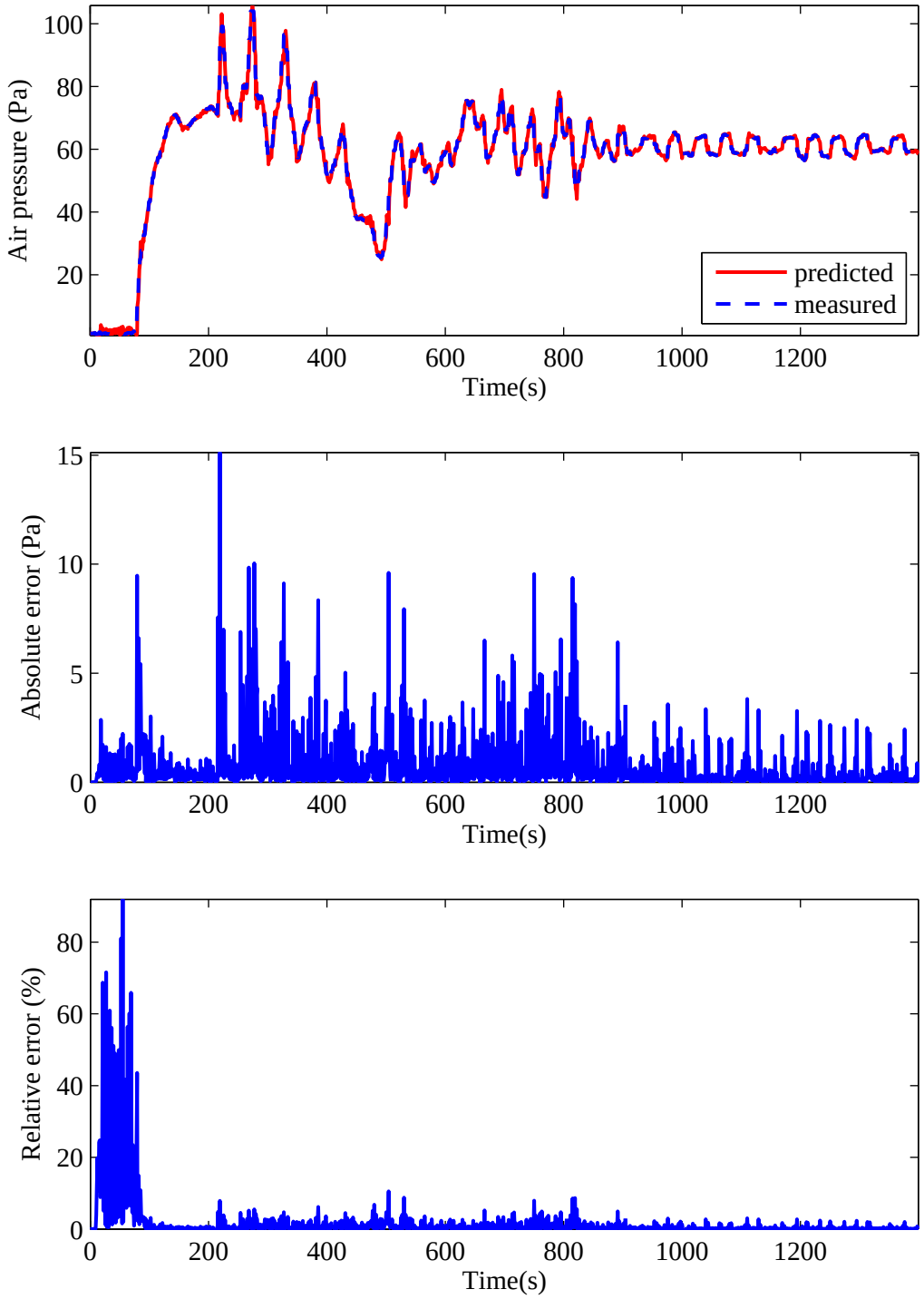

Figure 4.15: Comparison results of the output of the change room extract VAV model.

4.5 Identification of the MIMO models

The ARX models of the two subsystems are identified with the three parameter estimation methods presented in Section 4.3.4 respectively, the performance of which are compared by calculating the fitnesses of them. PEM resulted as the best parameter estimation method and has been applied to identify the subsystem models with the other two model structures: SS and TF. The predicted outputs of the identified models with the three model structures and the measured outputs are compared by plotting them in the same figures. The metrics introduced in Section 4.3.5 are calculated for analytical comparison. The comparison results shown below demonstrate that the ARX model of each subsystem performs the best. The measured data are collected from the real-time experiments ran in the cleanroom laboratory where each facility is controlled by a PI controller. The sample time of the controllers is one second.

4.5.1 Comparison of parameter estimation methods

The ARX models of the two subsystems are identified based on three parameter estimation methods: PEM, LS method and IV method. In order to find the best method, the performances of the identified models are compared depending on the goodness of fit. The comparison results are shown in Table 4.2.

Table 4.2: Goodness of fit for ARX models with three parameter estimation methods.

Subsystem	Output	PEM	LS	IV
AHU1 related subsystem	Small lab ACR	0.905	0.855	0.852
	Small lab AP	0.875	0.853	0.852
	Large lab ACR	0.972	0.964	0.954
	Large lab AP	0.921	0.903	0.893
AHU2 related subsystem	Change room ACR	0.984	0.984	0.983
	Change room AP	0.875	0.868	0.867

From Table 4.2, it is found that the models estimated by the PEM have the high-

est goodness of fit. In other words, the models identified by the PEM perform the best compared with the other two parameter estimation methods including LS and IV. For the four outputs in the AHU1 related subsystem, the comparison results clearly show that the PEM has the largest goodness of fit. The LS and IV have similar values, but they are 2-5% smaller than PEM. The AHU2 related subsystem has two outputs: for the change room ACR output, the goodness of fit values among three methods are almost the same; for the change room AP output, PEM has 1% larger value than LS and IV. Summarised from both outputs in the AHU2 related subsystem, PEM performs the best. Table 4.2 demonstrates that the PEM is the best method to estimate the parameters of the two subsystems while it would be used in the further estimation of the parameters for the other two model structures.

The LS and IV methods have similar performance in this situation. The PEM method has the larger goodness of fit values than the other two. Because the AHU1 related subsystem is more complex with more inputs and outputs than the AHU2 related subsystem, it is harder for the parameter estimation methods to reach great goodness of fit values. The less complex the model is, the easier the parameter estimation method can have high performance. For a simple enough model, different methods can perform quite similar with a very high goodness of fit which can approach 100%. The change room ACR output in the AHU2 related subsystem is an example of such situation.

4.5.2 Comparison between experiment and prediction results

AHU2 related subsystem

Figures 4.16-4.21 present the comparison between experiment and prediction results of the AHU2 related subsystem. The three sub-figures in each figure show the plotting of experiment and prediction results, the absolute errors and the relative errors, respectively. The first sub-figures of ARX and SS models for both outputs show a good fit between experiment and prediction results, and it is hard to determine which one is better visually. The difference between experiment and prediction results is significant for TF models which can be easily found from the

first sub-figures.

The calculation of the errors gives another direction to see which model performs better. The first output, the ACR in the change room, is provided in Figures 4.16-4.18 for three model structures: ARX, SS and TF, respectively. The relative errors of its ARX model are mostly below 1%, and the maximum point is smaller than 4%. The relative errors of its SS model are below 1% after 300 seconds, but its maximum point is more than 8%. Its TF model has the largest relative errors with more than 12% maximum point, and most time the errors are above 2%. Thus, the ARX model of the first output for the AHU2 related subsystem perform the best.

Figures 4.19-4.21 present the second output, the AP in the change room, for three model structures: ARX, SS and TF, respectively. The relative errors of ARX and SS models for the second output are similar. Both of them has about 15% maximum point. They are below 10% before 800 seconds and then decrease to smaller than 3%. The relative errors of its TF model are much larger than ARX and SS models. The maximum point can be more than 40%, and they are below 20% at most time. Thus, it is found that the ARX and SS models have high performance with smaller relative errors and the TF models perform much worse than the others.

In conclusion to Figures 4.16-4.21, TF models show much worse performance than ARX and SS models. The identification of the TF models estimates the parameters $G(z^{-1})$ from the measured data without including the disturbance. More data are needed to be identified to average out the effects of the disturbance.

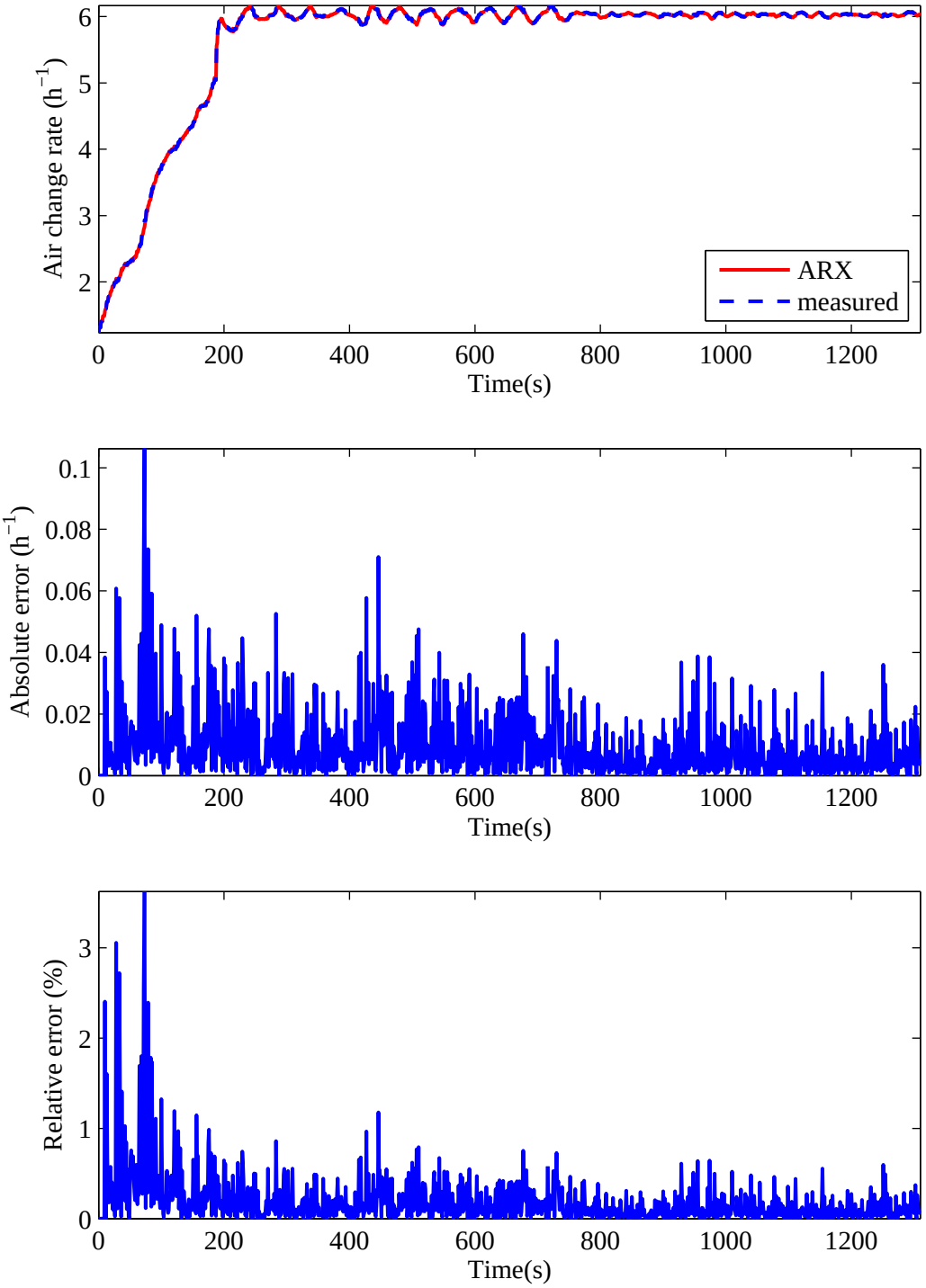

Figure 4.16: Comparison results of the output of the AHU2 related subsystem ARX model: ACR in the change room.

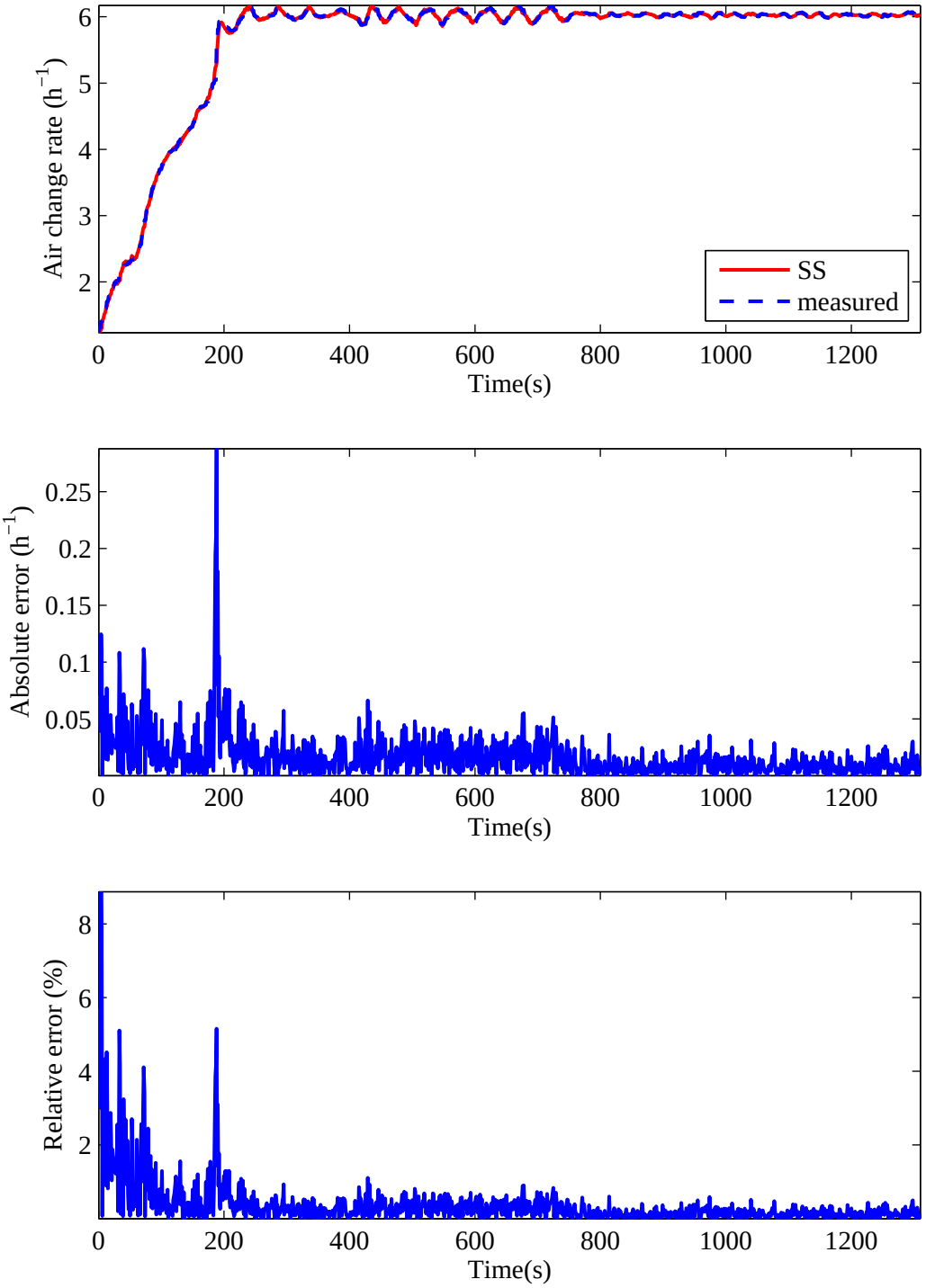

Figure 4.17: Comparison results of the output of the AHU2 related subsystem SS model: ACR in the change room.

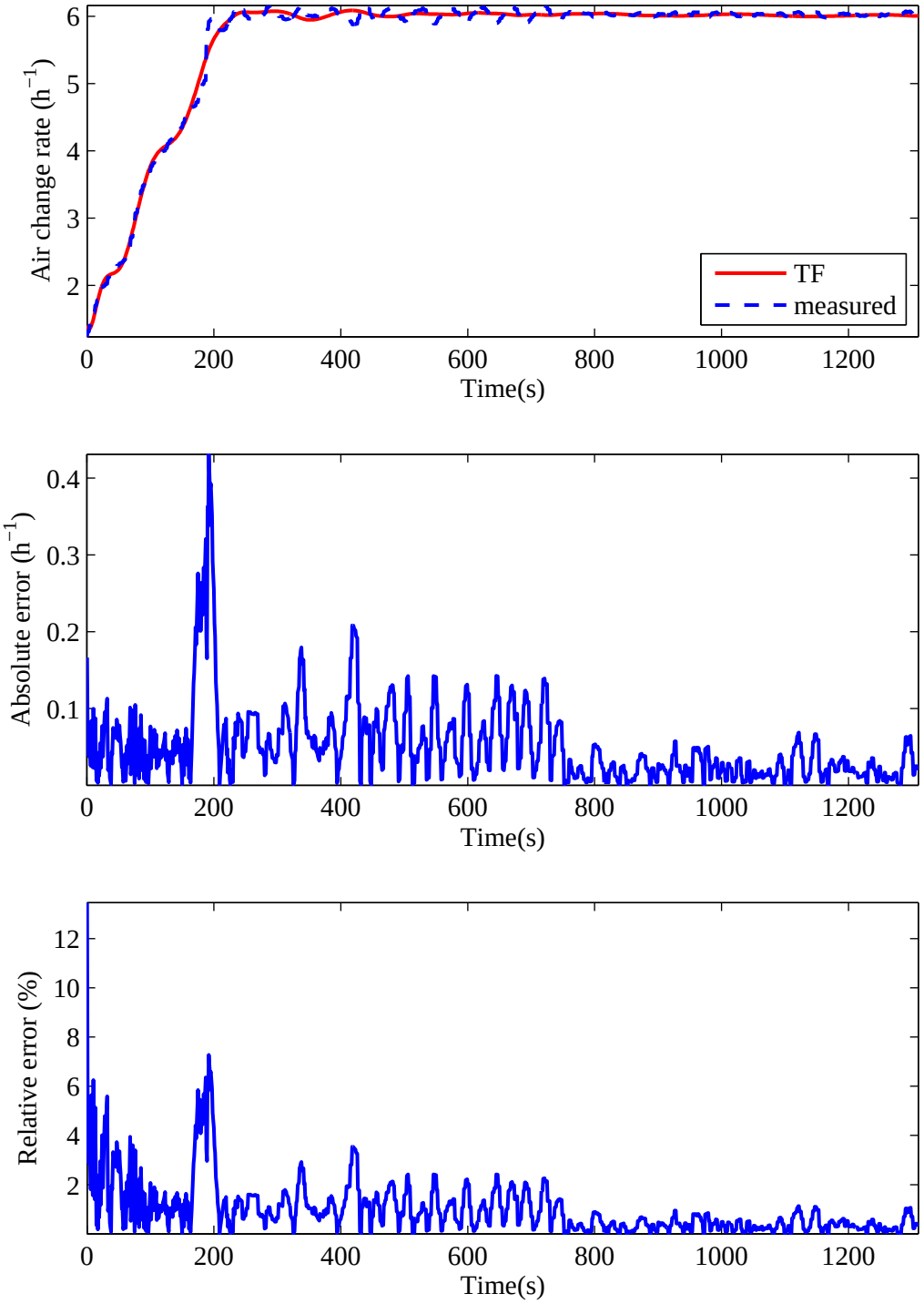

Figure 4.18: Comparison results of the output of the AHU2 related subsystem TF model: ACR in the change room.

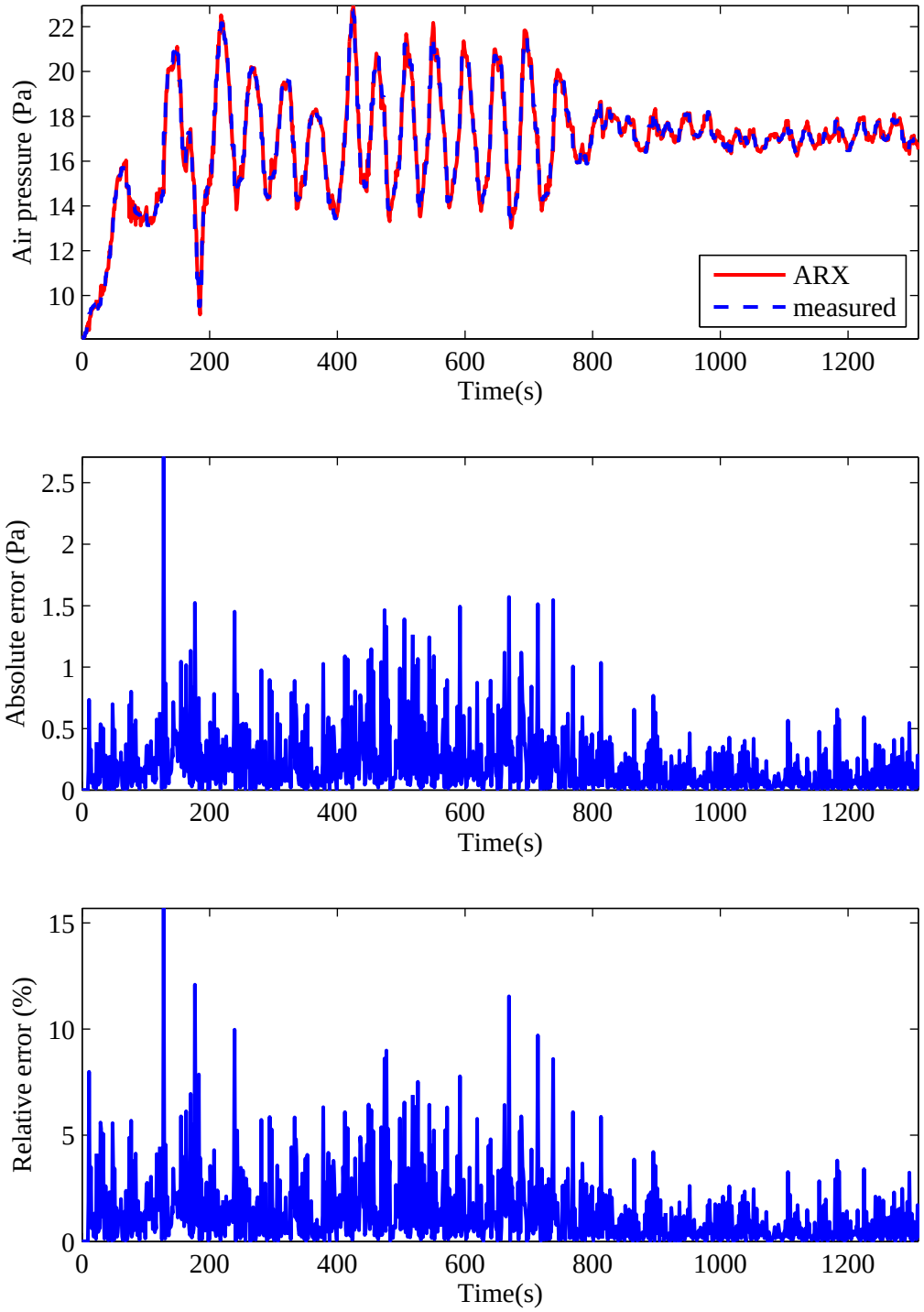

Figure 4.19: Comparison results of the output of the AHU2 related subsystem ARX model: AP in the change room.

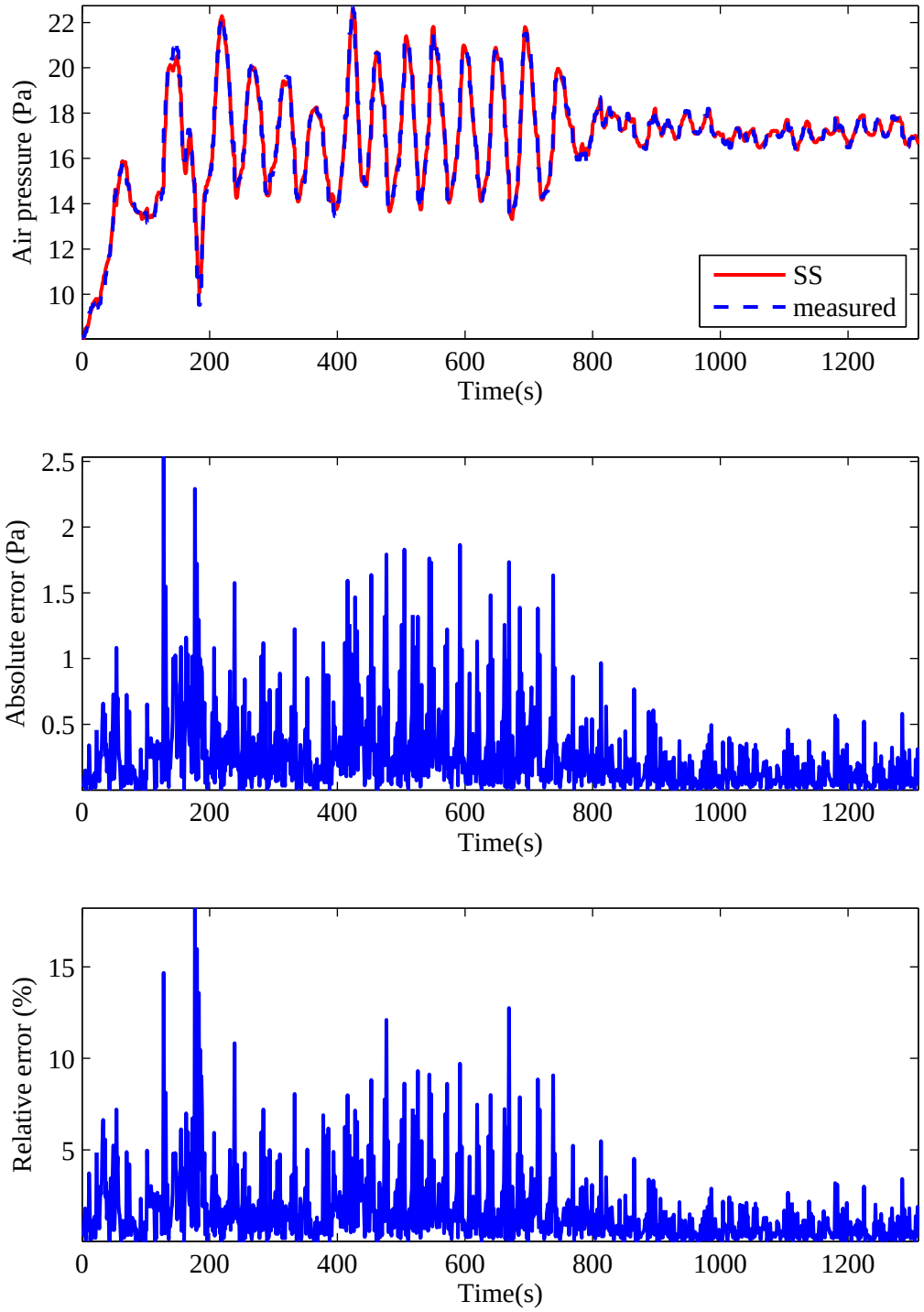

Figure 4.20: Comparison results of the output of the AHU2 related subsystem SS model: AP in the change room.

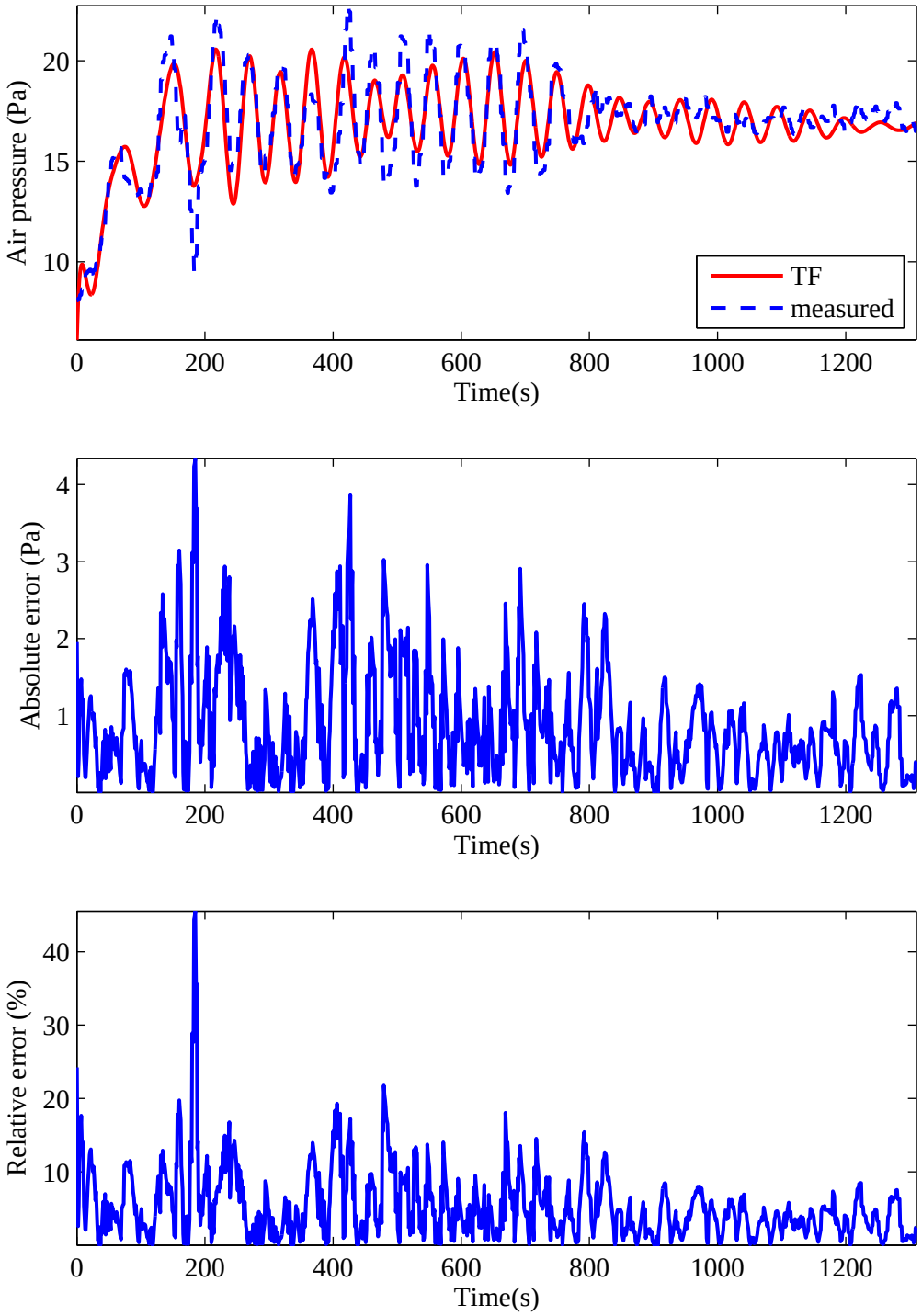

Figure 4.21: Comparison results of the output of the AHU2 related subsystem TF model: AP in the change room.

AHU1 related subsystem

The AHU1 related subsystem has four outputs. The comparison between experiment and prediction results are shown in Figures 4.22-4.33. The three sub-figures in each figure show the plotting of experiment and prediction results, the absolute errors and the relative errors, respectively. The first sub-figures of ARX and SS models for both outputs show a good fit between experiment and prediction results, and it is hard to determine which one is better visually. The difference between experiment and prediction results is significant for TF models which can be easily found from the first sub-figures. The relative errors of each output can then be used to compare the performance of different model structures.

The first output, the ACR in the small lab, is presented in Figures 4.22-4.24 for three model structures: ARX, SS and TF, respectively. The relative errors of the ARX and SS models are similar with about 25% maximum value and smaller than 10% at most time. The TF model apparently has much larger relative errors with more than 40% maximum point and smaller than 20% at most time. Thus, the performance of ARX and SS models are similar and better than TF model.

The second output, the AP in the small lab, is shown in Figures 4.25-4.27 for three model structures including ARX, SS and TF, respectively. The relative errors of the ARX models are below 20% before 800 seconds and can reach smaller than 2% after that. Its maximum is about 65% but only has several points. The relative errors of the SS model are below 20%, but its maximum is up to 160%. The TF model has smaller than 30% relative errors at most time and a 90% maximum point. Concluding from the relative errors of the three models, the ARX model performs the best.

The comparison results of the three models: ARX, SS and TF, for the third output, the ACR in the large lab, are given in Figures 4.28-4.30, respectively. The curves of relative errors for ARX and SS models have similar shapes and values. The values are larger than 10% in the beginning before 200 seconds. Then they go smaller than 2%. Another increasing happens between 400 seconds and 600 seconds which can be up to 40%. After that, the values go down to smaller than 2% until the end. The relative errors of the TF model have the similar shape to the other two

models, but the values are added with 10% to the full range. Thus, the ARX and SS models of this output perform similar and better than the TF model.

The measured data are collected from the original PI controllers. For the facilities in the AHU1 related subsystem, six PI controllers were implemented and worked in cooperation to maintain the steady state. The value of ACR is affected by both the supply fan and the supply VAV. The large lab ACR shown in Figures 4.28-4.30 drops to a low value at 500 seconds. It occurred when both the supply fan speed and the supply VAV position dropped to a low value. The wild fluctuations shown in Figures 4.22-4.27 are also caused by the cooperation between different PI controllers. The output variables are influenced by several drivers.

The comparison results of the three models, which contain ARX, SS and TF, for the fourth output, the AP in the large lab, are shown in Figures 4.31-4.33, respectively. Similar to the relative errors of the third output, the shapes and values of the ARX and SS models are similar. Both of the values are below 10% at most time with a maximum point 15%. TF models also have a similar shape with 10% addition. The TF model has the largest error, but the errors of the ARX and SS model are similar and difficult to compare.

From the comparison results as shown in these figures, TF models perform the worst, and ARX models and TF models have higher and similar performance. The model validation method should be introduced to determine the best model structure.

4.5.3 Model validation results

The metrics presented in Section 4.3.5 are used to validate the identified models. The comparison results of this metric for MIMO models are shown in Table 4.3. For both MIMO subsystem models, the TF models have much smaller goodness of fit values than those of ARX and SS models. The values of ARX and SS models are similar. For all the six outputs, the ARX models have 1-2% larger values than SS models. They all can reach larger than 80% values which provide high accuracy mathematical models to the design of MPC. Thus, the ARX models of both MIMO subsystems have the best performance. They would be used to design the MPC controllers as presented in Chapter 5.

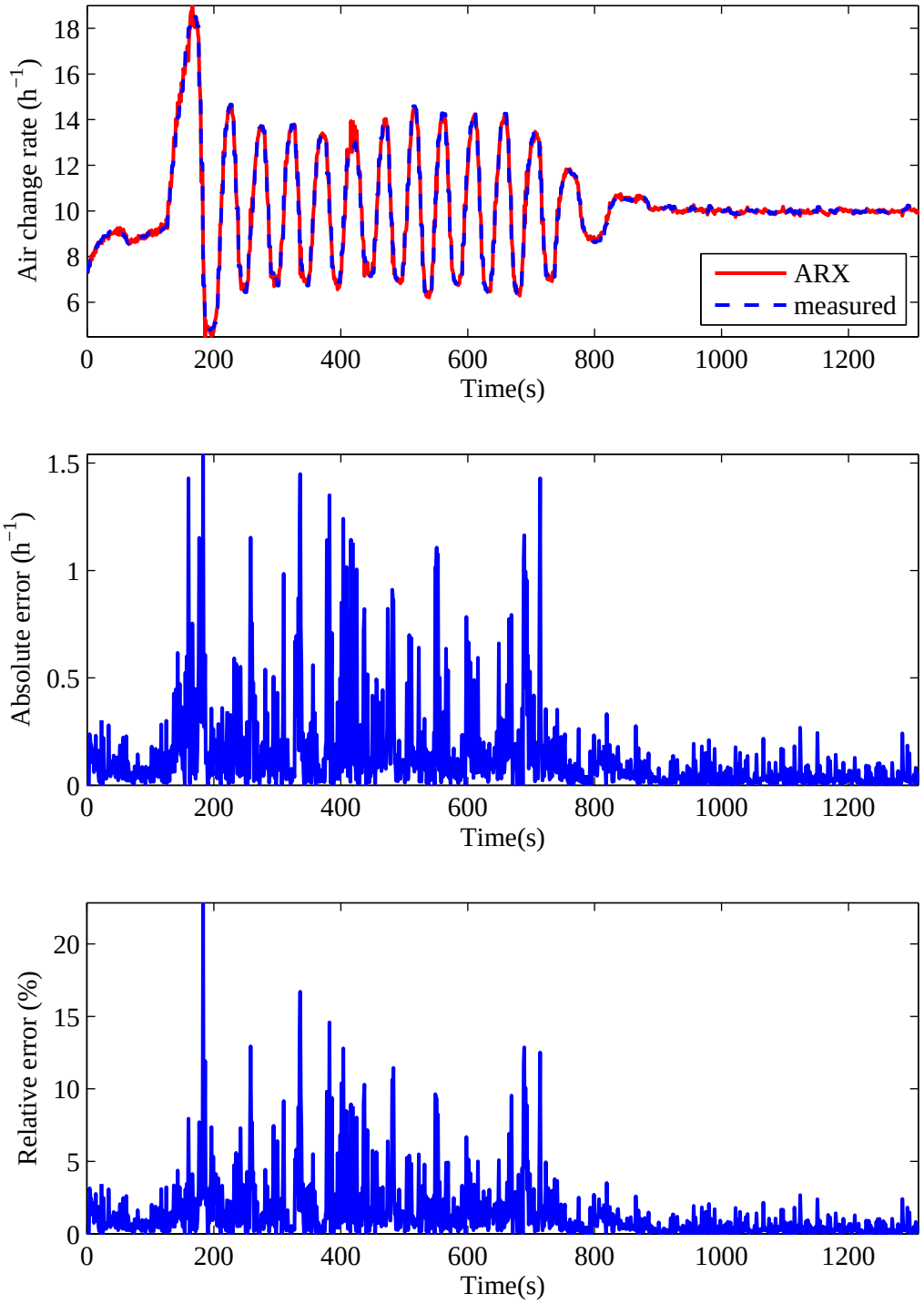

Figure 4.22: Comparison results of the output of the AHU1 related subsystem ARX model: ACR in the small lab.

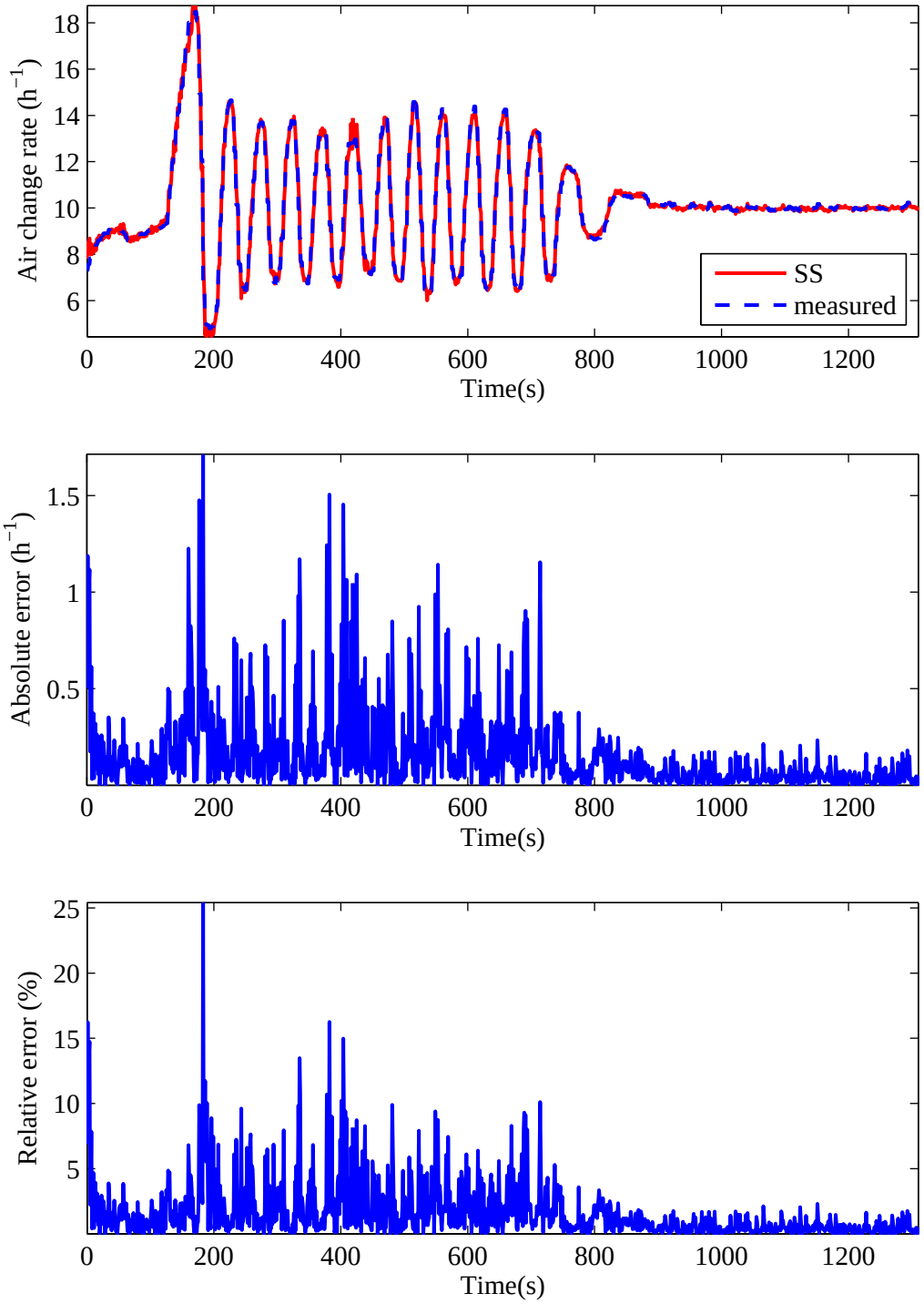

Figure 4.23: Comparison results of the output of the AHU1 related subsystem SS model: ACR in the small lab.

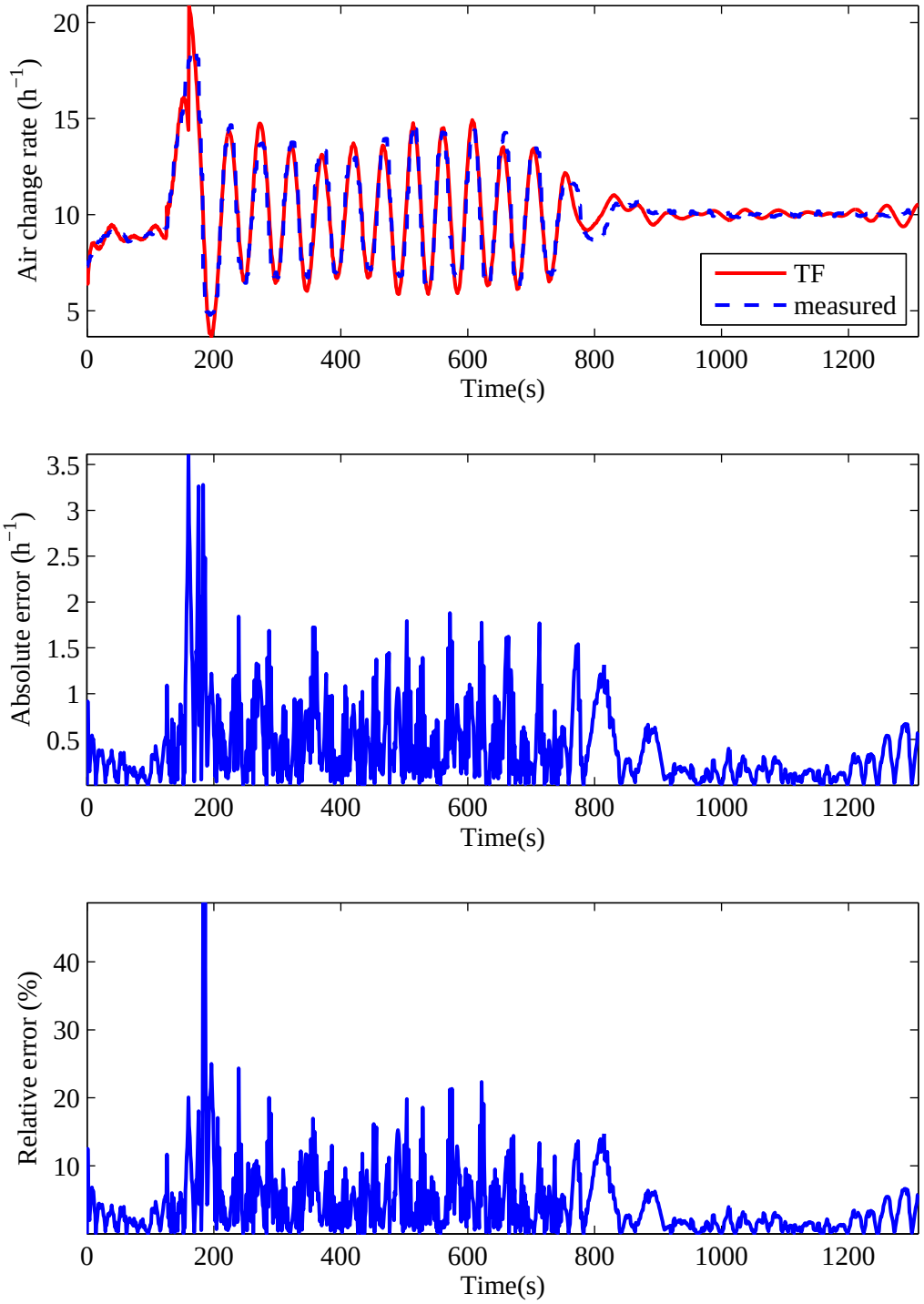

Figure 4.24: Comparison results of the output of the AHU1 related subsystem TF model: ACR in the small lab.

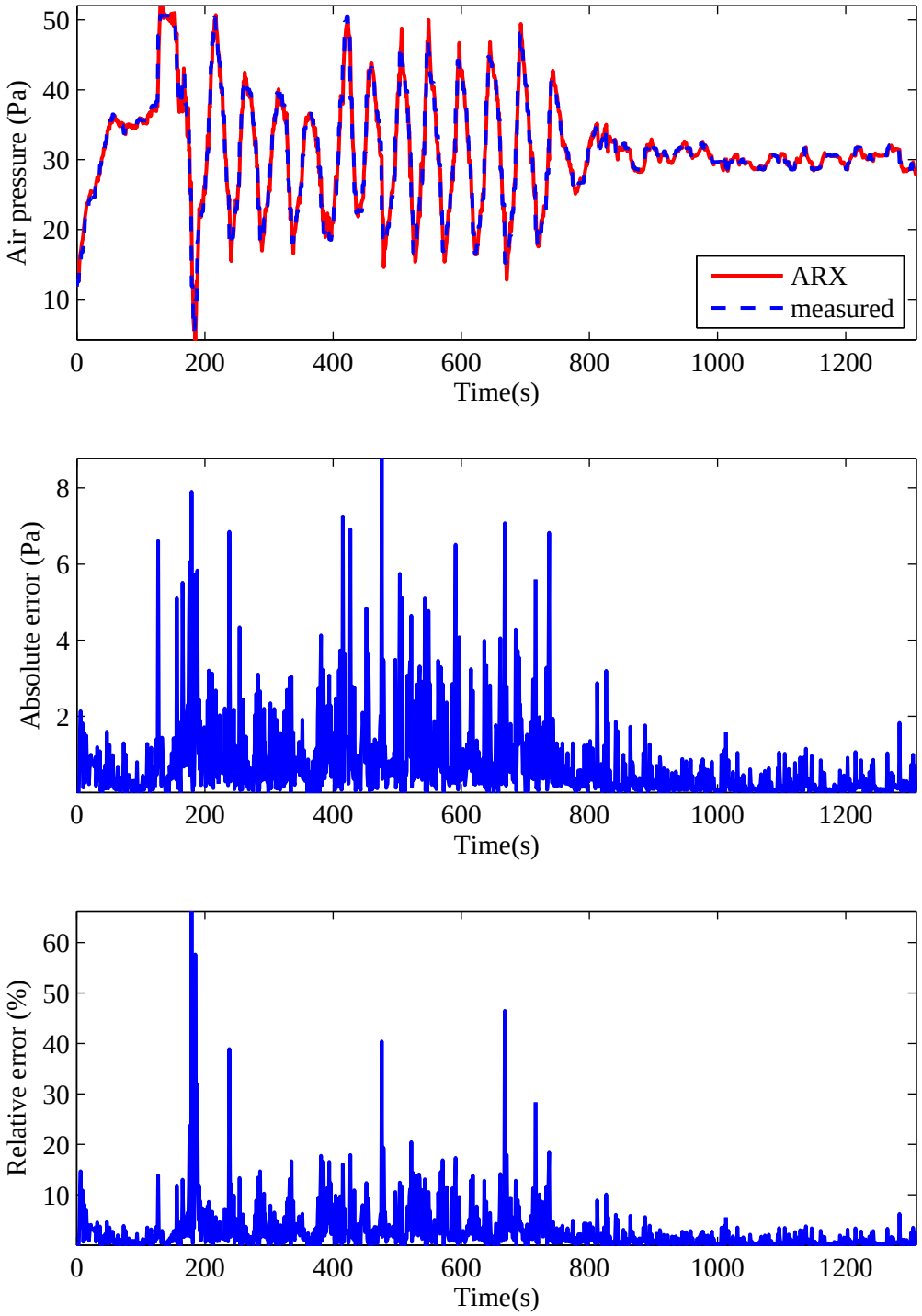

Figure 4.25: Comparison results of the output of the AHU1 related subsystem ARX model: AP in the small lab.

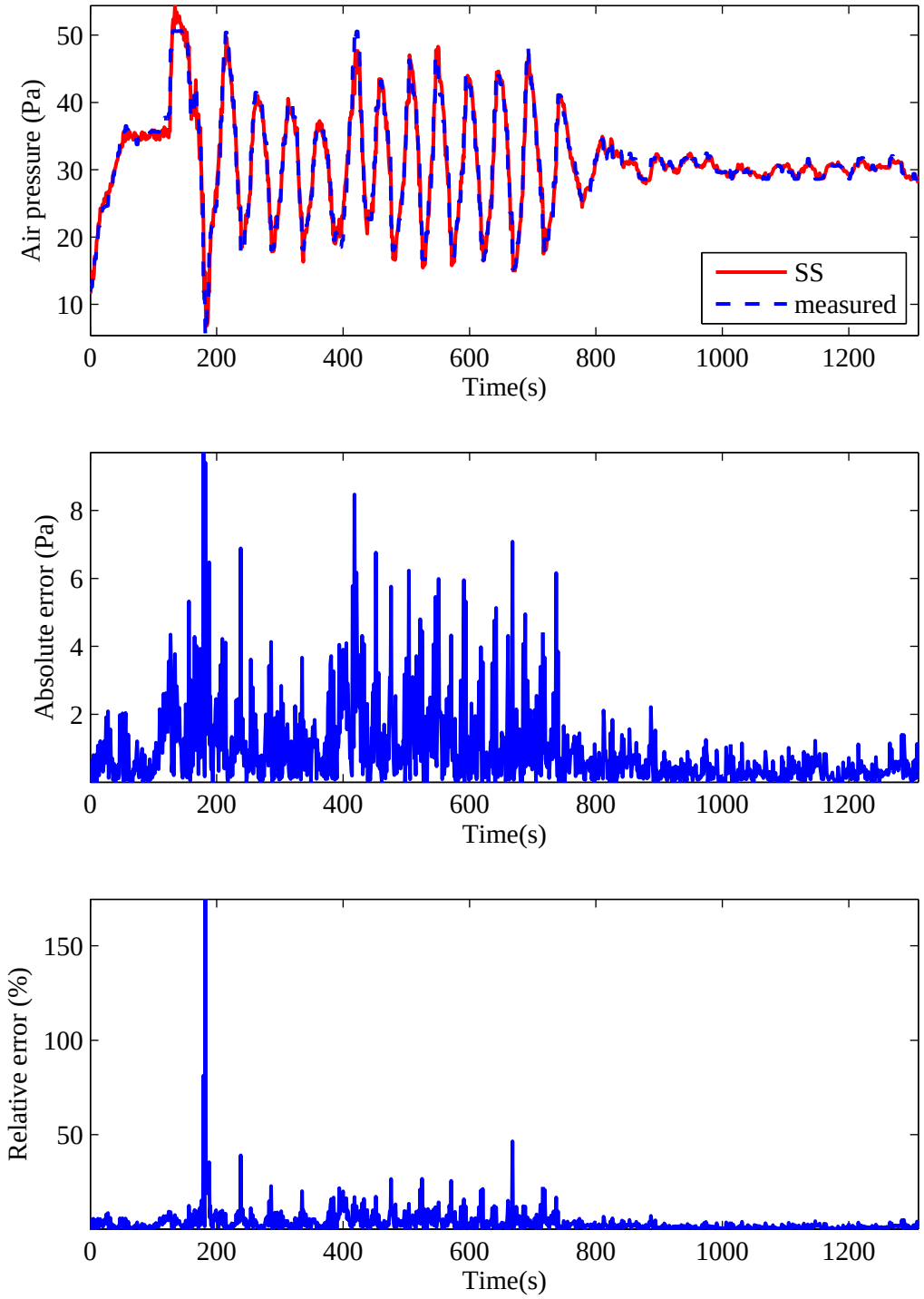

Figure 4.26: Comparison results of the output of the AHU1 related subsystem SS model: AP in the small lab.

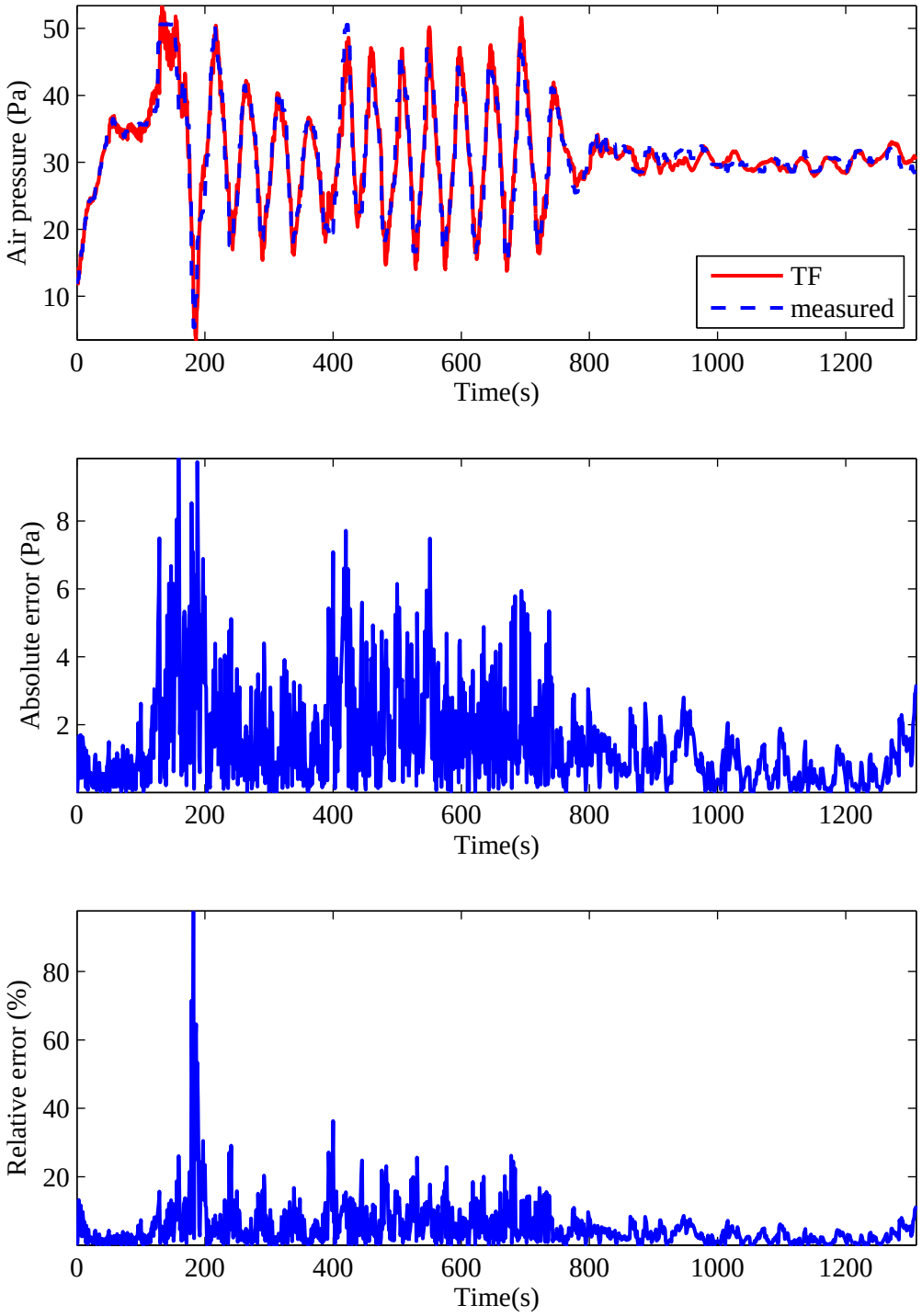

Figure 4.27: Comparison results of the output of the AHU1 related subsystem TF model: AP in the small lab.

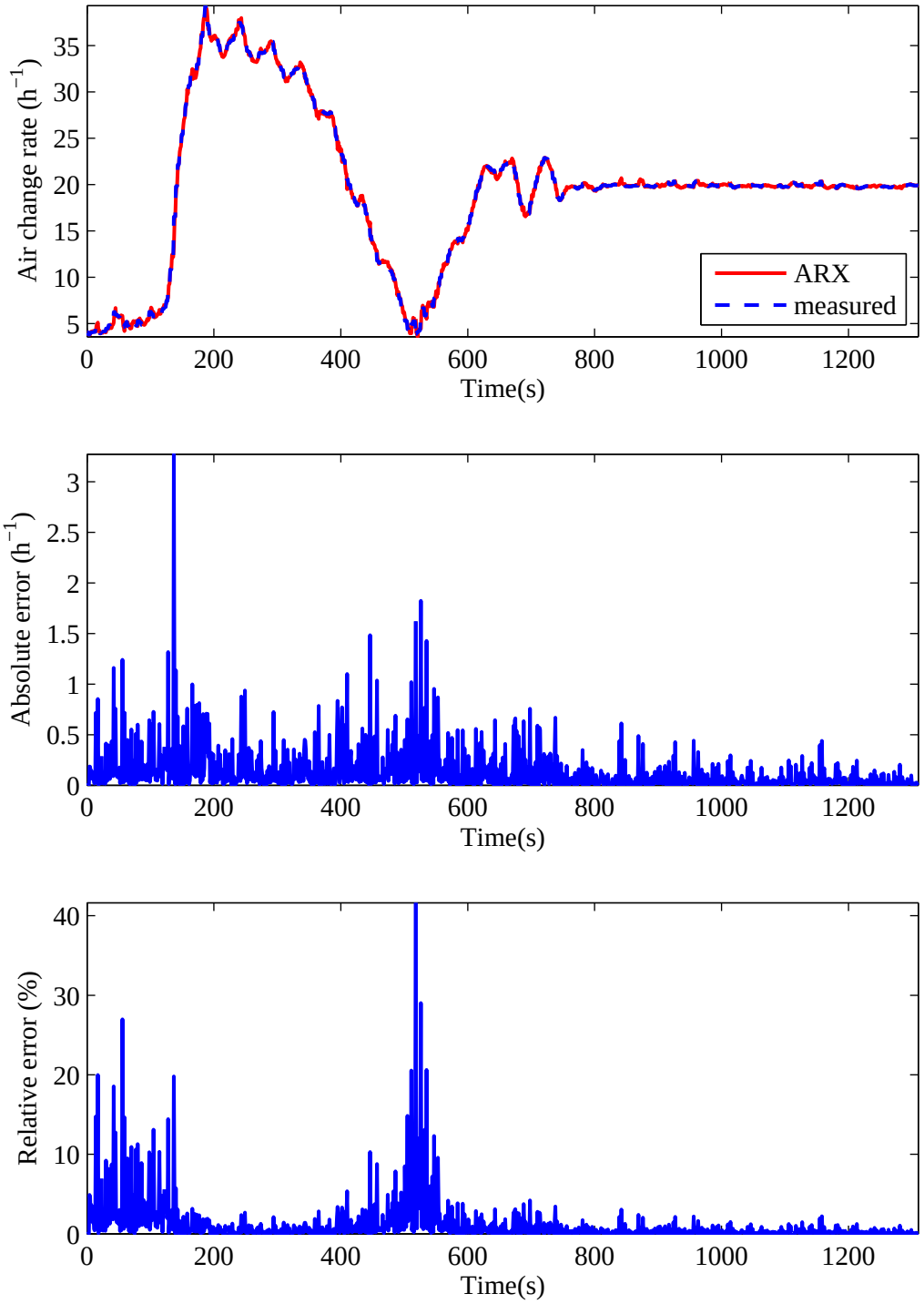

Figure 4.28: Comparison results of the output of the AHU1 related subsystem ARX model: ACR in the large lab.

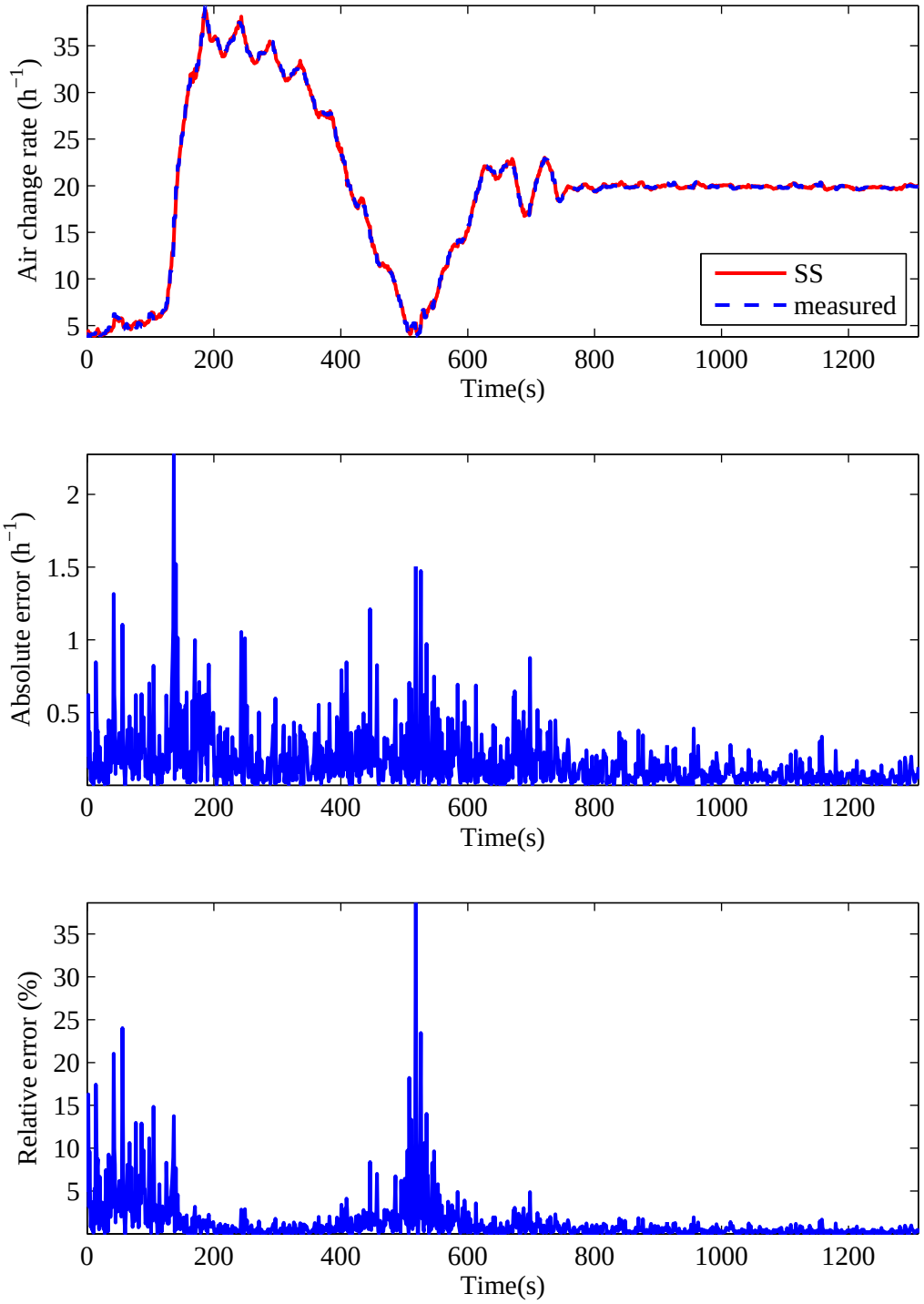

Figure 4.29: Comparison results of the output of the AHU1 related subsystem SS model: ACR in the large lab.

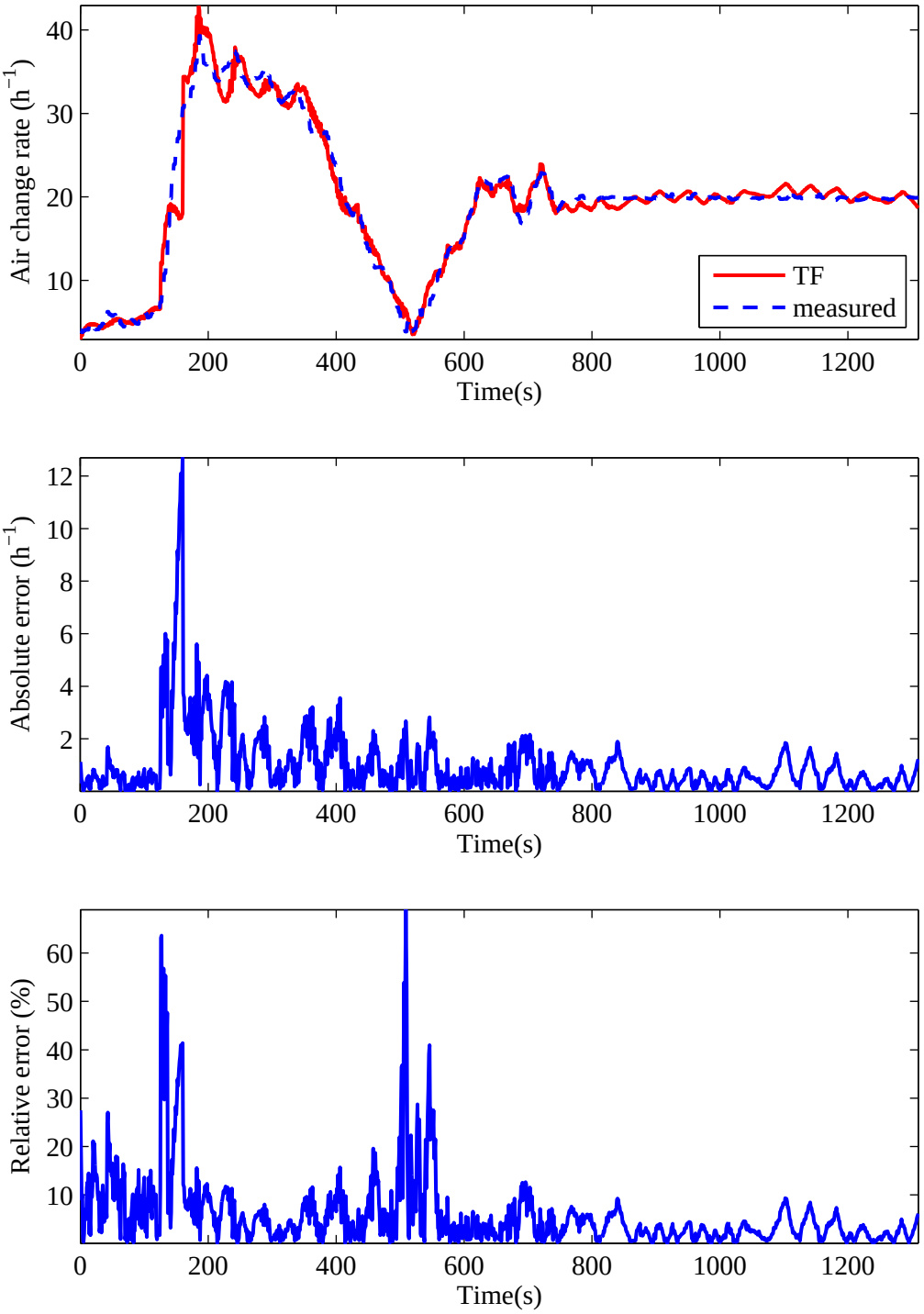

Figure 4.30: Comparison results of the output of the AHU1 related subsystem TF model: ACR in the large lab..

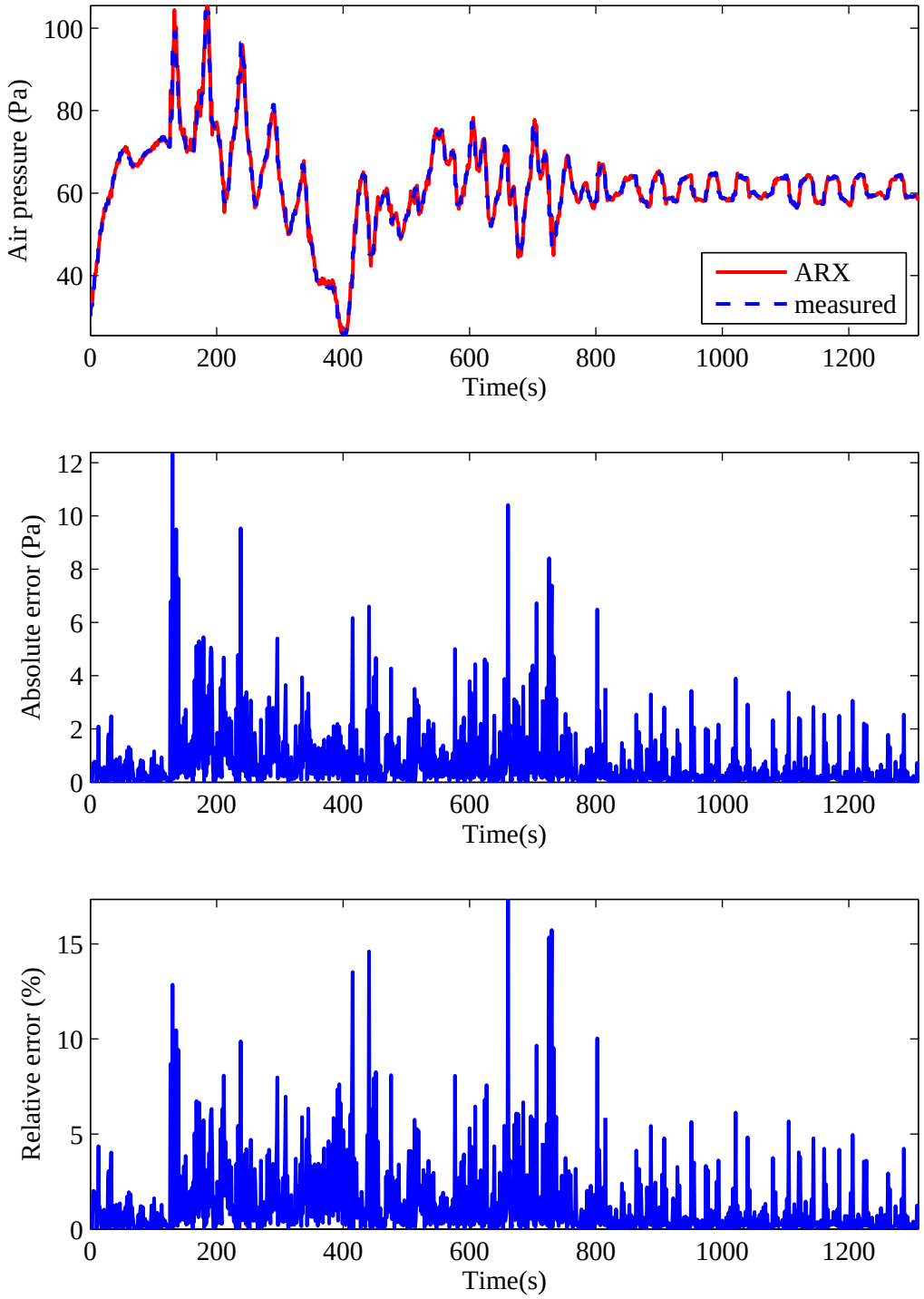

Figure 4.31: Comparison results of the output of the AHU1 related subsystem ARX model: AP in the large lab.

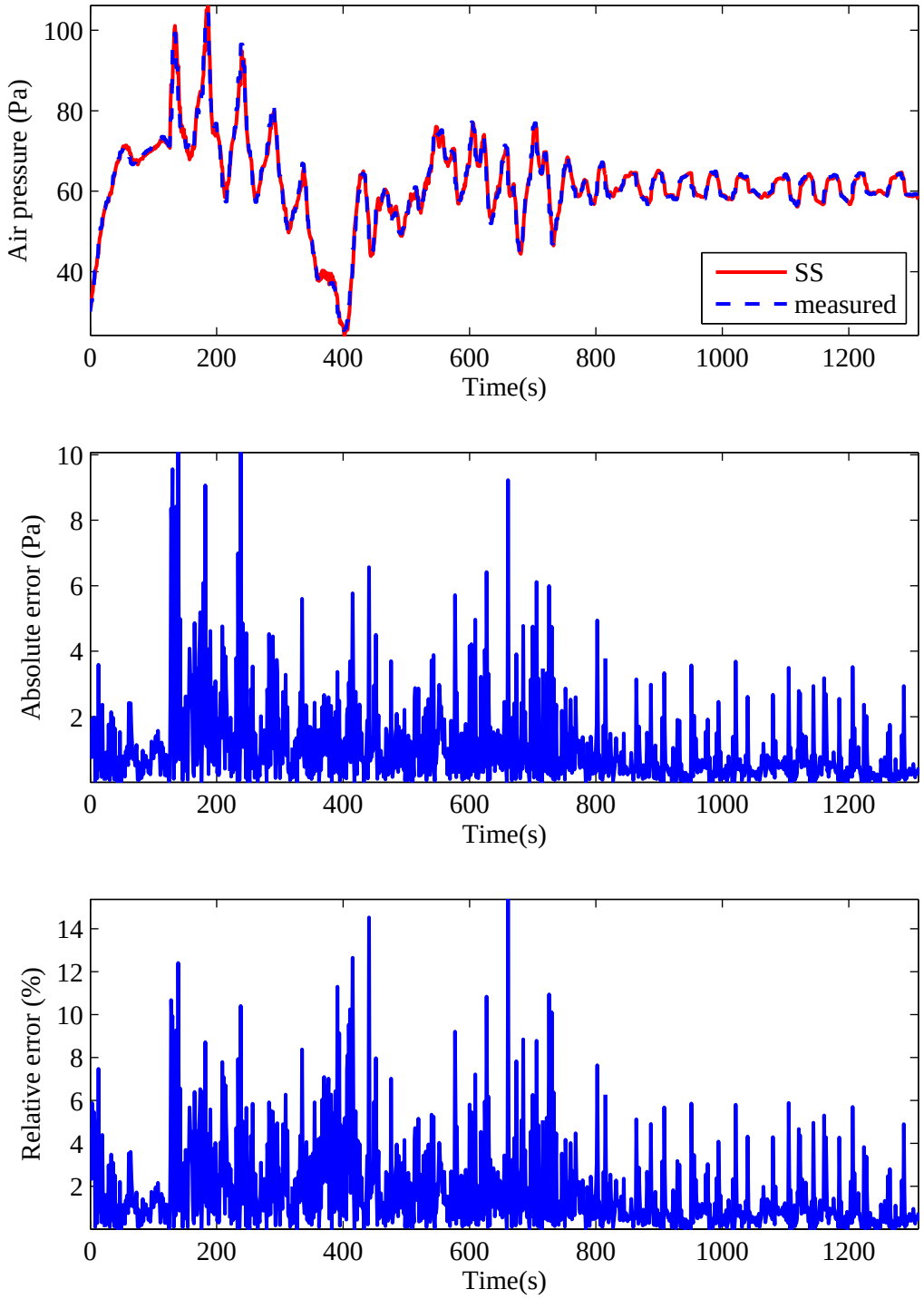

Figure 4.32: Comparison results of the output of the AHU1 related subsystem SS model: AP in the large lab.

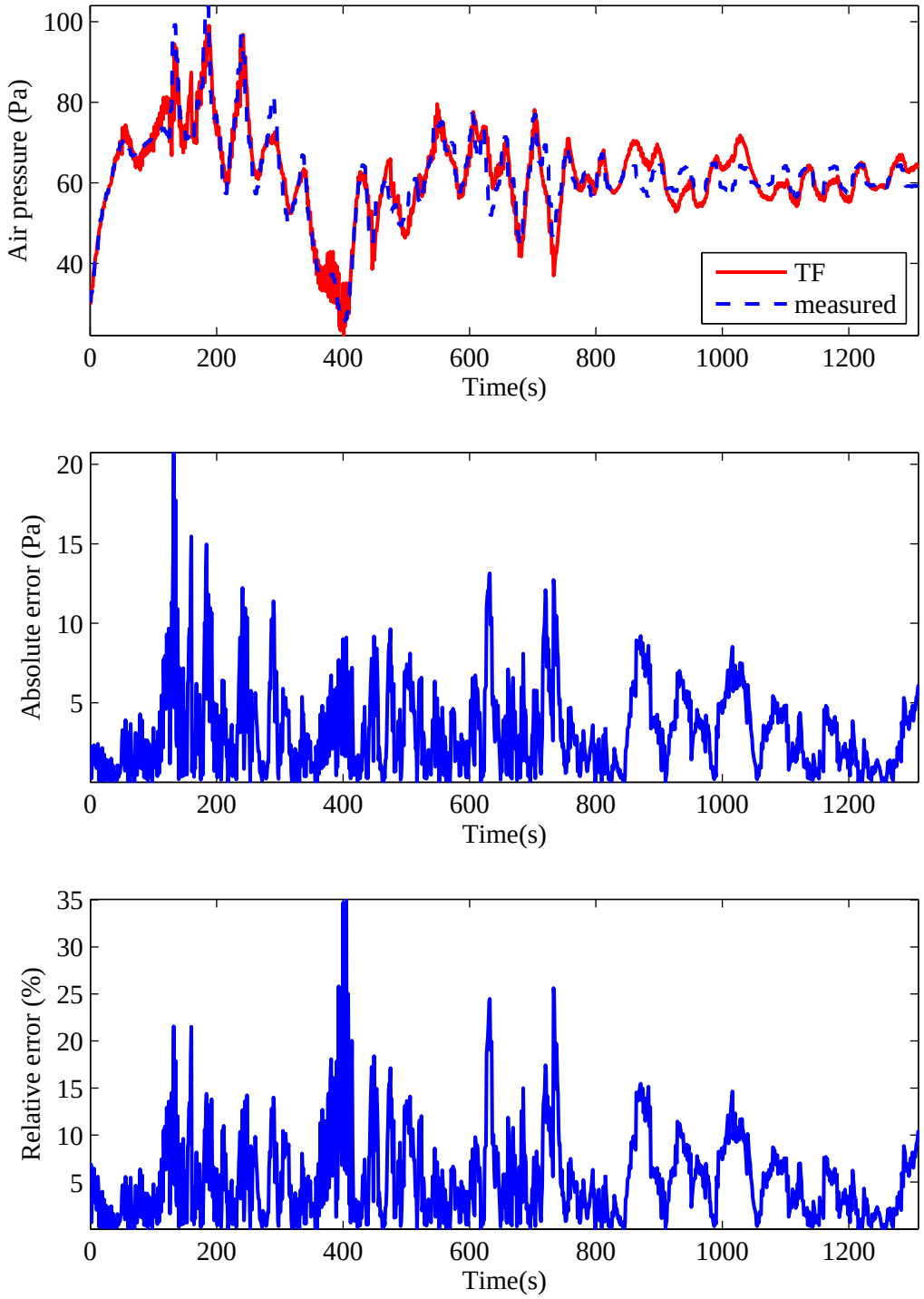

Figure 4.33: Comparison results of the output of the AHU1 related subsystem TF model: AP in the large lab.

Table 4.3: Comparison of goodness of fit for MIMO subsystem models.

Subsystem	Output	ARX model	SS model	TF model	Largest
AHU2 related	Change room ACR	98.6336	97.5228	92.9260	ARX model
	Change room AP	86.6895	84.1417	53.8819	ARX model
AHU1 related	Small lab ACR	89.4177	88.5812	74.2958	ARX model
	Small lab AP	82.7811	80.6683	72.1576	ARX model
	Large lab ACR	97.0737	96.9988	80.6156	ARX model
	Large lab AP	86.9755	84.9315	60.6922	ARX model

4.5.4 Mathematical models

AHU2 related subsystem

Table 4.3 gives the comparison results of the three model structures. The ARX model of the AHU2 related subsystem has the largest value of goodness of fit which indicates that the model identified in ARX model structure performs the best. From the comparison results presented above, the ARX model of the AHU2 related subsystem performs the best. The parameters of the ARX model have been estimated by the PEM resulting in a mathematical model as shown below.

The polynomials of output 1: ACR in the change room, are given:

$$\begin{aligned} A^1(z) &= 1 - 0.9308z^{-1} - 0.01683z^{-2} \\ A_2^1(z) &= 0.001459z^{-1} - 0.001247z^{-2} \\ B_1^1(z) &= 0.002881z^{-1} - 0.001584z^{-2} \\ B_2^1(z) &= 0.002455z^{-1} - 0.001917z^{-2} \\ B_3^1(z) &= -0.03288z^{-1} + 0.03575z^{-2} \\ B_4^1(z) &= -0.04089z^{-1} + 0.03974z^{-2} \end{aligned}$$

The polynomials of output 2: AP in the change room, are given:

$$\begin{aligned}
A^2(z) &= 1 - 0.9941z^{-1} + 0.02603z^{-2} \\
A_1^2(z) &= 6.582z^{-1} - 6.114z^{-2} \\
B_1^2(z) &= 0.001747z^{-1} + 0.01301z^{-2} \\
B_2^2(z) &= -0.01963z^{-1} + 0.02044z^{-2} \\
B_3^2(z) &= 0.6088z^{-1} - 0.5738z^{-2} \\
B_4^2(z) &= -0.08793z^{-1} + 0.07251z^{-2}
\end{aligned}$$

AHU1 related subsystem

The analytical comparison results of the AHU1 related subsystem are shown in Table 4.3 which demonstrate that the ARX model has the lowest ranking value. Thus the best model structure for the AHU1 related subsystem results as ARX. Since the comparison results demonstrate that the ARX model of the AHU1 related subsystem performs the best, it is necessary to conclude its mathematical model. The ARX model of the AHU1 related subsystem is calculated by estimating the parameters using PEM as shown below.

The polynomials of output 1: ACR in the small lab, are given:

$$\begin{aligned}
A^1(z) &= 1 - 0.8022z^{-1} - 0.1639z^{-2} - 0.1813z^{-3} + 0.2168z^{-4} \\
A_2^1(z) &= -0.1083z^{-1} + 0.07385z^{-2} + 0.03656z^{-3} - 0.01553z^{-4} \\
A_3^1(z) &= -0.01973z^{-1} - 0.03086z^{-2} + 0.03025z^{-3} + 0.0169z^{-4} \\
A_4^1(z) &= 0.02861z^{-1} - 0.02132z^{-2} - 0.008246z^{-3} + 0.0028z^{-4} \\
B_1^1(z) &= -0.01095z^{-1} + 0.01648z^{-2} \\
B_2^1(z) &= -0.004499z^{-1} - 0.005395z^{-2} \\
B_3^1(z) &= -0.02596z^{-1} + 0.03307z^{-2} \\
B_4^1(z) &= -0.03301z^{-1} + 0.02988z^{-2} \\
B_5^1(z) &= 0.1432z^{-1} - 0.1385z^{-2} \\
B_6^1(z) &= -0.03717z^{-1} + 0.03687z^{-2}
\end{aligned}$$

The polynomials of output 2: AP in the small lab, are given:

$$
\begin{aligned}
A^2(z) &= 1 - 0.7495z^{-1} - 0.2188z^{-2} - 0.3587z^{-3} + 0.3808z^{-4} \\
A_1^2(z) &= -0.1607z^{-1} + 0.4316z^{-2} - 0.3305z^{-3} + 0.4827z^{-4} \\
A_3^2(z) &= -0.1831z^{-1} + 0.2734z^{-2} + 0.05788z^{-3} - 0.08086z^{-4} \\
A_4^2(z) &= -0.00845z^{-1} + 0.00758z^{-2} + 0.00291z^{-3} + 0.01335z^{-4} \\
B_1^2(z) &= 0.1966z^{-1} - 0.08681z^{-2} \\
B_2^2(z) &= -0.109z^{-1} + 0.1028z^{-2} \\
B_3^2(z) &= -0.1807z^{-1} + 0.2016z^{-2} \\
B_4^2(z) &= -0.1393z^{-1} + 0.1492z^{-2} \\
B_5^2(z) &= 0.092z^{-1} - 0.07514z^{-2} \\
B_6^2(z) &= 0.02752z^{-1} - 0.02868z^{-2}
\end{aligned}
$$

The polynomials of output 3: ACR in the large lab, are given:

$$
\begin{aligned}
A^3(z) &= 1 - 0.946z^{-1} - 0.03805z^{-2} - 0.4217z^{-3} + 0.406z^{-4} \\
A_1^3(z) &= 0.001055z^{-1} - 0.01112z^{-2} - 0.08253z^{-3} + 0.08987z^{-4} \\
A_2^3(z) &= 0.03764z^{-1} - 0.02655z^{-2} - 0.008902z^{-3} - 0.00202z^{-4} \\
A_4^3(z) &= -0.01168z^{-1} + 0.00497z^{-2} + 0.00532z^{-3} + 0.00210z^{-4} \\
B_1^3(z) &= 0.01089z^{-1} - 0.01381z^{-2} \\
B_2^3(z) &= 0.006943z^{-1} - 0.001689z^{-2} \\
B_3^3(z) &= 0.01161z^{-1} - 0.01114z^{-2} \\
B_4^3(z) &= -0.06427z^{-1} + 0.06441z^{-2} \\
B_5^3(z) &= -0.003801z^{-1} + 0.007135z^{-2} \\
B_6^3(z) &= 0.06874z^{-1} - 0.06896z^{-2}
\end{aligned}
$$

The polynomials of output 4: AP in the large lab, are given:

$$
\begin{aligned}
A^4(z) &= 1 - 0.8709z^{-1} - 0.1222z^{-2} - 0.3426z^{-3} + 0.3981z^{-4} \\
A_1^4(z) &= 0.2811z^{-1} - 0.1524z^{-2} - 0.1576z^{-3} - 0.08642z^{-4} \\
A_2^4(z) &= -0.0539z^{-1} + 0.05125z^{-2} + 0.005547z^{-3} - 0.0545z^{-4} \\
A_3^4(z) &= -0.2866z^{-1} + 0.3599z^{-2} + 0.0447z^{-3} - 0.02202z^{-4} \\
B_1^4(z) &= 0.6384z^{-1} - 0.6058z^{-2} \\
B_2^4(z) &= 0.1249z^{-1} - 0.1333z^{-2} \\
B_3^4(z) &= 0.08775z^{-1} - 0.1226z^{-2} \\
B_4^4(z) &= -0.183z^{-1} + 0.2445z^{-2} \\
B_5^4(z) &= -0.123z^{-1} + 0.0977z^{-2} \\
B_6^4(z) &= 0.1712z^{-1} - 0.1762z^{-2}
\end{aligned}
$$

4.6 Conclusion

The black-box models of the cleanroom laboratory equipped with the HVAC system have been developed in this chapter. The SISO models are identified firstly from the original PI control loops. Two MIMO subsystems have been defined. By comparing the three parameter estimation methods: PEM, LS and IV, the best method PEM has been found and applied to identify the MIMO subsystem models with three types of model structures including ARX, SS and TF. The prediction results of these models have been compared with the measured outputs so that the one with the best performance for each subsystem has been found. The ARX models of both subsystems have the best performances.

Chapter 5

Model predictive control of airflow and air pressure of the cleanroom HVAC system

The SISO MPC controllers are designed based on the SISO models aiming to regulate the supply airflow rate and the AP. Also, the MIMO MPC of the cleanroom HVAC system is designed and tested based on the identified MIMO models to maintain the ACR and the AP in the change room, the small lab and the large lab. The performance of the MPC controllers is compared with that of PI controllers by comparing their integral performance indices which include the integral of absolute error (IAE), the integral of squared error (ISE), the integral of time multiplied absolute error (ITAE), and the integral of time multiplied squared error (ITSE). Both simulation and field test results are presented with the comparison of the integral performance indices. The comparison results show that MIMO MPC has the best performance and the least energy consumption.

5.1 Introduction

In buildings, a large amount of the electricity is consumed by the HVAC system. The improvement of the energy efficiency of buildings then become a problem

to improve the energy efficiency of the HVAC system. The development of effective control strategies can decrease the energy consumption of the HVAC system. Compared with PID control, which most industrial process controls rely on, MPC provides improved performance in the dynamics and energy efficiency, especially for field MIMO system. At each time-step, in MPC, control signals are generated by solving a constrained optimal control problem using a dynamic control model and a cost function.

Like most industrial plants, the HVAC system also exhibits a MIMO nature, which means that more than one variable has to be controlled [131]. Some researchers have investigated the dynamics and energy efficiency of MIMO HVAC systems with MPC. The multi-variable nonlinear adaptive control algorithms of temperature and humidity in HVAC systems were studied to achieve optimal energy-saving control [132]. Reference [133] presents the application of a Multi-variable Generalised Predictive Controller for simultaneous temperature and humidity control in an HVAC system. The multi-variable controlled process dynamics is modelled using a set of MISO models on-line identified from measured input-output process data. To control the air conditioning part of a system the designed multivariable predictive controller is considered in a cascade dual-rate control scheme with PID auxiliary controllers. The application of adaptive control for a class of multi-variable processes in HVAC systems is studied in Reference [134]. The thermal dynamics of a two zone fan-coil heating system and environmental zones are simulated by a nonlinear model. The adaptive controller can adapt to a wide range of operating conditions and can maintain the zone temperatures and the boiler temperature close to their respective set-points. MIMO MPC was used for the water flow valve in Reference [135] to control the temperature of multiple zones, and MPC was also applied to regulate the evaporator temperature and pressure by controlling the electronic expansion valve and compressor speed. In Reference [82] a MIMO controller to control the temperature and ventilation of multiple zones in a building with an MPC strategy is proposed. The MIMO controller for the indoor air temperature and relative humidity in a direct expansion air-conditioning system, based on the linearised dynamic model is presented in Reference [136], and in Reference [137]

MPC strategies for buildings with mixed-mode cooling are presented, and their potential performance bounds in terms of energy savings within the thermal comfort constraints are demonstrated.

The HVAC system exhibits a MIMO nature, which means that more than one variable has to be controlled. In this thesis, the controlled variables ACR and AP are coupled, and the interactions are not negligible. The cleanroom laboratory is considered as a MIMO system while MIMO MPC is necessary to be applied to the closed-loop system for the best performance.

5.2 Design of model predictive control

The corresponding MPC algorithm is introduced in this section. The performances of different control methods are compared based on the values of the integral performance indices as shown in this section.

5.2.1 Interface of control

As shown in Figure 5.1, the PI control is implemented by the BMS installed in the cleanroom laboratory. The measured data of the controller inputs and the system outputs of the closed-loops with PI control are collected from the BMS. Sensors and drivers are installed in the laboratory, in which the sensors are used to measure the system outputs, and the drivers receive the controller output data from the PI controllers in the BMS to operate the HVAC facilities. The communication between the sensors and drivers and the BMS is achieved by a MODBUS based OPC server. The data transferred to the OPC server can be collected by the OPC Toolbox in Simulink which can be used to identify the system models. The SISO MPC controllers can be built based on these models and tested through the OPC Toolbox.

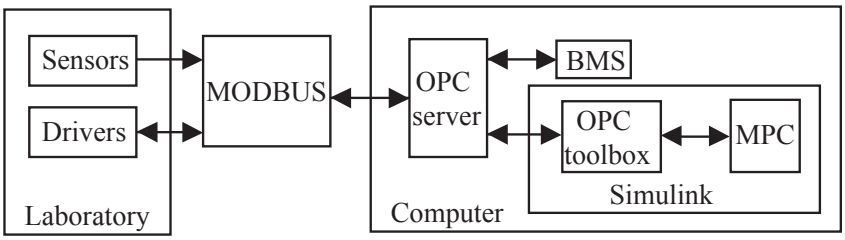

Figure 5.1: Interface of MPC with the laboratory.

5.2.2 Model predictive control algorithm

The MPC uses a system model to predict the future states of the system and generates a control vector that minimises a certain cost function over the prediction horizon in the presence of disturbances and constraints (see Figure 2.3). The system model can be identified using the system identification technology. The basic control law that MPC used is optimisation. At each time step in MPC, an optimal control problem is solved over a finite future horizon. The SS models can be used to formulate the MPC problem. In this chapter, the SS formulation in Reference [38] is used. The identified ARX models can be transferred into SS models which can then be formulated using the following algorithm.

Consider a discrete-time system with no disturbing and no measurement errors:

$$\begin{aligned} x(t+1) &= Ax(t) + Bu(t) \\ y(t) &= Cx(t) \end{aligned}$$

where A,B and C are system matrices, $x(t)$ is the state, $u(t)$ is the control input and $y(t)$ is the output. For SISO models, $y(t)$ and $u(t)$ are scalars and $x(t)$ is a vector. A MIMO process has the same description but with input vectors u of dimension m and y of dimension n.

The prediction for this model is given by [127]

$$\hat{y}(t+k|t) = C\hat{x}(t+k|t) = C[A^k x(t) + \sum_{i=1}^{k} A^{i-1} Bu(t+k-i|t)] \qquad (5.2.1)$$

Defining the control increment $\triangle u(t) = u(t) - u(t-1)$, the increment SS model

is derived:

$$\begin{bmatrix} x(t+1) \\ u(t) \end{bmatrix} = \begin{bmatrix} A\ B \\ 0\ I \end{bmatrix} \begin{bmatrix} x(t) \\ u(t-1) \end{bmatrix} + \begin{bmatrix} B \\ I \end{bmatrix} \triangle u(t) \tag{5.2.2}$$

$$y(t) = [C\ 0] \begin{bmatrix} x(t) \\ u(t-1) \end{bmatrix} \tag{5.2.3}$$

Defining a new state vector as $\hat{x}(t) = [x(t)\ u(t-1)]^T$, the incremental model takes the general form:

$$\hat{x}(t+1) = M\hat{x}(t) + N\triangle u(t) \tag{5.2.4}$$

$$y(t) = Q\hat{x}(t) \tag{5.2.5}$$

The cost function for SISO MPC has a general form:

$$J = \sum_{k=1}^{P} \|w^y[r(t+k) - y(t+k)]\|^2 + \sum_{k=1}^{M} \|w^{\triangle u}\triangle u(t+k-1)\|^2 \tag{5.2.6}$$

subject to the constrains

$$\begin{cases} u_{min} \leq u(t+k) \leq u_{max}, \ \ k = 0, \ldots, M-1 \\ \triangle u_{min} \leq \triangle u(t+k) \leq \triangle u_{max}, \ \ k = 0, \ldots, M-1 \\ y_{min} \leq y(t+k) \leq y_{max}, \ \ k = 0, \ldots, P \end{cases} \tag{5.2.7}$$

where t is the current sampling interval, $t+k$ is a future sampling interval (within the prediction horizon), P is the prediction horizon, w^y is the weight for the output, and $[r(t+k) - y(t+k)]$ is the predicted deviation at future instant $t+k$, M is the control horizon, $\triangle u(t+k-1)$ is the predicted adjustment in the MV at future (or current) sampling interval $t+k-1$ and $w^{\triangle u}$ is the weight for the adjustment of the MV.

In order to minimize the objective function (5.2.6), output predictions over the horizon must be computed resulting in:

$$\hat{y}(t+j) = QM^j\hat{x}(t) + \sum_{i=0}^{j-1} QM^{j-i-1}N\triangle u(t+i) \tag{5.2.8}$$

The estimation of the state vector $x(t)$ is calculated as:

$$\hat{x}(t|t) = \hat{x}(t|t-1) + K(y_m(t) - y(t|t-1)) \tag{5.2.9}$$

where $y_m(t)$ is the measured output. Thus, the predictions along the horizon are given by

$$y = \begin{bmatrix} \hat{y}(t+1|t) \\ \hat{y}(t+2|t) \\ \vdots \\ \hat{y}(t+P|t) \end{bmatrix} = \begin{bmatrix} QM\hat{x}(t) + QN\triangle u(t) \\ QM^2\hat{x}(t) + \sum_{i=0}^{1} QM^{1-i}N\triangle u(t+i) \\ \vdots \\ QM^P\hat{x}(t) + \sum_{i=0}^{P-1} QM^{P-1-i}N\triangle u(t+i) \end{bmatrix} \tag{5.2.10}$$

which can be expressed in vector form as

$$y = F\hat{x}(t) + Hu \tag{5.2.11}$$

where $u = [\triangle u(t)\ \triangle u(t+1) \dots \triangle u(t+M-1)]$ is the vector of future control increments, H is a block lower triangular matrix with its non-null elements defined by $H_{ij} = QM^{i-j}N$ and matrix F is defined as

$$F = \begin{bmatrix} QM \\ QM^2 \\ \vdots \\ QM^P \end{bmatrix} \tag{5.2.12}$$

The control sequence u is calculated minimizing the objective function 5.2.6, that can be written as:

$$J = w^y(r - Hu + F\hat{x}(t))^T(r - Hu + F\hat{x}(t)) + w^{\triangle u}u^Tu \tag{5.2.13}$$

Then an analytical solution exists that provides the optimum as:

$$u = (H^TH + w^{\triangle u}I)^{-1}H^T(r - F\hat{x}(t)) \tag{5.2.14}$$

As a receding horizon strategy is used, only the first element of the control sequence, $\triangle u(t)$, is sent to the plant and all the computation is repeated at the next sampling time.

In most applications, the controller's MVs should move freely (within a constrained region) to compensate for disturbances and set-point changes. An attempt to hold an MV at a point within the region would degrade output set-point tracking.

On the other hand, some plants have more MVs than output set-points. In such a plant, if all MVs are allowed to move freely, the MV values needed to achieve a particular set-point or to reject a particular disturbance would be non-unique. Thus, the MVs would drift within the operating space.

A common approach is to define set-points for "extra" MVs. These set-points usually represent operating conditions that improve safety, economic return, etc. The MIMO MPC design includes an additional term to accommodate such cases, as follows:

$$J_u = \sum_{k=1}^{M} \|w^u[r^u(t+k) - u(t+k-1)]\|^2 \tag{5.2.15}$$

where r^u is the set-point of the MV and w^u is the corresponding weight. By setting a small value of r^u, the minimisation of the control inputs can be implemented.

5.2.3 Integral performance indices

A performance index is a quantitative measure of the performance of a feedback control system that emphasizes those characteristics of the response [128]. The selection of an appropriate performance index is as much a part of the design process as calculating the final system. Commonly used performance indices are based on integral performance measures. In this chapter, the integral performance indices which are defined based on the system error $e(t)$ are calculated in order to give exact comparisons between MPC and PI control. Since the system is non-monotonic, the absolute values or square values of errors are necessary. Thus, four well-known integral performance indices are introduced: IAE, ISE, ITAE, and ITSE which are defined as follows [129] [130]:

$$IAE = \int_0^T |e(t)|dt \tag{5.2.16}$$

$$ISE = \int_0^T e^2(t)dt \tag{5.2.17}$$

$$ITAE = \int_0^T t|e(t)|dt \tag{5.2.18}$$

$$ITSE = \int_0^T te^2(t)dt \tag{5.2.19}$$

where $e(t)$ is the system error: $e(t) = r(t) - y(t)$, $r(t)$ is the reference signal and $y(t)$ is the measured system output. Each of the integral performance indices is calculated over the time interval $[0, T]$. The time T is chosen to span much of the transient response of the system so that a reasonable choice is the settling time.

IAE integrates the absolute error, and ISE integrates the square of the error $e(t)$ over the time interval $[0, T]$, both of which do not add weight to any of the errors in the system response. IAE gives simple mathematical treatment. ISE can deal with highly penalising large control errors which have larger setting time than IAE. ITAE integrates the absolute error multiplied by the time, and ITSE integrates the square of the error $e(t)$ multiplied by the time over the time interval $[0, T]$, both of which give higher weight to the error at the later time. ITAE has the similar effect to IAE which regards the permanence of the control error.

5.2.4 Parameter tuning

To verify the PI and MPC controllers, both discrete controllers have been simulated in Matlab/Simulink. Each SISO model identified above has a corresponding PI controller and MPC controller. The parameters of these controllers are shown in Tables 5.1 and 5.2 respectively. A sample time $T_s = 1s$ is used.

Table 5.1: Parameters of the PI controllers.

Model	K	T_i
AHU 1 supply fan	0.02	0.08
AHU 1 extract fan	0.16	0.18
AHU 2 supply fan	0.24	0.14
AHU 2 extract fan	0.11	0.11
Chang room supply VAV	0.1	0.29
Chang room extract VAV	1.06	0.37
Small lab supply VAV	0.35	0.19
Small lab extract VAV	-0.15	0.06
Large lab supply VAV	0.08	1
Large lab extract VAV	-0.09	0.05

Table 5.2: Parameters of the SISO MPC controllers.

Parameter	Symbol	Value
Weight on the outputs	w^y	1
Weight on the rate of change of inputs	$w^{\triangle u}$	1
Prediction horizon	P	10
Control horizon	M	2
Sampling time	T_s	5 s

The MIMO MPC controllers have been designed in Simulink. The parameters of the MIMO MPC controllers are set based on Table 5.3. The MIMO MPC controllers are designed based on the identified models presented in Chapter 3. The whole HVAC system is divided into two distinct subsystems where the interactions of the variables in each subsystem are taken into account.

Table 5.3: Parameter setting of the MIMO MPC controllers.

Facility	Parameter	Setting
Overall	Sample time	Sample time:5s
	Horizon	Prediction horizon:10, Control horizon:2
Input constraint	Fans	Value:[20,100], Rate:[-2,2]
	VAVs	Value:[0,100], Rate:[-2,2]
Output constraint	Air change rate	[0,40]
	Air pressure	[0,100]
Weights	Input	Value:0 for VAVs and 1 for fans, Rate:1
	Output	Value: 1

ACR is defined by ASHRAE [5] as "airflow in volume units per hour divided by the volume of the space on which the ACR is based in identical units." Thus ACR is calculated as:

$$N = \frac{Q}{V} \tag{5.2.20}$$

where:

- N = Number of air changes per hour (h^{-1})

- Q = Volumetric flow rate of air (l/s)
- V = volume of the room (m^3)

Because ACR is a major factor in particulate control in a cleanroom and is proportional to the airflow rate, the MIMO MPC regulates ACR instead of airflow rate to meet the industrial design standard.

5.3 Simulation results

Ten PI controllers are implemented by the BMS (see Figure 3.1). To compare the performance between PI and SISO MPC controllers, the PI controllers are replaced by the SISO MPC controllers. The MIMO MPC controllers have six outputs which exclude the fans. The parameters of PI and SISO MPC and MIMO MPC controllers are set as shown in Table 5.1, 5.2 and 5.3, respectively. Matlab/Simulink is used to simulate the controllers.

The original laboratory is constructed to simulate a real-time cleanroom with steady airflow rate and AP. The set-points of the simulation tests are set as constant values. The simulation tests verify the process that the plant is turned on at the beginning and runs in steady state after a while. The sample time is 1 second. The mathematical models identified in Chapter 4 are used to be the simulation plant in the simulation test. All the controllers have passed the simulation test since they can track the set-points within 20 minutes.

The four outputs related to the fans are not included in the MIMO MPC controllers. Figure 5.2 presents the simulation results for these four outputs of the PI and SISO MPC controllers. For the AHU1 supply AP, they have similar performance. However, SISO MPC controllers show much better performance for the other three outputs. They have much less settling time and less overshoot compared to PI controllers. The AHU1 supply extract AP MPC controller reaches steady state at about 150 seconds with a small overshoot, while the PI controller reaches at 1000 seconds with more than five large overshoots. The settling time of both two AHU2 MPC controllers is about 200 seconds. The settling time of the AHU2 PI controllers is more than 600 seconds. There is no overshoot with these two MPC controllers.

Moreover, PI controllers are difficult to get rid of the overshoot signals. Thus, for these four fan related outputs, the SISO MPC controllers perform better than the PI controllers.

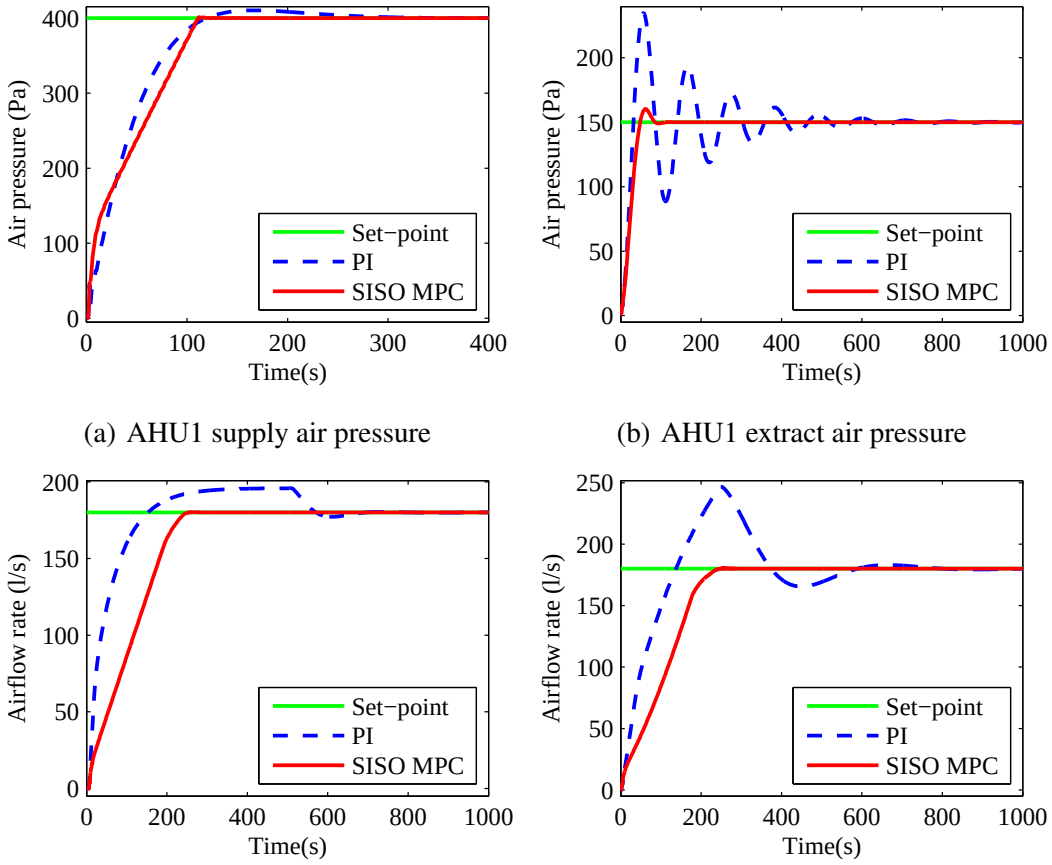

(a) AHU1 supply air pressure

(b) AHU1 extract air pressure

(c) AHU2 supply airflow rate

(d) AHU2 extract airflow rate

Figure 5.2: Comparison results between SISO MPC and PI control for the tracking response of the output variables related to fans (simulation results).

The MIMO MPC has been designed and simulated in Matlab/Simulink, the results of which are compared with PI and SISO MPC controllers. The simulation results for the MVs of the PI and MPC controllers are shown in Figures 5.3 and 5.4. The simulation results for the tracking response of PI and MPC controllers are presented in Figure 5.5. The results of the performance indices for the controllers are shown in Table 5.4.

The SISO MPC controllers show better performance with less settling time and

less overshoot than the PI controllers. Table 5.4 can demonstrate the results that the values of the performance indices of the SISO MPC controllers are smaller than those of PI controllers. The figures and the comparison of the performance indices clearly show that the SISO MPC controllers have better performance than PI controllers.

However, the results indicate that the MIMO MPC controllers do not perform well. The settling time of most outputs can be about 3000 seconds. Some of them have larger overshoot than SISO MPC and PI controllers. Also in Table 5.4, the performance indices of MIMO MPC controllers are larger than those of SISO MPC and PI controllers. The identified MIMO models are much more complex than the SISO models. The MIMO models have the smaller goodness of fit and cannot simulate the plant accurately. That makes the SISO controllers easy to reach the steady state with good performance.

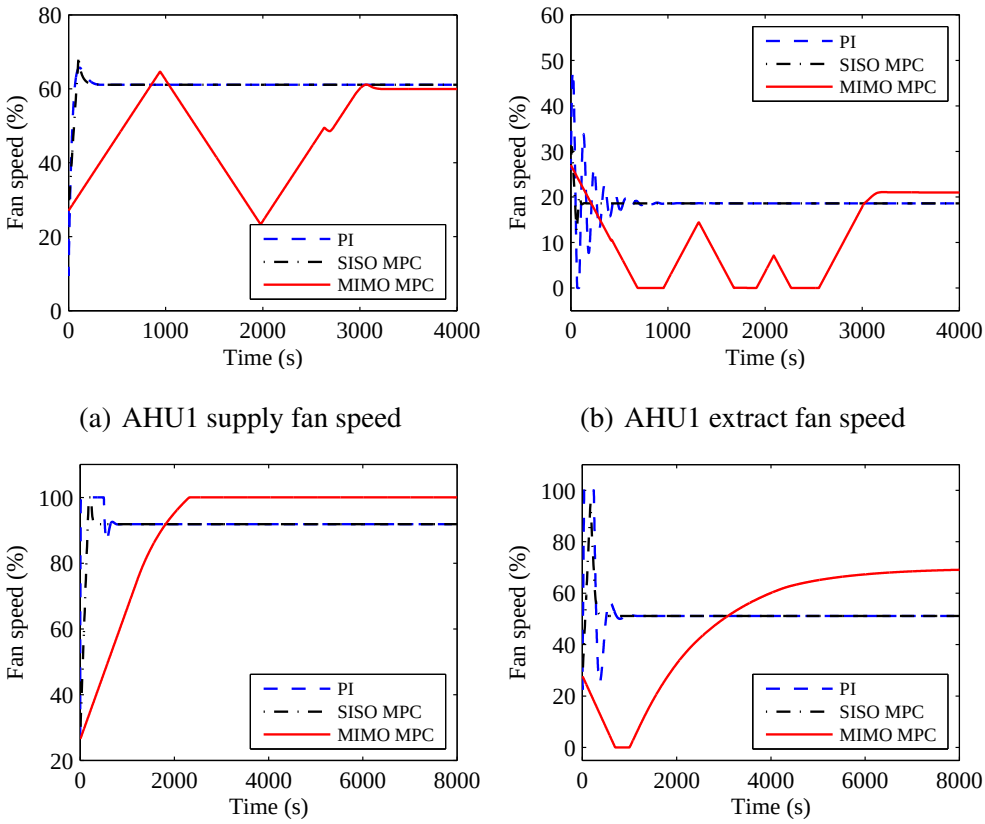

(a) AHU1 supply fan speed

(b) AHU1 extract fan speed

(c) AHU2 supply fan speed

(d) AHU2 extract fan speed

Figure 5.3: Comparison results between MPC and PI control for the MVs (simulation results, fan related).

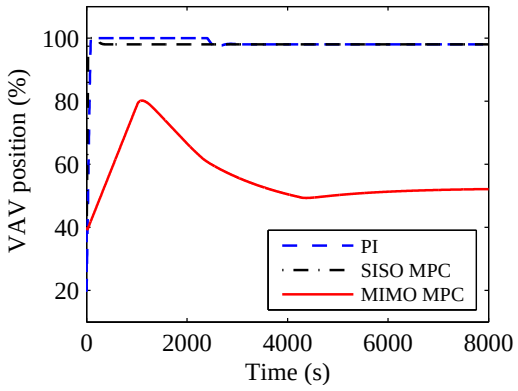

(a) Change room supply VAV position

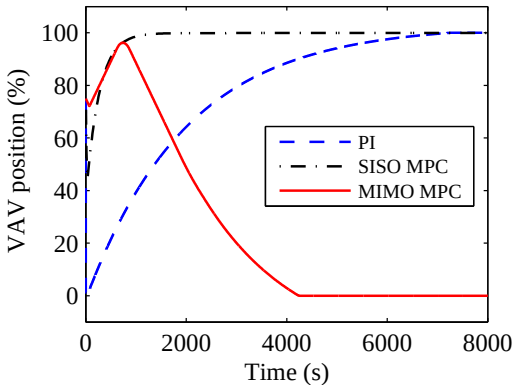

(b) Change room extract VAV position

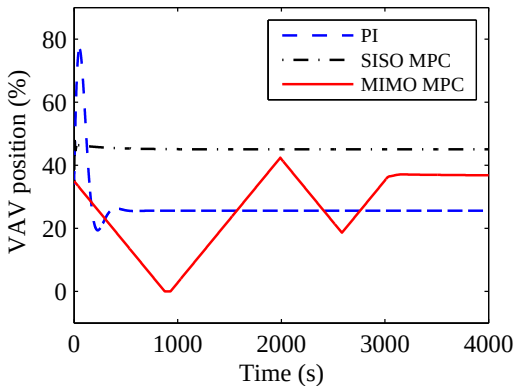

(c) Small lab supply VAV position

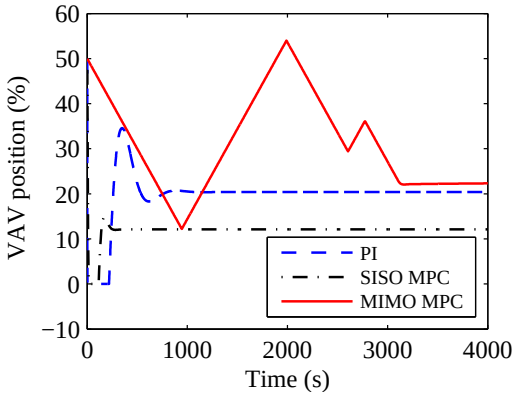

(d) Small lab extract VAV position

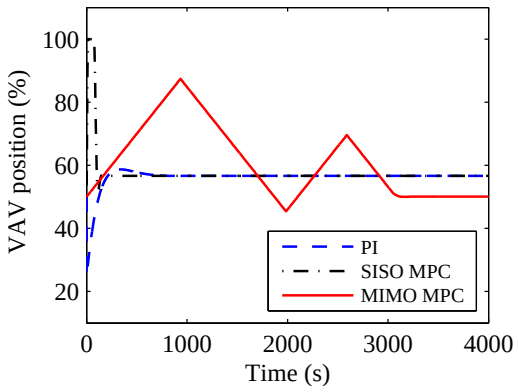

(e) Large lab supply VAV position

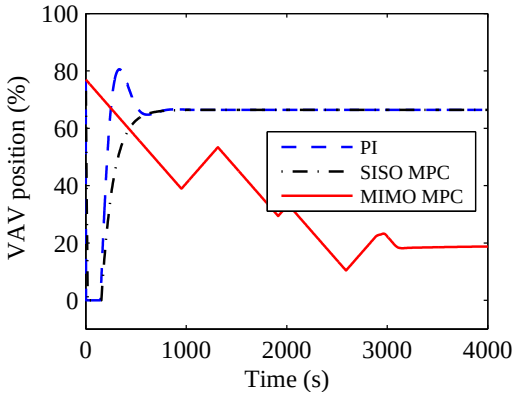

(f) Large lab extract VAV position

Figure 5.4: Comparison results between MPC and PI control for the MVs (simulation results, VAV related).

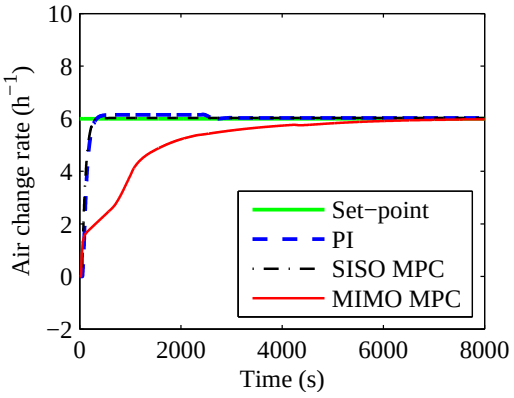

(a) Change room air change rate

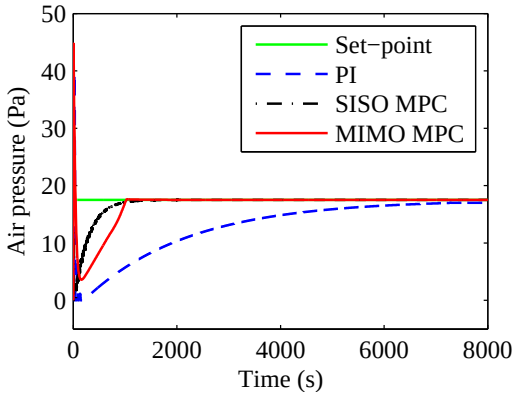

(b) Change room air pressure

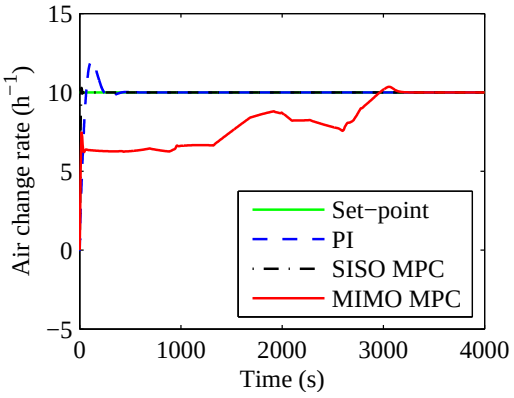

(c) Small lab air change rate

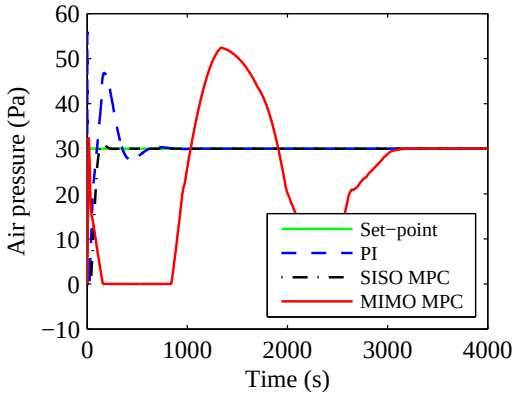

(d) Small lab air pressure

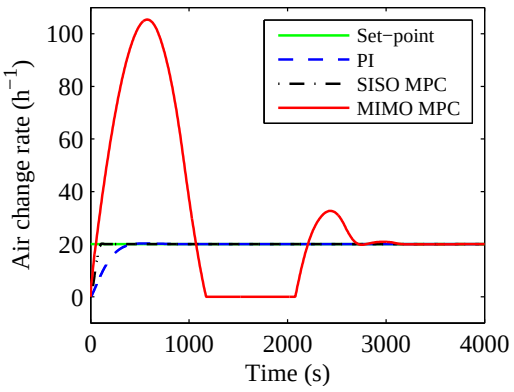

(e) Large lab air change rate

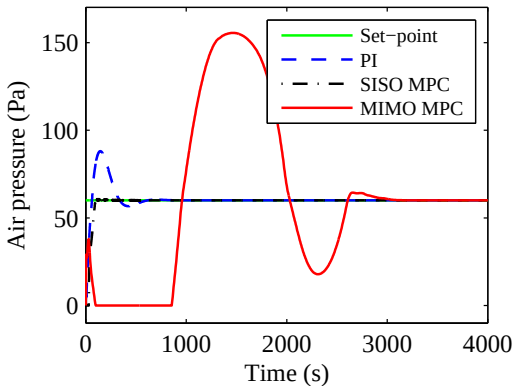

(f) Large lab air pressure

Figure 5.5: Comparison results between MPC and PI control for the tracking response of the output variables (simulation results).

Table 5.4: Comparison of the performance indices between PI controllers and MPC controllers (simulation results).

Output	Controller	IAE($\times 10^4$)	ISE($\times 10^6$)	ITAE($\times 10^6$)	ITSE($\times 10^8$)
Change room ACR	PI	2.7390	3.3837	4.2820	2.0430
	SISO MPC	2.0571	2.6719	1.5206	1.2796
	MIMO MPC	0.6285	0.0168	8.3925	0.0925
Change room AP	PI	1.8708	2.7054	1.4418	1.1823
	SISO MPC	5.2607	5.7088	1.1929	7.7034
	MIMO MPC	0.8449	0.0885	3.4658	0.2654
Small lab ACR	PI	0.1486	0.0574	0.0437	0.0047
	SISO MPC	0.0684	0.0429	0.0037	0.0015
	MIMO MPC	0.7689	2.3203	9.0766	0.2219
Small lab AP	PI	0.4278	0.0646	0.7487	0.0678
	SISO MPC	0.2252	0.0539	0.1029	0.0175
	MIMO MPC	5.3636	1.2215	6.6262	1.2977
Large lab ACR	PI	4.4823	8.0729	5.4331	5.6265
	SISO MPC	1.4802	3.0903	0.4699	0.7059
	MIMO MPC	8.0692	4.1970	7.4552	2.8468
Large lab AP	PI	0.6754	0.1665	1.0839	0.1690
	SISO MPC	0.3208	0.1454	0.1255	0.0331
	MIMO MPC	1.4267	9.4262	1.7357	1.1387

5.4 Field test results

The signal transferred to the hardware is overridden by the MPC controllers built in Matlab/Simulink. The communication of signals is implemented as presented in Section 5.2.1. A hardware-in-loop process is built where the MPC is run in Matlab/Simulink, and the control signal is sent to the hardware through OPC server. At each step, the MPC controller predicts one set of the outputs and transfer them into the hardware through OPC server. The prediction is based on the pre-identified subsystem models. The system is turned off initially. It is turned on at the same time

the controllers begin to work. The sample time of the PI controllers is 1 second. However, the sample time of the MPC controllers is 5 seconds because of the large delay between OPC server and Matlab.

5.4.1 Comparison among PI, SISO and MIMO model predictive control

Figure 5.6 shows the field test results for the tracking response related to fans of PI and SISO MPC controllers. These four outputs are not included in the MIMO MPC controllers. The SISO MPC controllers have less rise time than the PI controllers because the MPC controllers have to be run with large sample time to deal with the large delay. The SISO MPC controllers show better performance with fewer fluctuations and smaller overshoot.

Figures 5.7 and 5.8 present the field test results for the MVs of PI and MPC controllers. Figure 5.9 shows the field test results for the tracking response of PI and MPC controllers.

It can be found from Figure 5.9 that the AHU1 related subsystem reaches its steady state much faster with MIMO MPC controllers than with SISO MPC and PI controllers. Moreover, SISO MPC and PI controllers have more fluctuations than MIMO MPC controller during response time. The comparison results show that MIMO MPC controllers perform better than SISO MPC and PI controllers.

Figure 5.9 also presents the comparison results between MPC and PI control in the AHU2 related subsystem. The results show that the PI responses much faster than MPC when controlling the ACR. However, the response time of AP remains almost the same for MPC and PI control.

Table 5.5 compares the calculated integral performance indices for PI and MPC controllers. It is found that the performance indices of MIMO MPC controllers are smaller than those of SISO MPC and PI controllers. It can be concluded that MIMO MPC controllers perform better than SISO MPC and PI controllers in field tests.

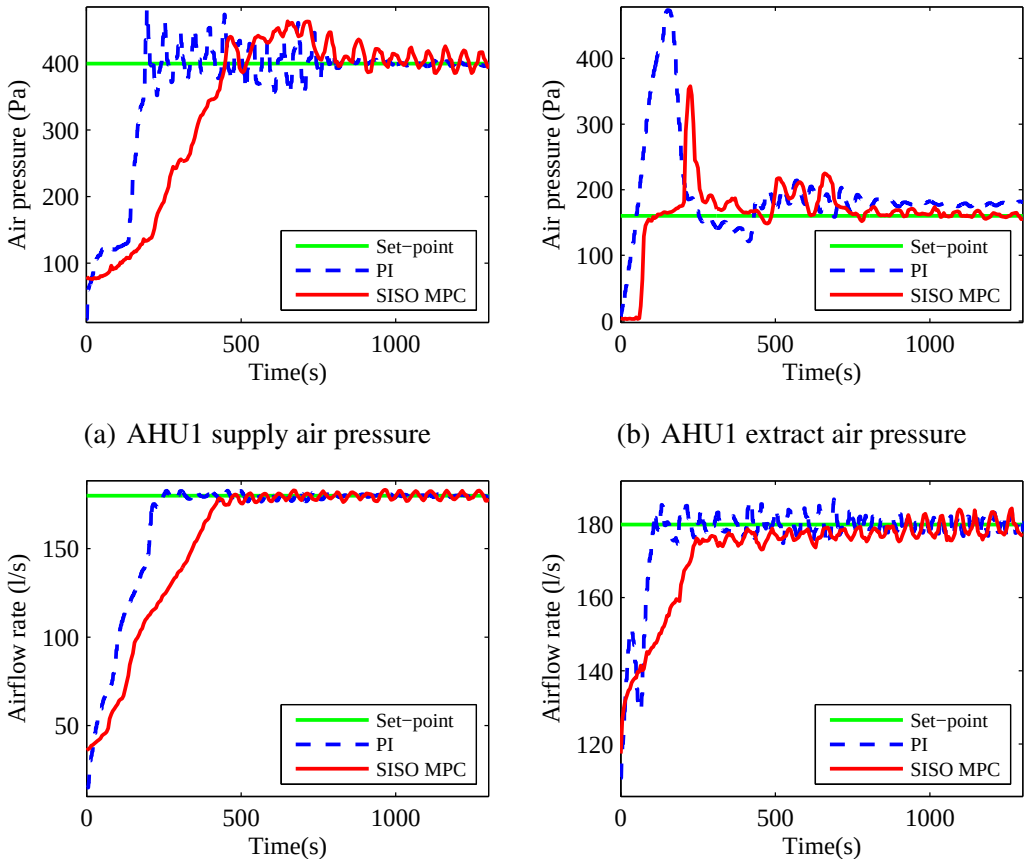

(a) AHU1 supply air pressure

(b) AHU1 extract air pressure

(c) AHU2 supply airflow rate

(d) AHU2 extract airflow rate

Figure 5.6: Comparison results between SISO MPC and PI control for the tracking response of the output variables related to fans (field test results).

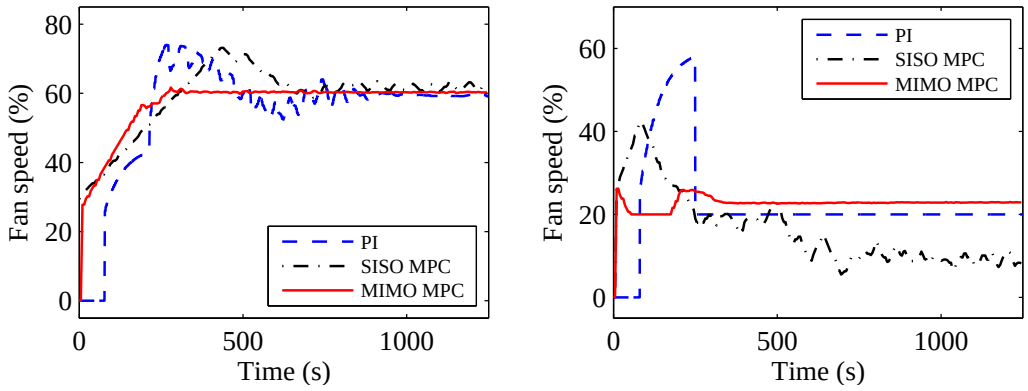

(a) AHU1 supply fan speed

(b) AHU1 extract fan speed

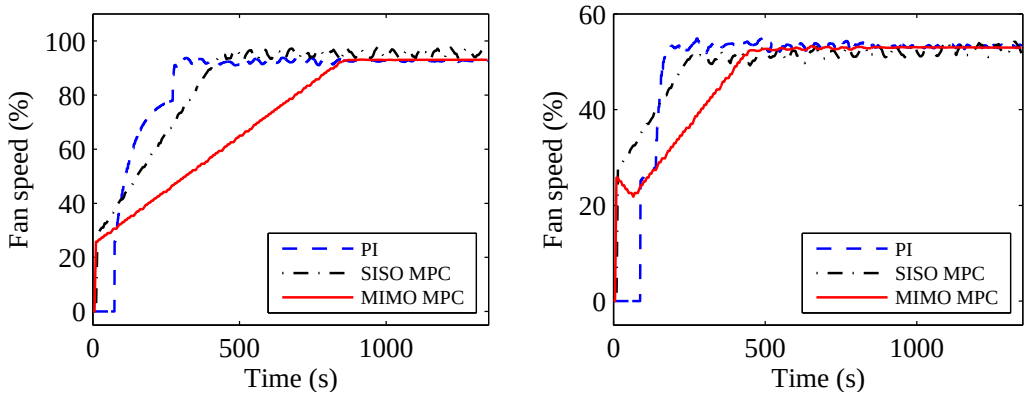

(c) AHU2 supply fan speed

(d) AHU2 extract fan speed

Figure 5.7: Comparison results between MPC and PI control for the MVs (field test, fan related).

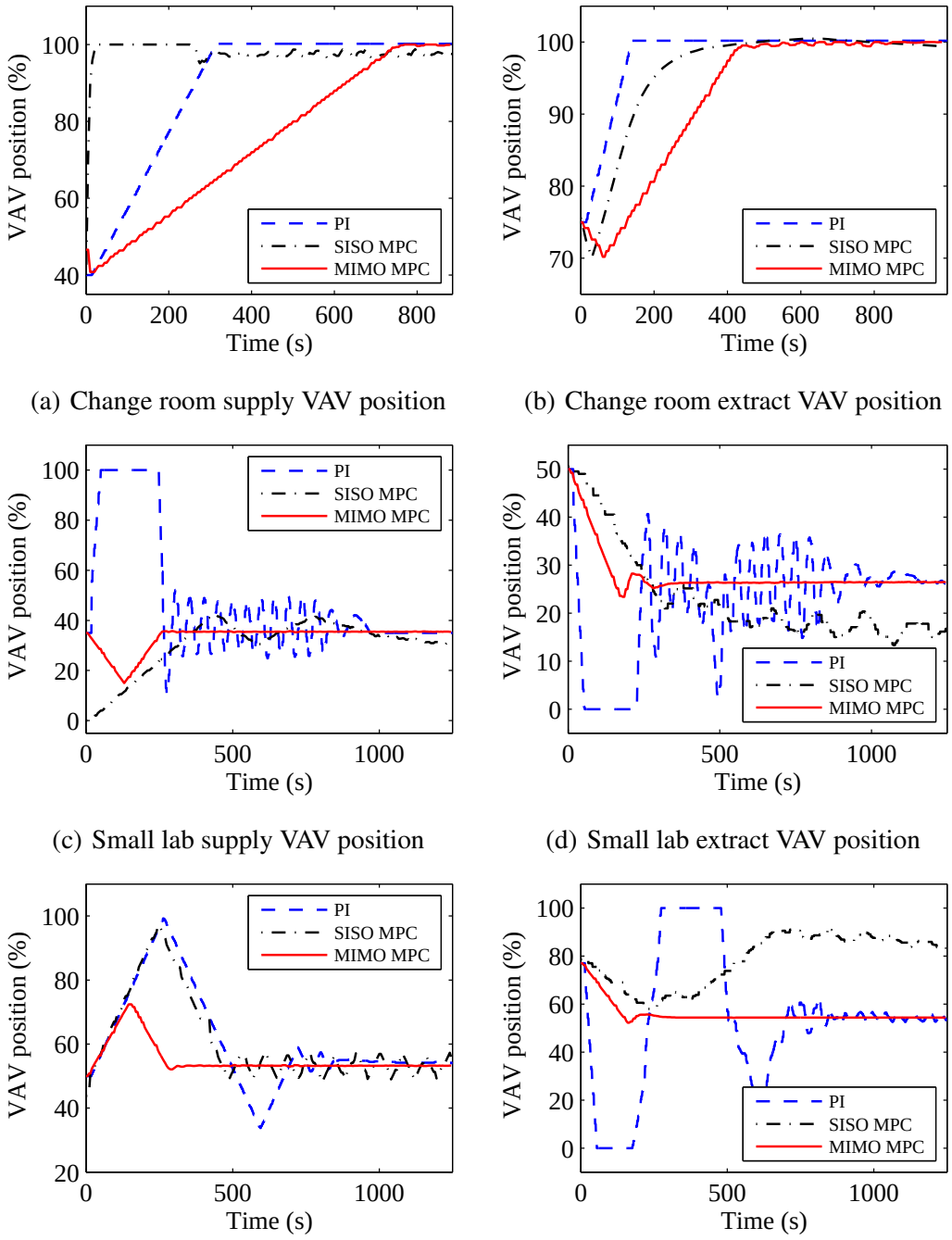

(a) Change room supply VAV position

(b) Change room extract VAV position

(c) Small lab supply VAV position

(d) Small lab extract VAV position

(e) Large lab supply VAV position

(f) Large lab extract VAV position

Figure 5.8: Comparison results between MPC and PI control for the MVs (field test, VAV related).

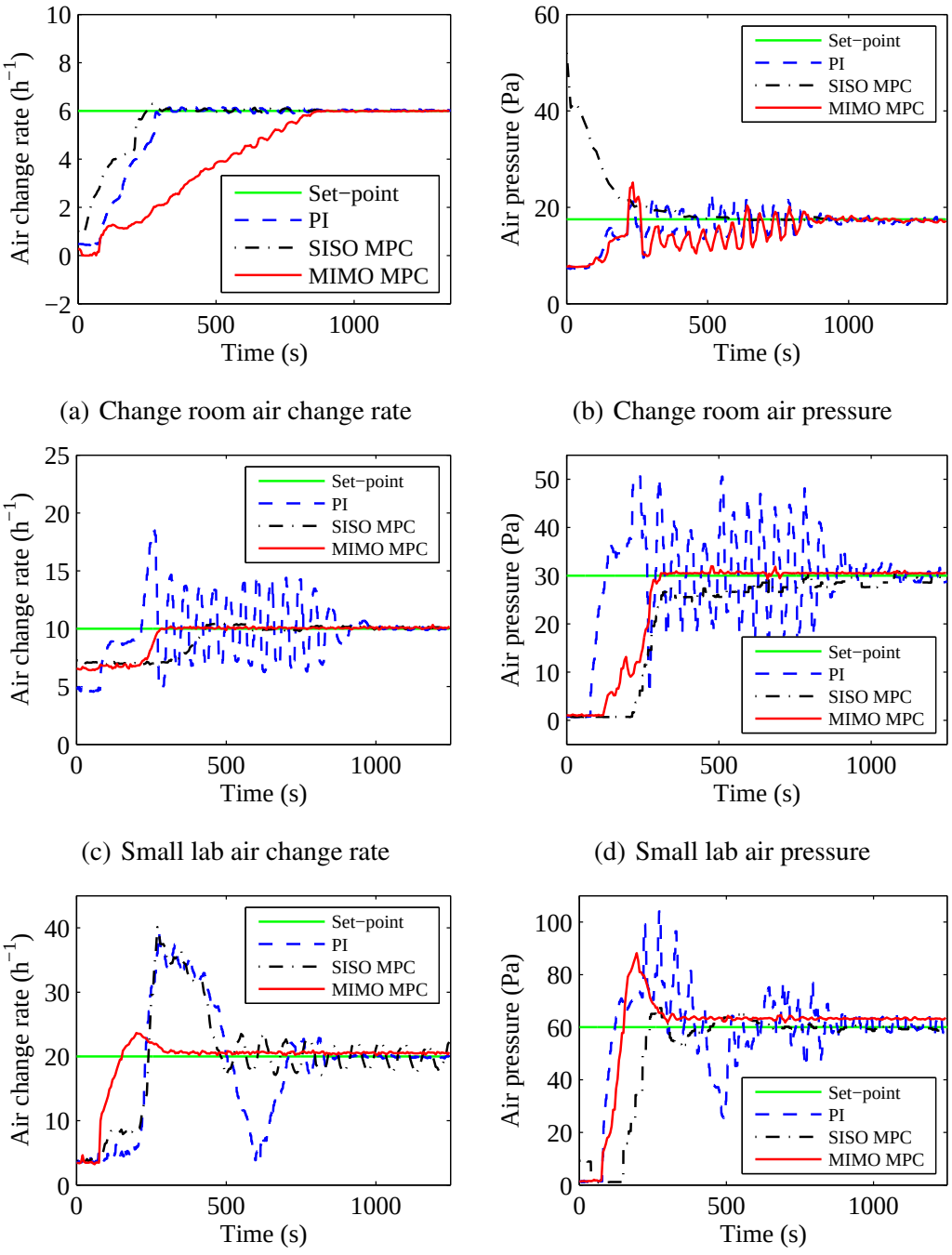

(a) Change room air change rate

(b) Change room air pressure

(c) Small lab air change rate

(d) Small lab air pressure

(e) Large lab air change rate

(f) Large lab air pressure

Figure 5.9: Comparison results between MPC and PI control for the tracking response of the output variables (field test).

Table 5.5: Comparison of the performance indices between PI and MPC controllers (field test).

Output	Controller	IAE($\times 10^4$)	ISE($\times 10^6$)	ITAE($\times 10^6$)	ITSE($\times 10^8$)
Change room ACR	PI	3.0968	3.8352	3.7400	3.1251
	SISO MPC	1.9528	1.8553	2.0579	1.1319
	MIMO MPC	0.2502	0.00999	0.6999	0.02039
Change room AP	PI	1.8805	2.2510	1.9909	1.0844
	SISO MPC	2.2442	2.3213	2.8657	1.3224
	MIMO MPC	0.4086	0.02473	1.4136	0.06075
Small lab ACR	PI	2.2972	0.7633	9.9290	2.6974
	SISO MPC	1.1604	0.2598	3.2089	0.4893
	MIMO MPC	0.3100	0.9105	1.5928	0.03469
Small lab AP	PI	0.9605	0.1467	3.8181	0.3753
	SISO MPC	1.0169	0.2258	2.5818	0.3218
	MIMO MPC	1.5153	2.5260	7.0412	0.7277
Large lab ACR	PI	12.9810	26.0990	41.4060	72.7590
	SISO MPC	10.1730	18.6740	2.8906	41.0350
	MIMO MPC	0.2480	2.4509	0.5550	0.0145
Large lab AP	PI	1.4514	0.4412	5.0430	0.7432
	SISO MPC	1.2667	0.57370	2.1001	0.5549
	MIMO MPC	1.1919	3.9475	3.2266	0.3394

In this situation, the differences between simulation and filed test are quite large. The field test results show that the MIMO MPC controllers perform the best, while in simulation test they perform the worst. The field test results are receivable. The test plant in the simulation test is the identified models. The simulation tests of the SISO and PI controllers use the identified SISO models as the test plant which cannot cover the whole HVAC system. The success of the SISO MPC in simulation test cannot demonstrate the success in the field test since the field test uses the entire system as the test plant. In the field test, the SISO MPC and PI controllers need to cooperate with each other. While the MIMO MPC already considers the interaction between variables in design part, so that it performs better than the simulation

program.

5.4.2 Energy consumption analysis

Based on Section 3.4, the compare of the energy consumption among different controllers can be represented by the compare of the integrals of the rotational speeds' cube for fans as presented in Figure 5.10. The blue bar represents the PI control, the green one represents the SISO MPC, and the red one represents the MIMO MPC. It is obvious to judge that the MIMO MPC consumes less energy than PI control and SISO MPC.

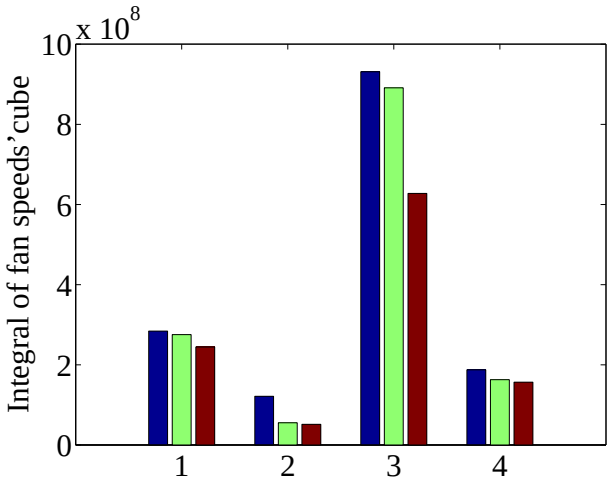

Figure 5.10: Comparison of integrals of fan speeds' cube among PI control(blue), SISO MPC (green) and MIMO MPC (red): 1 - AHU1 supply fan speed, 2 - AHU1 extract fan speed, 3 - AHU2 supply fan speed, 4 - AHU2 extract fan speed.

The field test of the controllers is almost the same as the real world small application. However, the real HVAC system has much larger scale than the laboratory which makes it difficult to define and identify the accurate system models. The cost to develop the MPC in the real word would be more expensive in data collection and identification part. However, PI control needs more time in parameter tuning which increases the cost. According to Figure 5.10, there is a large saving of energy consumption of MPC compared to PI control. If the saving is huge enough, it will save more than the extra cost of developing the MPC controllers.

5.5 Conclusion

The performances of PI and SISO MPC controllers in the cleanroom laboratory have been compared. Ten SISO MPC controllers have been designed to replace the original PI controllers in BMS. MIMO MPC of the cleanroom HVAC system has been designed and tested. The MIMO MPC has been designed based on the MIMO subsystem models identified in Chapter 4. It aims to maintain the ACR and AP in the cleanrooms.

Both simulation and field test have been done, and the integral performance indices have been calculated. The test results show that the MIMO MPC has better performance than SISO MPC and PI control. Also, the energy consumption of the HVAC system has been reduced with the largest amount by applying the MIMO MPC.

Chapter 6

Model predictive control of air cleanliness based on real-time data of particle counters for energy saving

This chapter investigates the design of MPC for controlling the particle concentration to a particular level, considering the reduction of energy consumption via the dynamic feedback control of the supply VAV position and the fan speed. Replacing the controlled output ACR with the particle concentration, the SISO model between the particle concentration and the supply VAV position is determined via black-box modelling approach. Moreover, the MIMO particulate model using both the supply fan and supply VAVs as the control inputs to control the particle concentration is identified. Based on those models, the change of particle concentrations is predicted, and the MPC is designed to minimise the particle concentration to a certain level, with reducing the energy consumption.

6.1 Particle counter

This section presents the specification of the particle counter, the results of the particle generation experiments and the standard of cleanroom classification based on particles.

6.1.1 Specification of particle counters

A particle counter is an instrument that detects and counts particles. A high-intensity light source is used to illuminate the particle as it passes through the detection chamber. The particle passes through the light source (typically a laser or halogen light), and if light scattering is used, then the redirected light is detected by a photo-detector. If direct imaging is used, a halogen light illuminates particles from the back within a cell while a high definition, high magnification camera records moving particles. Recorded video is then analysed by computer software to measure particle attributes. If light blocking (obscuration) is used, the loss of light is detected. The amplitude of the light scattered or light blocked is measured and the particle is counted and tabulated into standardised counting bins. Figure 6.1 shows a light scattering particle counter diagram.

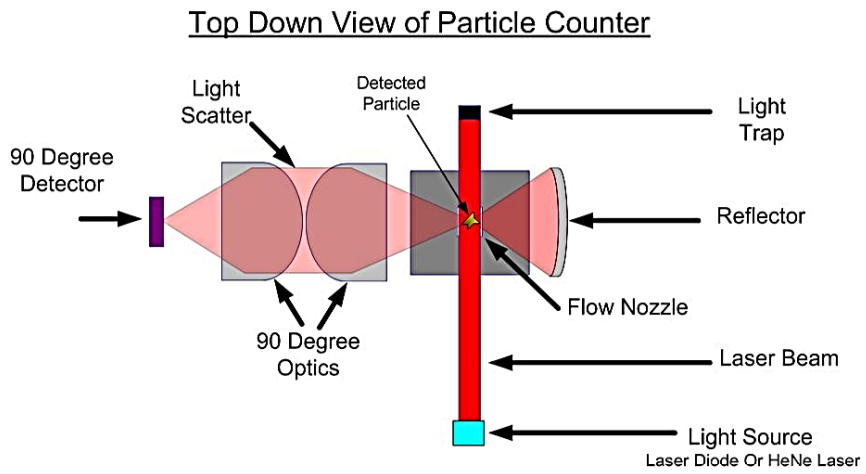

Figure 6.1: Diagram of a particle counter.

Aerosol particle counters are used to determine the air quality by counting and sizing the number of particles in the air. This information is useful in determining the number of particles inside a building or in the ambient air. It also is valuable in understanding the cleanliness level in a controlled environment. A commonly controlled environment aerosol particle counters are used in is a cleanroom. Clean-

rooms have defined particle count limits. Aerosol particle counters are used to test and classify a cleanroom to ensure its performance is up to a particular cleanroom classification standard.

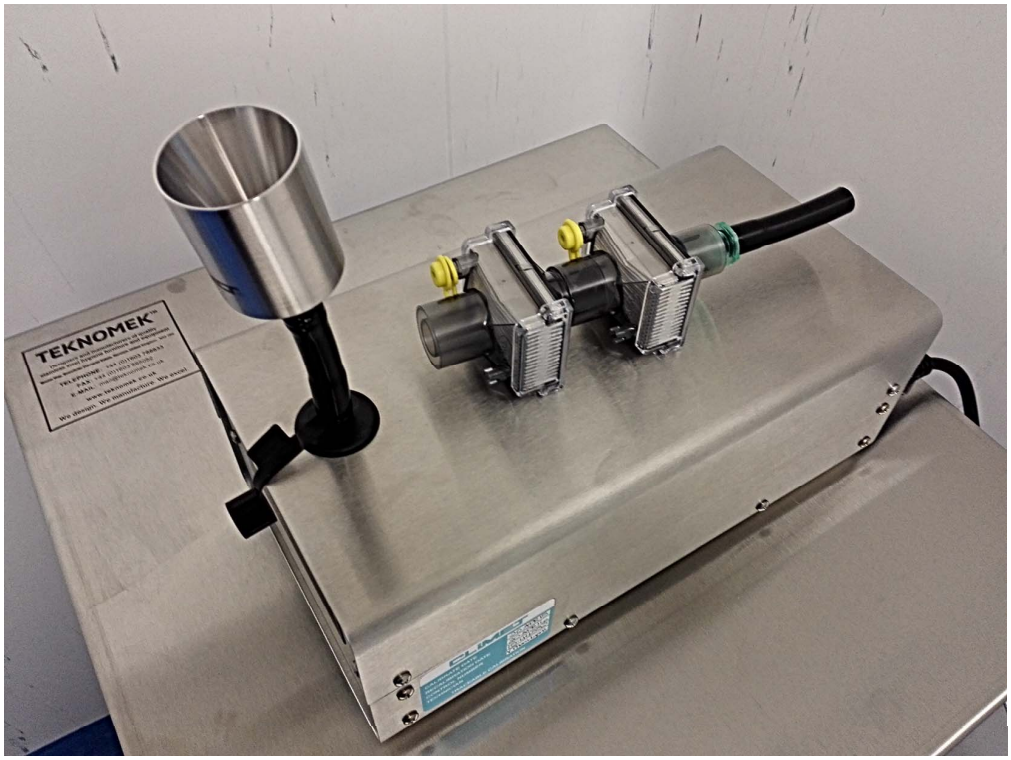

Figure 6.2: The particle counter [139].

The particle counter, shown in Figure 6.2 [139], is installed in the cleanroom laboratory. It is an aerosol particle counter which can monitor and control the particle contamination in cleanrooms. Its serial number is CI-3100-21, and it is produced by CLiMET. It is configured for integration into an Ethernet 10/100Base-T network using TCP/IP protocol. Particles are sized greater than 0.5 μm and 5.0 μm.

The particle counter samples air at a fixed sampling rate. The size of the air sample is therefore determined just by how long the measurement interval happens to be. The particle counter measures the air flow rate continuously and regulates the blower to keep the air flow within strict limits. If the fan is unable to control air flow correctly, the sample status will indicate a flow error.

The standard flow rate is 1.0 cubic feet per minute, which limits the allowable

concentration of particles to 1 million per cubic foot (CF) or 35.3 million per cubic meter (CM). The sample volume can be collected in CF mode or CM mode. The sample time for the CF mode is 1 minute while the sample time for the CM mode is 35.3 minutes. The Modbus protocol within the TCP/IP protocol (known as Modbus over Ethernet) or the HTTP web pages within the unit is used to communicate the sensor to the computer.

6.1.2 Particle generation experiments

Several particle generation experiments have been run and the results are shown in Figures 6.3-6.5. The particle greater than 0.5 μm is named as "fine particle" and that greater than 5.0 μm is called "coarse particle". The system is turned on with maximum airflow rate. Figure 6.3 shows the results when one person is entering the lab without wearing a guard. The measurement of the particle number is smaller than the ISO cleanroom standard which means the system can work in this situation. Figure 6.4 presents the results when one person is entering the lab wearing a guard. The particle number measurement is much smaller than the situation one person without wearing a guard. The above results show the importance of using guard when someone needs to enter the lab. Figure 6.5 presents the results when there are two persons inside the lab without wearing a guard. It takes a longer time to recover from dirty because more persons inside generate more particles. The air is dirtier than the previous situations, and the HVAC system is harder to remove them. The particle results are larger than the ISO standard even though the HVAC system is turned on. The particle generation test was run letting one person walk inside the lab. The value of PC3 is much higher than the other three counters because the person stayed longer time standing around PC3.

In summary, the particle generation experiments show the necessity of wearing guard if someone needs to get into a cleanroom and the particle generated from bodies of people can be colossal that the HVAC system cannot control it below the standard limitation. Most importantly, the particle counter can provide a real-time monitoring of the particle concentration level which then can be used to design a particle counter based real-time closed-loop controller.

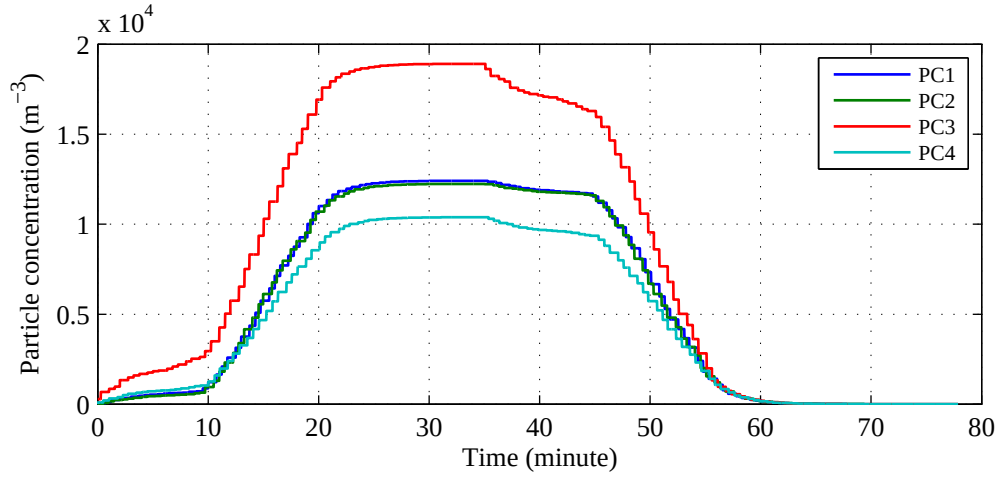

(a) Fine particle

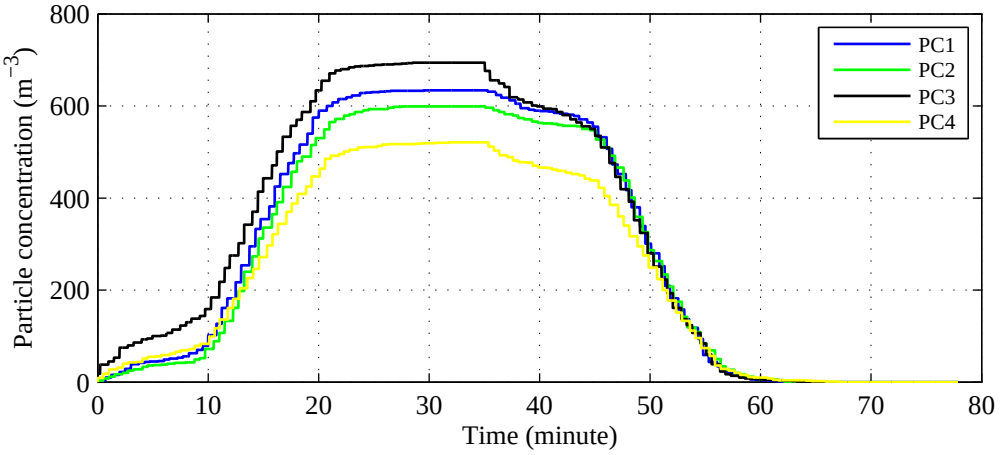

(b) Coarse particle

Figure 6.3: Results of the particle generation experiment, one person enter without wearing guard, HVAC system running (PC: particle counter).

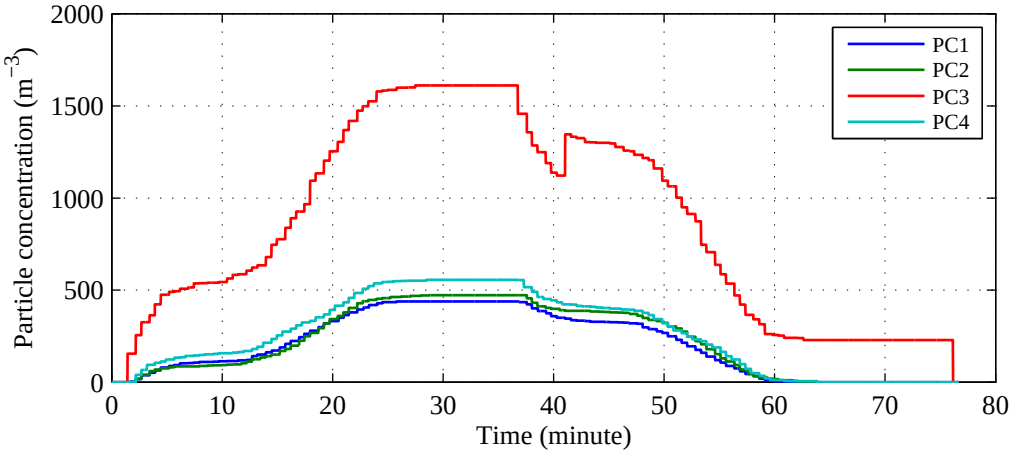

(a) Fine particle

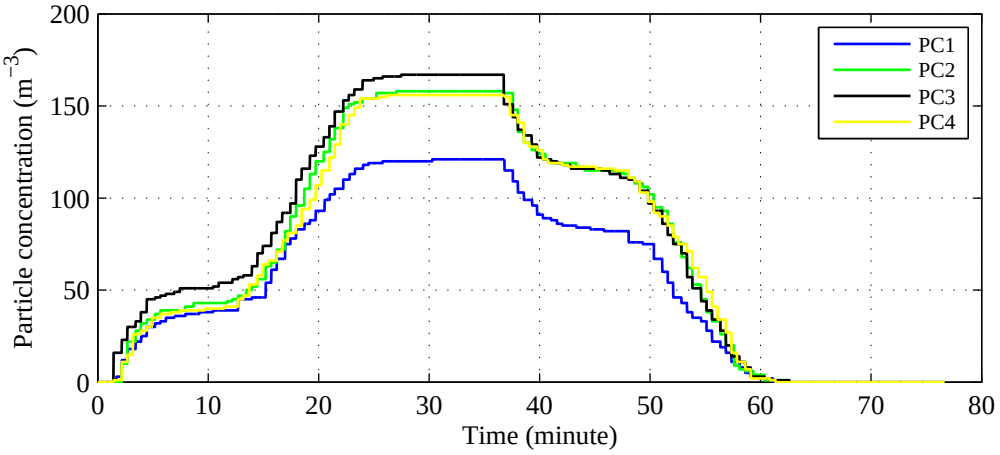

(b) Coarse particle

Figure 6.4: Results of the particle generation experiment, one person enter wearing guard, HVAC system running (PC: particle counter).

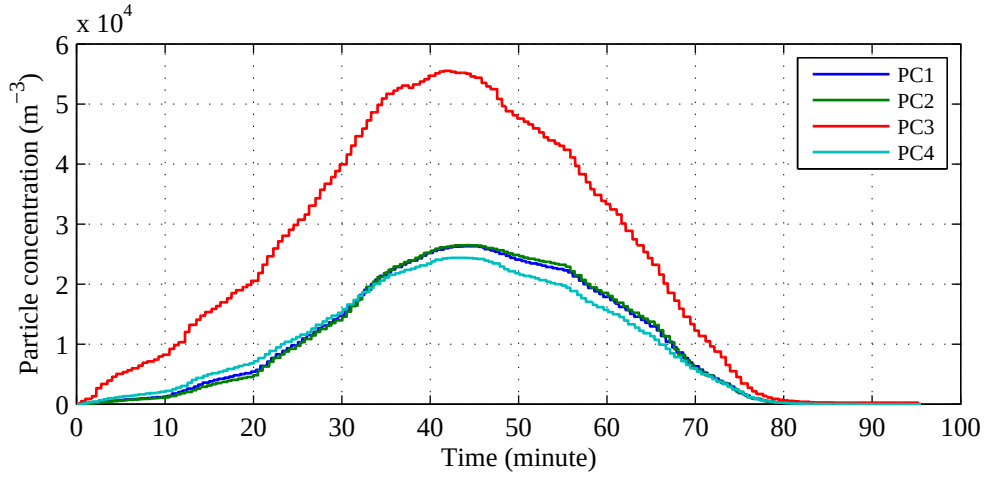

(a) Fine particle

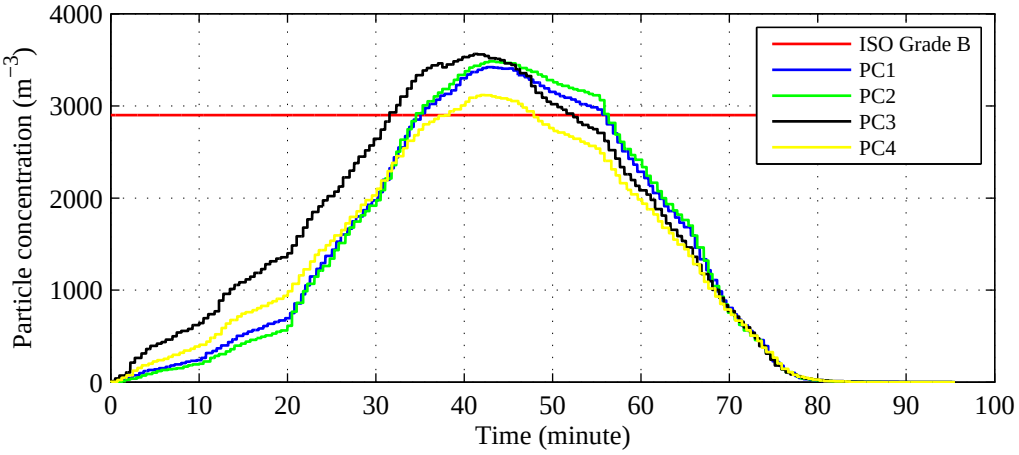

(b) Coarse particle

Figure 6.5: Results of the particle generation experiment, two person enter without wearing guard, HVAC system running (PC: particle counter).

6.1.3 Standard of cleanroom classification

The laboratory is built to test appropriate control of the HVAC system, based on the requirement of the cleanroom standard. The ISO produces a world-wide standard of cleanroom classification which is shown in Table 6.1 [2].

Table 6.1: Selected airborne particulate cleanliness classes for cleanrooms [2].

ISO classification Number (N)	Maximum concentration limits (particles/m^3 of air) for particles equal to and larger than the considered sizes shown below					
	0.1 μm	0.2 μm	0.3 μm	0.5 μm	1.0 μm	5.0 μm
ISO 1	10	2	n/a	n/a	n/a	n/a
ISO 2	100	24	10	4	n/a	n/a
ISO 3	1000	237	102	35	8	n/a
ISO 4	10000	2370	1020	352	83	n/a
ISO 5	100000	23700	10200	3520	832	29
ISO 6	1000000	237000	102000	35200	8320	293
ISO 7	n/a	n/a	n/a	352000	83200	29300
ISO 8	n/a	n/a	n/a	3520000	832000	293000
ISO 9	n/a	n/a	n/a	35200000	8320000	2930000

Cleanrooms of this laboratory are classified according to the primary activity and the cleanliness levels of the air within each room. For pharmaceutical cleanrooms, air cleanliness is either based on EU GMP guidance [4], which adopts alphabetic notations; or by using the International Standard ISO14644 [2], which adopts alphabetic notations. The standards define the air cleanliness based on some particle sizes. However, for a pharmaceutical factory, the concentration of particle sizes are $0.5\ \mu m$ and $5\ \mu m$. So the pharmaceutical standard the laboratory is based on is shown in Table 6.2.

Table 6.2: The airborne particulate classification for sterile medicinal products in the pharmaceutical factory [4].

		Maximum particles/m^3			
ISO	Pharmacy	At rest		In operation	
Particle size		0.5 μm	5 μm	0.5 μm	5 μm
5	Grade A	3520	20	3520	0
6	Grade B	3520	29	352000	2900
7	Grade C	352000	2900	3520000	29000
8	Grade D	3520000	29000	n/a	n/a

With EU GMP, Grade A is the highest grade (that is the "cleanest"), and Grade D is the lowest (that is the least "clean"). With ISO, the lower the number (such as "5") the "cleaner" the room class and the higher the number (such as "8") the place is considered to be "less clean." The four grades can be distinguished:

- Grade A: the local zone for high-risk operation.
- Grade B: the background environment for grade A zone.
- Grade C and D: clean areas for carrying out less critical stages in the manufacture of sterile products.

6.2 Model identification

In the small lab, only one particle counter is installed. Moreover, in the large lab, two particle counters are installed. The measured data from the particle counters give the number of particles in a specified air volume. The particle concentration is calculated by the ratio of the number of particles in the specified air volume. Since two kinds of particles are measured, for each particle size, these exist a concentration value maximising the particle concentration of every particle counters in the same lab. Thus, in each lab, there are two particle concentration values for each particle size.

The laboratory is designed to limit the concentrations of particles with both 0.5 μm and 5 μm under the cleanroom standard (see Table 6.2). The large lab of this

laboratory is designed with Grade B, and the small lab is designed with Grade C. A percentage value can be calculated by dividing the particle concentration values by the standard values. The particle concentration values in each lab are then quantified with the same scale as percentage values. The outputs of the SISO particulate model of each lab is defined by maximising the percentage of the particle concentration for each particle size. The inputs are the supply VAV positions of each lab. The model structure of the particle counter based SISO models is ARX.

6.2.1 SISO particle counter based models

Figure 6.6 presents the SISO particulate model in the small lab. A PI controller is designed to maintain the maximum particle concentration in the small lab by controlling the supply VAV. The data collected from this PI control loop are used to identify the SISO model. The identification results are shown in Figure 6.7. The measured and predicted outputs of the SISO model, the absolute error and the relative error are presented in Figures 6.7(a)-6.7(c), respectively. From the comparison results, it is found that the identified model has a good performance with small errors.

Figure 6.6: The small lab SISO particulate model.

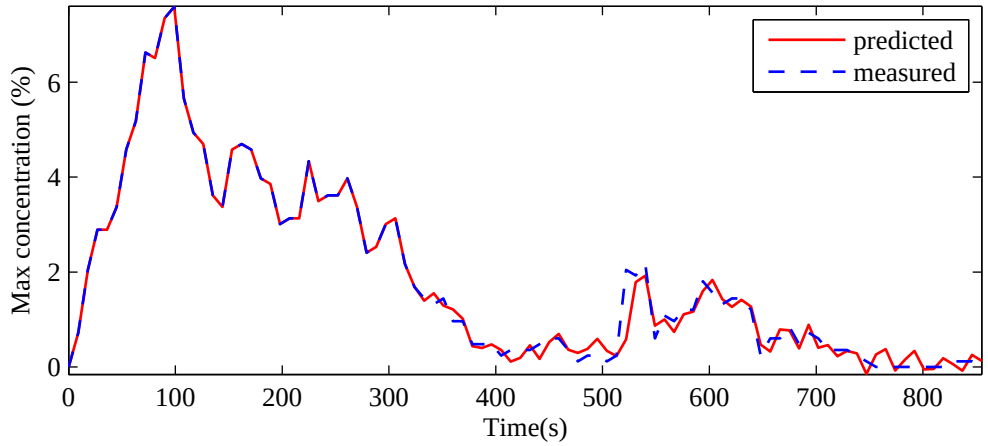

(a) Measured and predicted outputs of the small lab SISO particulate model.

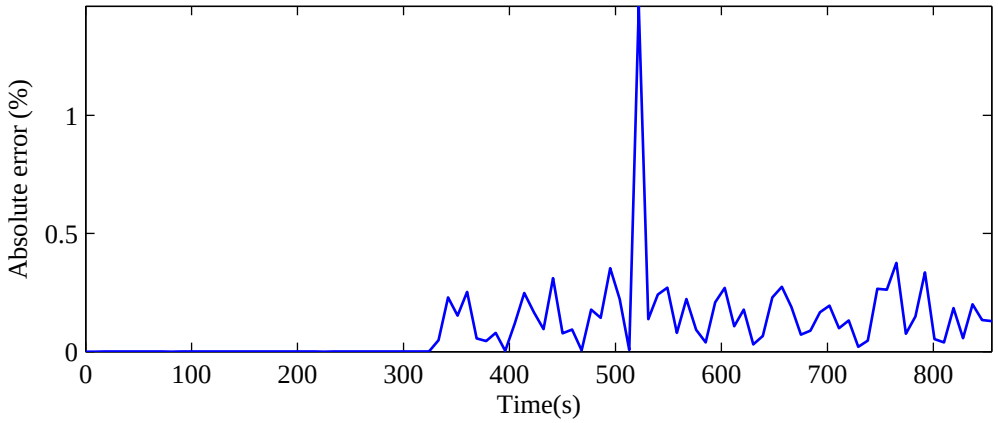

(b) Absolute error of the small lab maximum particle concentration

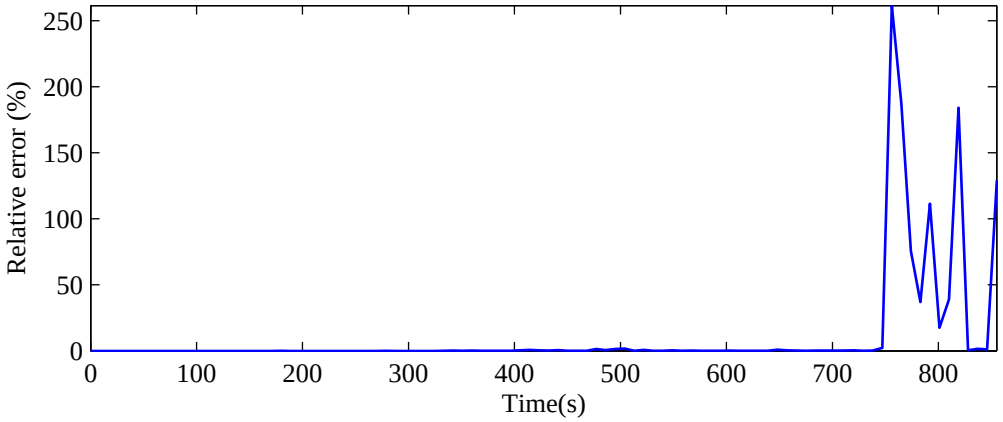

(c) Relative error of the small lab maximum particle concentration

Figure 6.7: Comparison results of the output of the small lab SISO particulate model.

Polynomials of the particle counter based small lab SISO ARX model:

$$\begin{aligned}
A^{small}(z) &= 1 - 0.7682z^{-1} - 0.1846z^{-2} + 0.7773z^{-3} - 0.6658z^{-4} - 0.1226z^{-5} \\
&+ 0.5613z^{-6} - 0.5436z^{-7} - 0.3972z^{-8} + 0.5696z^{-9} - 0.1149z^{-10} \\
&- 0.6536z^{-11} + 0.6308z^{-12} + 0.1819z^{-13} - 0.4854z^{-14} + 0.4016z^{-15} \\
&+ 0.244z^{-16} - 0.3917z^{-17} + 0.2402z^{-18} + 0.1182z^{-19} - 0.1586z^{-20} \\
B^{small}(z) &= 0.0001396z^{-4} + 0.0008664z^{-10} - 0.001626z^{-11} - 7.653e - 06z^{-12} \\
&+ 0.004834z^{-13} - 0.005905z^{-14} - 0.0001065z^{-15} + 0.003376z^{-16} \\
&- 0.0001499z^{-17} - 0.002376z^{-18} - 0.0001015z^{-19} + 0.00196z^{-20}
\end{aligned}$$

Figure 6.8 presents the SISO particulate model in the large lab. A PI controller is designed to maintain the maximum particle concentration in the large lab by controlling the supply VAV. The data collected from the PI control loop are used to identify the SISO model. The identification results are presented in Figure 6.9. Figure 6.9(a) shows the plot of measured and predicted outputs of the SISO model, Figure 6.9(b) presents the absolute error between them and Figure 6.9(c) gives the relative error. From the comparison results, it is found that the identified model has a good performance with small errors.

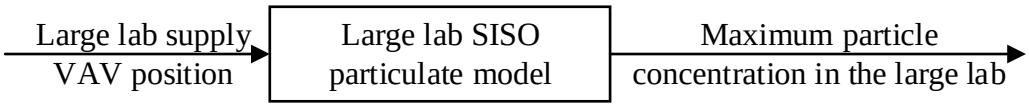

Figure 6.8: The large lab SISO particulate model.

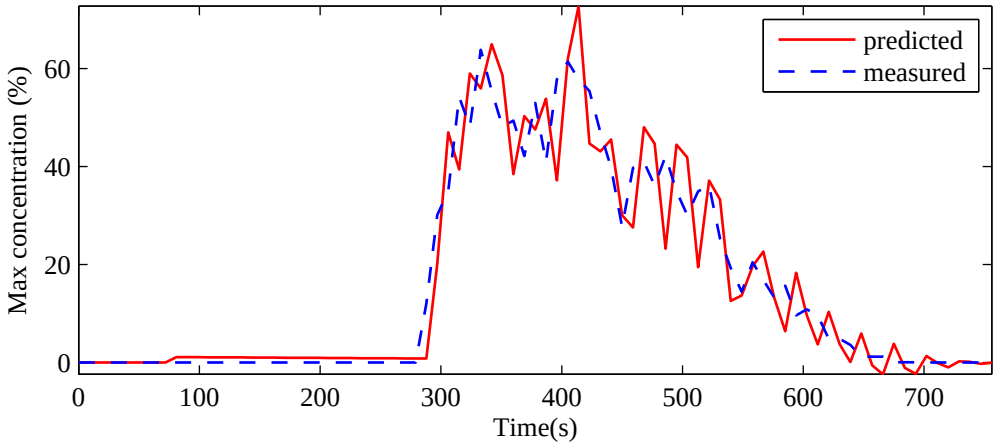

(a) Measured and predicted outputs of the large lab SISO particulate model.

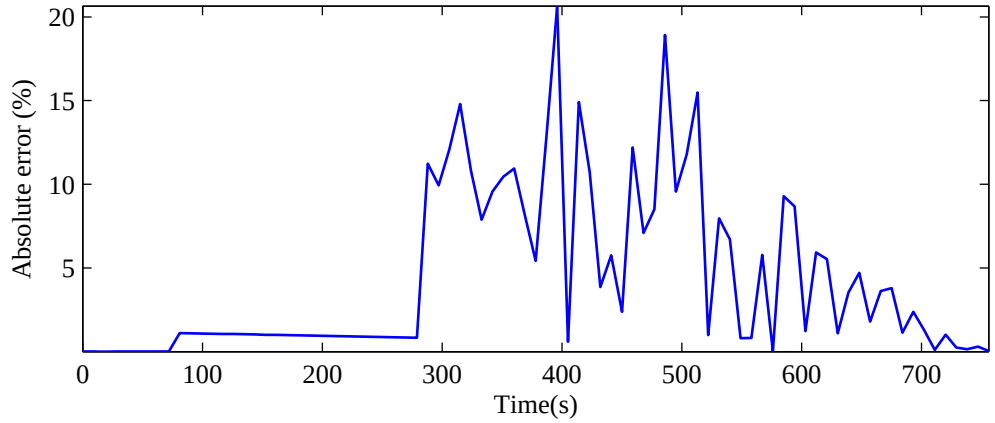

(b) Absolute error of the large lab maximum particle concentration

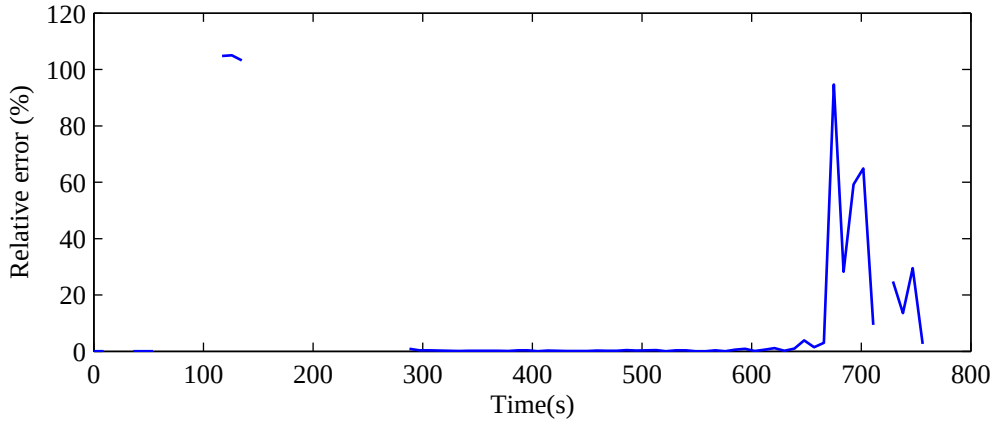

(c) Relative error of the large lab maximum particle concentration

Figure 6.9: Comparison results of the output of the large lab SISO particulate model.

Polynomials of the particle counter based large lab SISO ARX model:

$$
\begin{aligned}
A^{large}(z) &= 1 - 2.04z^{-1} + 0.5464z^{-2} + 1.074z^{-3} - 0.118z^{-4} - 0.8107z^{-5} \\
&+ 0.7349z^{-6} - 0.8108z^{-7} + 0.0995z^{-8} + 0.4042z^{-9} + 0.5522z^{-10} \\
&- 0.7134z^{-11} - 0.2327z^{-12} + 0.3096z^{-13} + 0.1574z^{-14} - 0.1878z^{-15} \\
&- 0.0605z^{-16} + 0.1823z^{-17} + 0.06057z^{-18} - 0.2624z^{-19} + 0.1321z^{-20} \\
B^{large}(z) &= 0.0001z^{-1} - 0.0003z^{-2} - 9.619e-05z^{-3} + 0.0008z^{-4} - 0.0001z^{-5} \\
&- 0.0011z^{-6} + 0.0004z^{-7} + 0.0006z^{-8} + 0.0004z^{-9} \\
&- 0.0020z^{-10} + 0.0017z^{-11} - 0.0007z^{-12} + 5.191e-05z^{-13} \\
&- 0.0005z^{-14} + 0.0023z^{-15} - 0.0011z^{-16} - 0.0018z^{-17} \\
&+ 0.0005z^{-18} + 0.0017z^{-19} - 0.0009z^{-20}
\end{aligned}
$$

6.2.2 MIMO particle counter based models

The inputs and outputs of the MIMO particulate model are defined in Figure 6.10. The corresponding mathematical model has been identified using black-box approach. Figures 6.11 and 6.12 present the identification results of the MIMO particle counter based model where both measured and predicted outputs are plotted, and the corresponding absolute errors and relative errors are given. The comparison results show that the identified MIMO particle counter based model has a good goodness of fit with small errors.

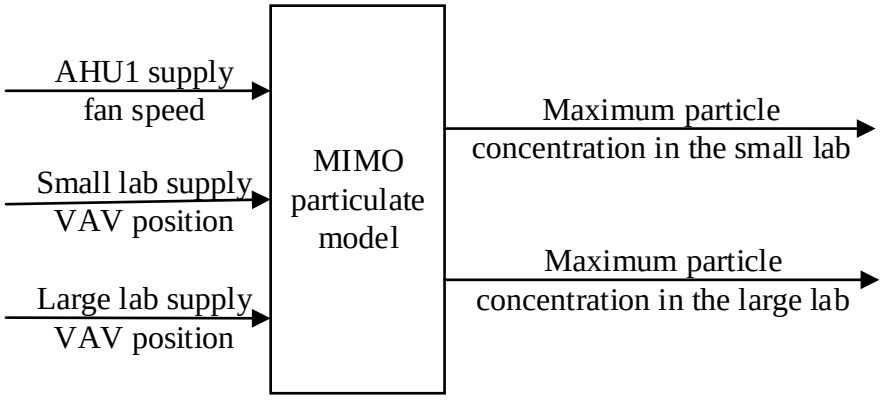

Figure 6.10: The MIMO particulate model.

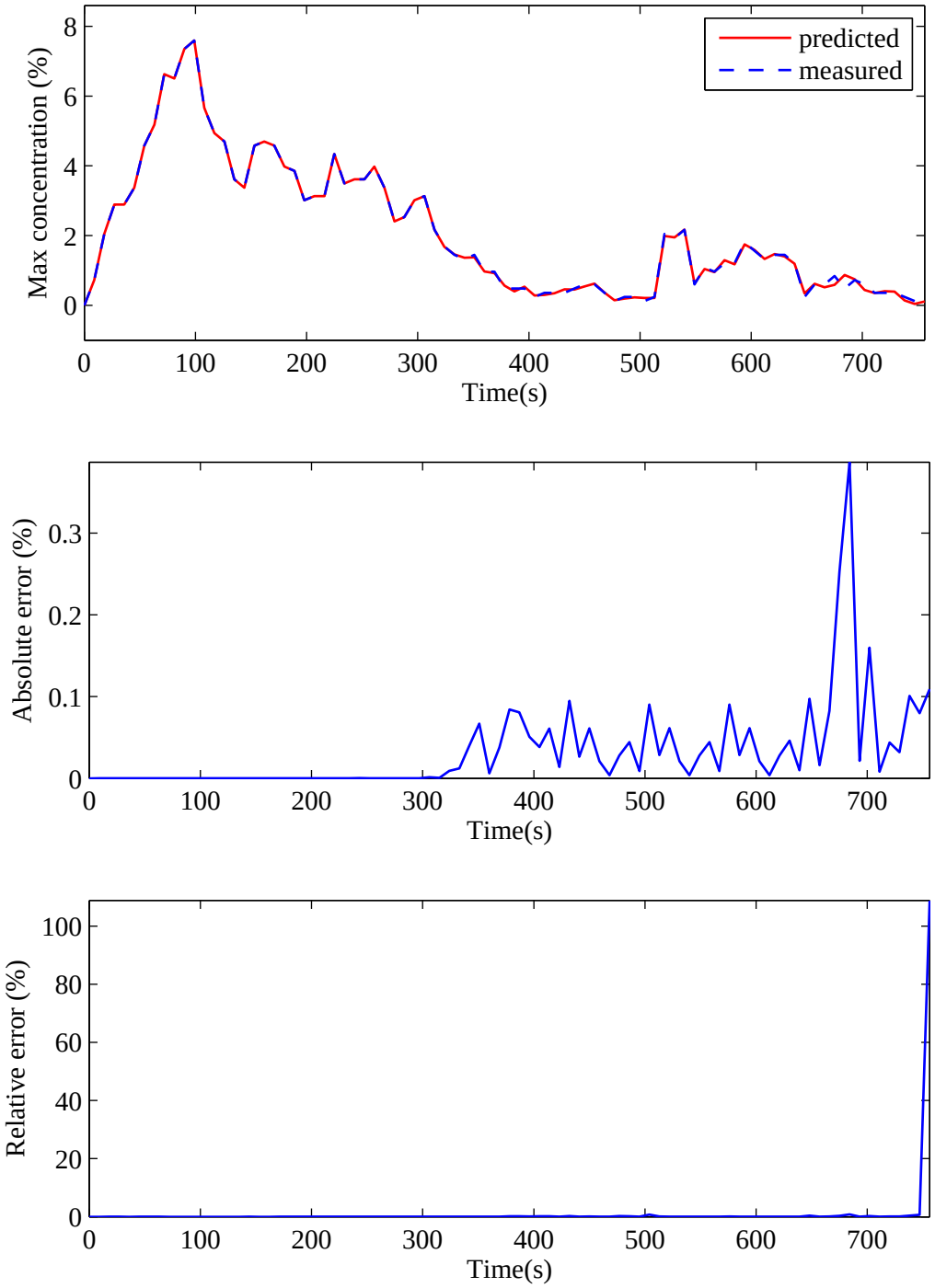

Figure 6.11: Comparison results of the output 1 of the MIMO particulate model: small lab maximum particle concentration.

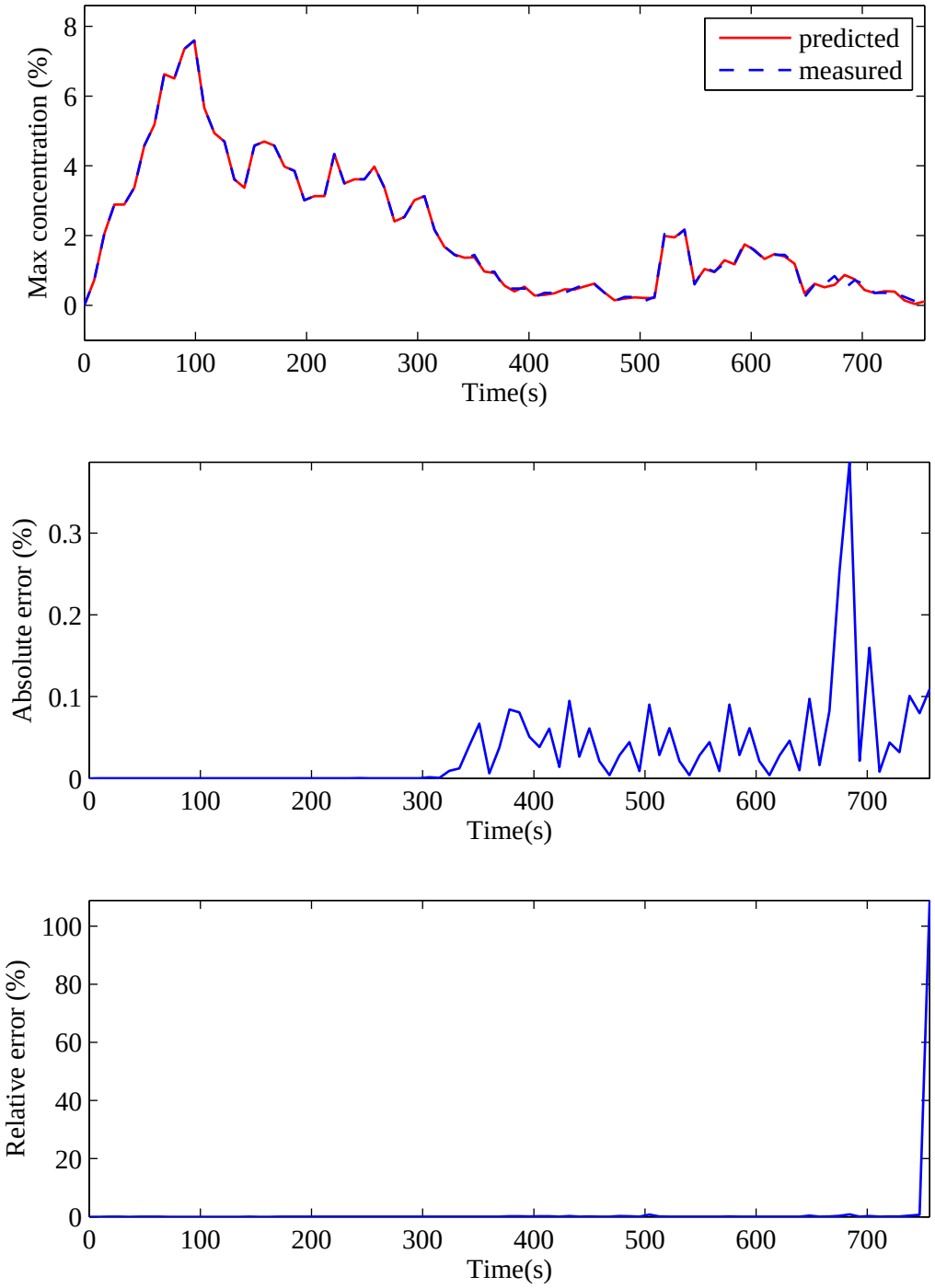

Figure 6.12: Comparison results of the output 2 of the MIMO particulate model: large lab maximum particle concentration.

The MIMO particle counter based model is identified as a MIMO ARX model. The polynomials of the outputs are shown below:

- Polynomials of output 1: small lab maximum particle concentration:

$$
\begin{aligned}
A^1(z) &= 1 - 0.814z^{-1} - 0.2114z^{-2} \\
A_2^1(z) &= -0.02488z^{-1} - 0.01846z^{-2} \\
B_1^1(z) &= -0.0086z^{-1} + 0.0035z^{-2} - 0.0103z^{-3} + 0.0030z^{-4} + 0.0065z^{-5} \\
&- 0.0025z^{-6} + 0.0013z^{-7} + 0.0113z^{-8} - 0.0012z^{-9} - 0.0033z^{-10} \\
&+ 0.0037z^{-11} - 0.0006z^{-12} + 0.0006z^{-13} - 0.0020z^{-14} \\
&+ 0.0016z^{-15} + 0.0136z^{-16} - 0.0002z^{-17} - 0.0029z^{-18} \\
&+ 0.0023z^{-19} + 0.0042z^{-20} \\
B_2^1(z) &= -0.01498z^{-1} + 0.0485z^{-2} - 0.0555z^{-3} + 0.0178z^{-4} - 0.0059z^{-5} \\
&+ 0.0022z^{-6} - 0.0002z^{-7} + 0.0078z^{-8} - 0.0072z^{-9} \\
&- 7.725e - 05z^{-10} - 0.0005z^{-11} + 0.0031z^{-12} - 0.0015z^{-13} \\
&- 0.0027z^{-14} + 0.0018z^{-15} + 0.0010z^{-16} + 0.0015z^{-17} \\
&- 0.0031z^{-18} - 0.0001z^{-19} - 0.0011z^{-20} \\
B_3^1(z) &= 0.0019z^{-1} + 0.0004z^{-2} + 0.0036z^{-3} - 5.699e - 05z^{-4} - 0.0001z^{-5} \\
&- 0.0021z^{-6} + 0.0001z^{-7} - 0.0058z^{-8} + 0.0017z^{-9} - 0.0002z^{-10} \\
&- 0.0002z^{-11} + 0.0019z^{-12} - 0.0023z^{-13} + 0.0005z^{-14} \\
&- 0.0019z^{-15} - 0.0009z^{-16} - 0.0025z^{-17} + 0.0007z^{-18} \\
&- 0.0035z^{-19} + 0.0021z^{-20}
\end{aligned}
$$

- Polynomials of output 2: large lab maximum particle concentration:

$$
\begin{aligned}
A^2(z) &= 1 - 0.2117z^{-1} + 0.05797z^{-2} \\
A_1^2(z) &= 3.865z^{-1} + 4.535z^{-2} \\
B_1^2(z) &= -0.0552z^{-1} + 0.1198z^{-2} - 0.1824z^{-3} - 0.1375z^{-4} \\
&- 0.0557z^{-5} - 0.2251z^{-6} - 0.0033z^{-7} - 0.1304z^{-8} - 0.1472z^{-9} \\
&- 0.03917z^{-10} - 0.07768z^{-11} - 0.1131z^{-12} - 0.1151z^{-13} \\
&- 0.1667z^{-14} - 0.1744z^{-15} - 0.157z^{-16} + 0.0052z^{-17} \\
&- 0.169z^{-18} - 0.02684z^{-19} + 0.0045z^{-20} \\
B_2^2(z) &= 0.5005z^{-1} + 0.6371z^{-2} - 0.8338z^{-3} + 0.3622z^{-4} + 0.0113z^{-5} \\
&- 0.0160z^{-6} + 0.0176z^{-7} - 0.0441z^{-8} + 0.0643z^{-9} \\
&- 0.0257z^{-10} + 0.0697z^{-11} - 0.0412z^{-12} + 0.0152z^{-13} \\
&+ 0.0016z^{-14} + 0.0037z^{-15} + 0.0197z^{-16} - 0.0174z^{-17} \\
&+ 0.0504z^{-18} - 0.0345z^{-19} + 0.0669z^{-20} \\
B_3^2(z) &= 0.0084z^{-1} - 0.0397z^{-2} + 0.0554z^{-3} + 0.0284z^{-4} \\
&+ 0.0958z^{-5} + 0.0254z^{-6} + 0.0895z^{-7} + 0.0150z^{-8} + 0.0668z^{-9} \\
&- 0.0091z^{-10} + 0.0585z^{-11} + 0.0535z^{-12} + 0.0537z^{-13} + 0.0453z^{-14} \\
&+ 0.1174z^{-15} + 0.0475z^{-16} + 0.0353z^{-17} + 0.0442z^{-18} + 0.0352z^{-19} \\
&- 0.0038z^{-20}
\end{aligned}
$$

6.3 Controller design

The introduction of the particle counters makes it possible to measure the particle concentrations. The closed-loop systems have been built to control the particle concentrations in the cleanroom laboratory. The SISO particle counter based MPC controller is designed based on the above identified model. The supply VAV in the each lab is overridden by Matlab programs while the other facilities are controlled by the PI controllers. The MIMO particle counter based MPC controller uses the mathematical MIMO models shown above to predict the future moves. Different

from SISO MPC, the MIMO MPC controller overrides the supply VAV in each lab and the supply fan in AHU1. Table 6.3 shows the parameters of the particle counter based MPC. The sample time is set to 9 seconds because the particle counter gives a value for each 9 seconds.

Table 6.3: Parameters of the particle counter based MPC.

Parameter	Symbol	Value
Weight on the outputs	w^y	1
Weight on the rate of change of inputs	$w^{\triangle u}$	1
Prediction horizon	P	10
Control horizon	M	2
Sampling time	T_s	9 s

6.4 Results

6.4.1 Simulation results

To verify the controllers designed above, the simulation tests have been done by Matlab/Simulink. Figure 6.13 shows the simulation results among MIMO MPC, SISO MPC and PI control of particle concentrations. A few particles are introduced at the beginning of the simulation. The results show that the particle counter based controllers can control the particle concentration at a particular level either in the small lab or large lab.

6.4.2 Field test results

The field tests of the designed controllers have been taken. The initial particles are introduced into cleanrooms that the researcher in ordinary dress walked inside for 10 minutes at each lab. Figure 6.14 shows the field test results among MIMO MPC, SISO MPC and PI control of the particle levels. The set-point of the maximum particle concentration in each lab is set as 1%. The results show that all the controllers can control the particle concentration at a particular level either in the

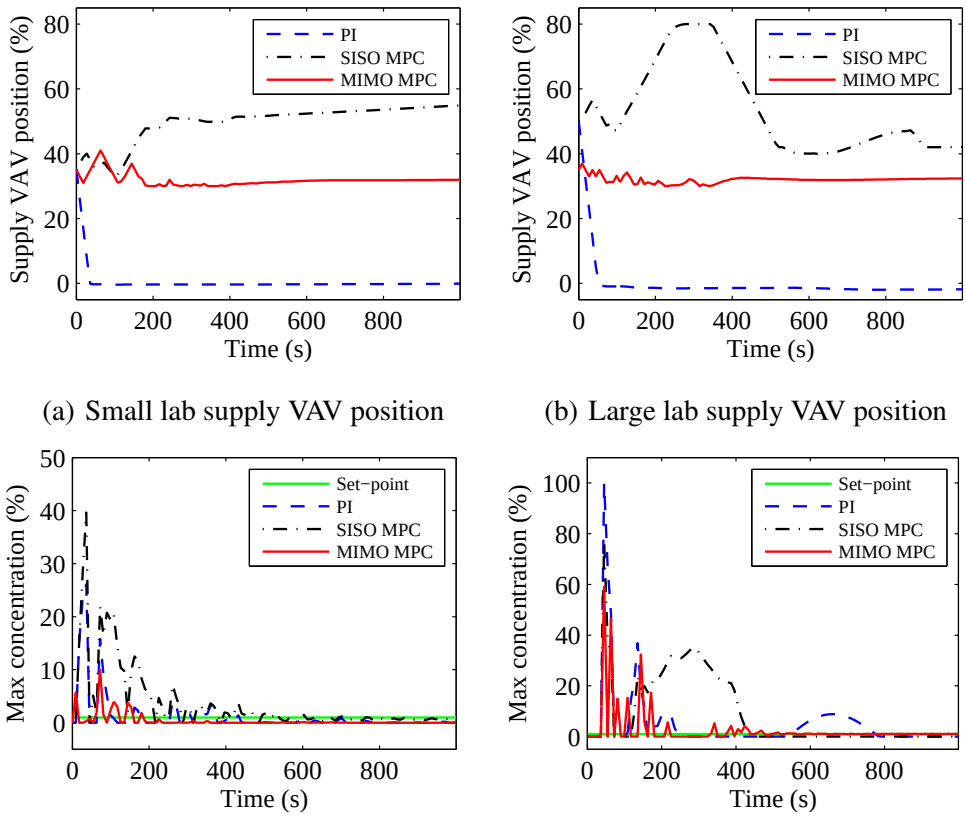

(a) Small lab supply VAV position

(b) Large lab supply VAV position

(c) Maximum particle concentration in the small lab

(d) Maximum particle concentration in the large lab

Figure 6.13: Comparison results among particle counter based MIMO MPC, SISO MPC and PI control (simulation results).

small lab or the large lab.

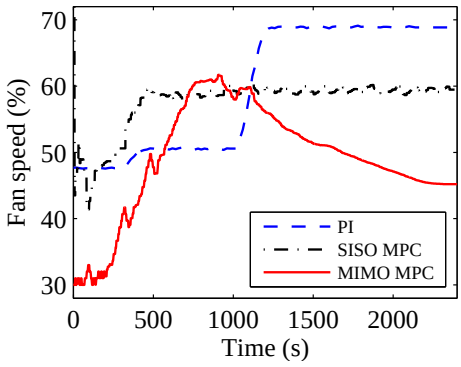

(a) AHU1 supply fan speed

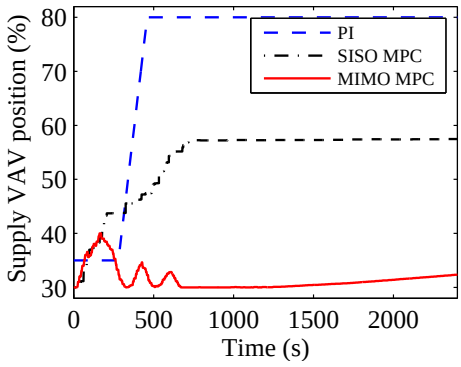

(b) Small lab supply VAV position

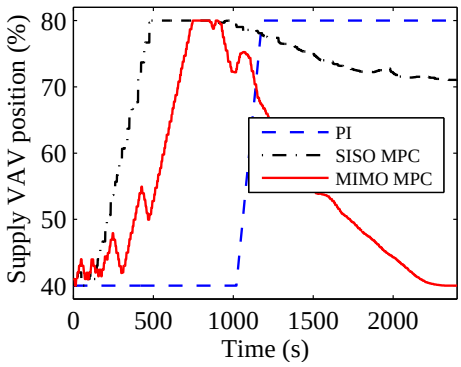

(c) Large lab supply VAV position

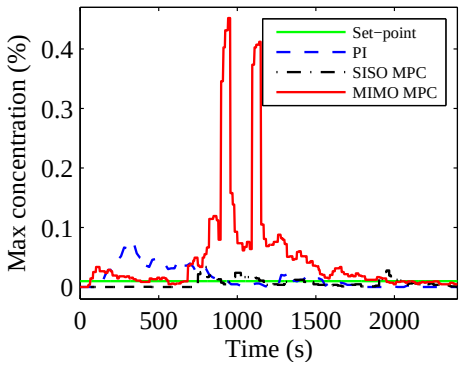

(d) Maximum particle concentration in the small lab

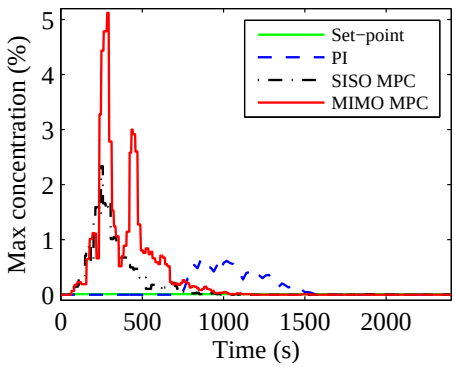

(e) Maximum particle concentration in the large lab

Figure 6.14: Field test results of the particle counter based MIMO MPC, SISO MPC and PI control.

6.4.3 Energy consumption analysis

Figure 6.15 presents a bar chart comparing the integrals of the AHU1 fan speeds' cube for particle counter based PI control, SISO MPC and MIMO MPC. As discussed in Section 3.4, the energy consumption of the HVAC system relates only to the fan speed and can be compared by calculating the integral of fan speeds. The comparison results show that the ranking of energy consumption from the lowest to the highest is MIMO MPC, SISO MPC and PI control.

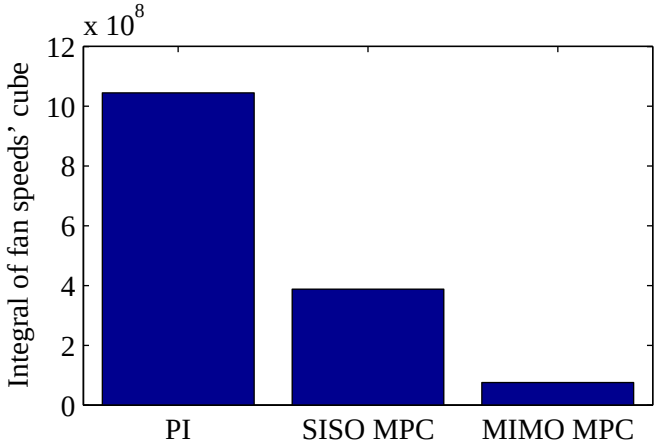

Figure 6.15: Comparison of integrals of fan speeds' cube among PI control and SISO MPC, MIMO MPC for particle counter based control.

6.5 Conclusion

In this chapter, the particle counter based MPC controllers have been designed and tested. The particle counter based PI control has been designed firstly, the measured data of which have been used to identify the particulate models. Both SISO and MIMO particulate models have been identified, and the corresponding MPC controllers have been designed. The simulation test and field test of these MPC controllers have been taken to verify the performance of MPC. The results show that both SISO MPC and MIMO MPC can maintain the particle concentration at the particular level. The comparison of energy consumption of these controllers results in a rank from the lowest to the highest: MIMO MPC, SISO MPC and PI control.

Chapter 7

PLC based implementation and experimental test

In this chapter, the Matlab programs proposed in the previous chapters have been transferred to PLC. A PLC platform produced by Beckhoff is installed. The run-time software, which is named as the Windows control and automation technology (TwinCAT), is embedded in the PLC platform supporting the running of PLC programs. Then, the PI control and MPC are implemented in cleanroom laboratory via the PLC platform. For regulating the airflow rate and AP:

- The Matlab based PI control is compared with the PLC based PI control for comparing the performance of the two platforms: Matlab and PLC.
- In PLC, the PI control and the MPC are tested to compare the two control methods including PI control and MPC.

The dynamic performances of these controllers are compared by calculating the integral performance indices including IAE, ISE, ITAE and IASE. The energy consumptions of them are compared by comparing the integral of fan speeds. The particle counters are connected with the PLC platform through the wireless network. The SISO and MIMO MPC of the particle concentration of the cleanrooms are implemented.

7.1 Introduction

A PLC is a special form of a microprocessor-based controller that uses programmable memory to save instructions and to implement functions such as logic, timing, sequencing, counting, and arithmetic to control machines and processes [140]. It is designed to be operated by engineers with perhaps a limited knowledge of computers and computing languages. A PLC is a digital computer used for automation of typical industrial processes, such as amusement rides, machinery on factory assembly lines and light fixtures.

PLCs are widely used in motion, positioning and torque control. The first PLC was developed in 1969. The use of PLCs now extends from small units for with perhaps 20 digital inputs/outputs to systems with up to thousands of inputs/outputs. PLCs can handle digital or analogue inputs/outputs, and carry out control algorithm such as PID control. The basic components of a typical PLC system contain processor unit, memory, power supply unit, input/output interface section, communications interface, and the programming device.

The functionality of the PLC has evolved process control, sequential relay control, motion control, distributed control systems, and networking. Compared with desktop computers, some modern PLCs have approximately equivalent functionalities in data handling, storage, processing power, and communication capabilities. In certain applications, the combination of PLC based programming with remote Input/Output (I/O) hardware allows the overlapping of a general-purpose desktop computer to some PLCs. Desktop computer controllers have not generally been accepted in heavy industries. The reason is that desktop computers run with less stability than PLCs, and the hardware of desktop computers is typically not designed to the same levels of tolerance to temperature, humidity, vibration, and longevity as that used in PLCs. Desktop logic applications are widely used in less critical situations, such as laboratory automation and small facilities with less demanding because they are much less expensive than PLCs.

PLCs have a great advantage that the same basic controller can be used with a wide range of control systems. An operator is designed necessarily to key in a different set of instructions to modify a control system. There is no need to rewire

since the result is a flexible, cost-effective system which varies quite widely in their nature and complexity [140]. PLCs are well adapted to a range of automation tasks including typically industrial processes where the cost of developing and maintaining the automation system is high relative to the total cost of the automation, and where changes to the system would be expected during its operational life. The input and output devices of PLCs are compatible with industrial devices and controls. PLC applications are typically highly customised with a low cost of a packaged PLC compared to the cost of a specific custom-built controller.

The PLC determines the logical operational sequence of the machine and assigns the motion controller to implement certain axis functions. Due to the increased performance of the controllers and the possibility to use higher-level programming languages (IEC 61131-3), complex machines can also be automated in this way. IEC 61131-3 is the third part of the open international standard IEC 61131 for PLCs and was first published in December 1993 by the IEC. It deals with programming languages and defines several PLC programming language standards:

- Ladder diagram
- Function block diagram
- Structured text
- Instruction list
- Sequential function chart
- Continuous Function Chart

MPC has become popular in the recent years due to its ability to handle MIMO systems with constraints. However, the computational effort required to solve the underlying algorithm usually limits the application of MPC to sufficiently slow systems [141]. This drawback makes it difficult to perform control tasks on hardware systems with limited performance and memory. A typical example is that PLCs are commonly used in industrial automation. In general, rather simple control strategies (such as PI control) are implemented on a PLC due to the limited resources.

The development of more powerful PLC devices makes it possible to handle the computing of the MPC algorithm in seconds. The cleanroom HVAC system presented in this thesis controls the ACR, AP and particle concentration in cleanrooms.

The process of this system is proved to be sufficiently slow that the PLC devices can be applied.

7.2 PLC based implementation

This section investigates how to implement the Matlab modules into the PLC based hardware. The PLC hardware is introduced with a detailed explanation of basic components. Two kinds of software are applied in the implementation, named TwinCAT and TE1400. The cooperation of them provides a way to transfer Simulink modules into PLC based programs.

7.2.1 PLC hardware

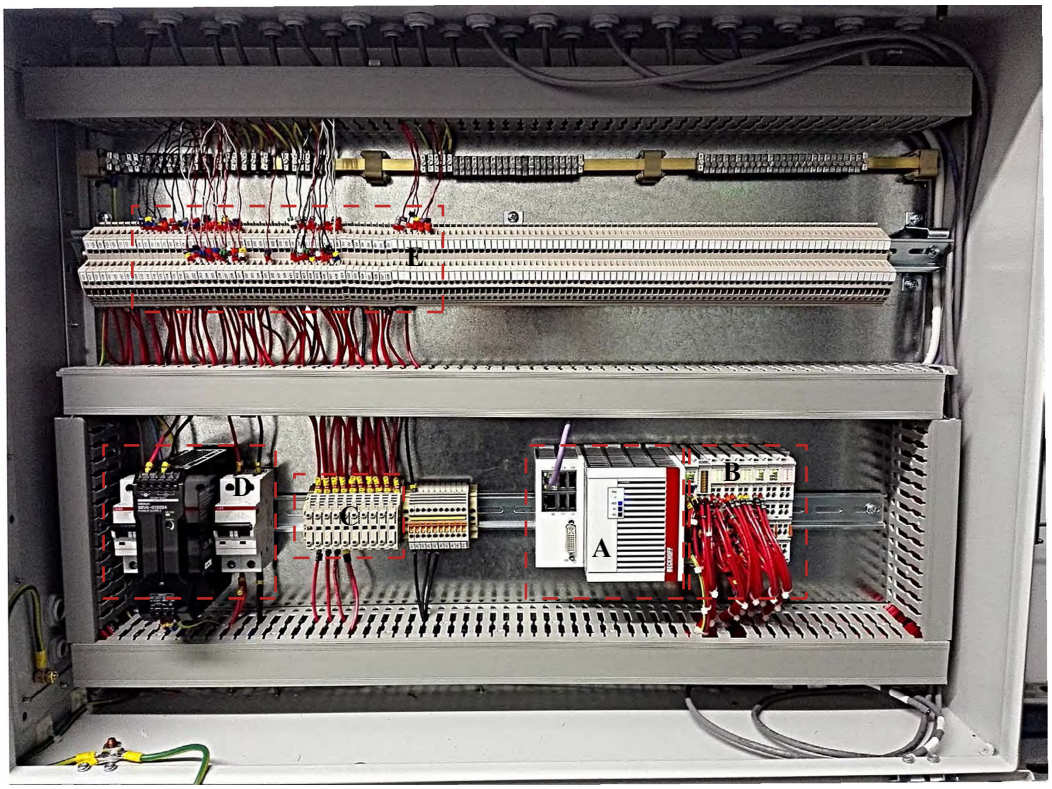

Figure 7.1: The panel where the PLC devices are installed [96].

Figure 7.1 [96] shows the panel where the PLC based workstation is installed. The PLC based programs have been implemented through the panel which contains several basic components:

A. The industrial PC.

   The IPC is an embedded PC based on an Intel Atom squad-core 1.91 GHz processor. The IPC can be used for implementing PLC projects with or without visualisation. The IPC is modelled for optimum interaction with Ethernet for control automation technology (EtherCAT). The EtherCAT connection is established via terminals where the extension modules B are attached. In terms of PLC, up to four virtual IEC 61131 CPUs can be programmed with up to four tasks each, with a minimum cycle time of 50 μs.

B. The extension modules.

   The extension modules are attached to the IPC through EtherCAT providing a terminal system. The EtherCAT terminal system is a modular emphasised system consisting of electronic terminal blocks such as input terminals, output terminals, serial interface terminals and feed terminals. Through the extended terminals, the data can be transferred between the IPC and the facilities.

C. The Transformers: 230 V to 24 V.

   The small transformers output the 24 V voltage to drive the terminals and facilities.

D. 230 V power supply to the IPC and the transformers.

E. Connection terminals transferring the data between the modules and the facilities.

   They connect the cables from the terminals with the cables from the facilities.

The block diagram of the PLC panel is shown in Figure 7.2. The controllers in IPC have the same algorithm as in Matlab. The control signals, u, are sent from the controllers to regulate the HVAC facilities. Through the main program in IPC and the output terminals, u are transferred to voltage signals 0-10 V. The VAVs receive the voltage signal and change its position from 0 to 90°. The inverters transfer the voltage signals to 0-50 Hz. The fans receive the frequency signals and regulate the fan speed from 0 to 3000 RPM. Taking pressure sensors (0-100 Pa) as exam-

ples, they measure the static pressure in cleanrooms and transfer pressure values to voltage signals. The voltage signals are finally transferred into pressure values, y, through input terminals and the main program in IPC. Thus, the controllers in IPC read the feedback signal from the sensors. The IPC, inverters and fans are powered by the 230 V electricity from the main grid. The transformers transfer 230 V to 24 V, driving the extension modules, VAVs and sensors.

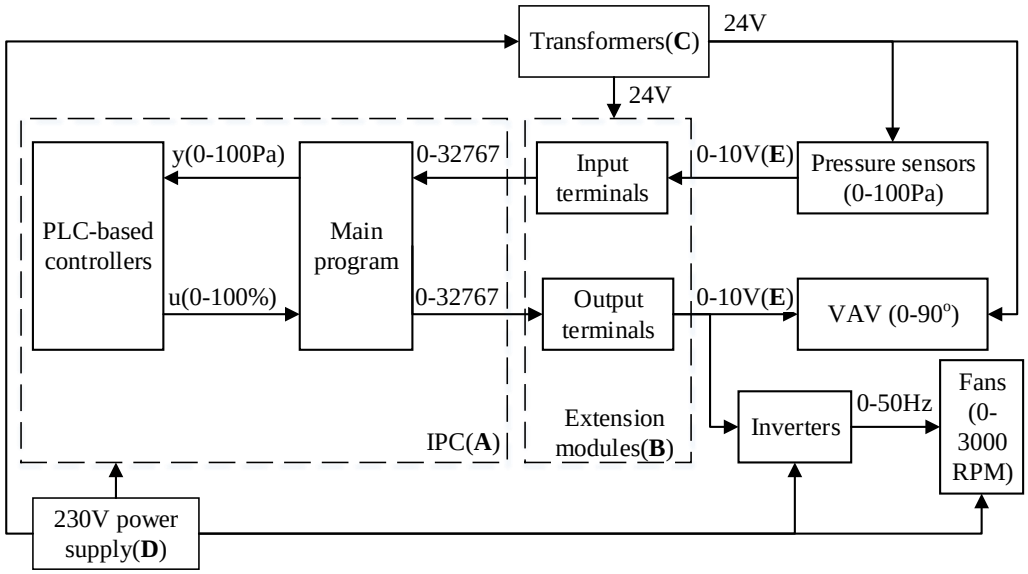

Figure 7.2: Block diagram of the PLC panel.

7.2.2 Implementation of Simulink modules in PLC

Figure 7.3 presents a block diagram of the implementation of Simulink modules, which contain the control algorithm, into the PLC based IPC. The software named TE1400 enables the user to generate real-time capable modules which can be executed in the IPC. These modules can be instantiated multiple times, parametrised and debugged in the IPC with TwinCAT. TE1410 provides an interface for data exchange between the TwinCAT and Simulink.

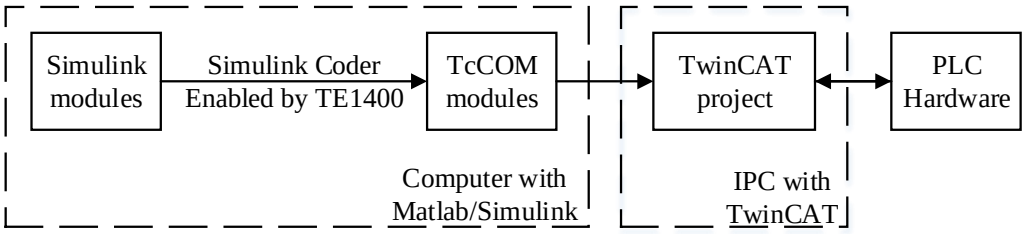

Figure 7.3: Implementation of Simulink modules in PLC.

The Simulink Coder generates real-time-capable C or C++ code from block diagrams implemented in Simulink. TE1400 uses the Simulink Coder to create a TwinCAT component object model (TcCOM) module with the input and output behaviour according to the source Simulink model. Generated modules can be instantiated in TwinCAT projects, where those can be parametrised using the TwinCAT in the IPC if parameter changes are necessary. After starting the TwinCAT, the module is executed in real-time and can thus be integrated into a real machine controller. The TwinCAT offers a software environment in which TwinCAT modules are loaded, implemented and managed. TwinCAT offers additional basic functions so that the system resources can be used (memory, tasks and hardware access, etc.).

7.3 Field test results

Since the PLC programs are transferred from the Matlab/Simulink programs proposed in previous chapters, the PLC based controllers have the same algorithm, inputs and outputs. To compare the performance of the controllers between Matlab and PLC, the PI controllers, MPC controllers and particulate controllers have been built and run in the IPC.

7.3.1 PI control: Matlab vs. PLC

To verify the performance of the PLC platform against Matlab, the PI control is also implemented in PLC. The PLC based PI controllers have been designed with the same parameters as in Matlab as shown in Table 5.1. The programs have been

transferred from Matlab/Simulink to PLC language.

The results obtained from the Matlab based PI control are compared with the proposed PLC based PI control. The control inputs of PI control for both Matlab and PLC based programs are plotted in Figures 7.4 and 7.5. The tracking response of the output variables for both controllers are shown in Figures 7.6 and 7.7. The comparison results show that the PLC based PI controllers have smaller rise time and shorter settling time.

The controllers in Matlab/Simulink communicate with the hardware through the OPC server. This data transmission causes a large delay to take the control actions. Also, the processor of the computer installed with Matlab is not powerful enough to supply good control performance. The PLC based controller communicate to the hardware directly through the MODBUS which apparently decrease the time delay. The PLC based IPC has a more powerful processor which can deal with the computation faster. Thus, the PLC based PI controllers show a better response than the Matlab based PI controllers.

Table 7.1 gives the comparison results of performance indices between Matlab based and PLC based PI control. Most PLC based controllers have smaller values of indices which demonstrate that the PLC based PI controllers perform better than Matlab based PI controllers.

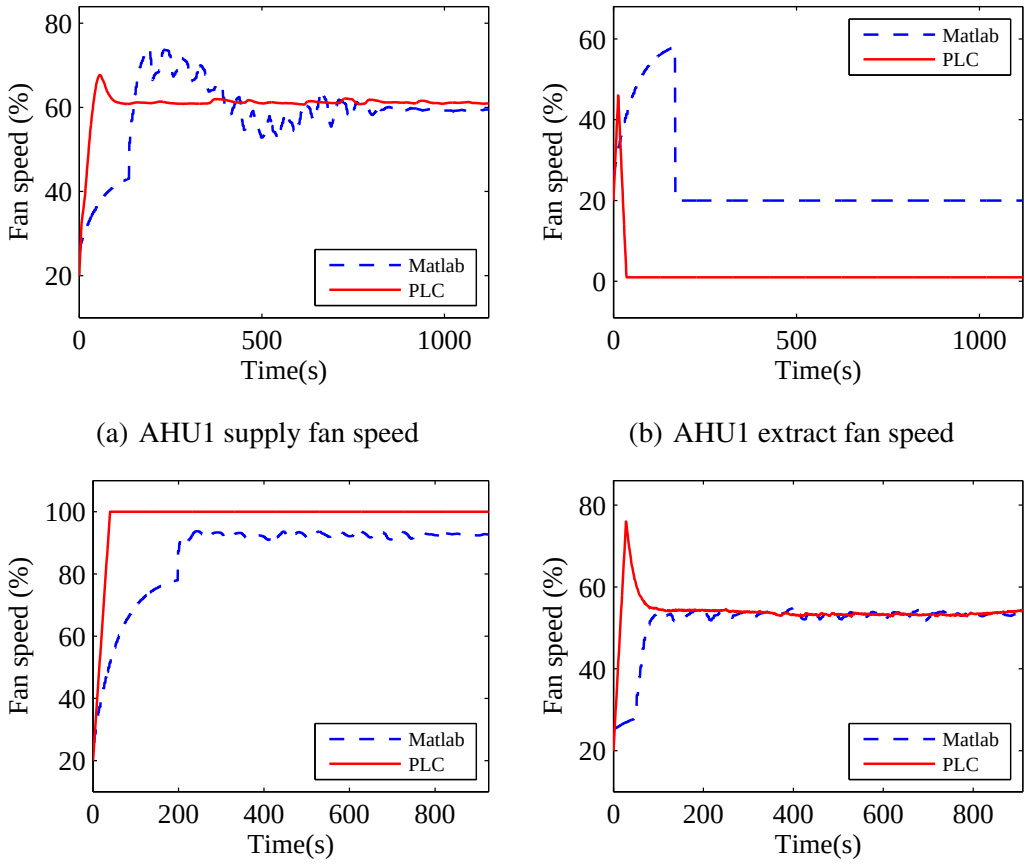

(a) AHU1 supply fan speed

(b) AHU1 extract fan speed

(c) AHU2 supply fan speed

(d) AHU2 extract fan speed

Figure 7.4: Comparison of PI control results between Matlab and PLC for the MVs related to fans.

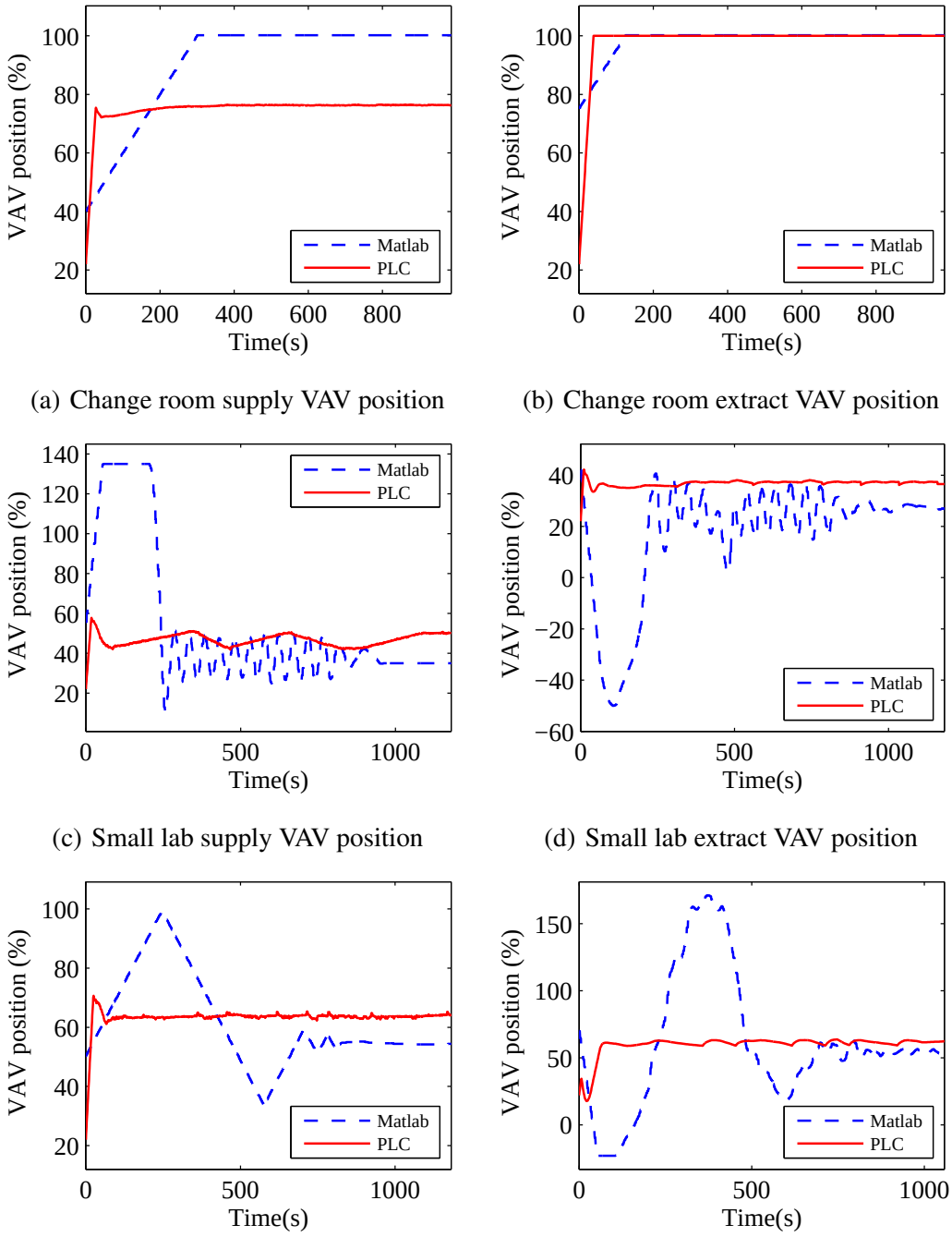

(a) Change room supply VAV position

(b) Change room extract VAV position

(c) Small lab supply VAV position

(d) Small lab extract VAV position

(e) Large lab supply VAV position

(f) Large lab extract VAV position

Figure 7.5: Comparison of PI control results between Matlab and PLC for the MVs related to VAVs.

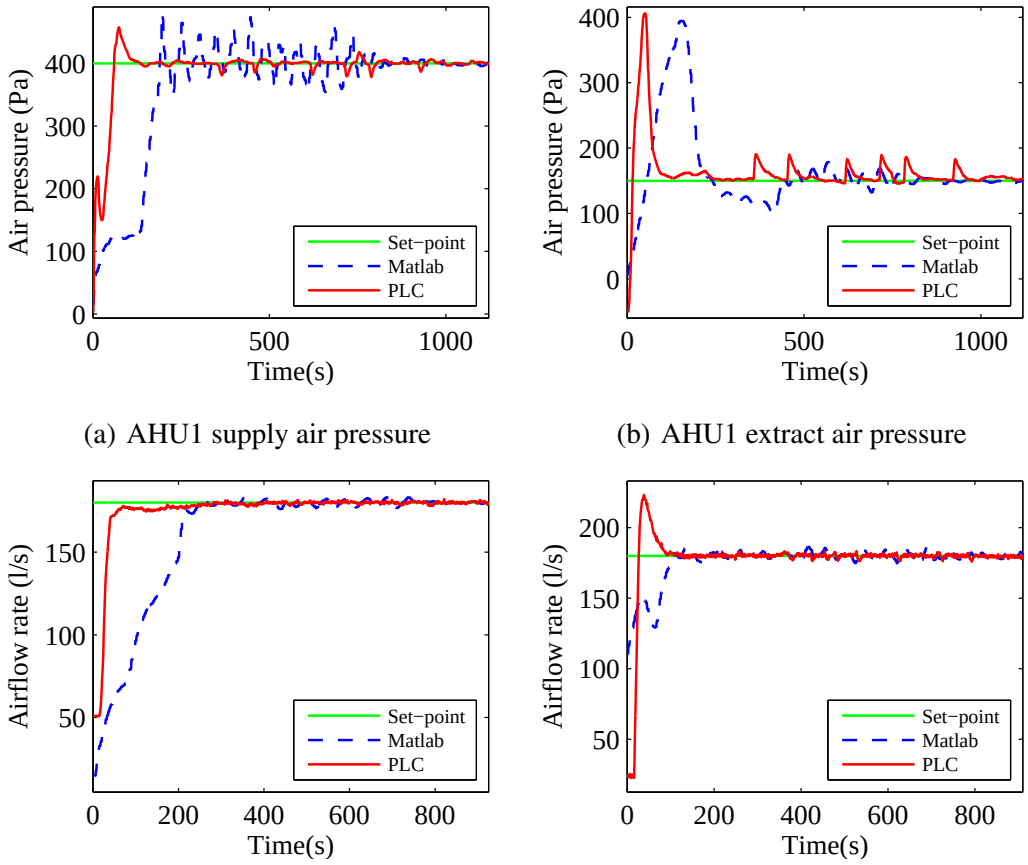

(a) AHU1 supply air pressure

(b) AHU1 extract air pressure

(c) AHU2 supply airflow rate

(d) AHU2 extract airflow rate

Figure 7.6: Comparison of PI control results between Matlab and PLC for the tracking response of outputs related to fans.

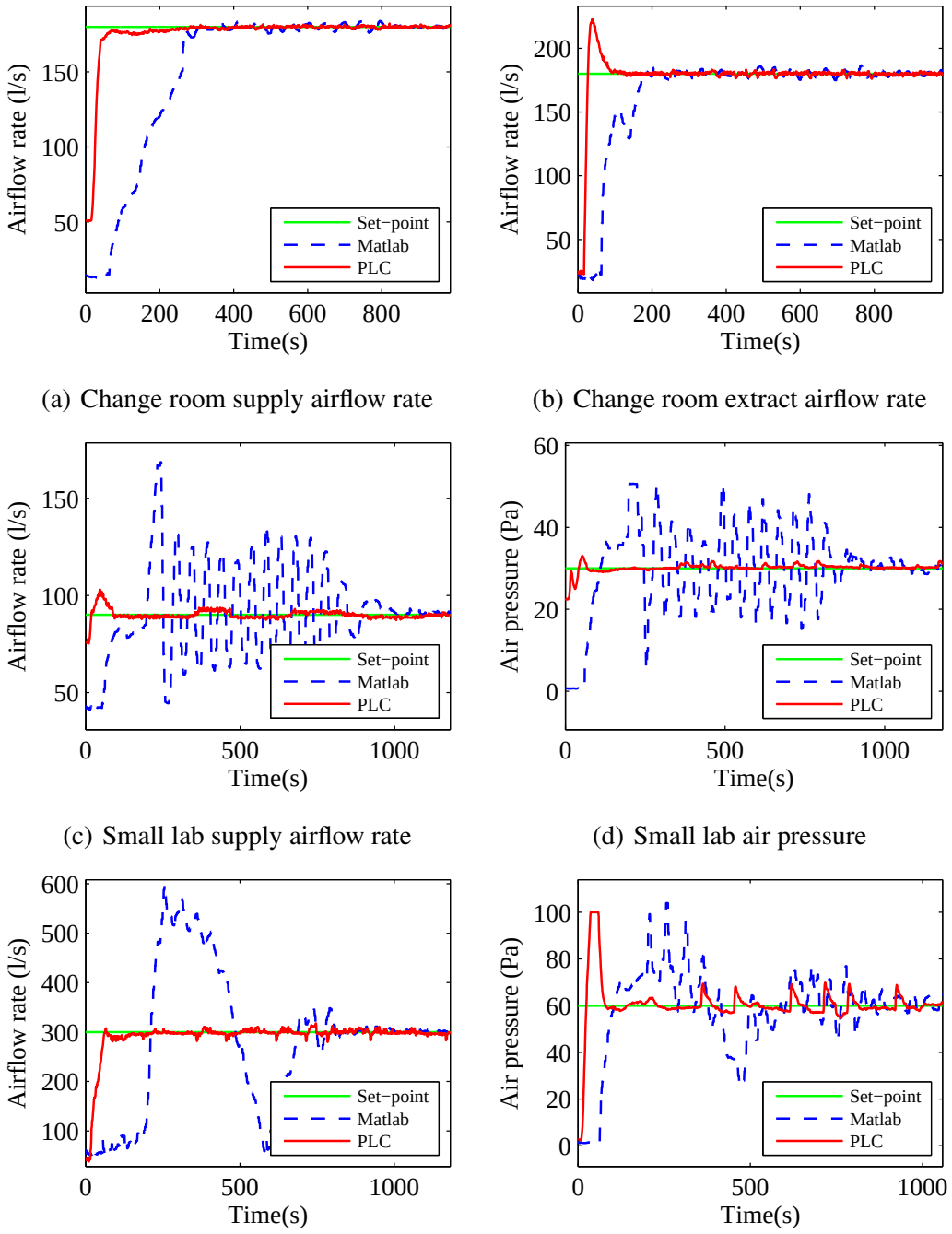

(a) Change room supply airflow rate

(b) Change room extract airflow rate

(c) Small lab supply airflow rate

(d) Small lab air pressure

(e) Large lab supply airflow rate

(f) Large lab air pressure

Figure 7.7: Comparison of PI control results between Matlab and PLC for the tracking response of outputs related to VAVs.

Table 7.1: Comparison of the performance indices of PI control, Matlab vs. PLC.

Model	Controller	IAE	ISE	ITAE	ITSE
AHU1	Matlab	1.3115e+4	2.3458e+4	6.0992e+5	5.2024e+7
supply fan	PLC	6.3574e+4	1.8098e+6	6.5221e+6	1.4251e+8
AHU1	Matlab	1.0616e+4	1.6906e+6	4.4941e+5	6.7330e+7
extract fan	PLC	9.7951e+3	1.4570e+6	3.9989e+5	5.3843e+5
AHU2	Matlab	4.4585e+3	4.1065e+3	2.2501e+5	5.5734e+6
supply fan	PLC	4.6124e+3	3.9020e+5	2.2771e+5	5.1931e+6
AHU2	Matlab	5.2841e+3	5.5326e+3	2.0163e+5	7.4639e+8
extract fan	PLC	4.5782e+3	4.9960e+5	2.7214e+5	5.8354e+6
Change room	Matlab	4.4592e+03	4.1072e+05	2.2502e+05	5.5734e+06
supply VAV	PLC	4.4808e+03	3.3872e+05	3.3985e+05	4.8228e+06
Change room	Matlab	5.2835e+03	5.5329e+05	2.0160e+05	7.4639e+06
extract VAV	PLC	4.3948e+03	4.4403e+05	2.2236e+05	4.8342e+06
Small lab	Matlab	8.03223+02	5.9635e+03	7.4216e+04	2.3424e+05
supply VAV	PLC	5.5152e+02	3.2414e+03	7.2082e+04	1.0319e+05
Small lab	Matlab	6.0336e+02	4.2634e+03	4.7960e+04	1.0145e+05
extract VAV	PLC	7.8525e+02	4.0373e+03	1.2473e+05	2.0702e+05
Large lab	Matlab	1.1022e+04	1.7487e+06	6.7903e+05	2.9674e+07
supply VAV	PLC	1.3480e+04	1.7007e+06	1.2585e+06	4.6455e+07
Large lab	Matlab	3.1671e+03	1.0714e+05	2.5236e+05	3.3713e+06
extract VAV	PLC	2.3445e+03	5.8141e+04	2.2771e+05	1.3706e+06

7.3.2 PI control vs. model predictive control in PLC

Several closed-loop systems have been built with MPC controllers implemented in PLC. To verify the performance of the MPC control strategy, the results of the field test of the PLC based MPC have been compared with the results from the PLC based PI control. The comparison results for both controllers are given in Figures 7.8-7.11. Figures 7.8 and 7.9 present the control inputs and Figures 7.10 and 7.11 show the tracking response of the output variables. The comparison results

demonstrate that both controllers have similar performance with similar rise time and settling time.

To compare them accurately, their integral performance indices have been calculated with the same response time. Table 7.2 presents the comparison results of the indices. Most MPC controllers have smaller values of indices than PI controllers. In other words, the MPC controllers have better performance than PI controllers in PLC.

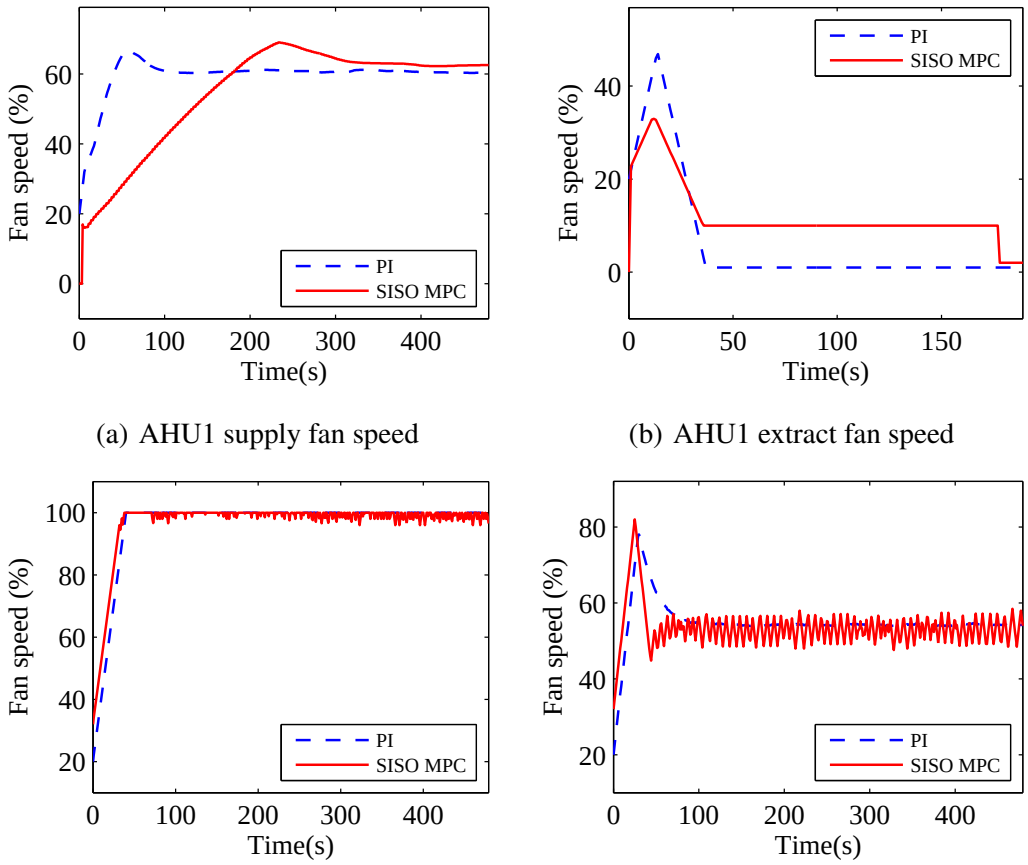

(a) AHU1 supply fan speed

(b) AHU1 extract fan speed

(c) AHU2 supply fan speed

(d) AHU2 extract fan speed

Figure 7.8: Comparison results between MPC and PI for the MVs related to fans in PLC.

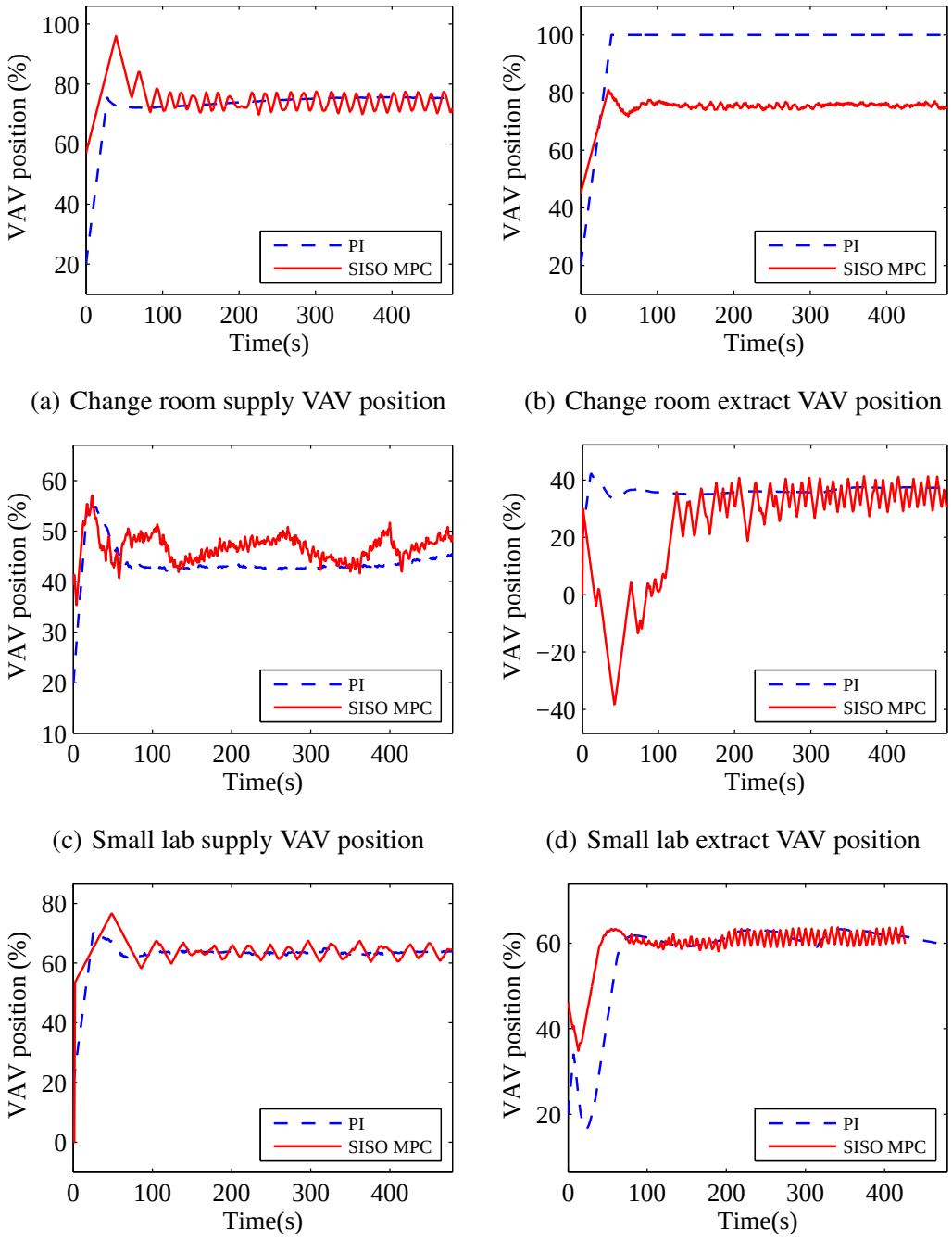

(a) Change room supply VAV position

(b) Change room extract VAV position

(c) Small lab supply VAV position

(d) Small lab extract VAV position

(e) Large lab supply VAV position

(f) Large lab extract VAV position

Figure 7.9: Comparison results between MPC and PI for the MVs related to VAVs in PLC.

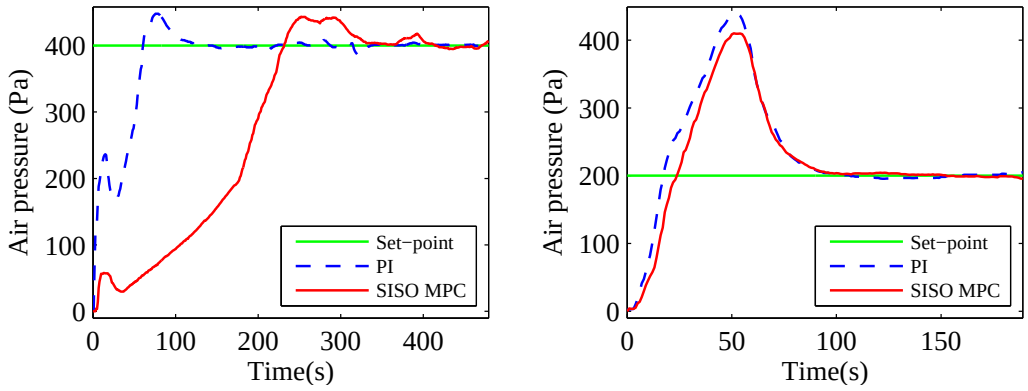

(a) AHU1 supply air pressure

(b) AHU1 extract air pressure

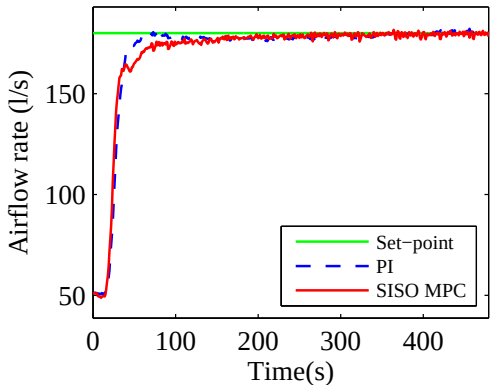

(c) AHU2 supply airflow rate

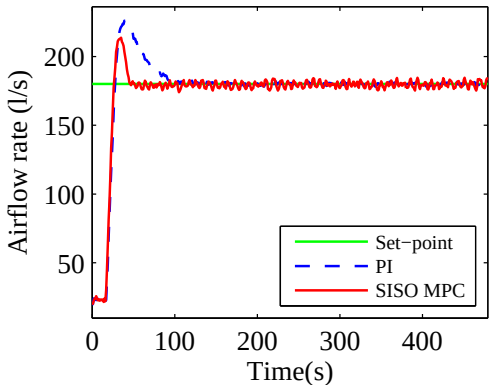

(d) AHU2 extract airflow rate

Figure 7.10: Comparison results between MPC and PI for the tracking response of outputs related to fans in PLC.

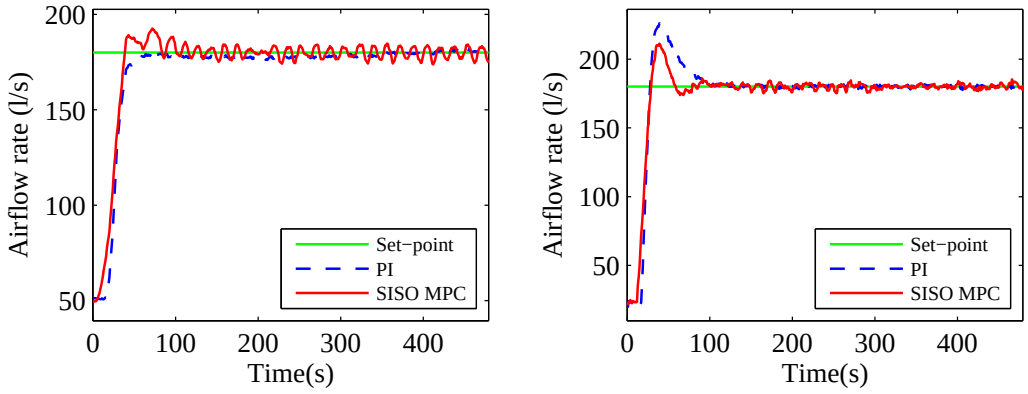

(a) Change room supply airflow rate

(b) Change room extract airflow rate

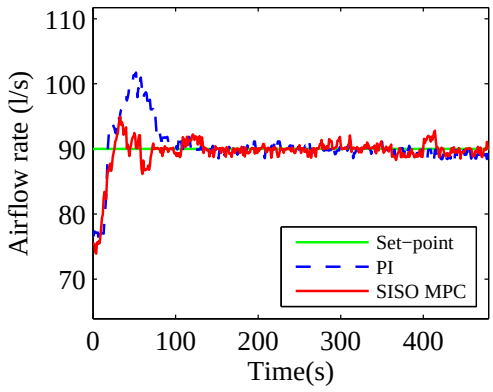

(c) Small lab supply airflow rate

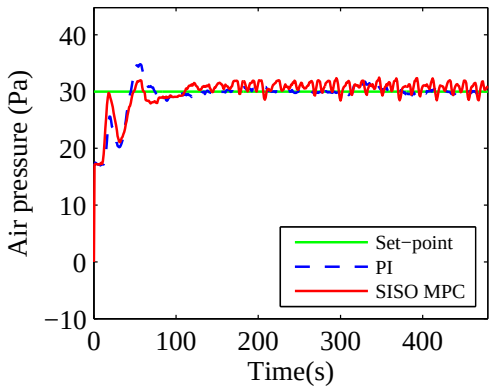

(d) Small lab air pressure

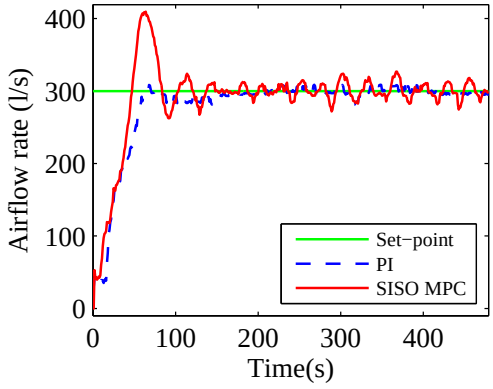

(e) Large lab supply airflow rate

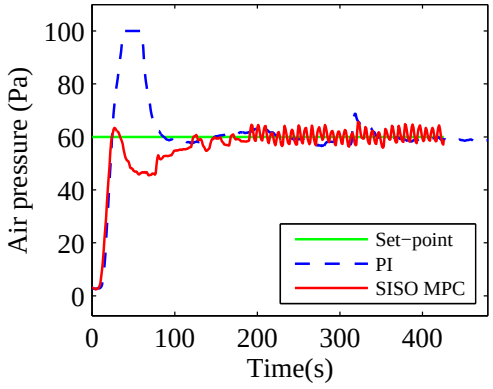

(f) Large lab air pressure

Figure 7.11: Comparison results between MPC and PI for the tracking response of outputs related to VAVs in PLC.

Table 7.2: Comparison of the performance indices between the PI and MPC controllers in PLC.

Model	Controller	IAE	ISE	ITAE	ITSE
AHU1	PI	1.3115e+4	2.3458e+4	6.0992e+5	5.2024e+7
supply fan	MPC	6.3574e+4	1.8098e+6	6.5221e+6	1.4251e+8
AHU1	PI	1.0616e+4	1.6906e+6	4.4941e+5	6.7330e+7
extract fan	MPC	9.7951e+3	1.4570e+6	3.9989e+5	5.3843e+5
AHU2	PI	4.4585e+3	4.1065e+3	2.2501e+5	5.5734e+6
supply fan	MPC	4.6124e+3	3.9020e+5	2.2771e+5	5.1931e+6
AHU2	PI	5.2841e+3	5.5326e+3	2.0163e+5	7.4639e+8
extract fan	MPC	4.5782e+3	4.9960e+5	2.7214e+5	5.8354e+6
Change room	PI	4.4592e+03	4.1072e+05	2.2502e+05	5.5734e+06
supply VAV	MPC	4.4808e+03	3.3872e+05	3.3985e+05	4.8228e+06
Change room	PI	5.2835e+03	5.5329e+05	2.0160e+05	7.4639e+06
extract VAV	MPC	4.3948e+03	4.4403e+05	2.2236e+05	4.8342e+06
Small lab	PI	8.03223+02	5.9635e+03	7.4216e+04	2.3424e+05
supply VAV	MPC	5.5152e+02	3.2414e+03	7.2082e+04	1.0319e+05
Small lab	PI	6.0336e+02	4.2634e+03	4.7960e+04	1.0145e+05
extract VAV	MPC	7.8525e+02	4.0373e+03	1.2473e+05	2.0702e+05
Large lab	PI	1.1022e+04	1.7487e+06	6.7903e+05	2.9674e+07
supply VAV	MPC	1.3480e+04	1.7007e+06	1.2585e+06	4.6455e+07
Large lab	PI	3.1671e+03	1.0714e+05	2.5236e+05	3.3713e+06
extract VAV	MPC	2.3445e+03	5.8141e+04	2.2771e+05	1.3706e+06

7.3.3 Particle counter based model predictive control in PLC

The introduction of the particle counters makes it possible to measure the particle concentrations. Two closed-loop systems have been built to control the particle concentrations in the cleanroom laboratory. The particle counter based SISO MPC controllers in these closed-loop systems have been transferred from Matlab to PLC. Thus, both two controllers can be run in PLC environment. The field test results of the two controllers are shown in Figure 7.12 which presents the supply VAV position

and the maximum particle concentration in the small lab and large lab. Other facilities are controlled in steady state by PI control. The results show that the particle counter based SISO MPC controllers can control the particle concentration either in the small or the large lab. The control inputs increased when the particle concentration rose high against the set-points. The control inputs decreased when the particle concentrations have fallen around the set-points. The operation of the VAVs by the SISO MPC controllers can maintain the particle levels in particular levels.

The particle counter based MIMO MPC is designed coupling both labs and the AHU1 supply fan together. Thus the controlling of the fan speed is taken into account. Figure 7.13 shows the control inputs and system outputs of the particle counter based MIMO MPC in PLC. The MIMO MPC controller is verified to maintain the air cleanliness at a particular level in the laboratory by regulating the AHU1 supply fans, the supply VAV in the small lab and the supply VAV in the large lab.

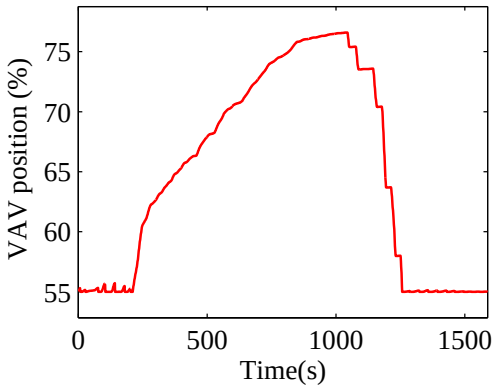

(a) Small lab supply VAV position

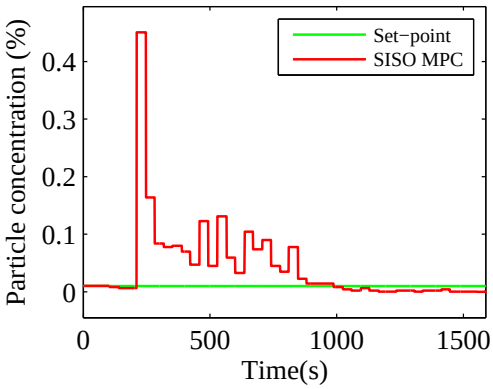

(b) Small lab maximum particle concentration

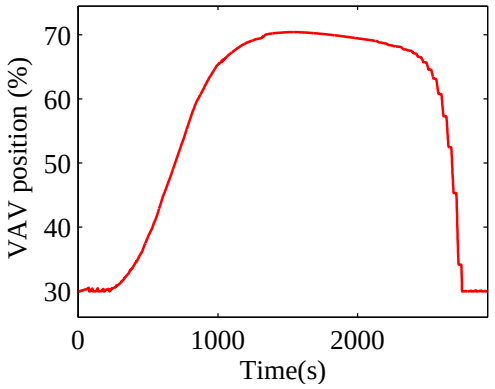

(c) Large lab supply VAV position

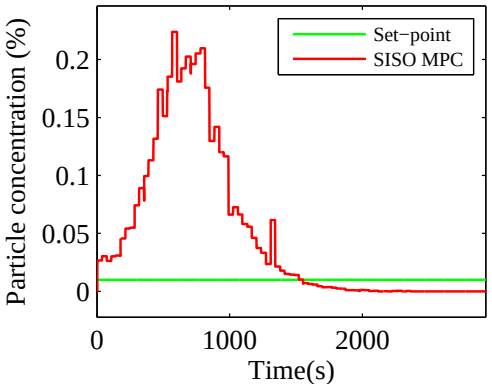

(d) Large lab maximum particle concentration

Figure 7.12: Field test results of the particle counter based SISO MPC in PLC.

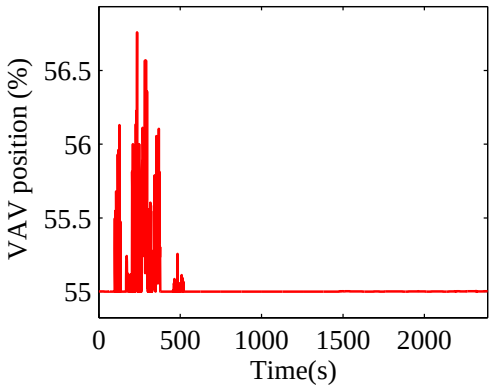

(a) Small lab supply VAV position

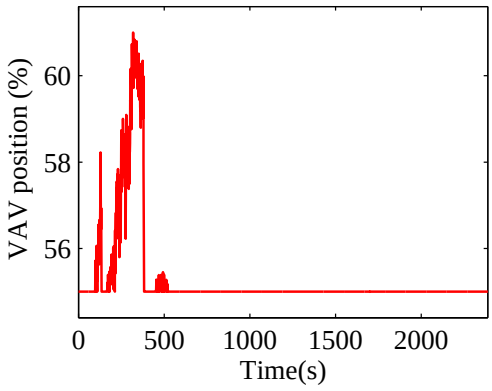

(b) Large lab supply VAV position

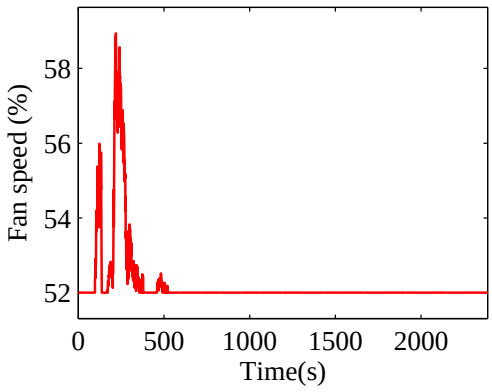

(c) AHU1 supply fan speed

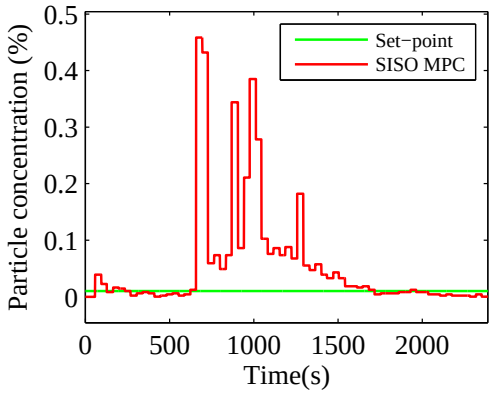

(d) Small lab maximum particle concentration

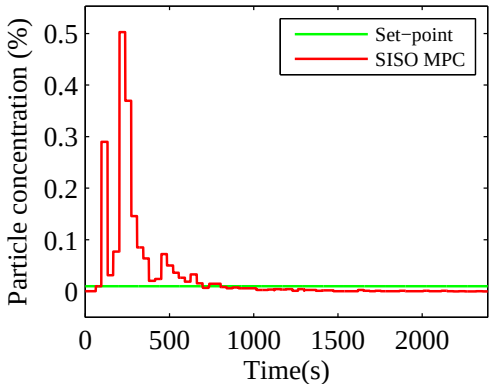

(e) Large lab maximum particle concentration

Figure 7.13: Field test results of the particle counter based MIMO MPC in PLC.

7.3.4 Energy consumption analysis

Figure 7.14 gives a bar chart to compare the integral of fan speeds' cube of PI control between Matlab and PLC, and MPC in PLC environment. Based on the analysis of energy consumption in Section 3.4, the compare of the integrals of fan speeds can reflect the compare of the energy consumption. Thus the energy consumption between different situations can be determined by Figure 7.14. The results demonstrate a rank of consumed energy from the highest to the lowest: Matlab based PI control, PLC based PI control and PLC based MPC.

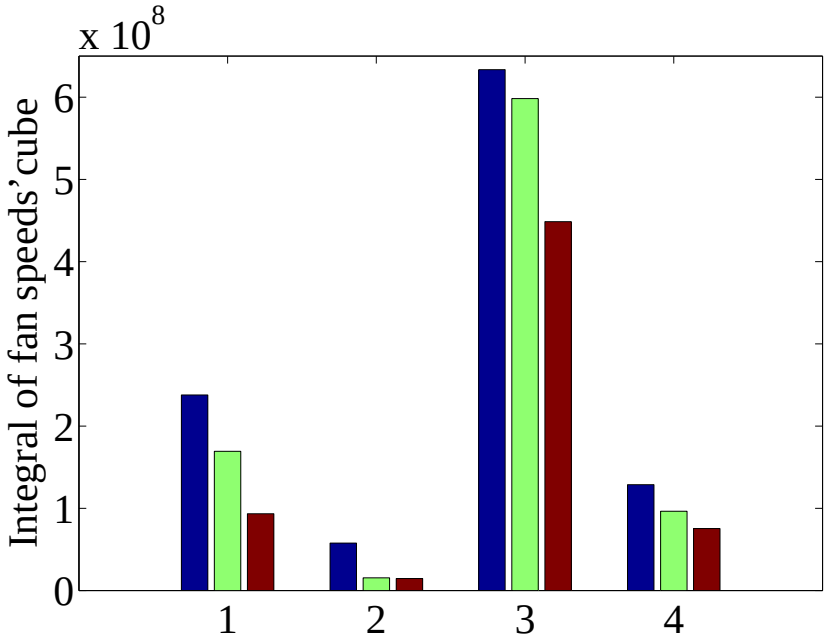

Figure 7.14: Comparison of integrals of fan speeds' cube among Matlab PI control(blue), PLC PI (green) and PLC MPC (red): 1 - AHU1 supply fan speed, 2 - AHU1 extract fan speed, 3 - AHU2 supply fan speed, 4 - AHU2 extract fan speed.

7.4 Conclusion

The PI control and MPC have been implemented in the laboratory via the PLC platform, and the experimental test has been done. The dynamic performances of different controllers are compared based on the comparison of the integral performance indices presented in Section 5.2.3. The energy consumptions of controllers

are compared by comparing the integral of fan speeds as shown in Section 3.4. To compare the performance of the two platforms: Matlab and PLC, the Matlab based PI control has been compared with the PLC based PI control. Moreover, to compare the performance of the two control methods in PLC, the PLC based PI control and MPC have been compared. The comparison results work out a rank of the dynamic performance from the best to the worst: PLC based MPC, PLC based PI control and Matlab based PI control, for the control of airflow rate and AP. Also, the results demonstrate a rank of consumed energy from the highest to the lowest: Matlab based PI control, PLC based PI control and PLC based MPC. Thus, for controlling the airflow rate and AP, the PLC based MPC has the best dynamic performance and consumes the lowest energy.

The particle counter based MPC has been implemented and tested on the PLC platform. Both SISO and MIMO MPC of the particle concentration have been tested in PLC. The field test results show that the controllers can maintain the particle concentration at a particular level.

Chapter 8

Conclusion and Future Work

8.1 Conclusion

The reduction of energy consumption has become main concerns given the growing focus on energy saving and environment protection in recent years, which desires proper design of the HVAC system with optimum energy efficiency with more accurate system model and advanced control of cleanrooms. Also, the control of air cleanliness in cleanrooms requires a way to control the particle concentration directly with the optimisation of the energy consumption. MPC has been implemented to meet the above requirements. This thesis has investigated and developed the MPC for a cleanroom HVAC system implemented by a constructed cleanroom laboratory. After completing this project, it is expected that there will be 40% energy saving compared to the current design.

Since the constructed cleanroom laboratory is a highly accurate simulation of a real-world pharmaceutical factory, the proposed method is applicable to other similar applications. All the facilities and software used in this project meet the industrial standard so that the solution is compatible with other cleanroom HVAC systems. The method proposed in this thesis presents a series of advantages for industrial applications:

- It is attractive to staff with only a limited knowledge of control because the concepts are very intuitive, and the tuning is relatively easy.

- It is a totally open methodology based on certain basic principles which allow for future extensions.
- It can reduce the energy consumption apparently.
- It has a dynamic control of the particle concentration.

Compared to the widely used PID controllers, it also has its drawbacks:

- Its derivation is more complex.
- It needs more computational load.
- The need for an appropriate model of the process to be available.

The main contributions of the thesis can be summarised as follows:

1. Modelling of the cleanroom laboratory

   A black-box approach has been proposed to identify the mathematical models of the cleanroom laboratory. The SISO system models of this laboratory have been identified based on the measured data of the laboratory controlled by PI controllers in the BMS. Based on the interactions of the controlled variables within the laboratory, the whole system has been divided into two MIMO subsystems whose mathematical models have also been identified. Three parameter estimation methods and three model structures have been investigated. The model structure of each system model with the best performance index has been found by comparing the prediction results with the experimental results. The PEM has estimated the model parameters the most accurately, and the ARX models have been chosen as the best-performed model structure.
2. Development of the SISO and MIMO MPC to replace the PI control

   The airflow rate and air pressure regulation using SISO MPC, which has been designed based on the identified SISO models, has been investigated. Both PI control and SISO MPC have been verified through simulation and field test. The transient performance and the energy consumption of the PI control and SISO MPC have been compared. The results show that the SISO MPC has better transient performance and less consumed power than the PI control.

   The MIMO MPC controllers have been proposed controlling the ACR and AP. The MIMO MPC uses the ACR instead of airflow rate because the ACR

is a more direct variable to reflect the ventilation situation in cleanrooms. The MIMO MPC can couple the relevant hardware which significantly improves the dynamics and reduce the energy consumption. By simulation and field test based on Matlab/Simulink, it is found that the MIMO MPC performs better and consume less power than the PI control and SISO MPC.

3. Introduction of the closed-loop control of particles

   The particle concentrations in the laboratory have been measured by particle counters as the feedback signals to build the closed-loop control of particle levels. The particle counter based PI, SISO MPC and MIMO MPC controllers have been designed to control the maximum particle concentration inside the small/large lab. Both simulation and field test results demonstrate that the particle counter based controllers can maintain the air cleanliness in a particularly low level. Based on the analysis of the energy consumption among the three controllers, MIMO MPC consumes the lowest power.

4. Test and implementation of MPC in PLC devices

   A PLC panel has been developed where the PLC based IPC has been installed, and the PI control and MPC have been implemented. The PLC devices provide a software-based PLC solution to deal with PLC based control problems. The hardware of the HVAC system is connected to the PLC panel through cables. The PI control and MPC programs have been transferred from Matlab/Simulink to PLC language. The field tests based on this PLC panel have been done to verify the performance of the PLC devices. The comparison results have given a rank of the transient performance from the best to the worst as PLC based MPC, PLC based PI control and Matlab based PI control for the regulation of the airflow rate and AP. The results also demonstrate a rank of consumed energy from the highest to the lowest: Matlab based PI control, PLC based PI control and PLC based MPC for controlling the airflow rate and AP. The particle counter based MPC controllers have been implemented and tested in the PLC panel. The field test results of the PLC based particulate control show that the controllers can maintain the particle concentration in particular low levels.

8.2 Future work

The possible future work is listed based on the following ideas.

1. For a new factory, the traditional MPC engineer needs to collect the data on-site with the facility running for enough time (sometimes takes weeks). The data will be used to identify the system models and design the MPC controllers. After the controllers have passed the simulation test, they will be tested on-site. Then the tuning process will be done. It normally takes months to make the MPC controllers working on-site. The currently developed system is manually tuned for the laboratory which can only provide optimal performance for the laboratory. For different clients, retuning process is required on-site which could be time-consuming, and the optimal performance also cannot be guaranteed. Thus automatic and optimal tuning is necessary for transferring the current lab-based design to a product. The real HVAC system can have a very large scale which makes it difficult to develop the accurate system models. The automatic algorithm should be adaptive to fit all kinds of HVAC system with different scales.
2. Current status: the value of the energy consumption of the whole system is collected once per half an hour which is much larger than the sample time of the controllers. It is impossible to put these data into closed-loop. If the measurement of the energy consumption is in a small enough sample time, it can be put into closed-loop. Thus the energy saving can be achieved directly by minimising the energy consumption in the optimisation process.
3. The traditional MPC controllers consider two optimisation process:
   - The tracking response of the output variables, the minimum of the difference between the measured output and the set-point.
   - The minimum of the increment of the MV, controlling the change rate of the input.

   The controllers can be upgraded with optimal tuning:
   - The difference between the MV and the set-point can be minimised. It can keep the driver in a low value which decreases the energy consump-

tion. The weight of each variable should be tuned which can balance the control performance and the energy consumption.

- The energy efficiency itself can be regarded as a variable of the performance index in the optimisation process. Then, the energy efficiency can be directly controlled.
- The measured energy consumption is usually an average value during a long time. However, the control strategy requires the instant value with a short time interval (seconds for this laboratory). The instant values can be put into closed-loop and optimisation process.

References

[1] C.Y. Khoo, C.C. Lee and S.C. Hu, "An experimental study on the influences of air change rate and free area ratio of raised-floor on cleanroom particle concentrations," *Building and Environment*, vol. 48, pp. 84-88, 2012.

[2] ISO 14644-1, *Cleanrooms and associated controlled environments - part 1: Classification of air cleanliness by particle concentration*, 2015.

[3] T. Sandle, "16 - Cleanrooms and environmental monitoring," in *Pharmaceutical Microbiology*, edited by Tim Sandle, Woodhead Publishing, Oxford, pp. 199-217, 2016.

[4] *Euradlex the rules governing medicinal products in the European community, Volume 4 - good manufacturing practice (GMP) guidelines, Annex 1 - manufacture of sterile medicinal products*, European Commission, Brussels, 2009.

[5] ASHRAE Standard 62.2, *Ventilation and acceptable indoor air quality in low-Rise residential buildings*, 2010.

[6] W. Whyte, N. Lenegan and T. Eaton, "Ensuring the air supply rate to a cleanroom complies with the EU GGMP and ISO 14644-3 recovery rate requirements," *Clean Air and Containment Review*, vol. 26, 2016.

[7] K. Sutherland, "Cleanroom management: using filters in the cleanroom," *Filtration & Separation*, vol. 45, no. 4, pp. 20-22, 2008.

[8] R.W. Haines and M.E. Myers, *HVAC systems design handbook*, McGraw-Hill Companies, Inc, 2010.

[9] R. McDowall, *Fundamentals of HVAC systems*, Elsevier, Oxford, 2007.

[10] R.D. Patil, S.P. Patil and V.H. Bankar, "A study on role of HVAC system in data center," *International Journal of Innovative Research in Computer and Communication Engineering*, vol. 4, no. 6, 2016.

[11] B.A. Rock and D. Zhu, *Designer's guide to ceiling-based air diffusion*, Atlanta, Ga: American Society of Heating, Refrigerating and Air-Conditioning Engineers (ASHRAE), 2002.

[12] *Handbook - fundamentals*, American Society of Heating, Refrigerating and Air-Conditioning Engineers (ASHRAE), 2009.

[13] F.C. McQuiston, J.D. Parker and J.D. Spitler, *Heating, ventilating, and air conditioning: analysis and design*, Wiley, 2000.

[14] S.C. Sugarman, *HVAC fundamentals*, Fairmont Press, Inc, 2016.

[15] L. Cui, *Methodology for design, calibration, system identification and operation of an experimental HVAC system*, Thesis, Department of Architectural Engineering, The Pennsylvania State University, 2013.

[16] *Communication from the commission to the European parliament*, The Council, The European Economic and Social Committee and the Committee of the Regions, 2010.

[17] R. Dixon, E. McGowan, G. Onysko and R. Scheer, "Us energy conservation and efficiency policies: challenges and opportunities," *Energy Policy*, 2010.

[18] *International energy outlook*, U.S. Energy Information Administration (EIA), 2016.

[19] *Annual energy outlook*, U.S. Energy Information Administration (EIA), 2013.

[20] Y. Yu, V. Loftness and D. Yu, "Multi-structural fast nonlinear model-based predictive control of a hydronic heating system," *Building and Environment*, vol. 69, pp. 131-148, 2013.

[21] M. Gruber, A. Trschel and J.O. Dalenbck, "Model-based controllers for indoor climate control in office buildings Complexity and performance evaluation," *Energy and Buildings*, vol. 68, part A, pp. 213-222, 2014.

[22] *White paper - energy efficiency in cleanrooms*, Energy Efficiency Consultancy (EECO2), 2017.

[23] C. Galitsky, S. Chang, E. Worrell and E. Masanet, *Energy efficiency improvement and cost saving opportunities for the pharmaceutical industry - an ENERGY STAR guide for energy and plant managers*, Environmental Energy Technologies Division, University of California, 2008.

[24] *The business of energy efficiency - a paper from Carbon Trust Advisory Services*, Carbon Trust, Available: https://www.carbontrust.com/media/135418/cta001-business-of-energy-efficiency.pdf.

[25] T. Xu, "Performance evaluation of cleanroom environmental systems," *Journal of the IEST*, vol. 46, no. 1, pp. 66-73, 2003.

[26] Q. Bi, W. Cai, Q. Wang, C.C. Hang, E. Lee, Y. Sun, K. Liu, Y. Zhang and B. Zou, "Advanced controller auto-tuning and its application in HVAC systems," *Control Engineering Practice*, vol. 8, pp. 633-644, 2000.

[27] U.S. Federal Standard FS209, *Clean room and work station requirements, controlled environment*, General Services Administration, 1973.

[28] IEST Recommended Practices (RP-12), *Considerations in cleanroom design*, 1978-2002.

[29] ISO 14644, *Cleanrooms and associated controlled environments - part 4: design, construction and start-up*, Geneva, Switzerland: International Organization for Standardization, 2001.

[30] D. Sartor, C. Lowell and C. Blumstein, *Cleanrooms and laboratories for high-tech industries*, Final Report, California Energy Commission, 1999.

[31] T. Xu and W. Tschudi, "Energy performance of cleanroom environmental systems," in *Proceedings of ESTECH 2002, the 48th annual technical meeting and the 16th ICCCS international symposium on contamination control*, Anaheim, California, USA: Institute of Environmental Sciences and Technology (IEST), 2002.

[32] W.K. Brown and C.A. Lynn, "Fundamental clean room concepts," *ASHRAE Transactions*, vol. 92, no. 1b, pp. 272-87, 1986.

[33] R.A. Jaisinghani, "Air handling considerations for cleanrooms," in *InterPhex conference*, Philadelphia, vol. 20-22, pp. 15, 2001.

[34] M. Kozicki, P. Robinson and S.A. Hoeniq, *Cleanrooms, facilities and practices*, New York: Van Nostrand Reinhold, 1991.

[35] P.W. Morrison, *Environmental control in electronic manufacturing*, New York: Van Nostrand Reinhold, 1973.

[36] W. Sun, "Conserving fan energy in cleanrooms," *ASHRAE Journal*, pp. 36-38, 2008.

[37] W. Sun, J. Mitchell, K. Flyzik, S.C. Hu, J. Liu, R. Vijayakumar and H. Fukuda, "Development of cleanroom required airflow rate model based on establishment of theoretical basis and lab validation," *ASHRAE Transactions*, vol. 116, no. 1, pp. 87-97, 2010.

[38] E.F. Camacho and C. Bordons, *Model predictive control*, Springer, 2007.

[39] D.Q. Mayne, "Model predictive control: Recent developments and future promise," *Automatica*, vol. 50, no. 12, pp. 2967-2986, 2014.

[40] C.E. Garcia, D.M. Prett and M. Morari, "Model predictive control: theory and practice - a survey," *Automatica*, vol. 25, no. 3, pp. 335-348, 1989.

[41] M. Morari and J.H. Lee, "Model predictive control: past, present and future," *Computers & Chemical Engineering*, vol. 23, no. 4-5, pp. 667-682, 1999.

[42] J. Richalet, A. Rault, J.L. Testud and J. Papon, "Model predictive heuristic control: applications to industrial processes," *Automatica*, vol. 14, no. 5, pp. 413-428, 1978.

[43] C.R. Cutler and B.L. Ramaker, "Dynamic matrix control - a computer control algorithm," in *AICHE national meeting*, Houston, Texas, 1979.

[44] D.M. Prett and R.D. Gillette, "Optimization and constrained multivariable control of a catalytic cracking unit," *AICHE national meeting*, Houston, Texas, 1979; also in *Proceedings of the joint automatic control conference*, San Francisco, California, 1980.

[45] L.A. Zadeh and B.H. Whalen, "On optimal control and linear programming," *IRE Transactions on Automatic Control*, vol. 7, no. 4, pp. 45-46, 1962.

[46] A.I. Propoi, "Use of LP methods for synthesizing sampled-data automatic systems," *Automation and Remote Control*, vol. 24, pp. 837, 1963.

[47] S.E. Dreyfus, "Some types of optimal control of stochastic systems," *Journal of the Society for Industrial and Applied Mathematics, Series A: Control*, vol. 2, no. 1, pp. 120-134, 1964.

[48] T.S. Chang and D.E. Seborg, "A linear programming approach to multivariable feedback control with inequality constraints," *International Journal of Control*, vol. 37, no. 3, pp. 583-597, 1983.

[49] S.J. Qin and T.A. Badgwell, "A survey of industrial model predictive control technology," *Control Engineering Practice*, vol. 11, no. 7, pp. 733-764, 2003.

[50] J. Richalet, A. Rault, J.L. Testud and J. Papon, "Algorithmic control of industrial processes," in *Proceedings of the 4th IFAC symposium on identification and system parameter estimation*, pp. 1119-1167, 1976.

[51] P. Grosdidier, B. Froisy, and M. Hammann, "The IDCOM-M controller," in *Proceedings of the 1988 IFAC workshop on model based process control*, Oxford: Pergamon Press, pp. 31-36, 1988.

[52] R. Rouhani and R. Mehra, "Model algorithmic control: basic theoretical properties," *Automatica*, vol. 18, no. 4, pp. 401-414, 1982.

[53] C.R. Cutler and B.L. Ramaker, "Dynamic matrix control - a computer control algorithm," in *Proceedings of the joint automatic control conference*, 1980.

[54] D.W. Clarke and C. Mohtadi and P.S. Tuffs, "Generalized predictive control - part I: the basic algorithm," *Automatica*, vol. 23, pp. 137-148, 1987.

[55] D.W. Clarke and C. Mohtadi and P.S. Tuffs, "Generalized predictive control - part II: extensions and interpretations," *Automatica*, vol. 23, pp. 149-160, 1987.

[56] D.W. Clarke and C. Mohtadi, "Properties of generalized predictive control," *Automatica*, vol. 25, no. 6, pp. 859-875, 1989.

[57] J. Richalet, *Practique de la commande predictive*, 1992.

[58] R.M.C. De Keyser, P.G.A. Van de Velde and F.G.A. Dumortier, "A comparative study of self-adaptive long-range predictive control methods," *Automatica*, vol. 24, no. 2, pp. 149-163, 1988.

[59] R.M. Dekeyser, "Application of extended prediction self-adaptive control," *Implementation of Self-tuning Controllers*, Ed. K Warwick. London, UK: Peter Peregrinus Ltd., 1988.

[60] B.E. Ydstie, A.H. Kemna and L.K. Liu, "Multivariable extended-horizon adaptive control," *Computers & Chemical Engineering*, vol. 12, no. 7, pp. 733-743, 1988.

[61] T.W. Yoon and D.W. Clarke, "Prefiltering in receding-horizon predictive control," *Internal Report 1995/93*, University of Oxford, Department of Engineering Science, 1993.

[62] A. Bemporad, M. Morari and N.L. Ricker, *Model predictive control toolbox for use with Matlab*, The MathWorks, 2005.

[63] J.L. Garriga and M. Soroush, "Model predictive control tuning methods: a Review," *Industrial & Engineering Chemistry Research*, vol. 49, no. 8, pp. 3505-3515, 2010.

[64] J.E. Seem, "A new pattern recognition adaptive controller with application to HVAC systems," *Automatica*, vol. 34, pp. 969-982, 1998.

[65] Y.G. Wang, Z.G. Shi and W.J. Cai, "PID autotuner and its application in HVAC systems," in *Proceedings of the 2001 American Control Conference*, Arlington, VA, vol. 3, pp. 2192-2196, 2001.

[66] G.Y. Jin, P.Y. Tan, X.D. Ding and T.M. Koh, "Cooling coil unit dynamic control of in HVAC system," in *2011 6th IEEE Conference on Industrial Electronics and Applications*, Beijing, pp. 942-947, 2011.

[67] I. Jetté, M. Zaheer-uddin and P. Fazio, "PI-control of dual duct systems: manual tuning and control loop interaction," *Energy Conversion and Management*, vol. 39, pp. 1471-1482, 1998.

[68] A.K. Pal and R.K. Mudi, "Self-tuning fuzzy PI controller and its applications to HVAC systems," *International Journal of Computational Cognition*, vol. 6, pp. 25-30, 2008.

[69] M. Zaheer-uddin and N. Tudoroiu, "Neuro-PID tracking control of a discharge air temperature system," *Energy Conversion and Management*, vol. 45, pp. 2405-2415, 2004.

[70] F. Tahersima, J. Stoustrup, H. Rasmussen and P.G. Nielsen, "Thermal analysis of an HVAC system with TRV controlled hydronic radiator," in *2010 IEEE International Conference on Automation Science and Engineering*, Toronto, ON, pp. 756-761, 2010.

[71] Y.A. Sha'aban, B. Lennox and D. Laur, "PID versus MPC performance for SISO dead-time dominant processes," *10th IFAC International Symposium on Dynamics and Control of Process Systems, IFAC Proceedings*, vol. 46, pp. 241-246, 2013.

[72] A. Afram and F. Janabi-Sharifi, "Review of modeling methods for HVAC systems," *Applied Thermal Engineering*, vol. 67, pp. 507-519, 2014.

[73] T. Zheng, *Model predictive control*, Published by Sciyo, 2010.

[74] P. Javid, A. Aeenmehr and J. Taghavifar, "Supply air pressure control of HVAC system using MPC controller," *International Journal of Mechanical, Aerospace, Industrial, Mechatronic and Manufacturing Engineering*, vol. 8, no. 1, pp. 90-93, 2014.

[75] G. Huang, "Model predictive control of VAV zone thermal systems concerning bi-linearity and gain nonlinearity," *Control Engineering Practice*, vol. 19, no. 7, pp. 700-710, 2011.

[76] S.J. Qin and T.A. Badgwell, "An overview of industrial model predictive control technology," in *AIChE Symposium Series*, New York, NY: American Institute of Chemical Engineers, 1971-c2002., vol. 93, no. 316, 1997.

[77] S.J. Qin and T. Badgwell, "An overview of nonlinear model predictive control applications," *IFACWorkshop on Nonlinear Model Predictive Control*. Assessment and Future Directions. Ascona, Switzerland, 1998.

[78] J.M. Martin-Sanchez and J. Rodellar, *Adaptive predictive control. from the concepts to plant optimization*, 1996.

[79] J.H. Lee, "Model predictive control: Review of the three decades of development," *International Journal of Control, Automation and Systems*, pp. 415-424, 2011.

[80] R. Kwadzogah, M. Zhou and S. Li, "Model predictive control for HVAC systems a review," in *2013 IEEE International Conference on Automation Science and Engineering (CASE)*, pp. 442-447, 2013.

[81] P.D. Moroan, R. Bourdais and D. Dumu, "Building temperature regulation using a distributed model predictive control," *Energy and Buildings*, vol. 42, no. 9, pp. 1445-1452, 2010.

[82] S. Yuan and R. Perez, "Multiple-zone ventilation and temperature control of a single-duct VAV system using model predictive strategy," *Energy and Buildings*, vol. 38, no. 10, pp. 1248-1261, 2006.

[83] H. Karlsson and C.E. Hagentoft, "Application of model based predictive control for water-based floor heating in low energy residential buildings," *Building and Environment*, vol. 46, no. 3, pp. 556-569, 2011.

[84] J. Ma, J. Qin, T. Salsbury and P. Xu, "Demand reduction in building energy systems based on economic model predictive control," *Chemical Engineering Science*, vol. 67, no. 1, pp. 92-100, 2012.

[85] M.S. Elliott, *Decentralized model predictive control of a multiple evaporator HVAC system*, MSc thesis, 2008.

[86] H. Lü, L. Jia, S. Kong and Z. Zhang, "Predictive functional control based on fuzzy T-S model for HVAC systems temperature control," *Journal of Control Theory and Applications*, vol. 5, no. 1, pp. 94-98, 2007.

[87] J. Rehrl and M. Horn, "Temperature control for HVAC systems based on exact linearization and model predictive control," in *2011 IEEE International Conference on Control Applications (CCA)*, Denver, CO, pp. 1119-1124, 2011.

[88] S. Prívara, J. Široký, L. Ferkl and J. Cigler, "Model predictive control of a building heating system: the first experience," *Energy and Buildings*, vol. 43, no. 2-3, pp. 564-572, 2011.

[89] J. Široký, F. Oldewurtel, J. Cigler and S. Prívara, "Experimental analysis of model predictive control for an energy efficient building heating system," *Applied Energy*, vol. 88, no. 9, pp. 3079-3087, 2011.

[90] X.C. Xi, A.N. Poo and S.K. Chou, "Support vector regression model predictive control on a HVAC plant," *Control Engineering Practice*, vol. 15, no. 8, pp. 897-908, 2007.

[91] A. Aswani, N. Master, J. Taneja, D. Culler and C. Tomlin, "Reducing transient and steady state electricity consumption in HVAC using learning-based model predictive control," *Proceedings of the IEEE*, vol. 100, no. 1, pp. 240-253, 2012.

[92] *AHU drawings*, Barkell Ltd, 2014

[93] *2008 ASHRAE handbook : heating, ventilating, and air-conditioning systems and equipment*, American Society of Heating, Refrigerating and Air-Conditioning Engineers (ASHRAE), Atlanta, Ga, 2008.

[94] *Variable speed drives catalogue*, Available: https://www.schneider-electric.com/ solutions/ww/en/med/ 4664898/ application/ pdf/577-vsd-eu_a4.pdf, Schneider Electric, 2008.

[95] *High efficiency free wheels backward curved and airfoil shaped blades for plenum fan*, Available: http://www.comefri.com/ sitoweb/ images/catalogues/NPL-NPA-TE%20C-0090%2001-14.pdf, Comefri UK Ltd, 2014.

[96] *User manual of the energy efficient cleanroom test bed*, Energy Efficiency Consultancy Ltd (EECO2), 2016.

[97] T.N. Aynur, Y. Hwang and R. Radermacher, "Simulation of a VAV air conditioning system in an existing building for the cooling mode," *Energy and Buildings*, vol. 41, pp. 922-929, 2009.

[98] *VMSM-05 Hi-speed Rotating Actuator*, Available: http://www. cmr-controls. com/ uk/ acatalog/ brochures/ main/ VMSM_05_GB_04_1_CAT_SM.pdf, CMR Controls Ltd, 2008.

[99] *Circular duct fans*, Available: http://planetaklimata.com.ua/ instr/ Systemair/ Systemair_Fans_KD_Data_sheet_Eng.pdf, Systemair.

[100] *Square duct fans*, Available: http://planetaklimata.com.ua/ instr/ Systemair/ Systemair_Fans_MUB_Data_sheet_Eng.pdf, Systemair.

[101] R. Liu, J. Wen and M.S. Waring, "Improving airflow measurement accuracy in VAV terminal units using flow conditioners," *Building and Environment*, vol. 71, pp. 81-94, 2014.

[102] S. Hall, *6 - fans, blowers, and compressors*, in Branan's Rules of Thumb for Chemical Engineers (Fifth Edition), Butterworth-Heinemann, Oxford, pp. 118-133, 2012.

[103] J. Rodellar and J.M. Martin-Sanchez, *Adaptive predictive control. from the concepts to plant optimization*, 1996.

[104] K. Kircher, X. Shi, S. Patil and K.M. Zhang, "Cleanroom energy efficiency strategies: modeling and simulation," *Energy and Buildings*, vol. 42, pp. 282-289, 2010.

[105] B. Tashtoush, M. Molhim and M. Al-Rousan, "Dynamic model of an HVAC system for control analysis," *Energy*, vol. 30, pp. 1729-1745, 2005.

[106] F. Scotton, L. Huang, S.A. Ahmadi and B. Wahlberg, "Physics-based modeling and identification for HVAC systems," in *Control Conference (ECC) European*, pp. 1404-1409, 2013.

[107] A. Kusiak and G. Xu, "Modeling and optimization of HVAC systems using a dynamic neural network," *Energy*, vol. 42, pp. 241-250, 2012.

[108] L. Ferkl and J. Široký, "Ceiling radiant cooling: comparison of ARMAX and subspace identification modelling methods," *Building and Environment*, vol. 45, pp. 205-212, 2010.

[109] A. Afram and F. Janabi-Sharifi, "Black-box modeling of residential HVAC system and comparison of gray-box and black-box modeling methods," *Energy and Buildings*, vol. 94, pp. 121-149, 2015.

[110] A. Kusiak, M. Li and Z. Zhang, "A data-driven approach for steam load prediction in buildings," *Applied Energy*, vol. 87, pp. 925-933, 2010.

[111] R. Blan, J. Cooper, K. Chao, S. Stan and R. Donca, "Parameter identification and model based predictive control of temperature inside a house," *Energy and Buildings*, vol. 43, pp. 748-758, 2011.

[112] A. Afram and F. Janabi-Sharifi, "Gray-box modeling and validation of residential HVAC system for control system design," *Applied Energy*, vol. 137, pp. 134-150, 2015.

[113] C. Khoo, C. Lee and S. Hu, "An experimental study on the influences of air change rate and free area ratio of raised-floor on cleanroom particle concentrations," *Building and Environment*, vol. 48, pp. 84-88, 2012.

[114] S.C. Esteves and F.C. Bento, "Implementation of air quality control in reproductive laboratories in full compliance with the Brazilian Cells and Germinative Tissue Directive," *Reproductive BioMedicine Online*, vol. 26, pp. 9-21, 2013.

[115] L. Strauss, J. Larkin and K.M. Zhang, "The use of occupancy as a surrogate for particle concentrations in recirculating, zoned cleanrooms," *Energy and Buildings*, vol. 43, pp. 3258-3262, 2011.

[116] What is OPC, Available: https://opcfoundation.org/about/what-is-opc/.

[117] L. Ljung, *System identification: theory for the user*, Prentice Hall PTR, 1999.

[118] K.J. Keesman, *System identification - an introduction*, Springer, 2011.

[119] P. Lindskog, *Algorithm and tools for system identification using prior knowledge*, Thesis, Department of Electrical Engineering, Linköping University, Linköping, Sweden, 1994.

[120] R.Z. Homod, "Review on the HVAC system modeling types and the shortcomings of their application," *Journal of Energy*, 2013.

[121] A. Afram and F. Janabi-Sharifi, "Theory and applications of HVAC control systems a review of model predictive control (MPC)," *Building and Environment*, vol. 72, pp. 343-355, 2014.

[122] M. Killian, B. Mayer and M. Kozek, "Effective fuzzy black-box modeling for building heating dynamics," *Energy and Buildings*, vol. 96, pp. 175-186, 2015.

[123] G. Mustafaraj, J. Chen and G. Lowry, "Thermal behaviour prediction utilizing artificial neural networks for an open office," *Applied Mathematical Modelling*, vol. 34, pp. 3216-3230, 2010.

[124] S. Wu and J. Sun, "A physics-based linear parametric model of room temperature in office buildings," *Building and Environment*, vol. 50, pp. 1-9, 2012.

[125] S. Soyguder and H. Alli, "Predicting of fan speed for energy saving in HVAC system based on adaptive network based fuzzy inference system," *Expert Systems with Applications*, vol. 36, pp. 8631-8638, 2009.

[126] A. Kusiak, G. Xu and Z. Zhang, "Minimization of energy consumption in HVAC systems with data-driven models and an interior-point method," *Energy Conversion and Management*, vol. 85, pp. 146-153, 2014.

[127] K.J. Aström, B. Wittenmark, *Computer controlled systems. theory and design*, Prentice-Hall. Englewood Cliffs, NJ, 1984.

[128] S.M. Shinners, *Modern control system theory and design*, John Wiley & Sons, 1998.

[129] R.C. Dorf and R.H. Bishop, *Modern control systems*, Addison Wesley Longman, Menlo Park, CA, 1995.

[130] M.S. Tavazoei, "Notes on integral performance indices in fractional-order control systems," *Journal of Process Control*, vol. 20, pp. 285-291, 2010.

[131] A. Preglej, J. Rehrl, D. Schwingshackl, I. Steiner, M. Horn and I. Škrjanc, "Energy-efficient fuzzy model-based multivariable predictive control of a HVAC system," *Energy and Buildings*, vol. 82, pp. 520-533, 2014.

[132] H. Lv, P. Duan, Q. Yao, H. Li and X. Yang, "A novel adaptive energy-efficient controller for the HVAC systems," in *2012 24th Chinese Control and Decision Conference (CCDC)*, Taiyuan, pp. 1402-1406, 2012.

[133] M. Gulan, M. Salaj and B. Rohal-Ilkiv, "Application of adaptive multivariable generalized predictive control to a HVAC system in real time," *Archives of Control Sciences*, vol. 24, no. 1, pp. 67-84, 2014.

[134] G. Singh, M. Zaheer-Uddin and R.V. Patel, "Adaptive control of multivariable thermal processes in HVAC systems," *Energy Conversion and Management*, vol. 41, no. 15, pp. 1671-1685, 2000.

[135] M.S. Elliott, *Decentralized model predictive control of a multiple evaporator HVAC system (MSc thesis)*, Texas A&M University, College Station, Texas, United States, 2008.

[136] Q. Qi and S. Deng, "Multivariable control of indoor air temperature and humidity in a direct expansion (DX) air conditioning (A/C) system," *Buildings and Environment*, vol. 44, no. 8, pp. 1659-1667, 2009.

[137] J. Hu and P. Karava, "Model predictive control strategies for buildings with mixed-mode cooling," *Buildings and Environment*, vol. 71, pp. 233-244, 2014.

[138] E. Camacho and C. Bordons, *Model predictive control*, Springer, 2007.

[139] *Operator's manual - CI3100 Ethernet OPT sensor*, CLiMET Instruments Company, 2013.

[140] W. Bolton, *Programmable logic controllers (Fifth Edition)*, Newnes, Boston, 2009.

[141] B. Käpernick and K. Graichen, "PLC implementation of a nonlinear model predictive controller," *IFAC Proceedings Volumes*, vol. 47, no. 3, pp. 1892-1897, 2014.